LEABHARLANN CHOLÁISTE NA TRÍONÓIDE, BAILE ÁTHA CLIATH | TRINITY COLLEGE LIBRARY DUBLIN
Ollscoil Átha Cliath | The University of Dublin

Terms and Conditions of Use of Digitised Theses from Trinity College Library Dublin

Copyright statement

All material supplied by Trinity College Library is protected by copyright (under the Copyright and Related Rights Act, 2000 as amended) and other relevant Intellectual Property Rights. By accessing and using a Digitised Thesis from Trinity College Library you acknowledge that all Intellectual Property Rights in any Works supplied are the sole and exclusive property of the copyright and/or other IPR holder. Specific copyright holders may not be explicitly identified. Use of materials from other sources within a thesis should not be construed as a claim over them.

A non-exclusive, non-transferable licence is hereby granted to those using or reproducing, in whole or in part, the material for valid purposes, providing the copyright owners are acknowledged using the normal conventions. Where specific permission to use material is required, this is identified and such permission must be sought from the copyright holder or agency cited.

Liability statement

By using a Digitised Thesis, I accept that Trinity College Dublin bears no legal responsibility for the accuracy, legality or comprehensiveness of materials contained within the thesis, and that Trinity College Dublin accepts no liability for indirect, consequential, or incidental, damages or losses arising from use of the thesis for whatever reason. Information located in a thesis may be subject to specific use constraints, details of which may not be explicitly described. It is the responsibility of potential and actual users to be aware of such constraints and to abide by them. By making use of material from a digitised thesis, you accept these copyright and disclaimer provisions. Where it is brought to the attention of Trinity College Library that there may be a breach of copyright or other restraint, it is the policy to withdraw or take down access to a thesis while the issue is being resolved.

Access Agreement

By using a Digitised Thesis from Trinity College Library you are bound by the following Terms & Conditions. Please read them carefully.

I have read and I understand the following statement: All material supplied via a Digitised Thesis from Trinity College Library is protected by copyright and other intellectual property rights, and duplication or sale of all or part of any of a thesis is not permitted, except that material may be duplicated by you for your research use or for educational purposes in electronic or print form providing the copyright owners are acknowledged using the normal conventions. You must obtain permission for any other use. Electronic or print copies may not be offered, whether for sale or otherwise to anyone. This copy has been supplied on the understanding that it is copyright material and that no quotation from the thesis may be published without proper acknowledgement.

The Role of microRNA-107 in Toll-like Receptor Signaling

Thesis Submitted to the

University of Dublin

For the

Degree of Doctor of Philosophy

By

Elizabeth J. Hennessy

School of Biochemistry & Immunology

Trinity College

Dublin

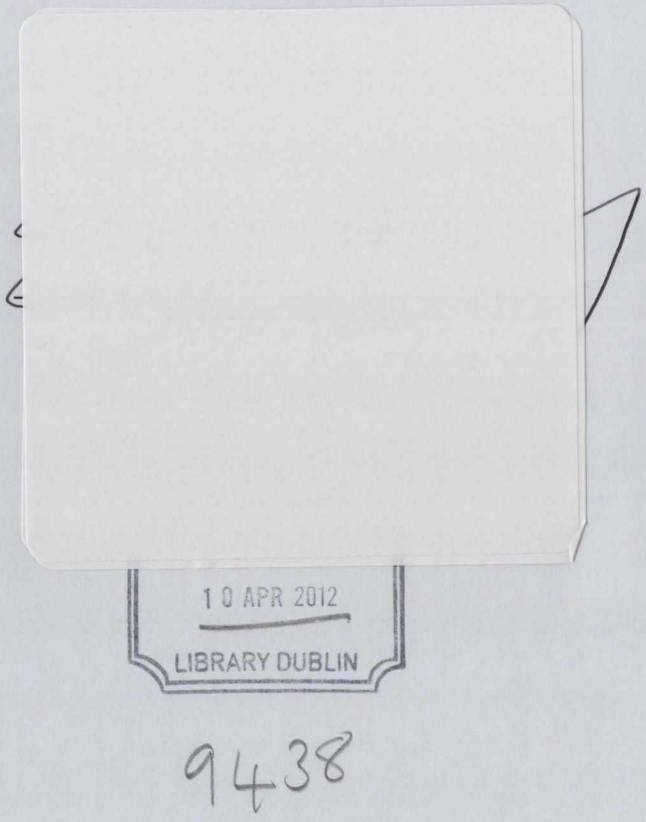
Ireland

September 2010

Declaration

This thesis is submitted by the undersigned to the University of Dublin for the examination of Doctorate of Philosophy. The work herein is entirely my own.

This work has not been submitted as an exercise for a degree to any other university. The library at Trinity College, Dublin, has my full permission to lend or copy this thesis upon request.



10 APR 2012
LIBRARY DUBLIN
9438

Acknowledgements

I owe a seriously big thank you to Luke O'Neill for taking a chance and letting me do this PhD under your supervision. You are truly a superior supervisor. I appreciate your intellectual guidance as well as taking us on all those nights out where we had some of the best brain storming/problem solving sessions.

Thank you everyone in the LON lab for being amazing people both scientifically and personally. This includes Eva, Kathy, Elaine, Sinead, Emma, Anne, Sarah, Andi, Seth, Jen, Gillian, Emer and Paulina.

I especially thank my office mates Becca and Dympna (a.k.a. B-money and D-money), you made life in the office fun but most importantly productive.

Thank you to past members of the LON lab, Christine, Claire McCoy, Susan and Caroline. It was a tough few months without you…

Fred Sheedy (a.k.a. Dawg) you made my time in Dublin totally memorable (Oh em gee). Thank you for making me feel so welcome in the lab and Ireland as well as introducing me to the amazing world of small RNA and Euro Pop.

Lastly, to my family, you made life over here a wee bit easier with your care packages, chocolate chip cookies and scratchies. I owe everything to youse.

This work was funded by the Health Research Board in Ireland under grant No. PhD / 20007/9.

I am ahead, I am advanced
I am the first mammal to make plans
I crawled the earth, but now I'm higher
2010, watch it go to fire
It's evolution
Do the evolution
- Eddie Vedder

Table of Contents

Declaration i
Acknowledgements ii
Table of Contents iii
List of Figures xi
List of Tables xvi
Abbreviations xvii
Abstract xx

CHAPTER 1 21

GENERAL INTRODUCTION 21

1.1. **The Immune System** 2

1.1.1. The Innate Immune Response 2

1.1.2. Phagocytosis 3

1.2. **TLRs** 5

1.2.1. Discovery of TLRs 5

1.2.2. Specificity of TLRs 6

1.2.3. TLR Signaling Pathways 7

1.2.4. TLRs and Disease 10

1.3. **A Role for MicroRNAs in the Innate Immune Response** 12

1.3.1. The History of Small, Non-coding RNAs 12

1.3.2. The Synthesis and Function of microRNAs 13

1.3.3. Bacteria and Small Non-coding RNAs 15

1.3.4. The Role of microRNAs in Cancer and Virus Invasion 16

1.3.4. The Role of microRNAs in Haematopoiesis 17

1.3.5. ImmunomiRs 18

1.4. **Aims and Objectives** 21

CHAPTER 2 ..... **22**

MATERIALS & METHODS **22**

2.1. **Reagents** 23

2.1.1. Stimulants 23

2.1.2. Antibodies 23

2.1.3. Cell Culture Reagents 23

2.1.4. Bacterial Strains 23

2.1.5. Cell Lines 23

2.1.6. PCR Reagents 24

2.1.7. Fluorescent Probes and Bacteria 24

2.1.8. RNA Oligonucleotides 24

2.1.9. DNA plasmids 24

2.1.10. Miscellaneous Reagents 24

2.1.11. Animals 25

2.2. **Cell Culture** 25

2.2.1. Maintenance of DC2.4 and THP1 Cell Lines 25

2.2.2. Maintenance of I-BMDM, Raw264.7, J774, A172, HEK293TLR4, Caco2 and MEF Cell Lines 25

2.2.3. Maintenance of L929 Cell Lines 26

2.2.4. Generating Primary Bone-marrow Derived Dendritic Cells 26

2.2.5. Generating Primary Bone-marrow Derived Macrophages 26

2.2.6. Isolation and Generation of Peripheral Blood Mononuclear Cells 27

2.2.7. Cryogenic Preservation of Cell Lines 27

2.3. **Stimulating Cells with TLR ligands** 27

2.4. **RNA Preparation** 27

2.4.1. Isolating RNA Using Qiagen RNeasy Kit to Extract Total RNA 27

2.4.2. Assessment and Quantification of RNA 28

2.5. **TaqMan miRNA PCR Analysis** 28

2.5.1. Generating cDNA using Reverse Transcription PCR 28

2.5.2. miRNA Specific Real Time PCR Amplification 29

2.5.3. Data Analysis 29

2.6. **TaqMan RT-PCR Analysis of Gene Expression** 30

2.6.1. Reverse Transcription 30

2.6.2. Gene Specific Real-time PCR Amplification 30

2.6.3. Gene Specific Real-time PCR Amplification using SYBR Green 30

2.7. **Enzyme-Linked Immunosorbent Assay of Cytokine Expression** 31

2.8. **Transfecting Cells with Anti-sense and Precursor miRNA Molecules** 31

2.8.1. Fluorescence Microscopy 32

2.8.2. Gentamicin Protection Assay 32

2.8.3. MTT Assay for Cell Proliferation 33

2.8.4. Scratch Assay to Simulate Wound Healing 33

2.9. **Western Blot Analysis of Protein Expression** 33

2.9.1. Cell lysis 33

2.9.2 Bradford Method for Determination of Protein Concentration 34

2.9.3. SDS-PAGE (sodium dodecyl sulfate – polyacrylamide gel electrophoresis) 34

2.9.4. Transfer Procedure 34

2.9.5. Blocking the Membrane 35

2.9.6. Immunodetection of Protein on Membrane 35

2.9.7. Stripping and Re-probing 35

2.10. **Luciferase Reporter Assays** 35

2.10.1. Preparation of Plasmid DNA 35

2.10.2. Transient Transfections and stimulations 36

2.10.3. Assay Procedure 36

2.11. **Bioinformatics** 37

2.11.1. Targetscan.org 37

2.11.2. MiRecords and G-profiler 37

2.12. **Statistical analysis** 38

CHAPTER 3 39

miRNA EXPRESSION 39

3.1. **Introduction** 40

3.2. **Analysis of miRNAs in murine cells in response to TLR ligands** 42

3.2.1. miRNA expression in DC2.4 cells in response to LPS 42

3.2.2. IL-6 and TNF-α are produced by DC2.4 cells in response to LPS over a 24 hour period 43

3.2.3. Analysis of expression levels of miR-146a and miR-107 in response to stimulation with recombinant TNF-α in DC2.4 43

3.2.4. Analysis of the expression levels miR-107 and miR-146a following stimulation with LPS in J774 cells 43

3.2.5. IL-6 is produced by J774 cells in response to LPS over a 24 hour period 43

3.2.6. Analysis of the expression levels of miR-107, miR-146a and miR-21 following stimulation with LPS in Raw264.7 cells 44

3.2.7. TNF-α is produced by murine Raw264.7 cells in response to LPS over a 24 hour period 44

3.2.8. Analysis of miR-107 and miR-146a expression following stimulation with TLR ligands in I-BMDM cells 44

3.2.9. IL-6 is produced by I-BMDM in response to LPS over a 24 hour period 44

3.2.10. Analysis of the expression levels of miR-107 and miR-146a following infection with heat-killed E. coli in I-BMDM 44

3.2.11. TNF-α is produced by I-BMDM in response to heat-killed E. coli in I-BMDM 45

3.2.12. Analysis of the expression levels of miR-107 and miR-146a following stimulation with LPS in primary bone marrow derived macrophages cells 45

3.2.13. TNF-α is produced by primary bone marrow derived macrophages in response to LPS 45

3.2.14. Analysis of the expression levels of miR-107, miR-146a and miR-21 following stimulation with LPS in primary bone marrow derived dendritic cells 45

3.2.15. TNF-α is produced by primary bone marrow derived dendritic cells in response to LPS 46

3.3. **Analysis of miRNAs in human cells in response to TLR ligands** 46

3.3.1. Analysis of miR-107, miR-146a and miR-149 expression following stimulation with TLR Ligands in human THP1 cells 46

3.3.2. IL-8 is produced by THP1 cells in response to LPS over a 24 hour period 46

3.3.3. Analysis of miR-107, miR-146a and miR-21 expression following stimulation with LPS in HEK293 and HEK293-TLR4 cells 47

3.3.4. IL-8 is not produced by human HEK293 but is produced by HEK293-TLR4 and THP1 cells in response to LPS over a 24 hour period 47

3.3.5. Analysis of the expression levels of miR-107 and miR-146a following stimulation with LPS in human glial cell line A172 48

3.3.6. Analysis of the expression levels of miR-107 and miR-146a following stimulation with recombinant TNF-α in human glial cell line A172 48

3.3.7. IL-6 is produced by the human glial cell line A172 in response to LPS 48

3.3.8. Analysis of the expression levels of miR-107and miR-146a following stimulation with LPS in human gut epithelial cell line Caco2 48

3.3.9. IL-6 is produced by the human gut epithelial cell line Caco2 in response to LPS 49

3.3.10. Analysis of the expression levels of miR-107, miR-146a and miR-21 following stimulation with LPS in peripheral blood mononuclear cells 49

3.3.11. TNF-α is produced by human PBMC in response to LPS 49

3.4. **Discussion** 50

CHAPTER 4 ..... **56**

MECHANISM OF miR-107 EXPRESSION **56**

4.1. **Introduction** 57

4.1.1. Biogenesis of small regulatory non-coding miRNA molecules 57

4.1.2. PanK1α, PPARα and the immune response 59

4.2. **Results** 62

4.2.1. Analysis of PanK1α and PPARα expression in DC2.4 cells following treatment with LPS over time 62

4.2.2. Analysis of PanK1α and PPARα expression in Raw264.7 macrophages following treatment with LPS over time 62

4.2.3. Analysis of PanK1α and PPARα expression in I-BMDM following treatment with LPS over time 62

4.2.4. Analysis of PanK1α and PPARα protein expression following treatment with LPS using SDS-PAGE and western blotting 63

4.2.5. Analysis of the expression levels of PanK1α and PPARα following infection with heat-killed E. coli in I-BMDM 63

4.2.6. Analysis of primary and precursor-miR-107 transcript expression in I-BMDM following LPS stimulation 63

4.2.7. Analysis of miR-107, PanK1α and PPARα expression in adaptor deficient I- BMDM following LPS stimulation 64

4.2.8. Analysis of primary and precursor-miR-107 transcripts in adaptor deficient I- BMDM following LPS stimulation 64

4.2.9. Rantes cytokine production is impaired in Trif deficient BMDM and TNF-α production is impaired in MyD88 deficient BMDM 64

4.2.10. Analysis of miR-107, PanK1α and PPARα expression in p65 deficient MEF following LPS stimulation 65

4.2.11. Analysis of primary and precursor-miR-107 transcript expression in p65 deficient MEF following LPS stimulation 65

4.2.12. Rantes cytokine production is elevated in the p65 deficient MEF but TNF-α production is impaired 66

4.2.13. Analysis of PPARα, PanK1α and miR-107 in murine macrophage cell line Raw264.7 following treatment with various doses of the PPARα specific agonist WY14643 66

4.2.14. Analysis of miR-107 and PPARα expression in I-BMDM following treatment with various doses of the PPARα specific agonist WY14643 for 8 or 24 hours 67

4.2.15. Production of TNF-α by macrophages pretreated with WY14643 before stimulation with LPS for 6 hours 67

4.2.16. Analysis of miR-107, PanK1α and PPARα expression in macrophages pretreated with WY14643 before stimulation with LPS for 6 hours 67

4.3. **Discussion** 69

CHAPTER 5 ..... **- 76 -**

miR-107 FUNCTION ..... **- 76 -**

5.1. **Introduction** ..... - 77 -

5.1.1. Functional Consequences of miR-107 Downregulation ..... - 77 -

5.2. **Results** ..... - 80 -

5.2.1. Identifying immunomiRs and target genes using in silico methods ..... - 80 -

5.2.2. Quantifying mRNA expression of miR-107 predicted target genes in response to LPS ..... - 80 -

5.2.3. Quantifying mRNA expression of published targets of miR-107 in response to LPS ..... - 81 -

5.2.4. Optimizing transfection efficiency of DC2.4 cells using two transfection reagents ..... - 82 -

5.2.5. Quantifying Cdk6 mRNA expression in I-BMDM transfected with antisense-miR-107 or precursor-miR-107 in response to LPS ..... - 83 -

5.2.6. miR-107 directly binds to CDK6 as shown using the 3`UTR luciferase reporter construct ..... - 83 -

5.2.7. Secreted TNF-α cytokine production is affected by transfection of miRNA molecules into DC2.4 and Raw264.7 cells ..... - 84 -

5.2.8. Fluorescence Microscopy shows that DC2.4 Cells Transfected with Pre-miR-107 show decrease in F-actin ..... - 84 -

5.2.9. Cells over-expressing miR-107, knocked down for CDK6 or CDK6 deficient BMDM exhibit less cellular proliferation ..... - 85 -

5.2.10. Mice deficient for CDK6 were less susceptible to the lethal effect of LPS and produced less TNF-α and enhanced IL-10 ..... - 87 -

5.2.11. Cells transfected with miR-107 molecules exhibited no differences in amount of apoptotic cells ..... - 87 -

5.2.12. Cells over-expressing miR-107 exhibit less migration ..... - 88 -

5.2.13. Cells over-expressing miR-107 exhibit less internalization of live *E. coli* ..... - 88 -

5.2.14. Effect on TNF-α and IL-6 cytokine secretion by cells transfected with miRNA molecules following infection with live E. coli ..... - 89 -

5.3. **Discussion** ..... - 90 -

CHAPTER 6 ..... **- 98 -**

FINAL DISCUSSION ..... **- 98 -**

CHAPTER 7 ..... **106**

REFERENCES **106**

CHAPTER 8 ..... **131**

APPENDICES **131**

Publication Record 132

Poster Abstracts 132

Published Articles 132

List of Figures

Chapter 1

1.1. The components of the innate and adaptive immune responses and timelines

1.2. Macrophages bear different pattern recognition receptors

1.3. Toll-like Receptor signaling pathways and the TLR4 crystal structure

1.4. The biogenesis of miRNA

1.5. ImmunomiRs miR-21, miR-155 and miR-146a and their target genes with roles in TLR signaling

Chapter 2

2.1. Stem-loop TaqMan PCR for miRNA expression and Real-time PCR amplification plot

Chapter 3

3.1. Expression levels of miR-155 and miR-214 in murine dendritic cell line DC2.4 in response to LPS

3.2. Expression levels of miR-21 and miR-146a in murine dendritic cell line DC2.4 in response to LPS

3.3. Expression levels of let-7e, miR-149 and miR-107 in murine dendritic cell line DC2.4 in response to LPS

3.4. Production of IL-6 and TNF-α cytokine by DC2.4 cells in response to LPS

3.5. Expression levels of miR-107 and miR-146a in murine dendritic cell line DC2.4 treated with TNF-α

3.6. Expression levels of miR-107 and miR-146a in murine J774 macrophages in response to LPS

3.7. Production of IL-6 cytokine by murine J774 macrophages in response to LPS

3.8. Expression levels of miR-107, miR-146a and miR-21 in murine Raw264.7 macrophages in response to LPS

3.9. Production of TNF-α cytokine by murine Raw264.7 macrophages in response to LPS

3.10. Expression levels of miR-107 and miR-146a in immortalized murine bone marrow derived macrophages (I-BMDM) in response to LPS

3.11. Production of IL-6 cytokine by I-BMDM in response to LPS

3.12. Expression levels of miR-107 and miR-146a in I-BMDM in response to *E. coli*

3.13. Production of TNF-α cytokine by I-BMDM in response to *E. coli*

3.14. Expression levels of miR-107 and miR-146a in primary murine bone-marrow-derived macrophages in response to LPS

3.15. Production of TNF-α cytokine by primary mouse bone marrow derived macrophages in response to LPS

3.16. Expression levels of miR-107, miR-146a and miR-21 in primary murine bone-marrow-derived dendritic cells in response to LPS

3.17. Production of TNF-α cytokine by primary mouse bone marrow derived dendritic cells in response to LPS

3.18. Expression levels of miR-107, miR-146a and miR-149 in human monocytic cell line THP1 in response to LPS

3.19. Production of IL-8 cytokine by human THP1 monocytic cell line in response to LPS

3.20. Expression levels of miR-107 and miR-146a in human embryonic kidney cells in response to LPS

3.21. Expression levels of miR-107, miR-146a and miR-21 in human embryonic kidney cells stably transfected with TLR4 in response to LPS

3.22. Production of IL-8 cytokine by human embryonic kidney cells and human embryonic kidney cells stably transfected with TLR4 cells in response to LPS

3.23. Expression levels of miRNA in human glial cell line A172 in response to LPS.

3.24. Expression levels of miR-107 and miR-146a in human glial cell line A172 in response to TNF-α

3.25. Production of IL-6 cytokine by human glial cell line A172 in response to LPS

3.26. Expression levels of miR-107 and miR-146a in human gut epithelial cell line Caco2 in response to LPS

3.27. Production of IL-6 cytokine by human gut epithelial cell line Caco2 in response to LPS

3.28. Expression levels of miR-107, miR-146a and miR-21 in human peripheral blood mononuclear cells in response to LPS

3.29. Production of TNF-α cytokine by human peripheral blood mononuclear cells in response to LPS

Chapter 4

4.1. The precursor miR-107 sequence is found in intron 5 of the PanK1α gene

4.2. Four PPRE are found in the promoter of PanK1α

4.3. Expression levels of PanK1α and PPARα in murine dendritic cell line DC2.4 in response to LPS

4.4. Expression levels of PanK1α and PPARα in murine macrophage cell line Raw264.7 in response to LPS

4.5. Expression levels of PanK1α and PPARα in murine macrophage cell line I-BMDM in response to LPS

4.6. Western blot analysis of PanK1α and PPARα protein expression in I-BMDM in response to LPS

4.7. Expression levels of PanK1α and PPARα in I-BMDM in response to *E. coli*

4.8. Expression levels of primary-miR-107 and precursor-miR-107 transcripts in murine macrophage cell line I-BMDM in response to LPS

4.9. Expression levels of miR-107, PanK1α and PPARα in adaptor deficient I-BMDM in response to LPS

4.10. Expression levels of primary-miR-107 and precursor-miR-107 transcripts in adaptor deficient I-BMDM in response to LPS

4.11. TNF-α and Rantes production in adaptor deficient I-BMDM in response to LPS

4.12. Expression levels of miR-107, mPanK1α and mPPARα in wild-type and p65 deficient mouse embryonic fibroblasts in response to LPS

4.13. Expression levels of primary-miR-107 and precursor-miR-107 transcripts in wild-type and p65 deficient mouse embryonic fibroblasts in response to LPS

4.14. TNF-α and Rantes production by wild-type and p65 deficient mouse embryonic fibroblasts in response to LPS

4.15. Expression levels of PPARα, PanK1α and miR-107 in murine macrophage cell line Raw264.7 in response to WY14643

4.16. Expression levels of PPARα and western blot analysis of PPARα protein expression in I-BMDM in response to WY14643

4.17. Production of TNF-α Cytokine in Raw264.7 and I-BMDM in response to pre-treatment with WY14643 before LPS stimulation

4.18. Expression levels of miR-107, PanK1α and PPARα in Raw264.7 in response to pre-treatment with WY14643 before LPS stimulation

Chapter 5

5.1. Common biological functions of miR-107 according to GProfiler

5.2. Expression of potential target genes in murine macrophage cell line I-BMDM in response to LPS

5.3. Expression of potential target genes in murine macrophage cell line I-BMDM in response to LPS

5.4. Expression levels of potential known target genes in murine macrophage cell line I-BMDM in response to LPS

5.5. Expression levels of mDicer1 in murine macrophage cell line I-BMDM and MEF in response to LPS

5.6. Expression level of CDK6 in murine macrophage cell line I-BMDM in response to LPS

5.7. Expression level of CDK6 in murine macrophage cell line I-BMDM in response to *E. coli*

5.8. Expression levels of mCDK6 in adaptor deficient murine macrophage cell line in response to LPS

5.9. Expression levels of mCDK6 in p65 deficient mouse embryonic fibroblasts in response to LPS

5.10. Optimizing Transfection Efficiency

5.11. Expression levels of mCDK6 in murine macrophage cell line I-BMDM in response to LPS

5.12. Illustration of luciferase construct containing 3`UTR of mouse Cdk6

5.13. CDK6 3`UTR luciferase expression in I-BMDM transfected with miRNA

5.14. Production of TNF-α in transfected mouse DC2.4 cells and Raw264.7 cells in response to LPS

5.15. Fluorescence microscopy of DC2.4 Cells Transfected with anti-miR-107 or pre-miR-107 in response to LPS

5.16. Cell Proliferation of I-BMDM in response to LPS

5.17. Cell Proliferation of I-BMDM in response to LPS

5.18. Cell Proliferation and TNF-α and IL-10 production of Primary BMDM in response to LPS

5.19. Expression level of miR-107 in CDK6 deficient BMDM in response to LPS

5.20. Survival of wild-type and CDK6 deficient mice in response to LPS injection and TNF-α and IL-10 in the serum of these mice

5.21 Percent of apoptotic I-BMDM in response to LPS

5.22. Cell migration of I-BMDM in response to LPS

5.23. Cell migration of I-BMDM in response to LPS

5.24. Intracellular bacteria counts of Raw264.7 cells infected with wild-type *E. coli*

5.25. TNF-α and IL-6 cytokine production of Raw264.7 cells transfected with miRNA RNA molecules and infected with *E.coli.*

Chapter 6

6.1. Regulation of cellular proliferation and migration via the decrease in miR-107 expression in response to LPS which leads to an increase in CDK6 expression

List of Tables

2.1. Primers used in this study

3.1. miR-107 expression in various mouse and human cell types

3.2. miR-146a expression in various mouse and human cell types

3.3. miR-21 expression in various mouse and human cell types

5.1. Selection of the predicted mouse genes targeted by miR-107 with a role in the immune response

5.2. Selection of the predicted human genes targeted by miR-107 with a role in the immune response

5.3. Potential miR-107 target genes that are induced in response to LPS.

Abbreviations

3` UTR	3` untranslated region
β –ME	β-mercaptoethanol
BACE1	β-amyloid precursor protein-cleaving enzyme 1
BMDC	marrow derived dendritic cells
BMDM	bone marrow derived macrophage cells
C57Bl6	C57 Black6
CDK6	cyclin-dependent kinase 6
CDKi	CDK inhibitors
cDNA	complementary DNA
CFUs	Colony forming units
CLL	chronic lymphocytic leukemia
CoA	Coenzyme A
CR1	type 1 complement receptor
C_t	Cycle Threshold
DAMPs	danger-associated molecular patterns
dsRNA	double stranded RNA
ECL	enhanced chemiluminescence
ELISA	Enzyme-Linked Immunosorbent Assay
FACS	Fluorescence Activated Cell Sorting
F-actin	filamentous actin
FCS	fetal calf serum
GIRE	glucose response element
HIF-1	Hypoxia-inducible factor 1
HSC	haematopoietic stem cells
IAPs	Inhibitors of apoptosis proteins
I-BMDM	immortalized bone marrow derived macrophages
IgG	immunoglobulin G
IKK	IκB kinase
IL-1RI	type I IL-1 receptor
ISRE	interferon sequence response element
IL-1β	interleukin-1β
IPD	invasive pneumococcal disease

IRAK-1	IL-1R-associated protein kinase
IRF3	IFN-regulatory factor 3
KSHV	Kaposi's-sarcoma-associated herpes virus
LBP	LPS-binding protein
LPS	lipopolysaccharide
LRR	leucine rich repeats
LTA	lipoteichoic acid
Mal	MyD88 adaptor-like
MAMPs	microbial associated molecular components
MAPK	Mitogen Activated Protein Kinase
MBL	mannose-binding lectin
MCP-1	monocytes chemoattractant protein-1
MDP	muramyl dipeptide
MEF	mouse embryonic fibroblasts
miRNAs	microRNAs
miR-107	microRNA-107
mRNA	messenger RNA
NEMO	NF-κB essential modulator
NF1-A	Nuclear factor 1 A-type
NF-κB	nuclear factor-kappa B
NLR	NOD-like receptor family
NOD	nucleotide oligomerization domain
P/S	penicillin/streptomycin
PAMPs	pathogen-associated molecular patterns
PanK1α	pantothenate kinase1-alpha
PBMC	peripheral blood mononuclear cells
PFA	paraformaldehyde
PI3K	phosphoinositide 3 kinase
PKAN	Pantothenate kinase-associated neurodegeneration
Poly I:C	Polyriboinosinic polyribocytidylic acid
PPARα	peroxisome proliferator-activated receptor-alpha
pre-miRNA	precursor-miRNA
pri-miRNA	primary miRNA

PRRs	Pattern recognition receptors
PVDF	polyvinylidene difluoride
Rab11FIP2	Rab-family interacting protein
Rb	retinoblastoma
RF-dH_20	RNase-free water
RISC	RNA-induced silencing complex
RNAi	RNA interference
RNase	RNA polymerase
RQ	relative quantification
SDN	small RNA degrading nuclease
SDS-PAGE	sodium dodecyl sulfate – polyacrylamide gel electrophoresis
SHIP-1	SH2-containing inositol 5-phosphatase 1
siRNA	small interfering RNAs
SMAC	Second mitochondria-derived activator of caspase
SOCS1	Suppressor of Cytokine Signaling 1
SREBP	sterol-regulatory element binding protein site
TACE	TNF-α converting enzyme
TAK-1	transforming growth factor-β-activated kinase
TIR	Toll-IL-1 receptor
TIRAP	Toll-IL-1 receptor domain containing adaptor protein
TLRs	Toll-like receptors
TRAF6	tumor necrosis factor receptor–associated factor
TRAM	Trif-related adaptor molecule
TRIF	Toll-IL-1 receptor domain-containing adaptor inducing IFN-β
Vamp	vesicle-associated membrane protein

Abstract

MicroRNAs (miRNAs) are a novel class of small non-coding RNA regulatory molecules which post-transcriptionally regulate genes in a fine-tuning manner. Multiple miRNAs have been shown to be regulated by Toll-like receptors (TLRs), including miR-146a, miR-155 and miR-21. In this study, I have found that the TLR4 ligand lipopolysaccharide (LPS) can down-regulate microRNA-107 (miR-107). miR-107 is downregulated in response to LPS in many cell lines as well as in primary mouse and human cells. This study focused primarily on the expression and function of miR-107 in an immortalized bone marrow derived macrophage cell line based on the degree and consistency of downregulation. I have found that the decrease in miR-107 expression is MyD88 and NF-κB-dependent. The primary-miR-107 transcript is encoded in intron 5 of the Pantothenate Kinase-1α gene (PanK1α) which is an essential enzyme needed for coenzyme A synthesis, one of the critical components of fatty acid oxidation. I have found that LPS stimulation decreases the mRNA and protein levels of PanK1α. This downregulation like miR-107 is also dependent on MyD88 and NF-κB signaling. The transcription factor PPARα which is known to regulate PanK1α expression is also downregulated in response to LPS stimulation in a MyD88 and NF-κB-dependent manner. Through the use of a chemical agonist specific for PPARα, WY14643, I have found that miR-107, PanK1α and PPARα are regulated together.

I went on to explore potential targets of miR-107 expression and found that the mRNA for Myosin9, Vinculin, Ankyrin1, HIF-1α, Dicer1, and cyclin-dependent kinase 6 (CDK6) all increase in response to LPS stimulation at the same time points as miR-107 downregulation suggesting that each of these genes could be potential targets of miR-107 regulation. I chose to focus this study on CDK6 based on consistency of upregulation in response to LPS. I provide evidence that increasing miR-107 limits the expression of cdk6 mRNA and protein levels resulting in a decrease in the proliferation and migration of immune phagocytic cell while indirectly affecting TNF-.α secretion, actin cytoskeletal rearrangement and phagocytosis of live bacteria. The data from this study therefore indicate a novel role for miR-107 in the regulation of TLR signaling.

CHAPTER 1

GENERAL INTRODUCTION

1.1. **The Immune System**

1.1.1. *The Innate Immune Response*

The mammalian innate immune response is a complex series of signal transduction pathways which ultimately leads to a successful defense against an assault on the body such as infection or tissue trauma. Innate, non-adaptive immune defenses act against infectious disease. The innate immune response is phylogenetically the oldest mechanism of defense against microbial invaders such as viruses, Gram-negative and Gram-positive bacteria, and fungi (Fearon and Locksley, 1996). Aspects of innate immunity are found in all multi-cellular organisms including plants and insects. The innate immune response can be divided into recognition, activation, and effector phases (Figure 1.1). Some components of innate immunity are active at all times, even before infection (Gordon, 2002).

Epithelial surfaces such as skin and the lining or mucosa of the respiratory and gastrointestinal tracts form barriers to prevent entry of foreign pathogens (Janeway and Medzhitov, 2002). However, upon entry of a pathogen into the body, activation of the host innate immune response depends on specific recognition of conserved microbial signature molecules called pathogen-associated molecular patterns (PAMPs) or microbial-associated molecular patterns (MAMPs) because they are recognized regardless of the degree of pathogenicity (Fearon and Locksley, 1996; Janeway and Medzhitov, 2002). These molecular patterns are highly conserved throughout evolution and are not likely to be mutated because they are essential for the survival of the microbe. These conserved structures can include nucleic acids or proteins unique to microbes, as well as lipids and carbohydrates synthesized by bacteria such as LPS and lipoteichoic acid (LTA). Pattern recognition receptors (PRRs) like TLRs act by specifically recognizing PAMPs. These transmembrane receptors act against infectious disease and are the first line of innate immune defense. The recognition of PAMPs leads to the binding, engulfment and subsequent destruction of the invading microbe as well as the activation of cell signaling cascades that lead to the inflammatory response and adaptive immunity. Principle effector cells of the innate immune system include mononuclear phagocytic cells such as

macrophages and neutrophils (Cohn, 1963; Fidalgo and Najjar, 1967). Phagocytes are cells with a primary function of identifying, ingesting, and destroying foreign microbes. Phagocytic cells were first identified by the Russian scientist Ilya Mechnikov in 1883 when he observed the ability of starfish larvae to engulf particles introduced to their bodies (Brown, 1995; Lokaj and John, 2008). His theory that white blood cells in the human body also had the ability to phagocytose microbes was initially ridiculed by other researchers but was later proven correct (Cook et al., 2003; Medzhitov and Janeway, 2000; Takeda and Akira, 2005).

Macrophages are cells that release cytokines and chemokines in response to an encounter with a foreign microbe. These chemical signals stimulate the cellular reaction of innate immunity called inflammation. During inflammation, leukocytes are recruited to the site of infection and activate proteins that eliminate the cause of the infection (García-Mauriño et al., 1999). Macrophages are strategically located throughout the host in tissues and sites where microbes may gain entry (Janeway and Medzhitov, 2002). They are actively recruited to the site of infection. They are found in the subepithelial connective tissue, in the interstitia of parenchymal organs, and in the lymphatic sinuses of the lymph nodes. Macrophages proceed through a series of sequential steps in the host innate immune response (Underhill and Ozinsky, 2002a).

1.1.2. *Phagocytosis*

Once microbes, apoptotic cells, necrotic cells and cellular debris are recognized by receptors like TLRs on the surface of phagocytic cells like macrophages they are internalized through a cytoskeleton-dependent process of engulfment called phagocytosis (figure 1.2) (Janeway and Medzhitov, 2002; Vieira et al., 2002). All mammalian cell types are capable of phagocytosing foreign particles, but the efficiency to which the cell ingests foreign matter varies greatly (Greenberg and Grinstein, 2002). Cells can be referred to as professional or non-professional phagocytes depending on the assistance or amount of priming or opsonization they need to phagocytose. When a ligand binds to a cell surface receptor a series of fusion events takes place leading to the invagination of the cell membrane, the formation of the phagocytic cup and ultimately the formation of the phagosome.

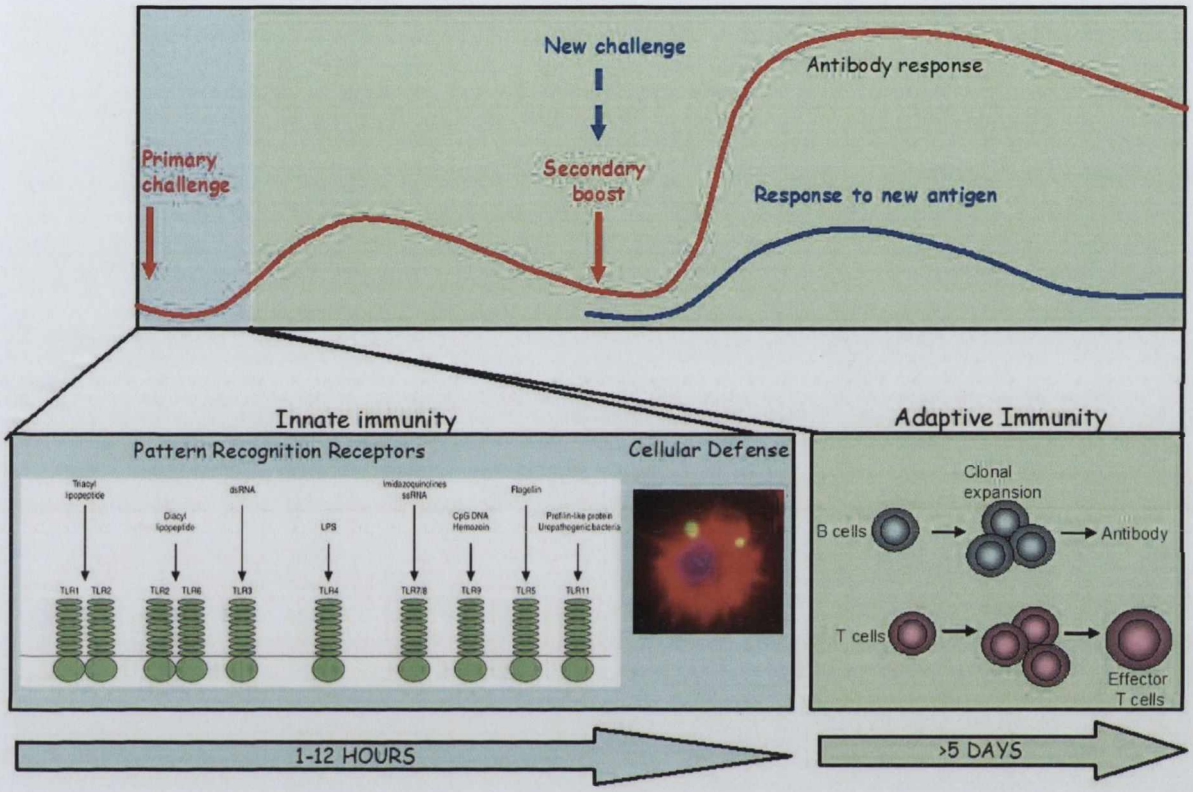


Figure 1.1. **The components of the innate and adaptive immune responses and timelines**. Pattern recognition receptors and cellular defenses like phagocytosis are involved in the innate immune response, which is followed by the adaptive response consisting of B and T cells and the formation of antibodies.

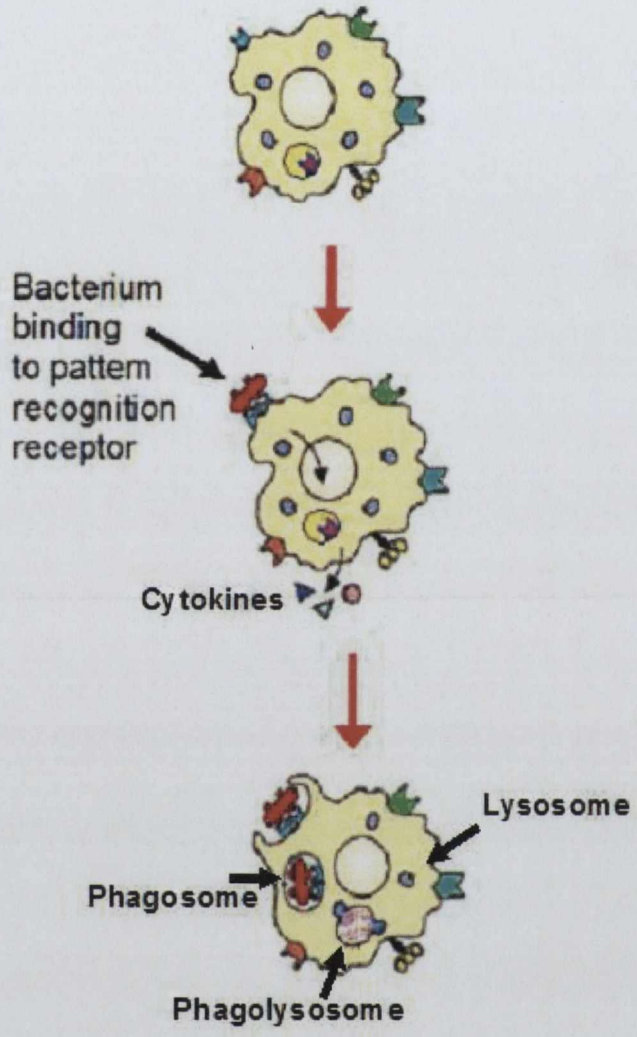


Figure 1.2. **Macrophages bear different pattern recognition receptors**. PRR like TLRs recognize microbial associated molecular components (MAMPs) such as the lipopolysaccharide found on the cell surface of gram-negative bacteria. This recognition leads to production of cytokines and the destruction of the invading microbe through the process of phagocytosis. The different colors in the diagram represent the many different PRR found on the outside and the inside of the cell.

After the phagocytic cup seals off, the newly formed vacuole or phagosome undergoes a complete transformation through a series of maturation steps resulting in major cellular changes. Yeast studies have demonstrated that phagocytosis in mammalian cells requires a properly functioning actin cytoskeleton (Lamaze et al., 1997). For years the role of the actin cytoskeleton in endocytosis was confusing. Researchers would use the drug Cytochalasin D on cells which destabilizes actin filaments. This would inhibit endocytosis in polarized cells at the apical end but not the basolateral surface of the cell. It was later shown that the actin filaments at the basolateral end were more resistant to the effects of the drug and the drug was actually preventing the formation of clathrin coated vesicles at the plasma membrane thus inhibiting phagocytosis. It is now known that all phagocytic processes are regulated by the actin cytoskeleton (May and Machesky, 2001). Following activation of the actin cytoskeleton, endosomes and the endoplasmic reticulum fuse with the phagocytic cup at the cell surface to create more membrane surface for more efficient engulfment (Stuart and Ezekowitz, 2005). The phagocytic cup then folds over the microbe, pinches off, and breaks away from the membrane forming an intracellular vacuole called a phagosome. The internalized microbe is then ingested, and the phagosome fuses with another organelle called the lysosome, forming a hybrid organelle called the phagolysosome. It is here that the microbicidal mechanisms of the macrophage are concentrated. These include a very low pH, hydrolytic enzymes, defensins, and the ability to generate toxic oxidative compounds (Janeway, 2001). Through the recognition of foreign particles via TLRs and the presentation of antigens on the cell surface, the process of phagocytosis acts as a "bridge" between the innate immune response and adaptive immunity.

Recognition of microbial PAMPs occurs through PRRs such as mannose receptors like mannose-binding lectin (MBL), nucleotide oligomerization domain (NOD)-like receptor family (NLR) and TLRs (Medzhitov and Janeway, 2000). Mannose receptors recognize terminal mannose and fucose residues of glycoproteins and glycolipids found on microbial cell surfaces. Glycoproteins and glycolipids on mammalian cell surfaces contain sialic acid or N-acetylgalactosimase residues which enable macrophages to distinguish between host cells and microbial cells (Rostand and Esko, 1997). Invading microbes are

coated with opsonins in a process called opsonization (Verhoef et al., 1979). This process allows "generic" receptors to mediate recognition, thus increasing the efficiency of the macrophage (Janeway, 2001). Opsonins include antibodies, complement proteins, and lectins (Rowley and Turner, 1964). Components of the complement system, in particular complement protein C3 and immunoglobulin G (IgG) are both potent opsonins. IgG is recognized by the Fc-gamma receptor and C3 is recognized by the type 1 complement receptor (CR1) found on the cell surface.

The NLRs are intracellular sensors of PAMPs or endogenous danger-associated molecular patterns (DAMPs). The NLR family consists of 22 cytoplasmic proteins including IPAF, APAF, the NOD and NALP (also known as NLRP) sub-families with the 14 NALPs representing the largest sub-family. When activated NLRs form oligomeric complexes which regulate pro-inflammatory cytokine production (Inohara et al., 2001; Kobayashi et al., 2002b; Martinon et al., 2009). There are three prototypical inflammasomes, the NALP1 inflammasome, the NALP3 inflammasome and the IPAF inflammasome. The NALP3 inflammasome is the best characterized and has been shown to be activated by a range of MAMPs/PAMPs and DAMPs including bacterial muramyl dipeptide (MDP), microbial toxins including nigericin, ATP, monosodium urate crystals, amyloid-β and the adjuvant alum. The activation of the NALP3 inflammasome requires several steps resulting in the maturation and secretion of pro-inflammatory cytokines like interleukin-1β (IL-1β).

1.2. **TLRs**

1.2.1. *Discovery of TLRs*

TLRs are expressed at high levels on immune phagocytic cells such as macrophages and dendritic cells as well as epithelial cells. The Toll gene was first discovered in the developing fruit fly *Drosophila melanogaster* where a mutation in the Toll gene resulted in abnormal development of the fly. The mutated flies were termed Toll the German for "wow". Adult fruit flies with the mutation were more susceptible to fungal infection and the activation of Toll resulted in the production of anti-fungal peptides. The *Drosophila* Toll protein was shown to

activate a transcription factor termed Dorsal which is a fly homologue of NF-κB (Medzhitov et al., 1997). The transcription factor NF-κB is activated in response to IL-1 and this activation is followed by the transcription of inflammatory genes. Importantly, the cytosolic signaling domain of the type I IL-1 receptor (IL-1RI) was shown to be homologous to Toll. IL-1 was one of the first cytokines to be described and it remains one of the most effective pro-inflammatory cytokines.

A more closely related mammalian homologue to *Drosophila* Toll was identified called hToll, which was subsequently renamed TLR4. This receptor was shown to induce the expression of the NF-κB signaling pathway and inflammatory genes. Mice that were resistant to the effects of LPS were found to have a mutation in their *TLR4* gene (Poltorak et al., 1998). In 1994, researchers discovered a plant protein that conveyed resistance to tobacco mosaic virus called N protein. This protein had homology to IL1-RI and Toll, the conserved domain being named the Toll-IL-1 receptor (TIR) domain (Whitham et al., 1994). The homology between the plant N protein, IL-1RI and the *Drosophila* Toll protein gave researchers reason to believe that proteins this similar must be very important in immune defense (Underhill and Ozinsky, 2002a). Thirteen mammalian TLRs have been identified in mouse and ten in human, each being responsible for the recognition of different PAMPs (Gordon, 2002; McCoy and O'Neill, 2008; Takeda and Akira, 2004).

1.2.2. *Specificity of TLRs*

The specificity of the TLRs has remained largely unchanged through the course of evolution allowing for an immediate response to invading threats and the ability for the host cell to distinguish between self and non-self and prevent auto-immune disorders from developing (Janeway and Medzhitov, 2002). TLRs recognize conserved structures of microbes or ligands from exogenous and endogenous (host-derived) sources. These can include bacterial or viral nucleic acids, the unmethylated CpG islands of pathogen DNA or proteins unique to microbes such as flagellin (Kawai and Akira, 2005a). Other TLR ligands include lipids and carbohydrates synthesized by bacteria such as LPS and LTA.

Each TLR has demonstrated its specificity for particular microbial components (Figure 1.3A). TLRs that recognize bacterial and fungal components are localized on the cell surface whereas TLRs that recognize viral or microbial nucleic acids are localized to intracellular membranes and encounter ligands in endosomal or phagosomal compartments. As mentioned earlier, TLR4 recognizes LPS on gram-negative bacteria and with the assistance of LPS-binding protein (LBP) this recognition is enhanced. LBP functions to carry LPS to the CD14 molecule where it is then presented to the MD-2/TLR4 complex (figure 1.3B and C) (Latz et al., 2002). TLR2 specifically recognizes components from gram-positive bacteria including LTA with the assistance of the scavenger receptor CD36. TLR2 can form a heterodimer with either TLR1 or TLR6. These TLRs are highly similar and were formed through an evolutionary gene duplication event. Through this collaboration of TLRs a more specific and wider array of microbial components can be recognized (Underhill et al., 1999). TLR5 recognizes flagellin, a constituent of bacterial flagella (Medzhitov and Janeway, 2000). TLR7 and TLR8 are found in endosomes of cells and recognize single-stranded RNA from viruses. TLR9 is also found in endosomes and acts as a receptor for unmethylated CpG islands found in bacterial and viral DNA. TLR3 recognizes double-stranded RNA which is produced by replicating viruses as well as Polyriboinosinic polyribocytidylic acid (Poly I:C). TLR3 is essential in inducing a protective effect against West Nile Virus by restricting its replication (Daffis et al., 2008).

1.2.3. *TLR Signaling Pathways*

All mammalian TLRs share the TIR domains followed by a transmembrane domain and multiple leucine rich repeats (LRR) (O'Neill and Bowie, 2007; O'Neill et al., 2003). Because these receptors are found across species, the importance of them in immunity became a focus for researchers and particularly the signaling cascades activated came into the spotlight. Some TLRs require additional molecules to facilitate the recognition of a ligand as well as the assistance of adaptor molecules. When TLRs are activated, adaptor molecules are recruited from within the cytoplasm of the cell and lead to the activation of signaling cascades. Adaptor molecules contain TIR domains like TLRs and it has been demonstrated that for signaling pathways to be initiated there needs to be an interaction between TIR domains. MyD88 was the first identified adaptor

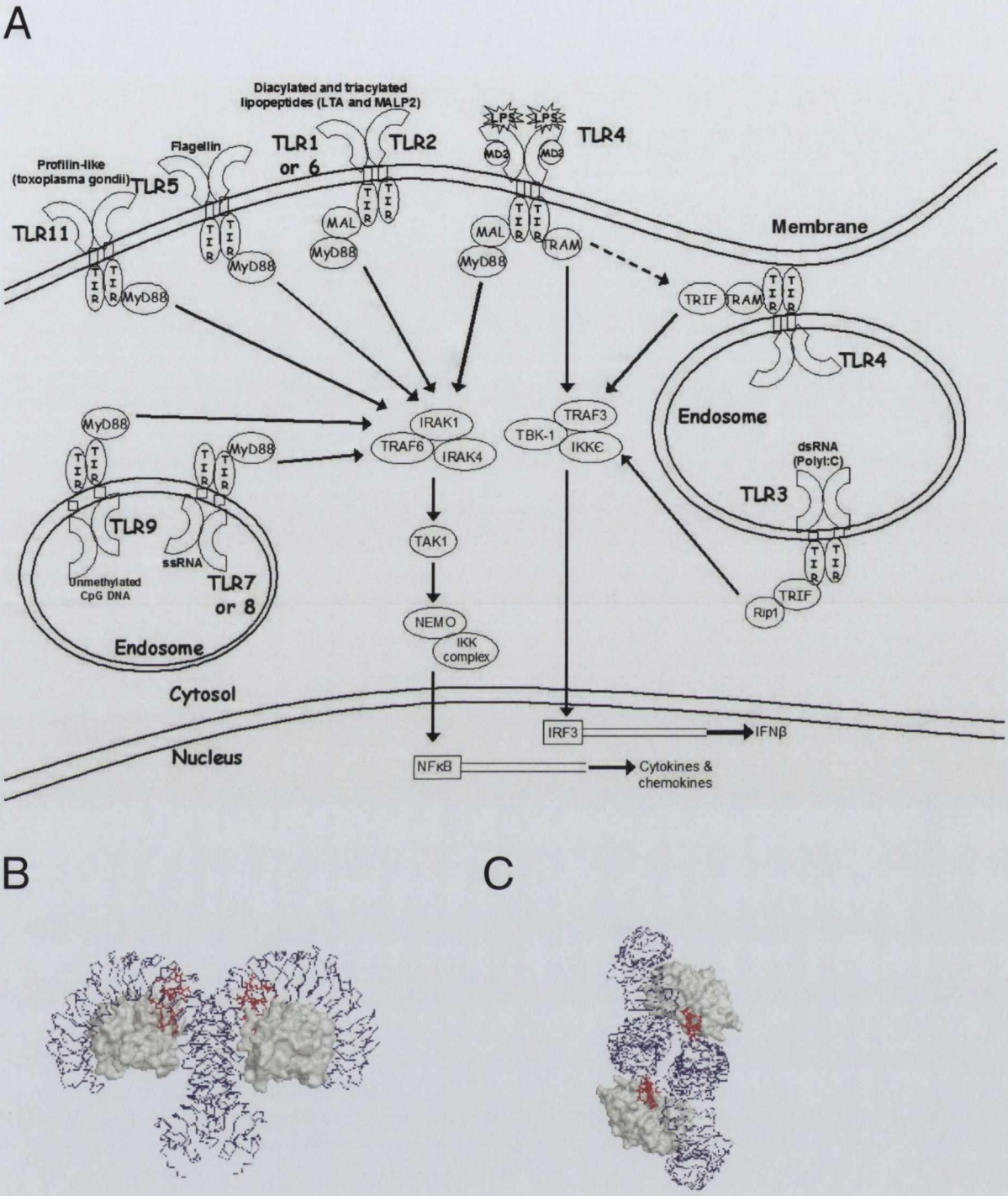


Figure 1.3. **Toll-like Receptor signaling pathways and the TLR4 crystal structure**. The complex series of TLR signaling pathways is illustrated, all converging to elicit either NF-κB or IRF signaling, which are required for cytokine production. The crystal structure for the TLR4 homodimer is illustrated from the side angle (B) and the top (C). LPS is in red. MD-2 is in grey.

molecule (Burns et al., 1998). It was first shown to associate with IL-1RI. Its activation leads to the synthesis of pro-inflammatory cytokines such as TNF-α and IL-1. The importance of MyD88 was demonstrated through the use of MyD88 knock-out mice. These mice were resistant to the effects of LPS, peptidoglycan and lipopeptides and also have defective T-cell proliferation. The knock-out mice exhibited no impairment of IFN-regulatory factor 3 (IRF3) activation in response to LPS leading to the idea that there are MyD88-independent TLR pathways where IFN-β is induced (Akira and Takeda, 2004).

The MyD88-independent pathway is mediated by Toll-IL-1 receptor domain-containing adaptor inducing IFN-β (TRIF). Trif is used by TLR3 and TLR4 and activates IRF3 which leads to the production of IFN-β. The activation of Trif-related adaptor molecule (TRAM) is TLR4 induced and leads to TRIF recruitment (Fitzgerald et al., 2003). Other adaptor molecules have been identified that enhance the specificity of individual TLR signaling pathways. MyD88 adaptor-like (Mal) also known as Toll-IL-1 receptor domain containing adaptor protein (TIRAP) is used in TLR2 and TLR4 signaling (Fitzgerald et al., 2001). Following the stimulation of TLRs and the recruitment of adaptor molecules to the receptor complex, other molecules like IRAK1 (IL-1R-associated protein kinase), IRAK4 and TRAF6 (tumor necrosis factor receptor–associated factor) are also recruited (Kaisho and Akira, 2006). This is followed by the disassociation of IRAK1 and TRAF6 from the receptor complex and their association with TAK-1 (transforming growth factor-β-activated kinase). TAK1 is a member of the Mitogen Activated Protein Kinase (MAPK) Kinase Kinase (MAPKKK) family (Sato et al., 2005) and is activated by LPS. It forms a complex with TAB1, TAB2 and TAB3. The activated TAK1 complex phosphorylates IκB kinase (IKK) whose kinase activity is regulated by NEMO (NF-κB essential modulator). It has been demonstrated that expression of TAK1 and TAB1 enhance activation of the transcription factor NF-κB (nuclear factor-kappa B) (Ninomiya-Tsuji et al., 1999). TAK1 is essential for TLR, IL-1RI, TNFR, and BCR signaling. See figure 1.3A for a detailed diagram of these molecules in the TLR pathways.

The NF-κB signaling pathway is highly conserved and is a key regulator of the inflammatory response (Sen and Baltimore, 1986). The activation of the pathway

occurs primarily via activation of IKK. When activated, the IκB kinase phosphorylates two serine residues located in an IκB regulatory domain. When phosphorylated on these serines, the IκB inhibitor molecules are modified by ubiquitination, which then leads them to be degraded by the proteasome (DiDonato et al., 1997). The NF-κB complex consisting of the p50 and p65 subunits is then freed to enter the nucleus where it can turn on the expression of specific genes that have DNA-binding sites or response elements for NF-κB nearby. The activation of these genes by NF-κB then leads to an inflammatory response, a cell survival response, or cellular proliferation. The activation of this pathway is not only implicated in mediating a protective inflammatory response against an invading pathogen, but it is also part of the pathogenic and virulence strategies of bacteria (Kawai and Akira, 2005b).

Other crucial signaling pathways are also activated in response to TLR ligands. These include the PI3K pathway. IRF pathway and MAPK pathways like JNK, p38 and ERK. Each of these pathways is responsible for the expression and activation of many immune regulatory genes. The PI3K (tyrosine phosphor-inositide 3-kinase) pathway recognizes phosphor-tyrosine residues in the intracellular regions of TLRs via its Src homology 2 (SH2) domain and subsequently activates its downstream kinase Akt. The IRF pathway responds to and activates the production of interferons which are critical for anti-viral responses. TLR3 and TLR4 both activate IRF3 via the TRIF pathway. TRIF engages TBK1 which leads to the phosphorylation of IRF3. Phosphorylated IRF3 then forms a homodimer and enters the nucleus where it binds to consensus sequence known as the interferon sequence response element (ISRE), found in the upstream region of promoter regions of interferon response genes. Typically, IFNβ and RANTES are induced by IRF3 (Fitzgerald et al., 2003). TLR7, TLR8 and TLR9 engage IRAK-1 and TRAF-6 and also activate IRF5 and IRF7 leading to the induction of IFNα (Kawai and Akira, 2005b; Uematsu and Akira, 2005). There are many other members of the IRF family, such as IRF1, IRF4 and IRF8 which although not directly activated by TLRs, play diverse roles in immunity including induction of other genes required for an inflammatory response such as caspase-1 (IRF1), correct T and B cell development (IRF4) and appropriate T

helper cell responses (IRF8). The RIG-I helicases can also activate IRFs through the activation of the RIP-1 kinase (Kawai and Akira, 2006).

MAPKs have also been implicated in TLR signaling and the cell cycle and proliferation of cells. Three major groups of MAPK are activated in response to TLR ligands, namely the c-Jun N-terminal kinase (JNK), p38 MAPK and the extracellular signal regulated kinases (ERK) (Kawai and Akira, 2005b; Takeda and Akira, 2004). MAPKs require phosphorylation on the threonine and tyrosine residues to become activated. This is perfomed by the MAPK kinases (MAPKK) which in turn are activated by serine/threonine phosphorylation. LPS is thought to activate JNK via the MEK1/MEK4 pathway and activates the p38 pathway through the activation of MEK3 (Barger et al., 2001; Kaisho and Akira, 2006; Underhill and Ozinsky, 2002b). p38 MAPK stabilizes the expression of various cytokine mRNA transcripts which contain AU-rich elements in the 3'UTR leading to enhanced expression. JNK activates the transcription factor c-Jun and c-Fos which can form the activation protein (AP-1) transcription factor complex. The role of ERKs p42 and p44 seems to be activation of c-fos which along with the activated c-Jun forms active AP-1 complexes (DiDonato et al., 1997).

1.2.4. *TLRs and Disease*

TLRs are essential regulators of innate and adaptive immune responses and their complexity continues to intrigue researchers (Cook et al., 2004; Fearon and Locksley, 1996). Because of their importance, when they are mutated and not functioning as they should auto-immune, inflammatory and infectious diseases can develop. Septic shock or excessive inflammation is possibly the most severe malfunctioning of TLRs. It is thought to result from an inadequate negative regulation of TLR signaling leading to excessive pro-inflammatory cytokine production (Sabroe et al., 2003).

Polymorphisms have been discovered in the genes encoding TLRs that are associated with disease progression (Reindl et al., 2003) and they demonstrate the importance of TLRs in a successful immune response. The best studied polymorphism is that of TLR4, D299G (Agnese et al., 2002; Kiechl et al., 2002; Reindl et al., 2003). It was first identified in human patients with a decreased

airway response to inhaled LPS. These patients had an increased risk of systemic inflammatory syndrome. The same polymorphism has also been associated with an increased risk of septic shock and decreased risk of atherosclerosis. A homozygous polymorphism in the Mal adaptor which is encoded by the TIRAP gene (S180L) has been linked with an increased susceptibility to invasive pneumococcal disease (IPD) (Khor et al., 2007). A TLR2 polymorphism, identified as R753Q is associated with a predisposition to staphylococcal infections or tuberculosis in humans (Lorenz et al., 2000). IRAK4 polymorphisms have also been identified. Children with homozygous polymorphisms have recurrent infections caused predominantly by gram-negative bacteria (Picard et al., 2003; Picard et al., 2007). These infections seem to become less over time because the immune system has a mechanism of compensating for the clearance of gram-negative pathogens.

Recent work has been done showing the manipulation of TLRs by pathogens, particularly virsuses (Bowie et al., 2000; Harte et al., 2003; Lysakova-Devine et al., 2010; Stack et al., 2005). Mechanisms have been identified where pathogens are able to avoid detection by TLRs. Strains of bacteria, such as uropathogenic *E. coli* secrete proteins that are taken up by cells such as macrophages and disable adaptor molecules like MyD88 leading to a non-functioning TLR signaling pathway and the successful survival of the pathogen. The Vaccinia virus produces a protein A52R that sequesters IRAK2 and TRAF6 from the pathway (Bowie et al., 2000). Some of the methods that bacteria and viruses use to manipulate TLR signaling are being used as therapies. Lipid A from *Rhodobacter sphaeriodes* and synthetic lipodisaccharide prevent activation of human TLR4 by LPS. This mechanism could possibly be used as a treatment for septic shock (Ulevitch, 2004). If more information can be uncovered regarding the methods bacteria use to manipulate TLRs in the host than more successful treatments can be used to eliminate infection.

Another area of research that has recently come into the spotlight and demonstrates the cleverness of TLRs is how they are needed to maintain homeostasis in the intestine (Rakoff-Nahoum et al., 2004). Microbial ligands are not only produced by pathogenic bacteria they are also produced by the

commensal microflora of the gut. TLRs on the surface on gastrointestinal cells are constantly being exposed to these ligands. It has been shown that commensal bacteria are recognized by TLRs under normal conditions and this recognition is essential for maintenance of homeostasis and a state of constant "controlled inflammation". When there is an imbalance of gut microflora, inflammatory bowel diseases like colitis and Crohn's Disease can develop.

As more and more genes in the TLR pathways are described it will become easier to manipulate the pathways to promote a defense against invading pathogens. In recent years molecules called miRNAs have been described that have a role in immune defense gene regulation (Sheedy and O'Neill, 2008). Some miRNAs have been described as negative regulators of TLR signaling acting as a break on the pathway while others act as positive regulators and act as an accelerator. These molecules bind complementary to messenger RNA (mRNA) of a target gene and prevent translation of the protein. Details of TLR signaling pathways like the discovery of the involvement of novel molecules like miRNA will lead to the ability to target specific immune processes thus preventing uncontrolled infection and inflammation.

1.3. **A Role for MicroRNAs in the Innate Immune Response**

1.3.1. *The History of Small, Non-coding RNAs*

Small, non-coding RNAs such as small interfering RNAs (siRNA) and miRNA are known to play important roles in regulating gene expression in many eukaryotic cell lineages. They are termed non-coding because they are transcribed from the genome into RNA but they are not translated into a functioning protein. These molecules were first identified in the nematode *Caenorhabditis elegans* in 1993 with the discovery of the lin-4 gene (Lee et al., 1993; Wightman et al., 1993). They were originally found to have a role in cellular development, differentiation, proliferation and apoptosis and are now known to function in cancer and immunity. siRNA and miRNAs regulate gene expression by targeting the 3`Untranslated (UTR) region of a target mRNA through either a targeted cleavage of the mRNA or translational inhibition. These small molecules share many similar characteristics, such as the method in which they are processed but

they differ in the way they are produced. siRNA is produced from double stranded RNA (dsRNA) that is processed to become siRNA. The source of the dsRNA can be endogenous or exogenous. miRNAs on the other hand originate as stem-loop precursor molecules and are endogenously produced. RNAi (RNA interference) is thought to have evolved as a defense mechanism against invading viral RNA to inhibit the replication of the virus within a cell.

1.3.2. *The Synthesis and Function of microRNAs*

miRNAs are transcribed from the genome of a cell within the nucleus (figure 1.4). They can be transcribed intronically from within a host gene or they can be found in exons and have their own promoter sequence. These small molecules originate from a longer double stranded RNA which is synthesized by the RNA polymerase (RNase) II into a stem-loop structure (Chen and Meister, 2005; Reinhart et al., 2002). The resulting primary miRNA (pri-miRNA) is ultimately cleaved by nuclear RNase III nuclease Drosha into a 60-70 nucleotide fragment named precursor-miRNA (pre-miRNA). The pre-miRNA is exported to the cytoplasm by the exportin5 complex where it is cleaved by the RNase III nuclease called Dicer. The resulting product is a double stranded duplex containing the mature miRNA and miRNA*. The duplex is unwound by the ribonucleoprotein complex called RISC (RNA-induced silencing complex) and the approximately 22 nucleotide mature miRNA binds to its target mRNA resulting in inhibition of translation or degradation of the mRNA.

The miRNA* strand has always been thought of as the carrier strand and it is degraded upon separation from the mature strand. They are less abundant than the mature miRNA but a 2008 study demonstrated that the miRNA* strand can bind to Argonaute proteins in the RISC (Okamura et al., 2008). It was thought that the mature miRNA is preferentially selected over the miRNA* for entry into the RISC based upon thermodynamic properties. It is now understood that each precursor-miR can produce two functioning mature miRNA products (Czech et al., 2009). The miRNA* strand is typically less abundant than their partners, but are often found at physiologically relevant levels. Unlike siRNAs which bind with complete complementarity to the sequence in the 3` UTR of the target mRNA, miRNAs do not have to bind perfectly to target mRNAs. A 7-8 nucleotide

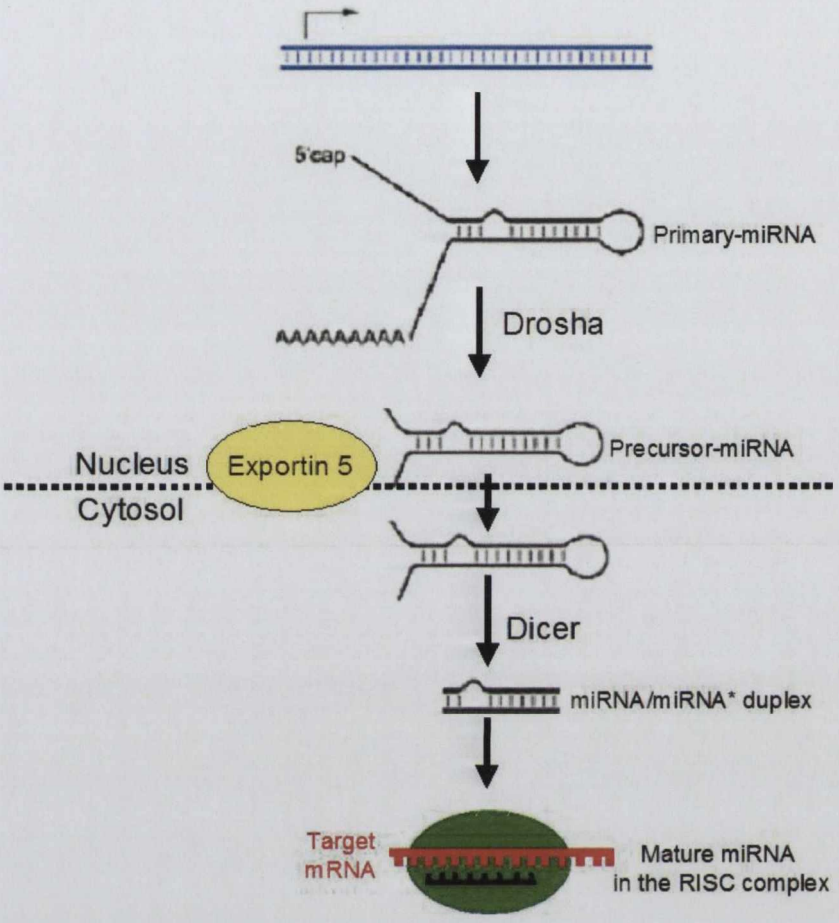


Figure 1.4. **The biogenesis of miRNA**. The primary miRNA transcript is encoded in the genome and following its transcription it is processed by a series of RNases to become the mature miRNA which functions to post-transcriptionally regulate mRNA.

sequence, called the seed sequence of the miRNA binds to the 3` UTR of the target mRNA. To date about 678 miRNAs have been identified in humans each potentially regulating hundreds of target mRNA (Belair et al., 2009; Lu and Liston, 2009). The importance of these molecules is demonstrated in that they are usually highly conserved across species and are found in all eukaryotic species.

The RISC is a multi-component complex which consists of members of the Argonaute (Ago) family of proteins, four of which occur in mammals, the most well studied being Ago-2 (Asirvatham et al., 2007; Chen and Meister, 2005). Ago are RNA-binding proteins that are highly conserved across species. Mature miRNA forms the RISC with these and other RNA-binding proteins including Fragile –X related protein (FXRP) and the nuclease Tudor-SN (Czech et al., 2009). In siRNA mediated gene silencing the siRNA sequence and the coding sequence of the mRNA are usually complementary leading to their entrance into the RISC. The cleaving enzyme in siRNA mediated silencing has been identified as Ago-2 (O'Carroll et al., 2007). miRNA mediated silencing differs in that target sites are found within the 3'UTR of target mRNA and the sequences are not always fully complementary to the mRNA. Partial complementarity usually occurs between nucleotides 2-7 from the 5' end of the miRNA. This is now known as the seed sequence of a miRNA. It is thought that when there is complete complementarity of the miRNA with the target mRNA, degradation of the target mRNA occurs. Whereas when incomplete complementarity occurs, repression of translation of the mRNA into protein occurs (Lewis et al., 2005).

The exact mechanism of translational inhibition is not fully understood but several models have been described. One idea is that miRNA activity interferes with the initiation of translation. The process of translation is subject to multiple levels of regulation. A group of proteins called the eukaryotic initiation factor (eIF) proteins are important for 5' cap-dependent translation. They facilitate binding to and initiate ribosome formation as well as ensure the tRNA enters into the correct reading frame of the mRNA. eIF4E has been shown to be inhibited by Ago2 activity in miRNA mediated silencing which also impacts the poly(A) tail function of the mRNA. Ago2 competes with eIF4E for binding to the 5' cap structure and thereby preventing translation (Czech et al., 2009; O'Carroll et al.,

2007). eIF46 has also been shown to be inhibited by Ago2 and inhibits the correct formation of the ribosome subunits 60s and 40s. It has been suggested that there is a circularization of the mRNA whereby the RISC located at the 3'UTR can inhibit processes at the 5'UTR (Asirvatham et al., 2007; Chen and Meister, 2005). Other reports suggest that there is an initial round of translation which is required before miRNA-mediated silencing can occur. The miRNA-mRNA duplex may block the dissociation of the ribosome from the mRNA. Protein synthesis may not be blocked at all but the nascent polypeptide if rapidly degraded (O'Carroll et al., 2007). miRNA mediated silencing can also occur via degradation or decay of the mRNA (Khabar, 2007). This is thought to occur through deadenylation of the target mRNA which is facilitated by a deadenylase complex and decapping enzymes which remove the poly(A) tail from the mRNA leading to decreased stability of the mRNA.

1.3.3. *Bacteria and Small Non-coding RNAs*

A part of this study focuses on a miRNA molecule with a possible role in bacterial pathogenesis, so the question has arisen if bacteria themselves produce miRNAs. Small non-coding RNAs have emerged as key regulators of gene expression (Vogel and Sharma, 2005). In the past few years, hundreds of small RNA molecules have been found in the bacterium *Escherichia coli* and homologues have been found in other prokaryotes. It was discovered in the 1980's that bacterial phages, transposons and plasmids use small anti-sense RNAs to regulate their expression in a bacterial cell. Recent evidence supports the idea that small RNAs are the "missing links" in bacterial genomes and regulons, and that they play key roles in the physiology of the cell. Bacterial small non-coding RNAs cannot be classified as miRNAs or siRNA because bacteria do not have the genes encoding the Dicer or RISC machinery used for RNA processing. Small RNAs in bacteria are not processed in the same manner as eukaryotic small RNAs. Whereas the eukaryotic miRNA will recognize its target gene sequence in the 3`UTR, prokaryotic small RNAs recognize a sequence in the 5`UTR leading to the stimulation of translation or the stabilization of mRNA (Gottesman, 2005).

1.3.4. *The Role of microRNAs in Cancer and Virus Invasion*

Recent studies have shown that miRNAs can function as tumor suppressors and oncogenes. miRNAs with a role in cancer have been termed "oncomiRs" (Cho, 2007). miRNAs are known to be cell-type specific and different types of tissue have different repertoires of miRNAs. They have a crucial role in cancer initiation and progression. miR-15 and miR-16 were the first oncomiRs to be discovered. They were found on the same region of a chromosome that is deleted in more than half of B-cell chronic lymphocytic leukemia (CLL). It was shown that in 68% of CLL cases, miR-15 and miR-16 were deleted or downregulated (Calin et al., 2002; Calin et al., 2007). These oncomiRs have also been shown to be negative regulators of Bcl2 overexpression in CLL cases by interacting with Bcl2. miRNAs miR-10b, miR-125b, and miR-145 are downregulated and miR-21 and miR-155 are upregulated in breast cancer cells (Iorio et al., 2005). miR-21 is greatly overexpressed in breast tumors compared to normal breast tissue (Si et al., 2007). It acts as an oncogene and controls tumorigenesis through the regulation of genes such as tropomyosin 1 which is a tumor suppressor (Zhu et al., 2007). miR-21 was identified to also have a role in head and neck cancer, leukemia and cervical cancer. The miR-17-92 polycistronic cluster of miRNAs is overexpressed in B cell lymphomas, chronic myeloid leukemia and breast, colon, lung and pancreatic tumors (Chow et al., 2010; Hayashita et al., 2005; Mu et al., 2009; Wong et al., 2010). Because of the negative regulation of oncomiRs, it may be possible to use them as therapy for the treatment of a variety of cancers.

miRNAs have been found in viruses and are thought to have viral origins. Homology has been found between viral miRNAs and human miRNAs. And it is because of this homology that they are classified as miRNAs. Viruses are able to use the miRNAs encoded in their genomes to assist in their invasion of a host. Simian virus 40 encodes miRNAs that target the T antigen (Stern-Ginossar et al., 2007). Downregulation of the T antigen leads to a decreased cytotoxic T lymphocyte response. Several other viruses such as Herpes simplex virus 1, encode miRNAs that also interfere with anti-viral host defense. Significant homology was found between miR-K12-11 miRNA encoded by Kaposi's-sarcoma-associated herpes virus (KSHV) and cellular miR-155, including the entire miRNA seed region. It is thought that this viral miRNA evolved to exploit a

pre-existing gene regulatory pathway in B cells, leading to B-cell tumor formation. This study showed that the homology between these two miRNAs would lead to similar mRNA targets (Gottwein et al., 2007). It is thought that cellular miRNAs with homology to viral miRNAs can possibly control viral infections and contribute to the host immune response.

1.3.4. *The Role of microRNAs in Haematopoiesis*

miRNAs are essential for organ development, cellular differentiation and homoeostasis. Their role in the immune system is expanding with recent studies demonstrating their role in haematopoiesis or the development of cells in the blood and in particular immune cells like lymphocytes. Using miRNA cloning or microarray analysis, researchers have identified groups of miRNAs that are expressed in different haematopoietic tissues. All blood cells begin as haematopoietic stem cells (HSC) in the bone marrow. Some HSC remain stem cells while others become myeloid and lymphoid progenitor cells. The interaction between miRNAs and transcription factors permits the proper generation of different cell types. Global miRNA expression profiles of progenitor and stem cells have been generated that identified certain miRNAs in these populations of cells. miR-196b is expressed in mouse short-term HSC and has a role in modulating HSC homeostasis and commitment to a cellular lineage (Popovic et al., 2009; Wang et al., 2010b). miR-126 expression increased colony formation of progenitor cells and is thought to regulate HOXA9, a homeobox gene needed to maintain HSC homeostasis (Shen et al., 2008). Overexpression of miR-21 and miR-196 blocked granulopoiesis whereas sustained expression of miR-155 increased the numbers of immature granulocytes (Merkerova et al., 2008; Velu et al., 2009). Certain miRNAs decrease during the development of certain types of cells. Members of the miR-17-92 and miR-106a-92 families decrease in expression during the differentiation of human haematopoietic progenitor cells into monocytes. The subsequent increase in the expression of their target genes like RUNX1 promoted the differentiation into monocytes (Fontana et al., 2007).

The role miRNA may play in B-cell differentiation was initially shown in mice with a haematopoietic defect in Ago2 which is part of the RISC machinery and crucial to the biogenesis of miRNA. This defect impaired the generation of mature

B-cells from early pro-B-cells (O'Carroll et al., 2007). miR-150 affects B-cell differentiation through the targeting of c-Myb, and overexpression of miR-150 results in a block from pro-B to pre-B cell transition (Xiao et al., 2007). T cell differentiation is also affected by miRNA expression. Dicer knockout mice displayed aberrant T-helper cell differentiation. T-cells could not be differentiated into CD8+ T cells and CD4+ T cells were generated but in very low numbers. When miR-150 was overexpressed in Dicer deficient cells, T cell differentiation was restored (Cobb et al., 2005; Muljo et al., 2005; Zhou et al., 2007). miR-181 expression is linked to a reduction in overall T-cell numbers (Chen et al., 2004). miR-155 deficiency promoted the differentiation of cells into T-helper 2 cells (Thai et al., 2007). Each of the miRNAs described is essential for proper balance between the different subsets of cells.

1.3.5. *ImmunomiRs*

A great deal of research has been conducted on the role of miRNAs in oncogenesis and viral invasion, but only recently has interest grown in miRNAs as regulators of the immune system. An LPS induced immune response results in an increase in the expression of several miRNAs including miR-146a, miR-155 and miR-21 (figure 1.5) (Moschos et al., 2007; O'Connell et al., 2007; Taganov et al., 2006). Two genes known to be involved in TLR4 signaling, those encoding TRAF6 and IRAK1 are targets of miR-146a. LPS induced activation of miR-146a is NF-κB-dependent and the increased expression of miR-146a leads to the subsequent degradation of TRAF6 and IRAK1 and a decreased pro-inflammatory immune response (Taganov et al., 2006). miR-146a acts as a negative regulator of TLR signaling and cytokine production. miR-155 expression was upregulated by LPS and Poly(I:C) through MyD88 and Trif signaling. Its expression also increased in response to IFN-β in a TNF-α dependent fashion (O'Connell et al., 2007). Mice deficient in miR-155 displayed decreased numbers of germinal center B cells and a diminished T- cell dependent antibody response. miR-155 knockout dendritic cells are unable to induce T-cell activation in response to antigens. Suppressor of Cytokine Signaling 1 (SOCS1) and SH2-containing inositol 5-phosphatase 1 (SHIP-1) are validated targets of miR-155. SOCS1 negatively regulates DC antigen presentation (Lu and Liston, 2009). SHIP-1 inhibits the activation of the kinase Akt by dephosphorylating the phosphoinositide 3 kinase

(PI3K). The overexpression of miR-155 *in vitro* and *in vivo* resulted in increased activation of Akt in response to LPS via the degradation of SHIP-1 (O'Connell et al., 2009). miR-21 has been linked to cell motility, invasion and adhesion, with target genes that include tropomyosin, PDCD4 and PTEN (Frankel et al., 2008). A study from 2010 confirmed that PDCD4 is a direct target of miR-21 and identified a novel role for PDCD4 in the anti-inflammatory immune response (Sheedy et al., 2010). PDCD4 acts as a pro-inflammatory gene, suppressing IL-10. When miR-21 expression increases in response to LPS, IL-10 production is enhanced through the degradation of PDCD4. Mice deficient in PDCD4 were protected from a lethal dose of LPS due to enhanced IL-10 production.

Other miRNAs have been implicated in TLR signaling including miR-9 which was upregulated in response to LPS in polymorphonuclear neutrophils and monocytes in a MyD88 and NF-κB dependent manner. miR-9 is also induced by TLR2 and TLR7/8 agonists and by the cytokines TNF-α and IL-1β. Overexpression of miR-9 led to decreased NF-κB activity suggesting a feedback loop (Bazzoni et al., 2009). miR-147 is also induced with multiple TLR stimuli in murine macrophages dependent on both MyD88 and Trif signaling (Liu et al., 2009). Let-7i is another miRNA involved in TLR4 signaling through an NF-κB/MyD88 dependent pathway (Chen et al., 2007). Infection of cholangiocytes with Cryptosporidium parvum led to a decrease in Let-7i expression. This decrease in expression is associated with TLR4 upregulation and through overexpression of Let-7i, it was determined that this miRNA is regulating TLR4 expression. miR-125b is also downregulated in response to TLR4 stimulation. TNF-α is a target gene of this miRNA so the downregulation of miR-125b is thought to be required for a proper pro-inflammatory response (Lu and Liston, 2009).

miRNAs also provide a level of control over the adaptive immune system. Proliferating T cells express genes with shorter 3'UTR compared to resting T cells. This results in less miRNA binding sites in the mRNA so the mRNA is less susceptible to miRNA regulation (Sandberg et al., 2008). Dicer knockout mice displayed a reduced number of mature T cells (Cobb et al., 2005; Muljo et al., 2005). miR-146a has recently been shown to be induced in human primary T

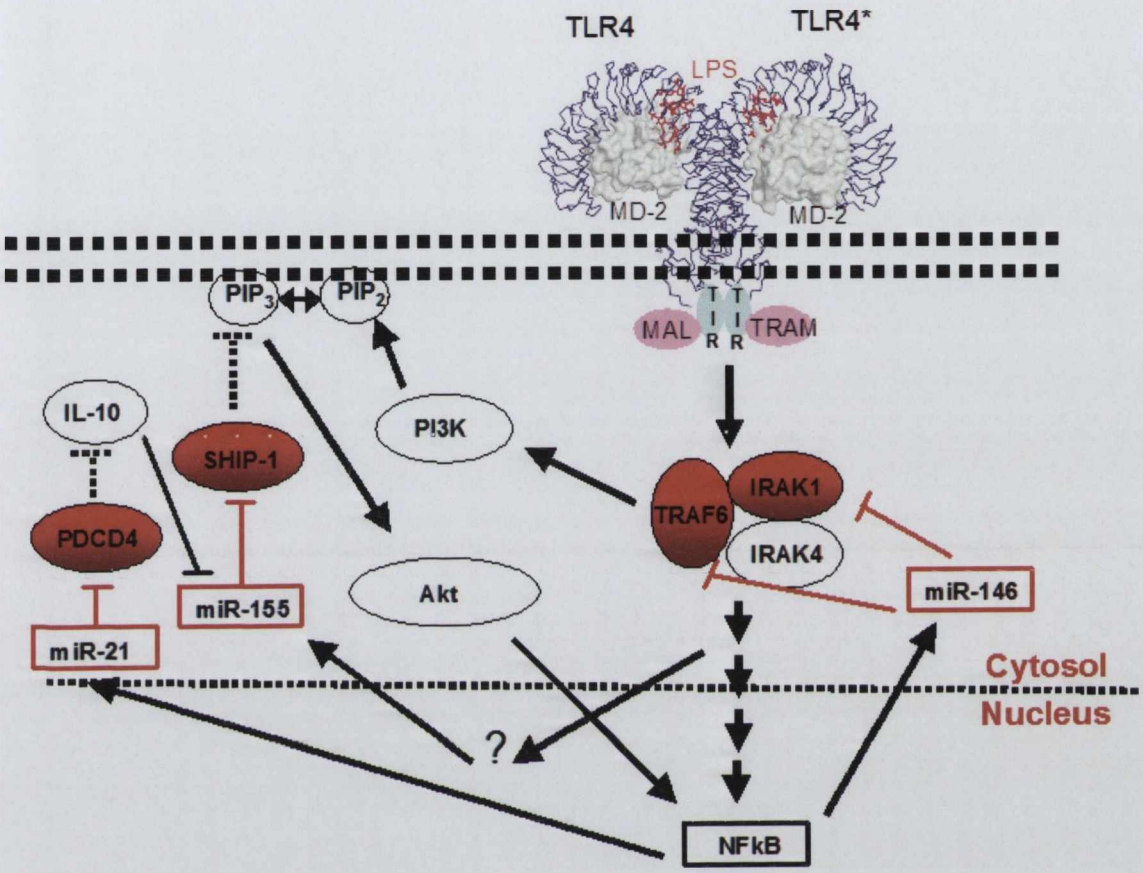


Figure 1.5. **ImmunomiRs miR-21, miR-155 and miR-146a and their target genes with roles in TLR signaling**. miR-21 targets PDCD4 to increase IL-10 production and subsequently decrease miR-155 expression. miR-155 induction leads to a suppression of SHIP-1 and a release on the break on the Akt pathway. miR-146a targets both TRAF6 and IRAK1 which would lead to a decrease in NF-κB activation.

lymphocytes upon T-cell receptor stimulation. Overexpression of miR-146a led to a decrease in AP-1 activity and IL-2 production (Curtale et al., 2010). miR-181 has been shown to positively regulate the T-cell receptor. The overexpression of miR-181 amplified T-cell receptor activation. There is speculation that miR-181 is regulating protein phosphorylation (Li et al., 2007). miR-155 seems to be the most pivotal miRNA in regulating the adaptive immune response. miR-155 knockout mice were immunodeficient and failed to develop protective immunity against *Salmonella typhimurium* following immunization (Rodriguez et al., 2007). miR-155 was shown to specifically regulate the germinal center reaction to produce a T cell-dependent antibody response in the knockout mice (Thai et al., 2007). miR-155 targets the transcription factor PU.1 which downregulates IgG1 antibody levels (Vigorito et al., 2007). T lymphocytes from the miR-155 knockouts also displayed reduced IL-2 and IFNγ production in response to antigens.

With all of the information gathered from previous studies regarding the role of miRNAs in the immune response, it seemed they are playing a crucial role in fine tuning such elaborate signal transduction cascades. In a screen conducted by Dr. F. Sheedy, observing the expression of 158 miRNAs in response to three TLR ligands, LPS, Pam_3CSK_4, and PolyI:C, several miRNA were implicated in the cellular response to all three. Some of the miRNAs were upregulated in response to all three. This group includes miR-146a, miR-155, miR-21, miR-214 and let-7e. Another group of miRNAs were downregulated in response to all three ligands, miR-149 and miR-107 are included in this group. This study focused on the downregulation in response to TLR ligands of miR-107, the mechanism, as well as the functional consequences of the downregulation.

1.4. **Aims and Objectives**

The regulation of immune genes by miRNAs is thought to bring about a balance of the components of the immune response. This study set out to examine the role and function of miR-107 in the mammalian innate immune response. The aims of this study are as follows:

1 To validate the miRNA screen of 150 miRNA in response to TLR stimuli
   - To confirm that miR-107 is downregulated in response to TLR stimulation, using miR-146a as a positive control
   - To quantitatively evaluate the downregulation of miR-107 in several cell types including primary cells and under various conditions

2 To determine the mechanism of miR-107 downregulation in response to LPS
   - To evaluate whether the effect is Trif or MyD88-dependent
   - To establish NF-κB-dependency
   - To determine if PanK1α is co-regulated with miR-107 because miR-107 is located within an intron in the PanK1α gene
   - To assess the role of PPARα in miR-107 regulation because PanK1α expression is regulated by PPARα

3 To determine the functional consequences of decreased miR-107 levels in response to LPS through the identification of target genes, specifically cyclin-dependent kinase 6 (CDK6)
   - To examine the significance of decreased miR-107 and increased CDK6 in the context of innate immunity and TLR signaling

Overall this study aimed to characterize a miRNA, miR-107, whose expression is downregulated by TLR4 and to determine the significance of this downregulation for TLR4 signaling. I have uncovered an important aspect of TLR4, whereby miR-107 downregulation is required for TNF-α secretion, phagocytosis and proliferation.

CHAPTER 2

MATERIALS & METHODS

2.1. **Reagents**

2.1.1. *Stimulants*

UltraPure LPS from *Escherichia coli* strain EH100 (Ra) was purchased from Alexis (Poole, Dorset, UK). WY14643 was purchased from Sigma (Poole, Dorset, UK).

2.1.2. *Antibodies*

The β-actin antibody was purchased from Sigma (Poole, Dorset, UK), The mouse monoclonal CDK6 antibody was purchased from Cell Signaling Technologies (Danvers, MA, USA). The rabbit polyclonal PanK1α antibody was a kind gift from Dr. Suzanne Jackowski (St. Jude Children's Research Hospital, Memphis, TN, USA). The PPARα antibody was purchased from BioVision (Mountain View, CA, USA).

2.1.3. *Cell Culture Reagents*

RPMI, DMEM and Opti-MEM were purchased from Gibco (Biosciences, Dun Laoghaire, Ireland). Fetal calf serum was obtained from Biosera (East Sussex, UK). Penicillin, streptomycin, gentamycin, blasticidin, trypsin, L-Glutamine and DMSO were obtained from Sigma (Poole, Dorset, UK). Cell culture flasks and plates were purchased from Starsted (Numbrecht, Germany).

2.1.4. *Bacterial Strains*

E. coli K12 was obtained from the Trinity College Dublin department of microbiology. *Yersinia enterocolotica* was obtained from Dr. Sinead Corr (TCD).

2.1.5. *Cell Lines*

The DC2.4 cell line was a gift from Dr. Kenneth Rock, University of Massachusetts, USA. J774 macrophages, THP1 human monocytic cell line, Caco2 gut epithelial cell line and HEK293 kidney epithelial cells were obtained from the European collection of Animal cell cultures (Salisbury, UK). The retrovirally immortalized bone marrow derived macrophages (I-BMDM), wild-type, MyD88-deficient and TRIF-deficient were a gift from Prof. Doug Gollenbock, University of Massachusetts, Worcester, MA, USA. P65-deficient and matched wild-type

control mouse embryonic fibroblasts (MEF) were a gift from Prof. Ron Hay, University of St. Andrews, Fife, UK. The HEK293 cell line stably transfected with TLR4, the A172 and the L929 cell lines were a gift from Dr. Kate Fitzgerald, University of Massachusetts, Worcester, MA, USA.

2.1.6. *PCR Reagents*

All reverse transcription kits, PCR mastermixes, gene expression assays and miRNA assays for real time PCR were purchased from Applied Biosystems (Huntington, UK). SYBR Green PCR master mix was purchased from Invitrogen, Biosciences (Dun Laoghaire, Ireland). Primers for SYBR green PCR were purchased from Eurofins MWG Operon (Ebersberg, Germany).

2.1.7. *Fluorescent Probes and Bacteria*

Fluorescently labeled Phalloidin stains Alexa Fluor 594 and 488 as well as FITC labeled heat-killed *E. coli* were obtained from Invitrogen, Biosciences (Dun Laoghaire, Ireland).

2.1.8. *RNA Oligonucleotides*

Antisense-miR inhibitors and precursor-miR molecules for miR-107 were obtained from Ambion (Huntington, UK) as well as non-targeting negative control molecules for each.

2.1.9. *DNA plasmids*

The CDK6-3`UTR-linked luciferase plasmid was purchased from Labomics (Nivelles, Belgium).

2.1.10. *Miscellaneous Reagents*

General lab chemicals were purchased from Sigma (Poole, Dorset, UK). RNase free water was obtained from the Milli-Q Advantage A10 water system (Millipore, Watford, UK) or purchased from Qiagen (Crawley, UK). ELISA duoset Kits were purchased from R&D Biosystems (Abingdon, UK). Pre-stained broad range protein molecular weight marker and 100 bp DNA ladder were purchased from New England Biolabs (Ipswitch, MA, USA). Enhanced chemoluminescent substrate reagent used was 20X LumiGlo and 20X peroxidase

from Cell Signaling Technologies (Danvers, MA, USA). Lipofectamine2000 was obtained from Invitrogen (Dun Laoghaire, Ireland). Coelentrazine was from Argus Fine Chemicals Vernio, France). 5X Passive lysis buffer was from Promega (Madison, WI, USA). Endotoxin-free plasmid purification maxi-kits and |RNA extraction mini-kit was purchased from Qiagen Crawley, UK).

2.1.11. *Animals*

Wild-type C57/BL6 mice were obtained from the Bioresources unit at Trinity College, Dublin. CDK6-deficient bone marrow was provided by Dr. David Santamaria (Centro Nacional de Investigaciones Oncológicas, Madrid Spain).

2.2. **Cell Culture**

2.2.1. *Maintenance of DC2.4 and THP1 Cell Lines*

DC2.4 and THP1 cells were grown in RPMI media supplemented with 10% fetal calf serum (FCS) and 5% penicillin (100U/mL)/streptomycin (100µg/mL) (P/S) in a 37°C incubator with 5% CO_2. When DC2.4 cells reached confluency they were trypsinized with 1X trypsin-EDTA for five minutes at 37°C and centrifuged at 1200 rpm for 5 minutes to pellet the cells. THP1 are suspension cells so they were simply centrifuged to pellet the cells. Supernatant was discarded and the pellet was resuspended in fresh media and counted. Cells were set-up at 2-3x10^5 cells/mL for experiments.

2.2.2. *Maintenance of I-BMDM, Raw264.7, J774, A172, HEK293TLR4, Caco2 and MEF Cell Lines*

I-BMDM, Raw264.7, J774, A172, HEK293TLR4, Caco2 and MEF cell lines were grown in DMEM media supplemented with 10% FCS and 5% P/S in a 37°C incubator with 5% CO_2. In addition HEK293TLR4 cells were supplemented with blasticidin at 10µg/mL and HygroGold at 50µg/mL. When all cells with the exception of Raw264.7 cells, reached confluency they were trypsinized with 1X trypsin-EDTA for five minutes at 37°C and centrifuged at 1200 rpm for 5 minutes to pellet the cells. The supernatant was discarded and the pellet was resuspended in fresh media and the cells were counted. Raw264.7 cells were scraped from the

bottom of the tissue culture flask and centrifuged for 5 minutes at 1000 rpm. Supernatant was discarded and the cells were resuspended in fresh media.

2.2.3. *Maintenance of L929 Cell Lines*

L929 cell line was grown in RPMI media supplemented with 10% FCS and 5% P/S in a 37°C incubator with 5% CO_2. Cells were left in flasks for seven days after which they had reached over-confluency. Cells were lifted by scraping gently. The cell/media mixture was transferred to 50 mL falcon tubes and centrifuged at 1200 rpm for 5 minutes. The supernatant, containing the M-CSF, was transferred to another falcon tube. The M-CSF containing media was filter sterilized, aliquoted and stored frozen at -20°C.

2.2.4. *Generating Primary Bone-marrow Derived Dendritic Cells*

The legs of three wild-type C57 Black6 (C57Bl6) mice were removed and all hair, skin and tissues were removed. The ends of the bones were clipped to expose the bone marrow. A 25 gauge needle was used to flush out the bone marrow with RPMI into a 50mL falcon tube. The marrow was resuspended by pipetting up and down. Marrow was spun down at 1500 rpm for 5 minutes. The media was removed and five mLs of red blood cell lysis buffer was added and let to sit at room temperature for two to three minutes. 25 mLs of 1X PBS was added to tube and cells were spun down 1500 rpm for 5 minutes. Cells were resuspended in 10mL of RPMI and cells were counted using a haemocytometer. GM-CSF (J558) was added to media for a final concentration of 40ng/mL. Media was changed four days after harvest and cells were then stimulated four days later. The cells were counted and set-up at a concentration of $2x10^6$ cells/mL in RPMI supplemented with 10% FCS and 5% P/S in a 37°C incubator with 5% CO_2.

2.2.5. *Generating Primary Bone-marrow Derived Macrophages*

Bone marrow was extracted as for the generation of BMDM with the exception that cells were grown in DMEM supplemented with 10-20% M-CSF (L929) media. Following isolation, cells were incubated for 24 hours and the non-adherent cells were removed and placed in the fresh plate with fresh media. Every 3 days fresh M-CSF containing media was added to the plates. BMDM were counted and set-up for experiments 8-10 days post-isolation. The cells were

counted and set-up at a concentration of $2x10^6$ cells/mL in DMEM supplemented with 10% FCS and 5% P/S in a 37°C incubator with 5% CO_2.

2.2.6. *Isolation and Generation of Peripheral Blood Mononuclear Cells*

20 mL of blood was taken form an anonymous healthy donor (Irish Blood Transfusion Board – IBTB). Blood was transferred to a 50 mL falcon tube and diluted 1:2 with 1X PBS. 20 mL of Ficoll paque plus Sigma) was used to separate the blood into red blood cells, PBMC and serum. The tubes were centrifuged at 2000 rpm for 30 minutes. The white blood cells ring was transferred into a new 50 mL tube using a Pasteur pipette. The volume was adjusted to 50 mL with PBS and was centrifuged again at 200 rpm for 10 minutes. The supernatant was removed and this step was repeated again and the pellet was resuspended in 10 mL PBS. The cells were counted and set-up at a concentration of $2x10^6$ cells/mL in RPMI supplemented with 10% FCS and 5% P/S in a 37°C incubator with 5% CO_2.

2.2.7. *Cryogenic Preservation of Cell Lines*

Cells were grown to a state of sub-confluency and were harvested and counted, as previously described. The cells were centrifuged and the pellet was resuspended at a concentration of $2x10^6$ cells/mL. Cells were resuspended in 40% of the media used to grow the cell line, 50% FCS and 10% DMSO. 1mL was placed in a 1.5 mL cryotube. These aliquots were placed into "Mr. Frosty" which allows for a slow freezing of the cells in the -80°C freezer. After 1 day the cells were placed for long term storage in liquid nitrogen.

2.3. **Stimulating Cells with TLR ligands**

$3x10^5$ cells/mL were plated in tissue culture treated plates and treated with 0.1 µg/ml of LPS over a 24 hour time course.

2.4. **RNA Preparation**

2.4.1. *Isolating RNA Using Qiagen RNeasy Kit to Extract Total (including small) RNA*

All steps were carried out in RNase-free conditions and on ice. Following stimulation with LPS cells were lysed in an appropriate volume of Buffer RLT containing 10% β-mercaptoethanol, ($<1x10^7$ cells = 350µL, $>1x10^7$ cells = 500µL). 1.5 volume of 100% ethanol was added to the lysate and the mixture was applied to the RNeasy spin column, and passed through by centrifugation at 8000rpm for 15 seconds. The column was washed twice using Buffer RW1. Following the washing steps, the column was placed into an RNase-free 1.5 mL eppendorf tube and 30µL of RNase-free water (RF-dH_20) was applied to the column which was subsequently centrifuged at 8000rpm for 1 minute to elute the RNA.

2.4.2. *Assessment and Quantification of RNA*

Isolated RNA samples were run on a 2% agarose-TAE gel and observed for the presence of 18s, 23s and small RNA fractions. Samples were also quantified using optical density spectrophotometry. Both a spectrophotometer and a Nanodrop were used for the samples. A 1:50 dilution was made in nuclease free water for use in the Spectrophotometer. Optical densities for each sample were recorded at A_{260} and A_{280} and concentrations were calculated using an extinction coefficient of 40µg.

2.5. **TaqMan miRNA PCR Analysis**

2.5.1. *Generating cDNA using Reverse Transcription PCR*

Following quantification using spectrophotometry RNA samples were diluted to a working stock concentration of 2ng/µL or 100ng/µL. The Applied Biosystems TaqMan RT-PCR kit was used to generate cDNA following the manufacturer's protocol with either random primers or stem-loop microRNA specific primers which were purchased from Applied Biosystems. The 15µL reaction consisted of 1.5 µL 10X reverse transcription buffer, 0.15µL 100mM dNTP mix, 0.19 µL RNase inhibitor, 1.0 µL MultiScribe reverse transcriptase, 3.0 µL 5X miRNA-specific stem-loop RT primer, 4.16 µL RF-dH_20 and 5µL of the 2ng/µL stock of RNA (10ng total). Following assembly of the reactions in a 96-well plate, the plates were sealed and placed into a 96-well thermocycler (Applied Biosystems Veriti) and the following program was run: 16°C 30 minutes, 42°C 30 minutes,

85°C 5 minutes 4°C HOLD. The stem-loop TaqMan PCR for miRNA expression is illustrated in figure 2.1.

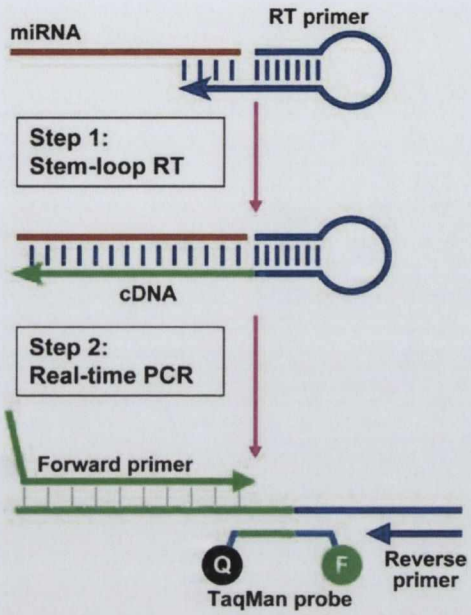
2.5.2. *miRNA Specific Real Time PCR Amplification*

Applied Biosystems TaqMan miRNA specific probes were used to quantify levels of specific miRNA in a sample of cDNA. The Applied Biosystems 7900 Fast System was used following the manufacturer's protocol. Reactions were set-up as follows: 5μL 2X TaqMan Universal Mastermix (No AMP erase UNG), 2.1μL RF-dH_20, and 0.5μL 10X miRNA specific primer/probe mix and 2.4μL miRNA-specific RT product. The 7900 Fast cycling program was as follows: 95°C 5 seconds, 60°C 30 seconds. Applied Biosystems SDS software was used to program the appropriate cycle. All probes used for miRNA-PCR were FAM labeled.

2.5.3. *Data Analysis*

Amplification plots for each PCR reaction were generated using the SDS software from which Cycle Threshold (C_t) values could be derived. Relative quantification was performed and the $\Delta\Delta C_t$ method was used to calculate fold changes of each miRNA relative to miRNA from unstimulated samples. Briefly summarized, the C_t values for each reaction – endogenous control and test probe for calibrator and test samples, were calculated using SDS software. For each detector/probe, the effect of loading and RNA normalization was corrected by subtraction of the C_t value for the endogenous control for each reaction giving the ΔC_t value. The ΔC_t value of the calibrator sample is subtracted from the ΔC_t value of each test sample. The resulting $\Delta\Delta C_t$ value is normalized using the $2^{(\Delta\Delta Ct)}$. Each cycle of amplification results in a doubling of the product thus the $2^{(\Delta\Delta Ct)}$. The resulting value is the fold-change in expression for a test sample relative to the calibrator sample for that particular detector/probe normalized using an endogenous control reference or the relative quantification (RQ). A representative amplification plot is shown in figure 2.1B.

A



B

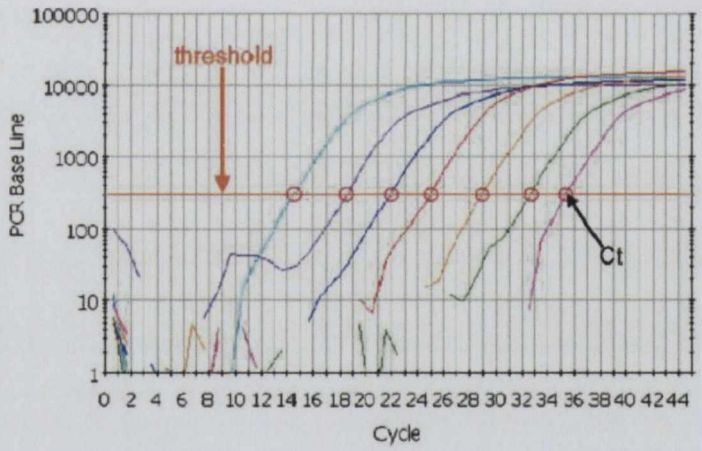


Figure 2.1. **Stem-loop TaqMan PCR for miRNA expression and Real-time PCR amplification plot.** RNA is amplified into complementary DNA (cDNA) with stem-loop primers specific for each miRNA. The cDNA is than quantified with real-time PCR and primer/FAM-labeled probes specific for the miRNA (A). The Ct value is the cycle where the fluorescence value has entered the exponential phase (B). Adapted from the Applied Biosystems website.

2.6. **TaqMan RT-PCR Analysis of Gene Expression**

2.6.1. *Reverse Transcription*

For generation of cDNA libraries from RNA samples the High Capacity cDNA Archive Kit II (Applied Biosystems) was used. 20µL reactions were prepared as follows, 2.0µL 10X reverse Transcription buffer, 0.8µL 100mM dNTP mix, 2.0µL Random Primer, 1.0µL Multiscribe Reverse Transcriptase and 5.2µL RF-dH_20. To this 8µL of the 100ng/µL stock RNA was added. Reverse transcription was performed in a 96-well PCR plate. When the plate was sealed it was centrifuged at 1000rpm for 30seconds. It was then placed in a thermocycler (Applied Biosystems Veriti) and the following cycling parameters were performed: 25°C 10 minutes, 37°C 2 hours, 4°C HOLD.

2.6.2. *Gene Specific Real-time PCR Amplification*

Gene-specific FAM labeled probes and primers were designed by Applied Biosystems (TaqMan Gene Expression Assays). The endogenous control probe, GAPDH was VIC labeled. PCR reactions were carried out in the AP7900 FAST machine in a 6-well FAST format. Briefly the reaction was prepared as follows: 5.0µL 2X TaqMan FAST Mix, 2.1µLRF-dH_20, 0.5µL 20X gene specific primer/probe mix 2.4µL cDNA. Cycling was performed as follows: 40 cycles of 95°C 5 seconds, 60°C 30 seconds. Amplification plots for each PCR reaction were generated using SDS software from which Cycle Threshold (C_t) values could be derived. Relative quantification was performed and the $\Delta\Delta C_t$ method was used to calculate fold changes in mRNA expression from unstimulated samples, as described in 2.5.3.

2.6.3. *Gene Specific Real-time PCR Amplification using SYBR Green*

Oligonucleotides were designed using Primer3 software and NCBI mRNA sequences. SYBR green Master mix (Invitrogen) was used to quantify amplification of cDNA into mRNA using the AB7900 FAST System following the manufacturer's protocol. Briefly the reaction was prepared as follows: 5.0µL SYBR green master mix, 0.2µL Rox reference dye, 0.8µL RF-dH_20, 1µL forward primer, 1µL reverse primer and 2.0µL cDNA. Cycling was performed as follows: 50°C 2 minutes, 40 cycles of 95°C 5 seconds, 60°C 30 seconds.

2.7. **Enzyme-Linked Immunosorbent Assay of Cytokine Expression**

Following treatment with TLR ligands, supernatants were collected at appropriate time points. IL-6, TNF-α, RANTES, IL-10 and IL-8 cytokine production was assayed in various cell types using R&D Bioscience Duoset Enzyme-Linked Immunosorbent Assay (ELISA) kit following the manufacturer's protocol. A standard curve is obtained by plotting the mean absorbance for each standard on the y-axis against the concentration on the x-axis. A curve is drawn through the points and the concentration of samples is extrapolated from the curve.

2.8. **Transfecting Cells with Anti-sense and Precursor miRNA Molecules**

Upon receipt of lyophilized RNA, oligonucleotides were resuspended in the appropriate volume of RF-dH_20 to obtain a 50μM stock of miRNA oligonucleotides and siRNA. For transient transfections with RNA oligonucleotides, cells were plated one day before transfection at a density of $3x10^5$ cells/mL in media containing no antibiotics and 1% FCS. Invitrogen Lipofectamine2000 and RNAiMAX were used to transfect RNA molecules into cells. Firstly, a mixture of 2% transfection reagent in OptiMem media (serum-free) was made-up and incubated at room-temperature for five minutes. The appropriate volume of RNA for each transfection was pipetted into an RNase-free eppendorf. The total volume of RNA was kept constant. To the diluted RNA, a volume of 2% transfection reagent/OptiMem was added. This mixture was then incubated at room temperature for 20 minutes before being added to the cells. 50μL total RNA/Transfection reagent/OptiMem was to a volume of 150μL in a well for a final volume of 200μL. RNA was diluted so the final concentration per well was 50nM. For most RNA experiments, cells were left for 24 hours to recover before stimulation with TLR ligands for the appropriate times. A FAM-anti-miR oligonucleotide was used as control of transfection and was assayed using Fluorescence Activated Cell Sorting (FACS) to determine transfection efficiency.

Company	Oligonucleotide Name	Sequence 5`- 3`
MWG	mGAPDH F	GAACGGGAAGCTTGTCATCAA
	mGAPDH R	CTAAGCAGTTGGTGGTGCAG
MWG	mEphA7 F	CCGGGAACAGTGTACGTCTT
	mEphA7 R	CGAACACCATGAACACCAAG
MWG	mMyosin9 F	GCCACCTGCACAGGTATTTT
	mMyosin9 R	TGCCGTAAGTCTCAATGCAG
MWG	mVinculin F	CTTCGATGAGGCTGAGGTTC
	mVinculin R	TGGTGAGTCAACTCCTGCTG
MWG	mTHY1 F	AAGGCCTCTGCCTGTAGTGA
	mTHY1 R	GAAGAGGCAGGTTGCAAGAC
MWG	mAnkyrin1 F	TACAGCCTTGCTGACCCTCT
	mAnkyrin1 R	GTCCTGCAGCGAGGAGTAAC
MWG	mRab11FIP2 F	CTGAAGCCAAAAGGCAAAAG
	mRab11FIP2 R	CCAGGGACCTGTGCATAACT
MWG	mRab11FIP4 F	CCCCAGGAGTTAGACATGGA
	mRab11FIP4 R	AATTGCTCCTCGTTGCTGAT
MWG	mVamp1 F	CTCCTCCCAACATGACCAGT
	mVamp1 R	CCTTTTTAGCTTGGCAGCAC
MWG	mVamp4 F	CACAGAAAGGGGCCATCTTA
	mVamp4 R	TGCATCTGAGGTCAGTCTGG
MWG	mVamp8 F	AAGTGCTGCTCAGTCCCTGT
	mVamp8 R	GAGGTCTTTATTGCCCACCA
MWG	mNf1-α F	CTCCCTGAGCATCTGGAGAC
	mNf1-α R	CTCCCTGAGCATCTGGAGAC
MWG	mBace1 F	AATCCTGCGTCACAGTTTCC
	mBace1 R	CCCCAACATGGGTAGAAATG
MWG	mHif1β F	TGCCTCATCTGGTACTGCTG
	mHif1β R	GAACATGCTGCTCACTGGAA
MWG	mHif1α F	TCAAGTCAGCAACGTGGAAG
	mHif1α F	TATCGAGGCTGTGTCGACTG
MWG	mDicer1 F	ATGCAAAAAGGACCGTGTTC
	mDicer1 R	CAAGGCGACATAGCAAGTCA
MWG	mCDK6 F	TGTTTCAGCTTCTCCGAGGT
	mCDK6 R	GACTGGAGCAGGACTTCTGG
MWG	pre-miR-107 F	GTGCTTTCAGCTTCTTTACAGTG
	pre-miR-107 R	TCTCTGTGCTTTGATAGCCCTGT
MWG	mPanK1α F	CTGCGGAGGAGGATGGACT
	mPanK1α R	CCACCGATATCCATACCAAACC
MWG	mPPARα F	GCAGCTCGTACAGGTCATCA
	mPPARα R	CTCTTCATCCCCAAGCGTAG

Applied Biosystems	Primary-miR-107	P.I.
Applied Biosystems	Antisense-miR-control	P.I.
Applied Biosystems	Antisense-miR-107	P.I.
Applied Biosystems	Precursor-miR-control	P.I.
Applied Biosystems	Precursor-miR-107	P.I.

P.I. = Proprietary Information

Table 2.1. **Primers used in this study.** Sequences for each gene were obtained from the NCBI database and entered into the Primer3 software.

2.8.1. *Fluorescence Microscopy*

DC2.4 cells were plated at $3x10^5$/mL per well on top of coverslips that were pre-treated with a 0.01% gelatin solution (1 mL added to coverslips and removed before addition of cells) in a 6-well tissue culture plate in antibiotic-free media containing 1% FCS. The cells were incubated at 37°C in a 5% CO2 incubator overnight to allow the cells to adhere to the coverslips. Cells were transfected with 50nM anti or precursor RNA molecules for 24 hours and then stimulated with 0.1µg/mL LPS for 18 hours. After this time the cells were fixed, permeabilized, and stained in unison. The staining solution contained 10 mL 4% paraformaldehyde (PFA) in PBS, 15 µl 20% Triton-X100 solution, and 30 µl Alexa Fluor 594 phalloidin stain (Molecular Probes), which fluorescently labels F-actin. The plate was covered with foil and left at room temperature for 1 hour. After this time, the wells and coverslips were washed three times with 1X PBS and the coverslips were laid on slides with 50 µl movial made with propyl gallate (40mg/mL) and placed at 4°C to allow the coverslips to adhere to slides.

2.8.2. *Gentamicin Protection Assay*

Eukaryotic cells were plated ($3x10^5$ cells/mL per well) in a twelve-well tissue culture plate in antibiotic-free media containing 1% FCS. The cells were incubated in a 37°C 5% CO2 incubator overnight to allow the cells to adhere to the bottom of the wells (Ramet et al 2002). Cells were transfected with RNA molecules following the above protocol. Cells were stimulated with live bacteria. Bacteria were added to cells in the 12-well plate at a ratio of 1:10. The plate was incubated in a 37°C 5% CO2 incubator for one hour. After this time, the plates were washed 3 times with ice cold 1X PBS. One mL of 100µg/ml gentamicin (Sigma) in DMEM was added to each well, and the plates were incubated with 37°C at 5% CO2 for 1 hour. After incubation, cells were washed 3 times in 1X PBS and then lysed with 100µl ice cold water for 5 minutes at room temperature. Serial dilutions of 1:10, 1:100 and 1:1000 were then made, and samples were spot plated (10µl) on LB plates containing selective antibiotics and incubated overnight at 37°C. Colony forming units (CFUs) were counted approximately 12 hours later and an internalization index was calculated comparing the initial number of bacteria to the bacteria internalized (Criss et al., 2001).

2.8.3. *MTT Assay for Cell Proliferation*

I-BMDM cells were seeded at $3x10^5$ cells/mL in 96-well plates and transfected with 50nm anti-sense or precursor miRNA oligonucleotides or 50nm siRNA-CDK6 or siRNA-Control. Cells were stimulated with LPS as indicated in the figure legend. Four hours before the end of stimulation, 20µl of 5mg/mL MTT (3-(4,5-Dimethylthiazol-2-yl)-2,5-diphenyltetrazolium bromide) reagent was added to the cells (Weichert et al., 1991). Following the four hour incubation media was removed and 100% isopropanol containing 4mM HCl was added and the plate was agitated for 15 minutes covered in foil at room temperature after which the optical density of the wells was read at 590nm with a reference filter of 620nm.

2.8.4. *Scratch Assay to Simulate Wound Healing*

I-BMDM cells were seeded at $3x10^5$ cells/mL in 96-well plates and transfected with 50nm anti-sense or precursor miRNA oligonucleotides for 24 hours. A sterile 10µl pipet tip was used to scratch wounds through the cell monolayer. After scraping, cells were washed twice in PBS to remove loose cells and new media was added. Cells were stimulated with LPS (100ng/ml) and incubated at 37°C as indicated in the figure legend. Digital images were taken at 0 and 18 hours after scraping. Images were superimposed with a 0.3mm x 0.3mm grid to quantify wound closure. Percent wound closure was calculated by comparing the number of grids in the defined wound area not occupied by cells after 18 hours of LPS stimulation (Slomiany et al., 2006).

2.9. **Western Blot Analysis of Protein Expression**

2.9.1. *Cell lysis*

Following stimulation with TLR ligands or bacteria, cells were lysed either directly with sample loading buffer containing β-mercaptoethanol or a low-stringency buffer containing inhibitors (50mM HEPES, pH 7.5, 100mM NaCl, 1mM EDTA, 10% glycerol, 0.5% Nonidet P40, supplemented with inhibitors - 10µg/mL PMSF, 30µg/mL aprotonin, 1µg/mL sodium orthovanadate and 1µg/mL leupeptin. The cells were incubated on ice for 30 minutes. Following this incubation, samples were centrifuged at 13,000 rpm for 20 minutes at 4°C. The supernatants were removed and assayed for protein and aliquots containing equal

amounts of protein were mixed with 5X SDS sample buffer (5mL glycerol. 10mL 10% SDS, 10mg bromophenol blue, 6.25mL 1M Tris pH 6.25, 28.75mL H_20). 50µL of β-mercaptoethanol (β –ME) was added per mL of sample buffer immediately prior to use. Samples were then boiled at 100°C for 5 minutes and centrifuged gently prior to loading on SDS-PAGE gels.

2.9.2 *Bradford Method for Determination of Protein Concentration*

Samples were diluted 1:5 in water in triplicate and 250µL Bradford reagent (0.01% (w/v) Coomassie Brilliant Blue G250, 4.7% (v/v) ethanol, 8.5% (v/v) orthophosphoric acid) was added to each sample. The reaction was allowed to develop for 5 minutes after which time the plates were read at OD_{570} using Dynatech MR5000 plate reader. Protein concentrations were determined using a standard curve constructed using BSA concentrations in the range of 0-20µg/µL.

2.9.3. *SDS-PAGE (sodium dodecyl sulfate – polyacrylamide gel electrophoresis)*

Samples were resolved in SDS polyacrylamide gel using constant current of 25 mA per gel. Approximately 25µl of sample was loaded into each well. Samples were first run through a 12% stacking gel (1mL 30% bisacrylamide mix, 0.75mL 1M Tris pH 6.8, 60µl 10% (w/v) ammonium persulfate and 6µl TEMED made up to 6mL with water) to condense the protein. The protein was then resolved according to size using a 12% polyacrylamide gel (30% bisacrylamide mix, 3.75mL 1M Tris pH 8.8, 150µl 10% (w/v) ammonium persulfate and 6µl TEMED made up to 15mL with water). Samples were run with 7µl pre-stained protein markers (New England Biolabs) as molecular weight standards.

2.9.4. *Transfer Procedure*

The resolved proteins were transferred to polyvinylidene difluoride (PVDF) using wet transfer system with all components soaked in transfer buffer (25mM Tris-HCL pH 8, 0.2M glycine, 20% methanol). PVDF was activated by first soaking in 100% methanol. The gel was immersed in 1x transfer buffer and placed onto a layer of filter paper and sponge. The gel was covered in PVDF. A second piece of filter paper was placed on top followed by the second sponge. The entire assembly was placed in a cassette and an electric current of 150 mA was applied for two hours.

2.9.5. *Blocking the Membrane*

Once the proteins from the gel had transferred onto the membrane it was removed and placed in 50mL of blocking solution (5% marvel in Tris Buffered Saline/Tween). The PVDF membrane was allowed to rock gently in blocking solution for one hour at room temperature.

2.9.6. *Immunodetection of Protein on Membrane*

The blot was placed into a 50mL falcon tube containing a 1:1000 dilution of the primary antibody. The tube was left to roll at 4°C overnight. The blot was then removed and washed in TBS/Tween three times for five minutes each. The blot was then placed into another 50mL falcon tube containing secondary antibody (1:1000) depending on the host species. The tube was left to roll for one hour at room temperature and then washed three times in TBS/Tween for five minutes each wash. Blots were developed by enhanced chemiluminescence (ECL) (Amersham) according to the manufacturer's protocol.

2.9.7. *Stripping and Re-probing*

The blot was washed one time in TBS/Tween to remove ECL. The membrane was stripped by placing it in 4mL of re-blot solution (Chemicon International) for 15 minutes at room temperature rocking. The membrane was re-blocked with 5% marvel solution for one hour and probed with primary and secondary antibodies as described previously.

2.10. **Luciferase Reporter Assays**

2.10.1. *Preparation of Plasmid DNA*

Plasmids were purified from *E. coli* DH5α host cells using growth in kanamycin (30μg/mL) for the CDK6 3`UTR plasmid as a selection agent. 100μL of a pre-culture was added to 100mL of Luria Bertani LB) broth containing the antibiotic. The cultures were grown overnight at 37°C with gentle agitation. The cultures were transferred to 50mL tubes and centrifuged at 6000 x g for 15 minutes at 4°C. The DNA was then harvested using the Qiagen Maxi prep for DNA isolation. Briefly, the bacterial pellets were resuspended in 10mL buffer P1. 10mL of buffer

P2 was then added and the tubes were mixed vigorously. They were incubated at room temperature for 5 minutes. 10mL of pre-chilled buffer P3 was added to the lysate, and mixed thoroughly. The lysate was poured into the barrel of a QIAfilter cartridge and incubated for 10 minutes at room temperature. The cap was removed from the cartridge and the plunger was inserted and the cell lysate was placed into a clean 50mL tube. 2.5mL of buffer ER was added to the lysate and mixed and inverted 10 times. This was then incubated on ice for 30 minutes. A Qiagen tip was equilibrated by applying 10mL of buffer QBT. The column was left to empty by gravity flow. The filter lysate was added to the Qiagen tip and left to empty by gravity flow. The tip was washed 2 x 30mL of buffer QC. The DNA was eluted with 15mL of buffer QN. The DNA was precipitated by the addition of 10.5mL of isopropanol. This was centrifuged at 6000 x g for 60 minutes. The DNA pellet was washed with 5mL of endotoxin free 70% ethanol and centrifuged at 6000 x g for 30 minutes. The supernatant was removed and the pellet was left to air dry for 10 minutes and subsequently resuspended in between 200-500µL of endotoxin free buffer TE.

2.10.2. *Transient Transfections and stimulations*

For luciferase assays, cells were set-up in 96-well plates at $2x10^5$ cells/mL, 100µL per well. When cells had reached 80% confluency they were transfected with DNA plasmids as described in 2.8. Cells were either co-transfected with RNA molecules. Cells were left 18-24 hours to recover again before stimulation with LPS or vehicle control for 24 hours.

2.10.3. *Assay Procedure*

Cells were washed with PBS then lysed for 15 minutes at room temperature with 50µL of 1X passive lysis buffer with shaking at 300rpm. 20µL of the lysed cell mix was taken and tested for firefly luciferase activity and 20µL of the lysed cell mix was tested for Renilla luciferase activity. Firefly luciferase activity was assays by the addition of 40µL of the luciferase assay mix (20mM tricine, 1.07 mM $(MgCO_3)_4Mg(OH)_2.5H_2O$, 2.67 mM MgS)4, 0.1 M EDTA, 33.3 mM DTT, 270 mM coenzyme A, 470 mM luciferin, 530 mM ATP) to the sample and Renilla was read by the addition of 40µL of a 1:1000 dilution of Coelentrazine in PBS. Luminescence was read using Mediators PHL luminometer. Firefly luminescence

readings were corrected for Renilla activity and expressed as fold stimulation over unstimulated negative control.

2.11. **Bioinformatics**

2.11.1. *Targetscan.org*

Many databases exist for the purpose of identifying potential gene targets for miRNAs. They can also be used to identify possible miRNAs involved in the regulation of a particular gene of interest. Targetscan.org is one of the preeminent sites for either identifying target genes or identifying interesting miRNAs. This database presents the user with a list of genes and provides p-values which are calculated based on the series of rules. Context score calculated based on:

1. Site-type contribution: the type of seed match (8mer, 7mer-m8, and 7mer-1A)
2. 3' pairing contribution: consequential miRNA-target complementarity outside the seed region
3. Local AU contribution: transcript AU content 30 nucleotides upstream and downstream of predicted site
4. Position contribution: distance to nearest end of UTR of target.

The context score is the sum of the scores and a more negative score is associated with a more favorable site.

2.11.2. *MiRecords and G-profiler*

A database designed by The University of Minnesota and the University of Houston in 2008 (http://mirecords.umn.edu/miRecords/) uses an algorithm that allows a user to combine several different database filters to find a much more condensed list of target mRNAs for a given miRNA. This list can then be entered into the G-profiler (http://biit.cs.ut.ee/gprofiler/) database to find common biological functions amongst the targets.

2.12. **Statistical analysis**

All statistical tests were carried out on the mean results of at least three independent experiments unless otherwise indicated. A paired two-tailed and two-sample student t-test was performed to determine if samples were significantly different with Microsoft Excel (Microsoft, WA). Levels of significance are indicated using asterisks: * $P \leq 0.05$, ** $P \leq 0.01$, *** ≤ 0.001.

CHAPTER 3

miRNA EXPRESSION

3.1. **Introduction**

Since the discovery of small non-coding RNA including siRNA and miRNA over a decade ago, interest in the area of RNA biology has grown tremendously. The therapeutic potential of small non-coding RNA is currently being explored in clinical trials to treat cancer and hepatitis C infection. miRNAs act as key regulators of embryological development (Wienholds and Plasterk, 2005) and haematopoietic cell differentiation (Chen et al., 2004). Their dysregulation has been linked to many types of cancer and it is thought that they play a crucial role in regulating the immune response. The role miRNAs play in the immune response has only been realized in the last five years. It is thought that the human genome contains more genes for non-coding small RNA than protein-coding genes (Birney et al., 2007). One of the most interesting aspects of miRNAs is the tissue specificity of their expression and that levels of miRNAs vary between different cell types and in different developmental stages. Because of this they are being used as diagnostic biomarkers in the identification of cancers, autoimmune disorders and rheumatic diseases (Alevizos and Illei, 2010; Kosaka et al., 2010a; Schuster et al., 2010; Wittmann and Jack, 2010). Screens have been conducted examining the expression of miRNAs in different tissues and organs and in response to different stimuli (Liang et al., 2007). The more information that is obtained regarding their tissue specificity, how their expression is regulated and the functional consequences of their expression the greater the therapeutic potential (Lu et al., 2005).

When TLRs are activated the expression profile of hundreds of genes is altered perhaps due to the fine-tuning mechanism of miRNAs. Prior to the start of this study a screen measuring the expression of over a hundred miRNAs in response to three different TLR ligands was performed in a dendritic cell line. I examined the miRNAs from this screen that were most upregulated or downregulated in response to LPS and validated their expression in the DC2.4 cell line used in the initial study. I then examined the miRNAs that were most consistently upregulated or downregulated and examined their expression in a dozen cell types including immune cells, brain cells and epithelial cells. Based the data gathered from this study and past studies I can conclude that miRNAs play a key role in the

regulation of innate immune responses. Their expression patterns are now well documented but the functional outcomes of their expression is not well studied and remains difficult to assess because of the global scope of their targeting. In this chapter, I explore the expression of various miRNAs in response to the TLR4 ligand LPS in a wide-range of cell types from immune cells to epithelial cells to obtain a better understanding of the cell-type and tissue specificity of miRNAs.

3.2. **Analysis of miRNAs in murine cells in response to TLR ligands**

3.2.1. *miRNA expression in DC2.4 cells in response to LPS*

A screen of 158 miRNAs was conducted by Dr. F. Sheedy where three TLR ligands were used to stimulate dendritic cells and miRNA expression was measured using TaqMan technology. miRNAs that have since been shown to have a role in TLR signaling were uncovered in the screen. These include miR-155, miR-146a and miR-21 (McCoy et al., 2010; O'Connell et al., 2009; Sheedy et al., 2010; Taganov et al., 2006). I first attempted to confirm and validate that LPS could increase the expression of miR-155 and miR-214 as found in the screen. Figure 3.1A shows the induction of miR-155 expression by nearly 15 fold following 24 hours of LPS stimulation. Figure 3.1B shows a nearly 8 fold induction of miR-214 at about 18 hours post-stimulation with LPS

I next examined the expression of miR-21 in response to LPS. Figure 3.2A shows that LPS stimulation for 24 hours resulted in a 4 fold increase in expression. The expression of a previously characterized miRNA miR-146a was examined next. This miRNA has two isoforms, miR-146a and miR-146b but in several studies, miR-146a was shown to have a more significant role in innate immunity (Perry et al., 2009; Xia et al., 2009). miR-146a expression gradually increased following 24 hours of LPS stimulation as shown in figure 3.2B reaching a 20 fold increase in expression. Figure 3.2C shows that let-7e expression increases approximately 3 fold at 2 hours post LPS stimulation but quickly returns to basal levels.

Following verification that some of the miRNAs from the initial miRNA screen could be repeatedly upregulated, two of the downregulated miRNAs from the screen were examined. Figure 3.3A shows miR-149 expression decreased nearly 4 fold between 8 and 18 hours post-LPS stimulation. miR-107 expression was examined next in the DC2.4 cell line. Following 4 hours of LPS stimulation, miR-107 expression decreased about 5 fold and remained decreased until 18 to 24 hours when it returned to basal levels as shown in figure 3.3B. The remainder of this study chose to focus on the expression of miR-107 based on consistency of downregulation in response to LPS.

3.2.2. *IL-6 and TNF-α are produced by DC2.4 cells in response to LPS over a 24 hour period*

Murine dendritic cell line DC2.4 was used to validate the initial miRNA data. To ensure that cells were responding to various TLR stimuli, IL-6 and TNF-α were measured. Figure 3.4A shows the production of IL-6 in response to LPS over a 24 hour period and figure 3.4B shows the production of TNF-α over a 24 hour period in response to LPS. Cells responded to LPS and over time, with the highest cytokine production at 24 hours.

3.2.3. *Analysis of expression levels of miR-146a and miR-107 in response to stimulation with recombinant TNF-α in DC2.4*

DC2.4 cells were stimulated with recombinant TNF-α to analyze if direct TNF-α cell stimulation has a greater effect on miR-107 downregulation than direct LPS stimulation. There is evidence that the transcription factor that may regulate miR-107 expression is directly affected by TNF-α. Figure 3.5 shows that in DC2.4 cells, miR-107 decreased nearly 5 fold after 8 hours of treatment followed by an increase after 18 hours and a decrease to basal levels after 24 hours. miR-146a expression increased marginally in response to TNF-α treatment.

3.2.4. *Analysis of the expression levels miR-107 and miR-146a following stimulation with LPS in J774 cells*

The expression of miR-107 and miR-146a in response to LPS was examined in the murine J774 peritoneal macrophage cell line. miR-107 expression is shown in figure 3.6A and it is downregulated about 2 fold 4 hours post-LPS stimulation but returned to slightly above basal levels after 18 and 24 hours of stimulation. miR-146a expression is shown in figure 3.6B and it is increased about 50 fold after 18 hours of LPS stimulation.

3.2.5. *IL-6 is produced by J774 cells in response to LPS over a 24 hour period*

To ensure that the murine macrophage cell line J774 was responding to TLR stimuli, IL-6 was measured. Figure 3.7 shows that J774 cells start to produce IL-6 at 18 hours.

3.2.6. *Analysis of the expression levels of miR-107, miR-146a and miR-21 following stimulation with LPS in Raw264.7 cells*

The expression of miR-107 and miR-146a was next examined in the murine peritoneal macrophage cell line Raw264.7. Figure 3.8A shows miR-107 is downregulated after 2 hours and stays decreased nearly 10 fold through 24 hours. Both miR-21 and miR-146a are upregulated in response to LPS as shown in figures 3.8B and 3.8C respectively. miR-146a is upregulated 5 fold after 2 hours and increases to about 15 fold after 24 hours, whereas miR-21 does not increase until 18 hours and then is up about 10 to 15 fold through 24 hours.

3.2.7. *TNF-α is produced by murine Raw264.7 cells in response to LPS over a 24 hour period*

To ensure that the murine macrophage cell line Raw264.7 was responding to TLR stimuli, TNF-α was measured. Figure 3.9 shows the production of TNF-α over a 24 hour period by Raw264.7 cells. TNF-α starts to be produced in response to LPS at 4 hours and there is a gradual increase reaching the highest concentration at 24 hours.

3.2.8. *Analysis of miR-107 and miR-146a expression following stimulation with TLR ligands in I-BMDM cells*

Figure 3.10A shows the downregulation of miR-107 in the immortalized murine bone marrow derived macrophage cell line I-BMDM in response to LPS following 18 hours of stimulation and remaining decreased through 24 hours. miR-146a increases about 6 fold in I-BMDM treated with both LPS as shown in figure 3.10B.

3.2.9. *IL-6 is produced by I-BMDM in response to LPS over a 24 hour period*

To ensure that the I-BMDM were responding to TLR stimuli, IL-6 was measured. Figure 3.11 shows that I-BMDM cells start to produce IL-6 at 18 hours.

3.2.10. *Analysis of the expression levels of miR-107 and miR-146a following infection with heat-killed E. coli in I-BMDM*

We next wanted to examine the expression of miR-107 and miR-146a in response to a heat-killed *E. coli* infection in the I-BMDM to examine any differences

between ligand induced downregulation of miR-107 and the whole bacteria. Figure 3.12A shows the expression of miR-107 in response to heat-killed *E. coli* and its expression decreases from 1 to 4 hours post-infection. miR-146a expression was measured next and it increased in response to the heat-killed infection to about 4 fold as shown in figure 3.12B.

3.2.11. *TNF-α is produced by I-BMDM in response to heat-killed E. coli in I-BMDM*

I-BMDM were infected with heat-killed *E. coli* for different time points and assessed for TNF-α production. Figure 3.13 shows TNF-α production gradually increasing over time in response to heat-killed *E. coli* but at marginal levels of 200 to 300 pg/mL 3 hours post-infection.

3.2.12. *Analysis of the expression levels of miR-107 and miR-146a following stimulation with LPS in primary bone marrow derived macrophages cells*

The downregulation of miR-107 in primary murine bone marrow derived macrophage cells (BMDM) is shown in Figure 3.14A. miR-107 expression decreases at 4 hours post-LPS stimulation and continues to decrease over the 24 hour stimulation period. miR-146a is not upregulated to previously seen levels in the cell lines but does increase approximately 2.5 fold at about 24 hours post-stimulation as shown in figure 3.14B.

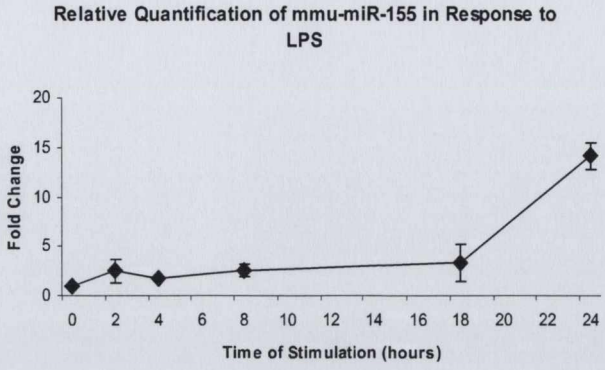
3.2.13. *TNF-α is produced by primary bone marrow derived macrophages in response to LPS*

Primary murine BMDM were harvested, stimulated with LPS for different time points and assessed for TNF-α production. Figure 3.15 shows TNF-α production gradually increasing over time and reaching a maximum 18 hours post-stimulation.

3.2.14. *Analysis of the expression levels of miR-107, miR-146a and miR-21 following stimulation with LPS in primary bone marrow derived dendritic cells*

miR-107 expression was next examined in primary murine bone marrow derived dendritic cells (BMDC) in response to LPS and this is shown in figure 3.16A. miR-107 expression did not change drastically and only decreased to about 3 fold

A



B

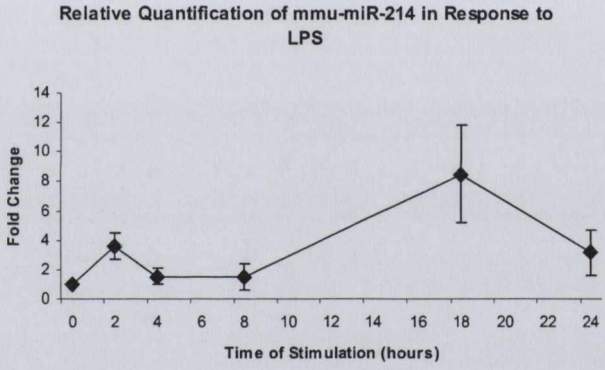
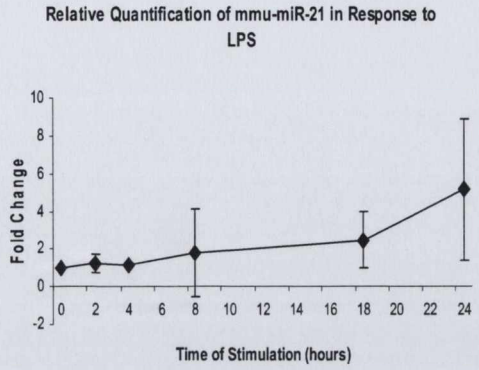
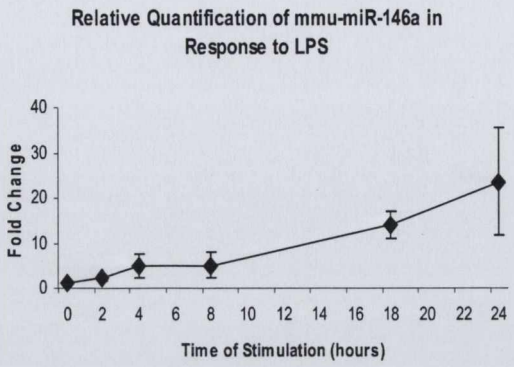


Figure 3.1. **Expression levels of miR-155 and miR-214 in murine dendritic cell line DC2.4 in response to LPS.** DC2.4 ($3x10^5$ cells/mL) were plated and incubated with LPS (0.1μg/mL) or left unstimulated. RNA was extracted and analyzed using miRNA TaqMan PCR with probes specific to miR-155 (A) and miR-214 (B). Fold changes in miRNA expression were calculated using ΔΔCt method with RNA from unstimulated cells as a calibrator and U6 rRNA as an endogenous control. The data shown is the mean expression ± S.E.M. of three separate experiments, each carried out in triplicate.

A



B



C

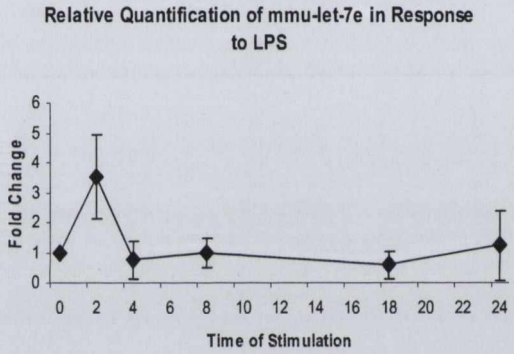
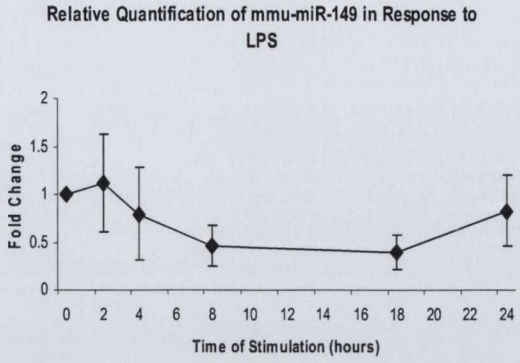


Figure 3.2. **Expression levels of miR-21, miR-146a and let-7e in murine dendritic cell line DC2.4 in response to LPS.** DC2.4 ($3x10^5$ cells/mL) were plated were plated and incubated with LPS (0.1μg/mL) or left unstimulated. RNA was extracted and analyzed using miRNA TaqMan PCR with probes specific to miR-21 (A) miR-146a (B) and let-7e (C). Fold changes in miRNA expression were calculated using ΔΔCt method with RNA from unstimulated cells as a calibrator and U6 rRNA as an endogenous control. The data shown is the mean expression ± S.E.M of three separate experiments, each carried out in triplicate.

A



B

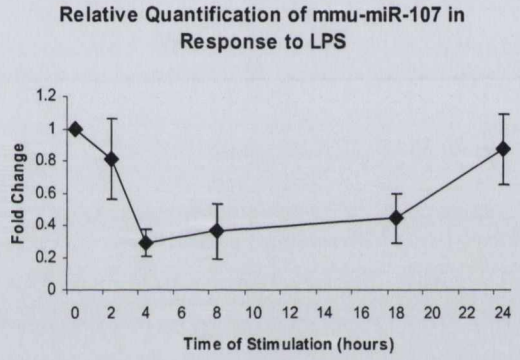
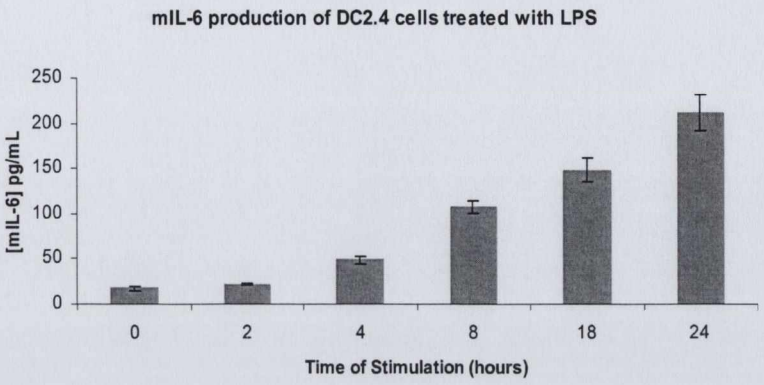


Figure 3.3. **Expression levels of miR-149 and miR-107 in murine dendritic cell line DC2.4 in response to LPS.** DC2.4 ($3x10^5$ cells/mL) were plated and incubated with LPS (0.1μg/mL) or left unstimulated. RNA was extracted and analyzed using miRNA TaqMan PCR with probes specific miR-149 (A) and miR-107 (B). Fold changes in miRNA expression were calculated using ΔΔCt method with RNA from unstimulated cells as a calibrator and U6 rRNA as an endogenous control. The data shown is the mean expression ± S.E.M. of three separate experiments, each carried out in triplicate.

A



B

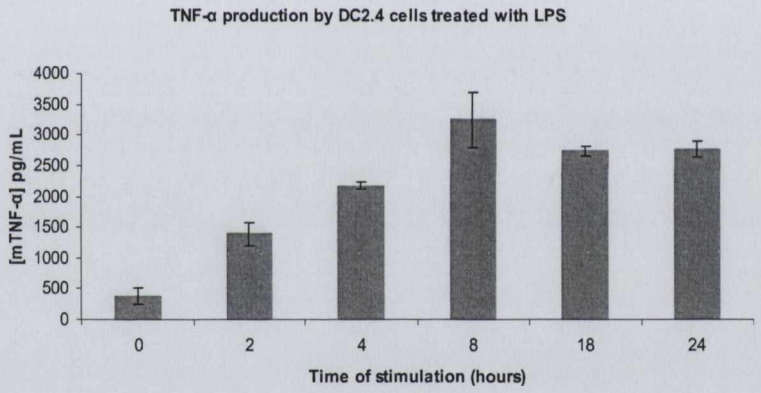


Figure 3.4. **Production of IL-6 and TNF-α cytokine by DC2.4 cells in response to LPS.** DC2.4 ($3x10^5$ cells/mL) were plated and incubated with LPS (0.1μg/mL) or left unstimulated. Time 0 = unstimulated cells. Supernatants were collected at various time points and analyzed by ELISA for IL-6 (A) and TNF-α (B) production. The data shown is the mean expression ± S.E.M. of three separate experiments, each carried out in triplicate.

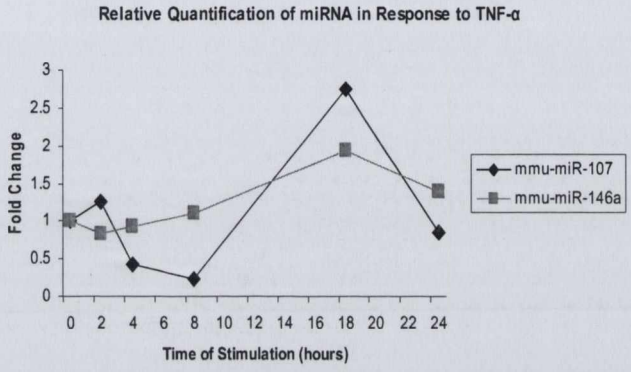
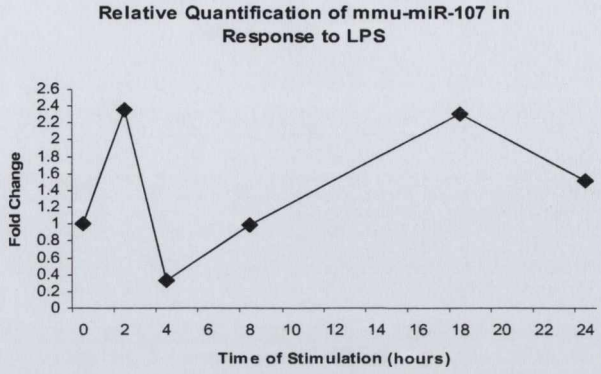


Figure 3.5. **Expression levels of miR-107 and miR-146a in murine dendritic cell line DC2.4 treated with TNF-α.** DC2.4 ($3x10^5$ cells/mL) were plated and incubated with mouse recombinant TNF-α (20ng/mL) or left unstimulated. RNA was extracted and analyzed using miRNA TaqMan PCR with probes specific for miR-107 and miR-146a. Fold changes in miRNA expression were calculated using ΔΔCt method with RNA from unstimulated cells as a calibrator and U6 rRNA as an endogenous control. The data shown is representative of an experiment done in triplicate.

A



B

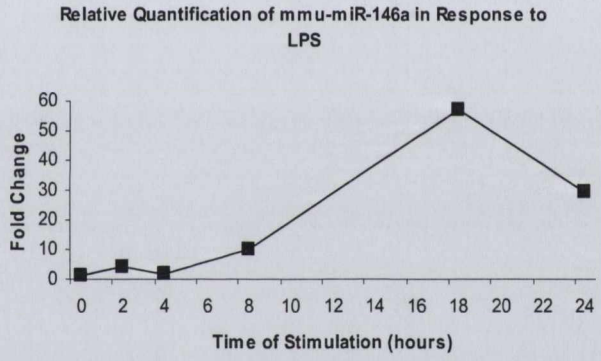


Figure 3.6. **Expression levels of miR-107 and miR-146a in murine J774 macrophages in response to LPS.** J774 ($3x10^5$ cells/mL) were plated and incubated with LPS (0.1μg/mL) or left unstimulated. RNA was extracted and analyzed using miRNA TaqMan PCR with probes specific to miR-107 (A) or miR146a (B). Fold changes in miRNA expression were calculated using ΔΔCt method with RNA from unstimulated cells as a calibrator and U6 rRNA as an endogenous control. The data shown is representative of an experiment done in triplicate.

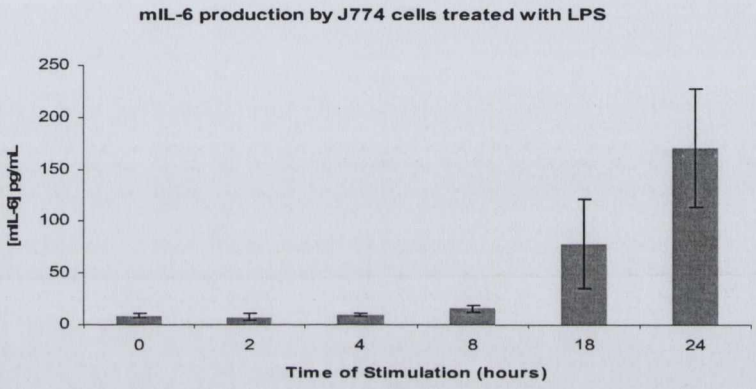
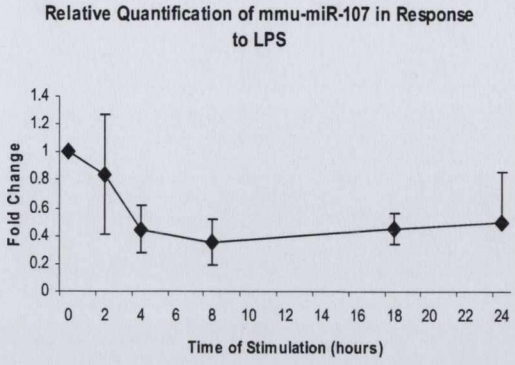
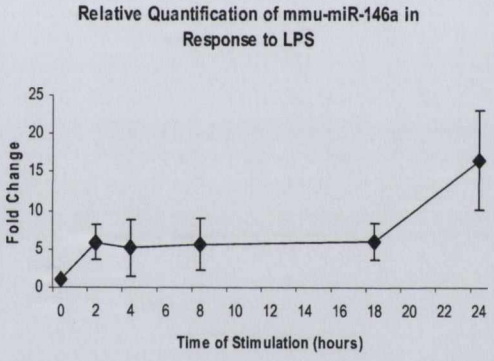


Figure 3.7. **Production of IL-6 cytokine by murine J774 macrophages in response to LPS.** J774 ($3x10^5$ cells/mL) were plated and incubated with LPS (0.1μg/mL) or left unstimulated. Supernatants were collected at various time points and analyzed by ELISA for IL-6 production. The data shown is representative of an experiment done in triplicate.

A



B



C

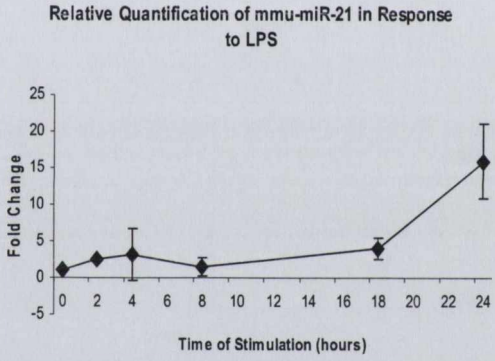


Figure 3.8. **Expression levels of miR-107, miR-146a and miR-21 in murine Raw264.7 macrophages in response to LPS.** Raw264.7 ($3x10^5$ cells/mL) were plated and incubated with LPS (0.1μg/mL) or left unstimulated. RNA was extracted and analyzed using miRNA TaqMan PCR with probes specific to miR-107 (A), miR146a (B) or miR-21 (C). Fold changes in miRNA expression were calculated using ΔΔCt method with RNA from unstimulated cells as a calibrator and U6 rRNA as an endogenous control. The data shown is the mean expression ± S.E.M. of three separate experiments, each carried out in triplicate.

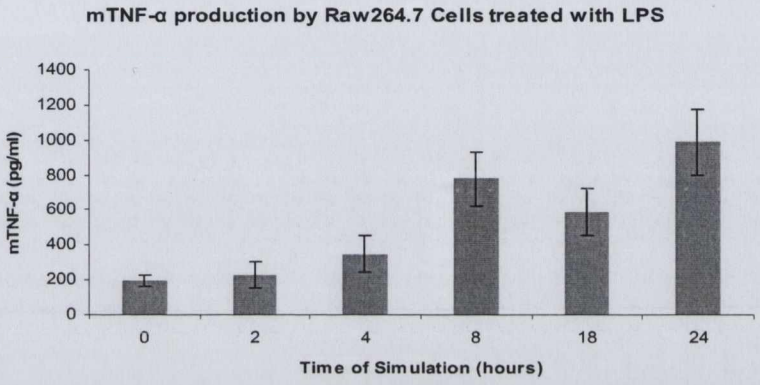
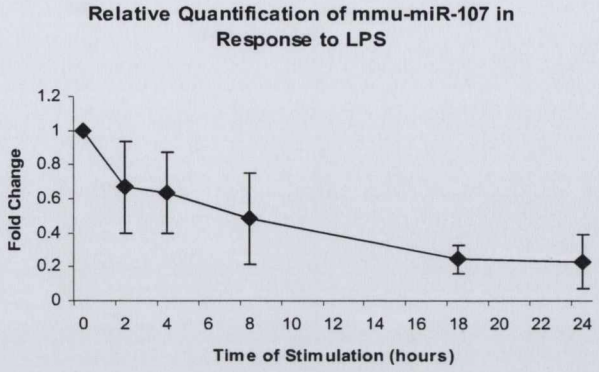


Figure 3.9. **Production of TNF-α cytokine by murine Raw264.7 macrophages in response to LPS.** Raw264.7 ($3x10^5$ cells/mL) were plated and incubated with LPS (0.1μg/mL) or left unstimulated. Supernatants were collected at various time points and analyzed by ELISA for TNF-α production. The data shown represent mean cytokine level $\pm$ S.E.M. from three separate experiments, each carried out in triplicate.

A



B

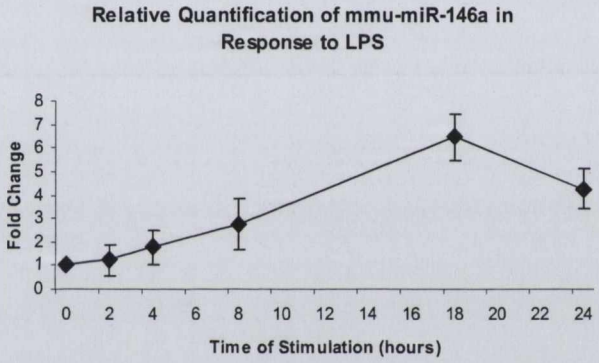


Figure 3.10. **Expression levels of miR-107 and miR-146a in immortalized murine bone marrow derived macrophages (I-BMDM) in response to LPS.** I-BMDM ($3x10^5$ cells/mL) were plated and incubated with LPS (0.1μg/mL) or left unstimulated. RNA was extracted and analyzed using miRNA TaqMan PCR with probes specific to miR-107 (A) or miR146a (B). Fold changes in miRNA expression were calculated using ΔΔCt method with RNA from unstimulated cells as a calibrator and U6 rRNA as an endogenous control. The data shown is the mean expression ± S.E.M. of three separate experiments, each carried out in triplicate.

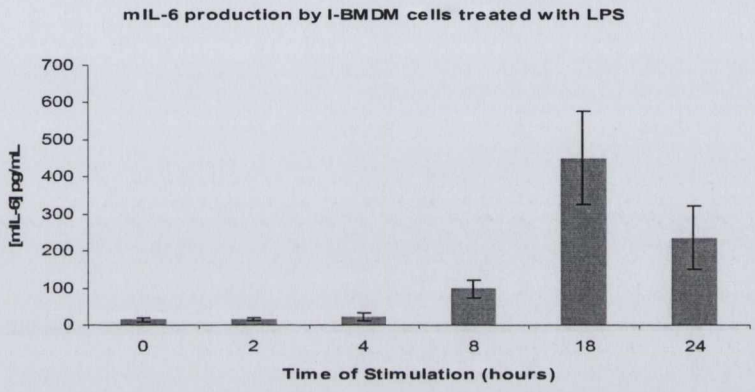
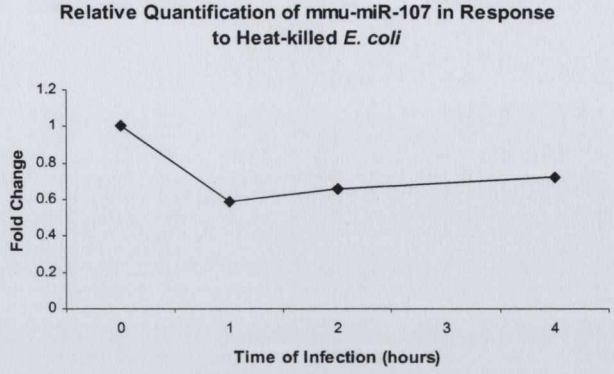


Figure 3.11. **Production of IL-6 cytokine by I-BMDM in response to LPS.** I-BMDM ($3x10^5$ cells/mL) were plated and incubated with 0.1μg/mL LPS or left unstimulated. Supernatants were collected and analyzed by IL-6 ELISA. The data shown represent mean cytokine level ± S.E.M. from three separate experiments, each carried out in triplicate.

A



B

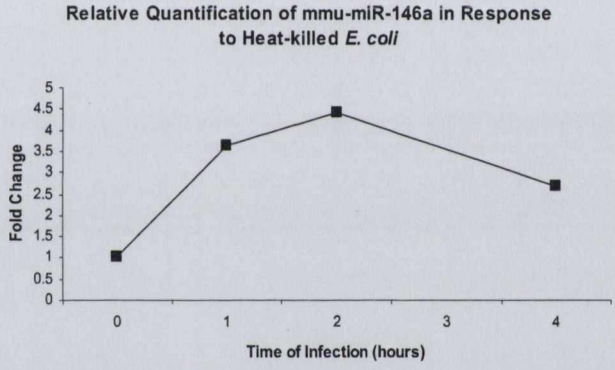


Figure 3.12. **Expression levels of miR-107 and miR-146a in I-BMDM in response to *E. coli*.** I-BMDM ($3x10^5$ cells/mL) were plated and incubated with heat-killed (MOI of 40:1) *E. coli* or left unstimulated. RNA was extracted and analyzed using miRNA TaqMan PCR with probes specific to miR-107 (A) and miR-146a (B). Fold changes in miRNA expression were calculated using ΔΔCt method with RNA from unstimulated cells as a calibrator and U6 rRNA as an endogenous control. Data shown is from a single experiment done in triplicate and is representative of three separate experiments.

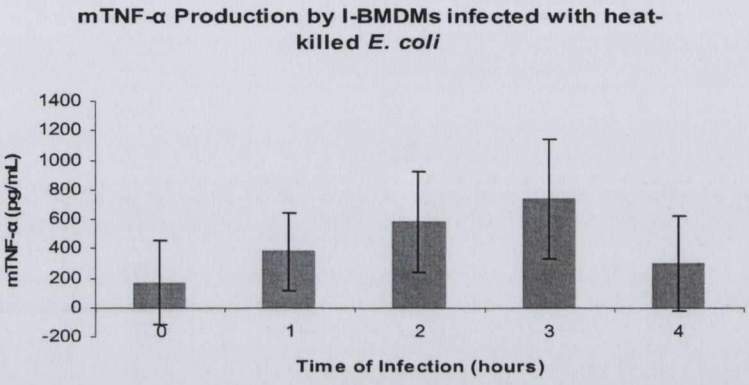
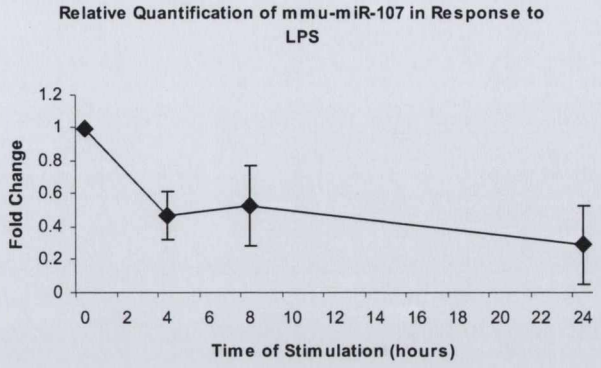


Figure 3.13. **Production of TNF-α cytokine by I-BMDM in response to *E. coli*.** I-BMDM ($3x10^5$ cells/mL) were plated and incubated with heat-killed (MOI of 40:1) *E. coli* or left unstimulated. Supernatants were collected at various time points and analyzed by ELISA for TNF-α production. The data shown is the mean expression ± S.E.M. of three separate experiments, each carried out in triplicate.

A



B

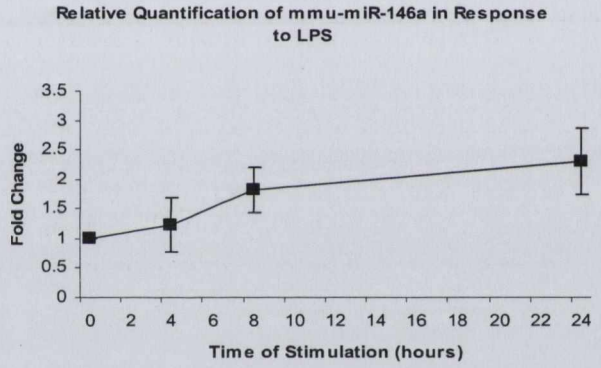


Figure 3.14. **Expression levels of miR-107 and miR-146a in primary murine bone-marrow-derived macrophages in response to LPS.** Primary BMDM ($3x10^5$ cells/mL) were plated and incubated with LPS (0.1μg/mL) or left unstimulated. RNA was extracted and analyzed using miRNA TaqMan PCR with probes specific to miR-107 (A) and miR146a (B). Fold changes in miRNA expression were calculated using ΔΔCt method with RNA from unstimulated cells as a calibrator and U6 rRNA as an endogenous control. The data shown is the mean miRNA expression ± S.E.M. of three separate experiments, each carried out in triplicate.

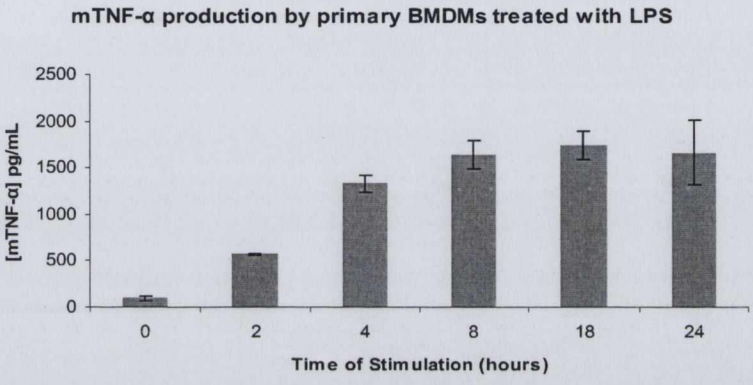
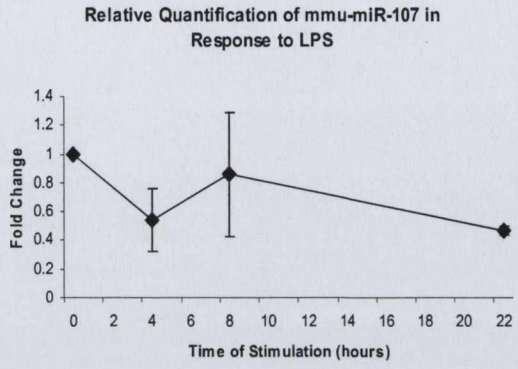
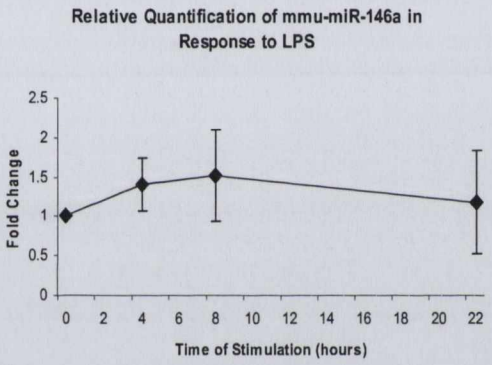


Figure 3.15. **Production of TNF-α cytokine by primary mouse bone marrow derived macrophages in response to LPS.** BMDM ($3x10^5$ cells/mL) were plated and incubated with LPS (0.1μg/mL) or left unstimulated. Supernatants were collected at various time points and analyzed by ELISA for TNF-α production. The data shown is the mean expression ± S.E.M. of three separate experiments, each carried out in triplicate.

A



B



C

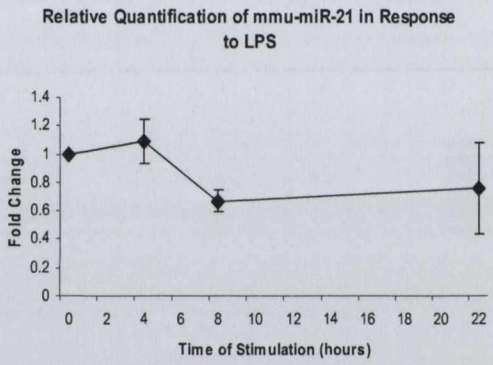


Figure 3.16. **Expression levels of miR-107, miR-146a and miR-21 in primary murine bone-marrow-derived dendritic cells in response to LPS.** Primary BMDC ($3x10^5$ cells/mL) were plated and incubated with LPS (0.1μg/mL) or left unstimulated. RNA was extracted and analyzed using miRNA TaqMan PCR with probes specific to miR-107 (A), miR-146a (B) or miR-21 (C). Fold changes in miRNA expression were calculated using ΔΔCt method with RNA from unstimulated cells as a calibrator and U6 rRNA as an endogenous control. The data shown is the mean expression ± S.E.M. of three separate experiments, each carried out in triplicate.

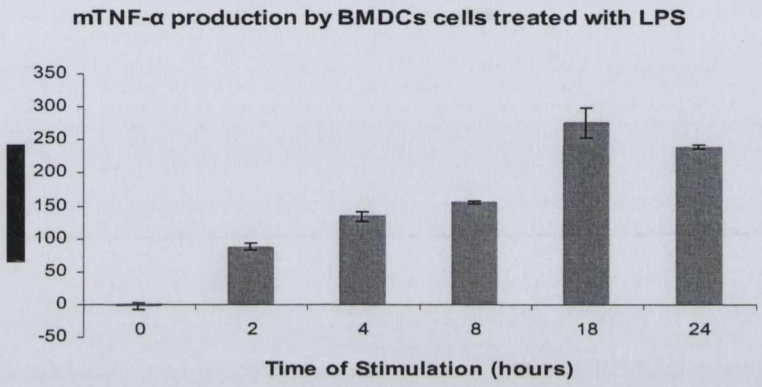


Figure 3.17. **Production of TNF-α cytokine by primary mouse bone marrow derived dendritic cells in response to LPS.** BMDC ($3x10^5$ cells/mL) were plated and incubated with LPS (0.1μg/mL) or left unstimulated. Supernatants were collected at various time points and analyzed by ELISA for TNF-α production. The data shown is the mean expression ± S.E.M. of three separate experiments, each carried out in triplicate.

following 24 hours of LPS stimulation. miR-146a expression was examined next in response to LPS and it did not increase in response to LPS as shown in figure 3.16B. miR-21 expression also did not increase in response to LPS as shown in figure 3.16C. These results suggest that the cells did not respond to LPS.

3.2.15. *TNF-α is produced by primary bone marrow derived dendritic cells in response to LPS*

Murine BMDC were harvested, stimulated with LPS for different time points and assessed for TNF-α production. Figure 3.17 shows TNF-α production gradually increasing over time in response to both ligands but at very marginal levels of 200 to 300 pg/mL following 18 hours of stimulation.

3.3. **Analysis of miRNAs in human cells in response to TLR ligands**

3.3.1. *Analysis of miR-107, miR-146a and miR-149 expression following stimulation with TLR Ligands in human THP1 cells*

The human monocytic cell line THP1 was the first human cell used to analyze the expression of miRNA in this study. Figure 3.18A shows the slight upregulation of miR-107 in response to LPS at 4 hours followed by decrease to basal levels from 8 to 24 hours in the THP1 cell line. miR-146a expression increases about 15 fold in response to LPS after 18 hours followed by a decrease after 24 hours as demonstrated in figure 3.18B. miR-149 expression was also examined in THP1 cells in response to LPS. At 8 hours post-LPS stimulation there is a decrease in miR-149 expression shown in figure 3.18C.

3.3.2. *IL-8 is produced by THP1 cells in response to LPS over a 24 hour period*

To examine if the THP1 cells were responding to LPS, IL-8 ELISA for cytokine production was measured. Figure 3.19 shows the production of IL-8 by THP1 cells starting at about 8 hours post-stimulation and increasing over the next 16 hours.

3.3.3. *Analysis of miR-107, miR-146a and miR-21 expression following stimulation with LPS in HEK293 and HEK293-TLR4 cells*

Human embryonic kidney cells HEK293 were first examined as a negative control cell line to see if miR-107 would still be downregulated in a cell line that does not express TLRs. Figure 3.20A shows the slight downregulation of miR-107 after 2 hours of stimulation but expression increased to basal levels after 18 hours and decreased again after 24 hours possibly indicating unstable expression of the miRNA. The uneven distribution of miR-107 expression suggests that miR-107 expression does not change in cells lacking TLRs. miR-146a was also measured and its expression is shown in figure 3.20B. Its levels increase about 6 fold following 8 hours of LPS stimulation.

HEK293 cells stably transfected with TLR4 were than used to examine if the effect of LPS stimulation on expression of miR-107 was in fact TLR4 dependent. Figure 3.21A shows the downregulation of miR-107 from 4 to 18 hours followed by miR-107 levels returning to basal levels by 24 hours. Because the downregulation of miR-107 was more consistent in the cells stably transfected with TLR4, this suggests that miR-107 may have a direct role in TLR4 signaling. miR-146a expression in response to LPS is shown in figure 3.21B. Its expression increases from 2 to 8 hours but returns to basal levels after 18 hours of stimulation. I cannot conclude a definitive result from this part of the study but based on the data that is presented here, the mechanism of miR-146a upregulation is TLR4 independent and the mechanism of miR-107 downregulation is TLR4-dependent. miR-21 expression was also examined and is shown in figure 3.21C. Its expression levels increase slightly following 2 hours of LPS stimulation but quickly return to basal levels.

3.3.4. *IL-8 is not produced by human HEK293 but is produced by HEK293-TLR4 and THP1 cells in response to LPS over a 24 hour period*

To see if human cell lines HEK293 and HEK293-TLR4 were responding to TLR4 stimuli IL-8 was measured. Figure 3.22A shows the lack of production of IL-8 by HEK293 cells over a 24 hour period. Figure 3.22B shows the production of IL-8 by HEK293-TLR4 cells from 8-24 hours in response to LPS.

3.3.5. *Analysis of the expression levels of miR-107 and miR-146a following stimulation with LPS in human glial cell line A172*

Human glial A172 cells were next used to examine miRNA expression in human cells. Figure 3.23A shows the downregulation of miR-107 reaching its maximum of nearly 10 fold at 4 hours post LPS stimulation. miR-146a expression is shown in figure 3.23B and it increased about 3 fold at 18 hours post-LPS stimulation.

3.3.6. *Analysis of the expression levels of miR-107 and miR-146a following stimulation with recombinant TNF-α in human glial cell line A172*

Several papers have been published suggesting a possible role for miR-107 in the progression of neurodegenerative diseases (Nelson and Wang, 2010; Wang et al., 2010a). A172 cells were stimulated with recombinant TNF-α to analyze if direct cell stimulation with TNF-α has a greater effect on miR-107 downregulation than direct LPS stimulation. Figure 3.24A illustrates that in A172 cells, miR-107 decreased nearly 5 fold after 8 hours of treatment followed by an increase after 18 hours and a decrease to basal levels after 24 hours. miR-146a expression increased about 3.5 fold following 24 hours of treatment with recombinant TNF-α as demonstrated in figure 3.24B.

3.3.7. *IL-6 is produced by the human glial cell line A172 in response to LPS*

To examine if the human cell line A172 was responding to LPS, IL-6 was measured. Figure 3.25 shows the production of IL-6 by A172 cells starting at 2 hours post-stimulation and increasing over-time.

3.3.8. *Analysis of the expression levels of miR-107and miR-146a following stimulation with LPS in human gut epithelial cell line Caco2*

The human cell line Caco2 was stimulated with LPS to analyze the expression of miR-107 and miR-146a in the gut. miR-107 expression does not change in response to LPS as shown in figure 3.26A. miR-146a expression also does not change as seen in figure 3.26B. These experiments could mean that the LPS did not stimulate the cells or these cells simply have a different repertoire of miRNA expressed.

3.3.9. *IL-6 is produced by the human gut epithelial cell line Caco2 in response to LPS*

To see if Caco2 cells were responding to LPS, IL-6 was measured. Minimal amounts of IL-6 were produced, but there is evidence that the cells did respond to LPS as shown in figure 3.27. So it seems that Caco2 do respond to LPS but they do not express miR-107 or miR-146a.

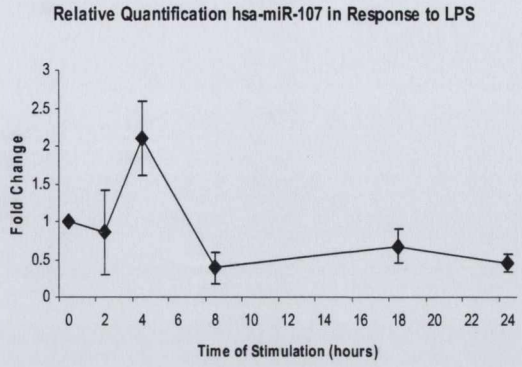
3.3.10. *Analysis of the expression levels of miR-107, miR-146a and miR-21 following stimulation with LPS in peripheral blood mononuclear cells*

I next examined PBMC isolated from human blood. Figure 3.28A shows miR-107 downregulation in PBMC in response to LPS at 4 hours post-stimulation followed by a slight increase at 8 hours and a return to basal levels at 24 hours. miR-146a is upregulated at 4 to 8 hours post-stimulation and stays increased about 6 fold after 24 hours as shown in figure 3.28B. miR-21 expression is shown in figure 3.28C and like miR-146a it increased at 8 hours post-stimulation but returns to basal levels after 24 hours.

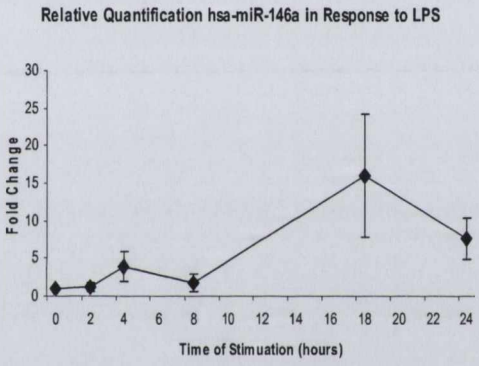
3.3.11. *TNF-α is produced by human PBMC in response to LPS*

PBMC were stimulated with LPS at different time points and assessed for TNF-α production. Figure 3.29 shows TNF-α production reached it maximum at 8 hours post-stimulation and then starts to decrease.

A



B



C

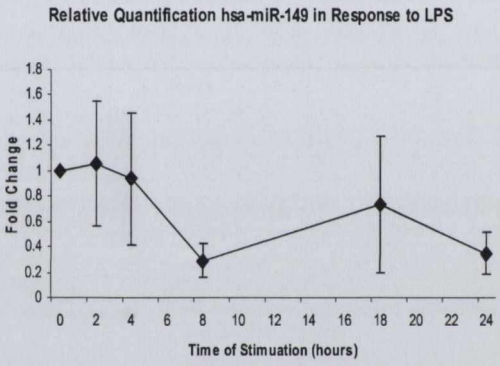


Figure 3.18. **Expression levels of miR-107, miR-146a and miR-149 in human monocytic cell line THP1 in response to LPS.** THP1 ($3x10^5$ cells/mL) were plated and incubated with LPS (0.1μg/mL) or left unstimulated. RNA was extracted and analyzed using miRNA TaqMan PCR with probes specific to miR-107 (A), miR-146a (B) or miR-149 (C). Fold changes in miRNA expression were calculated using ΔΔCt method with RNA from unstimulated THP1 cells as a calibrator and U6 rRNA as an endogenous control. The data shown is the mean miRNA expression ± S.E.M. of three separate experiments, each carried out in triplicate.

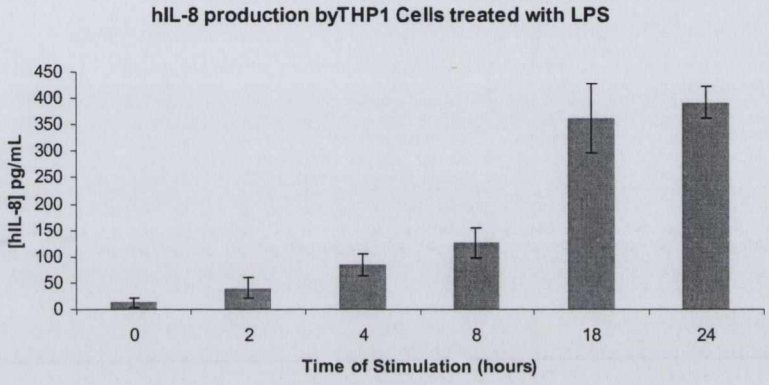
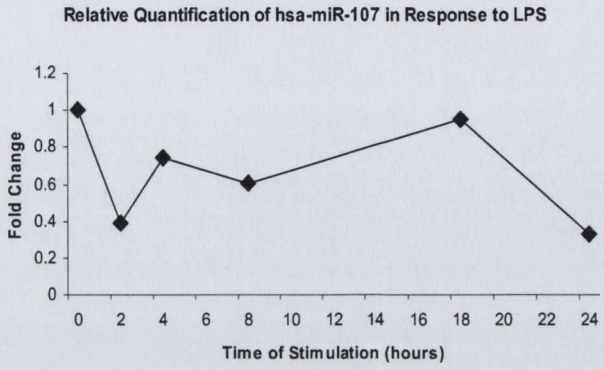


Figure 3.19. **Production of IL-8 cytokine by human THP1 monocytic cell line in response to LPS.** THP1 ($3x10^5$ cells/mL) were plated and incubated with LPS (0.1μg/mL) or left unstimulated. Supernatants were collected at various time points and analyzed by ELISA for IL-8 production. The data shown represent mean cytokine level ± S.E.M. from three separate experiments, each carried out in triplicate.

A



B

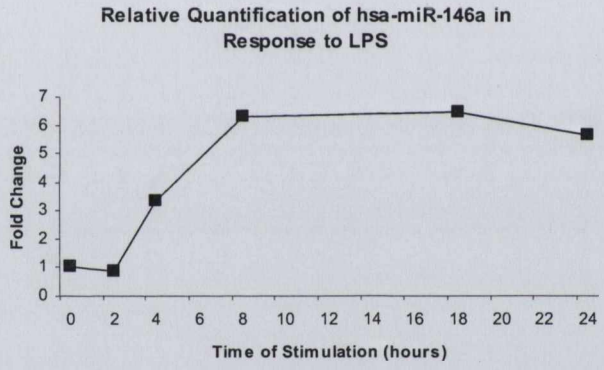
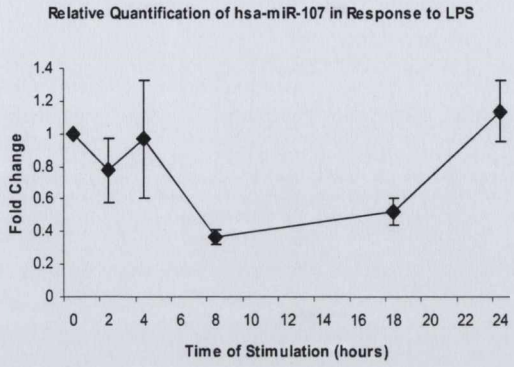
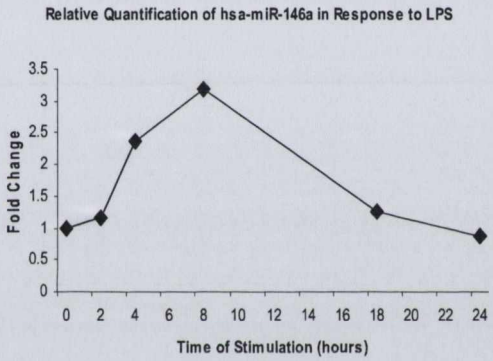


Figure 3.20. **Expression levels of miR-107 and miR-146a in human embryonic kidney cells in response to LPS.** HEK293 ($3x10^5$ cells/mL) were plated and incubated with LPS (0.1μg/mL) or left unstimulated. RNA was extracted and analyzed using miRNA TaqMan PCR with probes specific to miR-107 (A) and miR-146a (B). Fold changes in miRNA expression were calculated using ΔΔCt method with RNA from unstimulated cells as a calibrator and U6 rRNA as an endogenous control. The data shown is representative of an experiment done in triplicate.

A



B



C

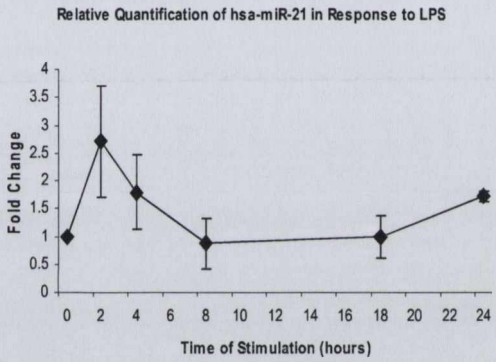
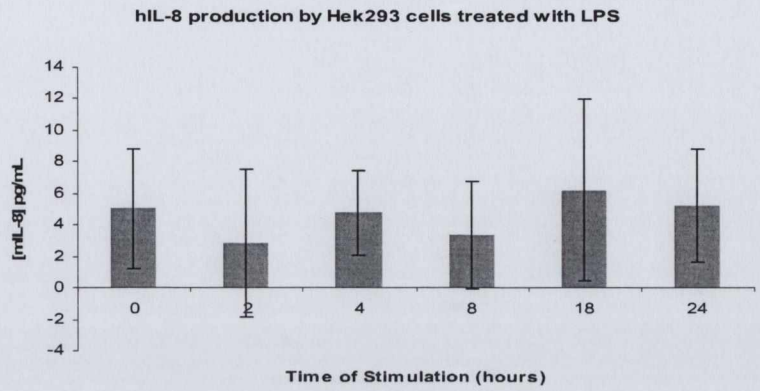


Figure 3.21. **Expression levels of miR-107, miR-146a and miR-21 in human embryonic kidney cells stably transfected with TLR4 in response to LPS.** HEK293-TLR4 ($3x10^5$ cells/mL) were plated and incubated with LPS (0.1μg/mL) or left unstimulated. RNA was extracted and analyzed using miRNA TaqMan PCR with probes specific to miR-107 (A), miR146a (B) or miR-21 (C). Fold changes in miRNA expression were calculated using ΔΔCt method with RNA from unstimulated HEK293-TLR4 cells as a calibrator and U6 rRNA as an endogenous control. The data shown in figures A and C are the mean miRNA expression ± S.E.M. of three separate experiments, each carried out in triplicate. The data shown in B is representative of an experiment done in triplicate.

A



B

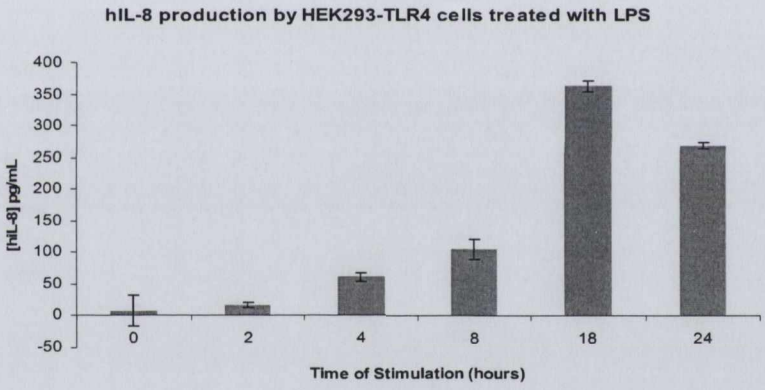
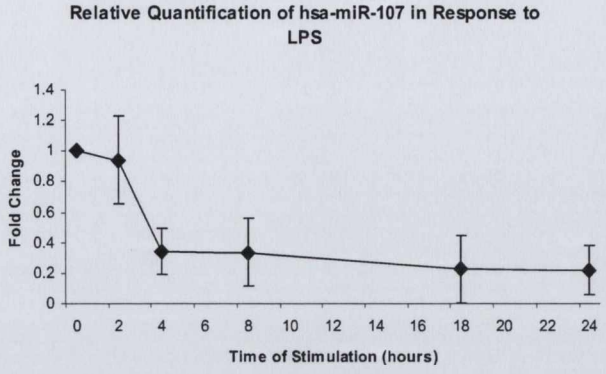


Figure 3.22. **Production of IL-8 cytokine by human embryonic kidney cells and human embryonic kidney cells stably transfected with TLR4 cells in response to LPS.** HEK293 (A) or HEK293-TLR4 (B) ($3x10^5$ cells/mL) were plated and incubated with LPS (0.1μg/mL) or left unstimulated. Supernatants were collected at various time points and analyzed by ELISA for IL-8 production. The data shown represent mean cytokine level ± S.E.M. from three separate experiments, each carried out in triplicate.

A



B

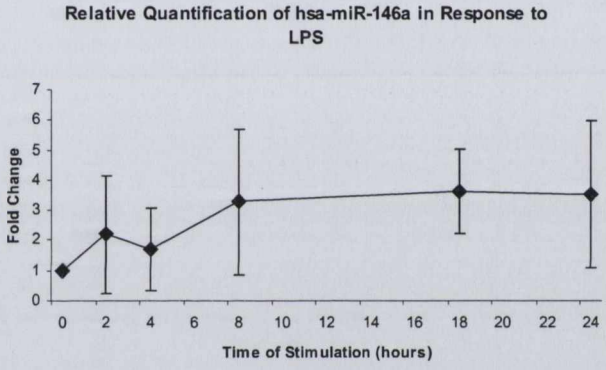
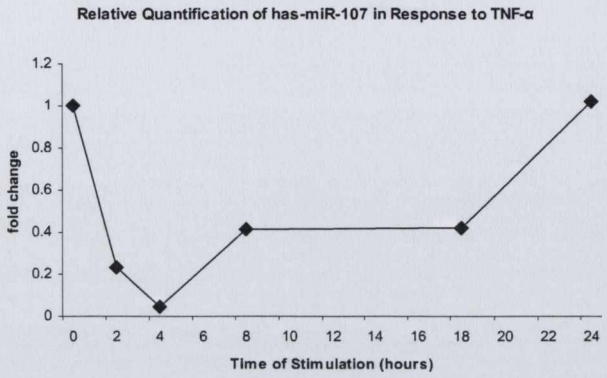


Figure 3.23. **Expression levels of miRNA in human glial cell line A172 in response to LPS.** A172 ($3x10^5$ cells/mL) were plated and incubated with LPS (0.1μg/mL) or left unstimulated. RNA was extracted and analyzed using miRNA TaqMan PCR with probes specific to miR-107 (A) or miR146a (B). Fold changes in miRNA expression were calculated using ΔΔCt method with RNA from unstimulated cells as a calibrator and U6 rRNA as an endogenous control. The data shown is the mean miRNA expression ± S.E.M. of three separate experiments, each carried out in triplicate.

A



B

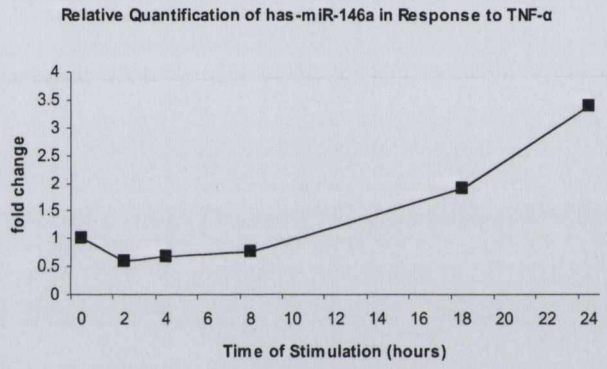


Figure 3.24. **Expression levels of miR-107 and miR-146a in human glial cell line A172 in response to TNF-α.** A172 ($3x10^5$ cells/mL) were plated and incubated with mouse recombinant TNF-α (20ng/mL) or left unstimulated. RNA was extracted and analyzed using miRNA TaqMan PCR with probes specific for miR-107 (A) and miR-146a (B). Fold changes in miRNA expression were calculated using ΔΔCt method with RNA from unstimulated cells as a calibrator and U6 rRNA as an endogenous control. Data shown is from a single experiment done in triplicate and is representative of three separate experiments.

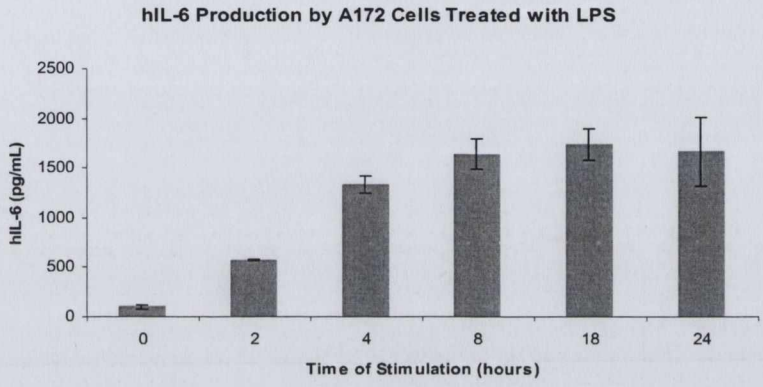
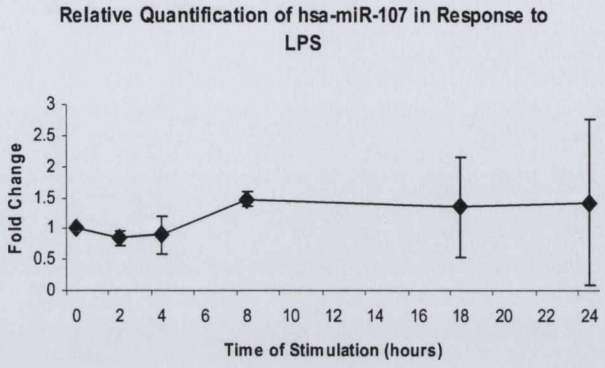


Figure 3.25. **Production of IL-6 cytokine by human glial cell line A172 in response to LPS.** A172 ($3x10^5$ cells/mL) were plated and incubated with LPS (0.1μg/mL) or left unstimulated. Supernatants were collected at various time points and analyzed by ELISA for IL-6 production. The data shown represent mean cytokine level ± S.E.M. from three separate experiments, each carried out in triplicate.

A



B

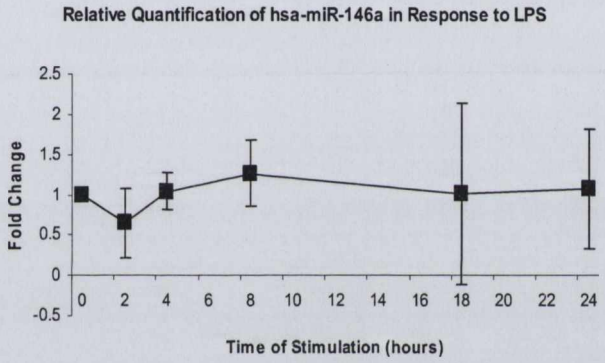


Figure 3.26. **Expression levels of miR-107 and miR-146a in human gut epithelial cell line Caco2 in response to LPS.** Caco2 ($3x10^5$ cells/mL) were plated and incubated with LPS (0.1μg/mL) or left unstimulated. RNA was extracted and analyzed using miRNA TaqMan PCR with probes specific to miR-107 (A) or miR146a (B). Fold changes in miRNA expression were calculated using ΔΔCt method with RNA from unstimulated cells as a calibrator and U6 rRNA as an endogenous control. The data shown is the mean miRNA expression ± S.E.M. of three separate experiments, each carried out in triplicate.

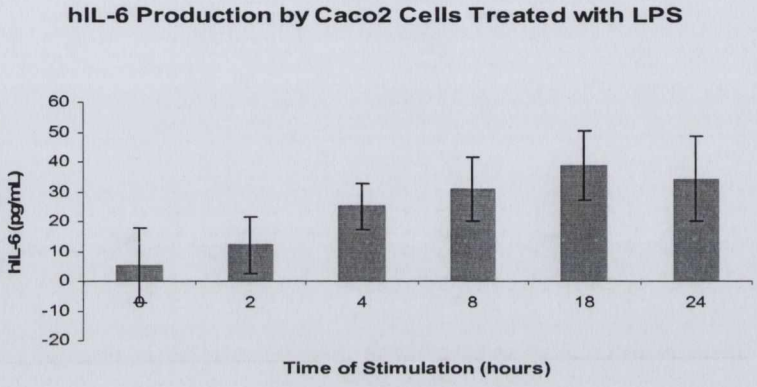
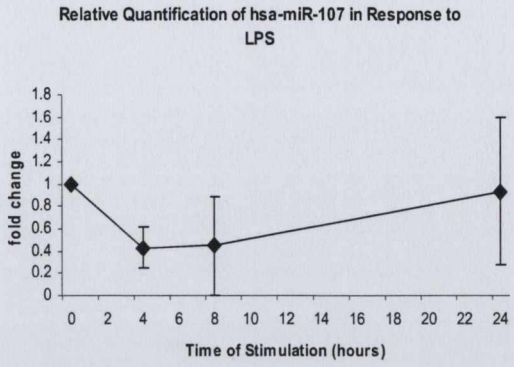
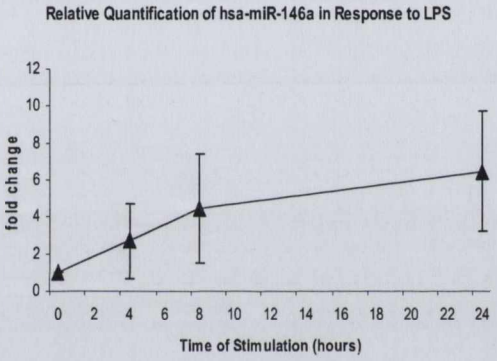


Figure 3.27. **Production of IL-6 cytokine by human gut epithelial cell line Caco2 in response to LPS.** Caco2 ($3x10^5$ cells/mL) were plated and incubated with LPS (0.1μg/mL) or left unstimulated. Supernatants were collected at various time points and analyzed by ELISA for IL-6 production. The data shown represent mean cytokine level ± S.E.M. from three separate experiments, each carried out in triplicate.

A



B



C

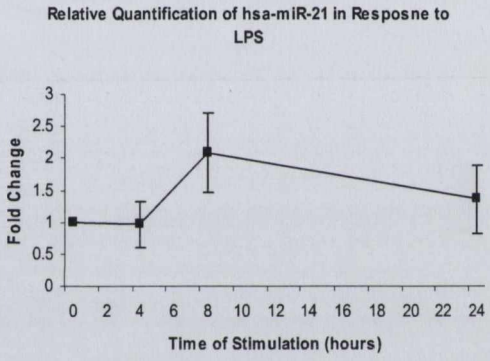


Figure 3.28. **Expression levels of miR-107, miR-146a and miR-21 in human peripheral blood mononuclear cells in response to LPS.** PBMC ($3x10^5$ cells/mL) were plated and incubated with LPS (0.1μg/mL) or left unstimulated. RNA was extracted and analyzed using miRNA TaqMan PCR with probes specific to miR-107(A), miR146a (B) or miR-21 (C). Fold changes in miRNA expression were calculated using ΔΔCt method with RNA from unstimulated PBMC as a calibrator and U6 rRNA as an endogenous control. The data shown is the mean miRNA expression ± S.E.M. of three separate experiments, each carried out in triplicate.

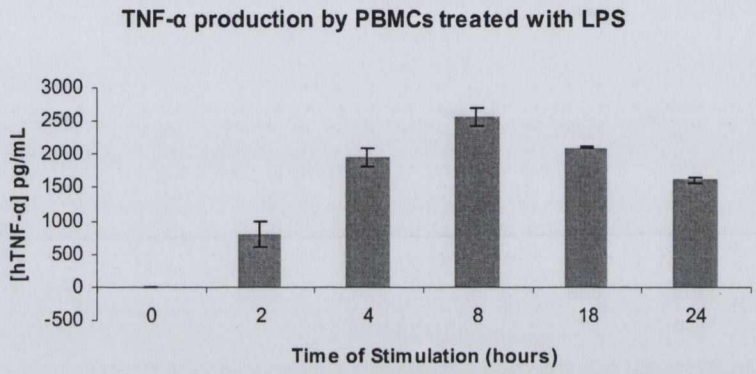


Figure 3.29. **Production of TNF-α cytokine by human peripheral blood mononuclear cells in response to LPS.** PBMC ($3x10^5$ cells/mL) were plated and incubated with LPS (0.1μg/mL) or left unstimulated. Supernatants were collected at various time points and analyzed by ELISA for TNF-α production. The data shown represent mean cytokine level ± S.E.M. from triplicate determinations and are representative of three experiments.

3.4. **Discussion**

A study in 2007 examined the expression of 345 miRNAs in normal human tissue (Liang et al., 2007). This study strengthened the point that miRNA expression is extremely tissue specific. A group of 15 miRNAs were expressed at similar levels in all the tissues examined. These miRNAs could be involved in fundamental functions of the healthy cell such as metabolism. Understanding the expression patterns of a particular miRNA from healthy to disease state is important if it has therapeutic potential. My study initially set out to find novel miRNAs with roles in TLR signaling and I have identified a miRNA, miR-107 that is significantly and consistently downregulated in response to LPS. According to the 2007 study, miR-107 expression is highest in the human brain, the liver and kidney (Liang et al., 2007). I have examined the expression of miR-107 in response to TLR signaling in several cell lines using miRNAs with known roles in immune signaling, miR-146a, miR-155 and miR-21 as positive controls of TLR induction. Each expression study used a U6 ribosomal RNA as an endogenous control of TLR induction. This ribosomal RNA control is highly expressed in the cell so any changes in its expression will affect the expression of the miRNA it is compared to, so any slight changes need to be considered. miRNAs have a significant role in the differentiation of cells so this study examined miRNA expression in dendritic cells and macrophages which undergo differentiation to become mature antigen presenting cells

The murine dendritic cell line DC2.4 was used to examine the expression of several miRNAs that were upregulated or downregulated in response to TLR ligands in Dr. Sheedy's initial study (Sheedy et al., 2010). I found that miR-155 expression is increased in response to the TLR4 ligand LPS. miR-155 expression is the only miRNA studied so far that is both MyD88 and Trif-dependent (O'Connell et al., 2007). miR-155 is one the most studied and characterized miRNA. It was first reported to be upregulated in response to LPS in the human monocytic cell line THP1 (O'Connell et al., 2008; O'Connell et al., 2007). The basal level of expression of miR-155 is much lower compared to other miRNAs such as miR-21 (O'Connell et al., 2009). miR-155 has been shown to directly target SOCS1 and SHIP-1. Mice lacking miR-155 have defects in B cell

differentiation, as well as having severe deficiencies in immune responses when exposed to pathogens (McCoy et al., 2010; O'Connell et al., 2009; Yin et al., 2008).

Several previously unexplored miRNAs were uncovered in this study including miR-214 which was the next miRNA examined in the DC2.4 and I showed that its expression increased in response to LPS. This miRNA has been linked to the expression of PTEN (Jindra et al., 2010; Yang et al., 2008a). The downregulation of PTEN protein has been detected in ovarian cancers and the mechanism of this downregulation was thought to be due to promoter hypermethylation but it is now known to be due to elevated levels of miR-214 in ovarian tumors targeting PTEN protein translation. Inhibition of PTEN leads to the activation or suppression of the Akt pathway, depending on the cell type which induces LPS-induced MAPK and NF-κB signaling cascades (Androulidaki et al., 2009). miR-214 expression is deregulated in ovarian cancer and is upregulated following T-cell activation. Its overexpression led to an increase in proliferation following stimulation and an increase in cell survival.

miR-146a, miR-21 and let-7e expression were examined next in response to LPS. These miRNAs are upregulated in response to LPS. Like miR-155 these miRNAs have been studied and are known to have direct roles in the innate immune response. miR-146a acts as a negative regulator of TLR signaling and cytokine production. Two genes known to be involved in TLR4 signaling, TRAF6 and IRAK1 are targets of miR-146a and it has been shown that LPS induced activation of miR-146a is NF-κB-dependent (Taganov et al., 2006). miR-146a was used a positive control for miRNA function in this study because of its consistent upregulation in many cell types. Table 3.2 provides a summary of miR-146a expression in the various cell types where it was measured. miR-21 has been linked to cell motility, invasion and adhesion, with target genes that include tropomyosin, PDCD4 and PTEN. It was recently shown to negatively regulate the immune response by promoting the anti-inflammatory response through the elimination of PDCD4 and up-regulation of IL-10 (Frankel et al., 2008; Sheedy et al., 2010). Table 3.3 gives a summary of miR-21 expression in the few cell types where it was measured. Let-7e expression increased in the DC2.4 3.5 fold

following 2 hours of LPS stimulation. A study using Akt knockout macrophages showed that LPS stimulation induced let-7e expression in wild-type cells but failed to in the knockout cells (Androulidaki et al., 2009).

miRNA expression can also be down-regulated in response to LPS and TLR4 activation. Let-7i regulates TLR4 signaling through post-transcriptional modification of the TLR4 mRNA via an NF-κB/MyD88 dependent pathway (Chen et al., 2007). Mature let-7 is down-regulated in response to *Cryptosporidium parvum* infection leading to an induction of TLR4 signaling. Another miRNA miR-125b is also down-regulated in response to LPS and TNF-α stimulation. The 3'UTR of TNF-α was identified as a target for miR-125b through the use of a luciferase construct. However, the miRNA expression of miR-125b is never measured, a northern blot is used and it is not the best quality. The down-regulation of miR-125b is thought to be required for a proper inflammatory response (Lu and Liston, 2009; Tili et al., 2007).

I have measured two miRNAs that were downregulated in response to LPS in Dr. Sheedy's initial study of miRNA expression, miR-149 and miR-107 (Sheedy et al., 2010). miR-149 expression was also examined in the DC2.4 in response to LPS. Its expression decreased in response to both TLR ligands. This miRNA has been implicated in renal cell carcinoma (Liu et al., 2010a). Loss of miR-149 led to gain of function of the oncogenes KCNMA1, LOX. miR-149 may also have a role in Hepatitis C entry and replication in the cell (Liu et al., 2010b). A recent study identified Akt1 and E2F1 to be two direct targets of miR-149*. Overexpression of this miRNA induced apoptosis. They found that the pro-apoptotic function of miR-149* could not be reduced by transfecting cells with excess miR-149 which would act as an anti-sense molecule. This result suggests that different cellular mechanisms induce miR-149* and miR-149.

I then examined the expression of miR-107 in response to LPS. miR-107 was consistently downregulated in response to LPS in all cell types except the gut epithelial cell line Caco2 and HEK293. The expression of miR-107 in the different cell types is summarized in table 3.1. This is the first study to link miR-107 expression with innate immune signaling. miR-107 expression has been

implicated in hypoxia, Alzheimer's disease, lung cancer, pancreatic cancer, breast cancer and acute promyelocytic leukemia (Dolt et al., 2007; Garzon et al., 2007; Lee et al., 2009; Martello et al., 2010; Nelson and Wang, 2010; Takahashi et al., 2009; Wang et al., 2008; Wang et al., 2010a; Yamakuchi et al., 2010). miR-107 was first linked to hypoxia in a 2006 study of high altitude yak (*Bos grunniens*). The yak has successfully adapted to the chronic condition of hypoxia from living at high altitudes where oxygen is limited (Dolt et al., 2007). Hypoxia-inducible factor 1 (HIF-1) acts as a global regulator of oxygen homeostasis and consists of the subunits HIF-1α and HIF-1β. When hypoxic conditions arise the cell activates HIF-1α and stabilizes it through post-translational modifications. Abnormal HIF-1α expression has been linked to many hypoxia related diseases. A bioinformatics search found potential miRNAs that could be regulating HIF-1α expression and miR-107 was a strong match. A 2007 study examined miRNAs in hypoxia in the context of cancer. Hypoxia is a key feature of the neoplastic tumor environment (Kulshreshtha et al., 2007). The less oxygen needed by a tumor the more resistant it is to therapies and the more successful it is at invasion. This study showed that hypoxia leaves a miRNA signature in an assortment of cell types. miR-107 was included in the group of miRNAs identified as induced in a hypoxic environment.

Approximately 6% of human miRNAs exhibit HIF-1 sites in their seed sequences. This is thought to signify the functional importance of miRNAs in hypoxia. LPS is a known inducer of hypoxia signaling in a time and dose-dependent manner (Blouin et al., 2004). NF-κB is a critical activator of HIF-1α under both basal and hypoxic conditions (Rius et al., 2008). The cellular process of proliferation is affected by hypoxia. The cell cycle slows down or even stops during oxygen deprivation (Kulshreshtha et al., 2008). Many miRNAs that are predicted to act in hypoxia are also potential regulators of the cell cycle. There may be a coordinated induction of these genes that needs to be tested further. A study from 2010 identified HIF-1β as a direct target for miR-107 (Yamakuchi et al., 2010). When a cell undergoes hypoxia or other cellular stress the tumor suppressor p53 is activated to inhibit cell growth and induce apoptosis. Mutations in p53 are associated with tumor growth and there have been suggestions that p53 is involved in the hypoxic response but the pathway is not known (Yu et al., 2002). A screen for miRNAs expressed in colon cancer samples and regulated by p53

was carried out. These miRNAs were further analyzed to establish a possible role in hypoxia. miR-107 was first characterized and reporter constructs were made containing the upstream region of miR-107 and the gene it is encoded in PanK1α and they found that p53 directly regulated miR-107 expression. They also found that HIF-1 signaling is primarily regulated through the HIF-1β subunit. This study is important because it shows that the tumor suppressor p53 induces miR-107 which targets HIF-1β leading to a decrease in angiogenesis and tumor growth.

miR-107 expression has also been associated with traumatic brain injury and neurodegenerative disease (Redell et al., 2009; Wang et al., 2008; Wang et al., 2010a). A study in 2007 examined the brains from Alzheimer's disease patients. miRNA expression arrays were used to determine the expression patterns from four groups of patients with varying degrees of the disease. miR-107 expression decreased significantly in all patients. *In silico* analysis predicted β-amyloid precursor protein-cleaving enzyme 1 (BACE1) mRNA to be a target for miR-107. In the same patient samples, BACE1 mRNA levels were increased as miR-107 expression decreased. This study also found at least one miR-107 seed sequence within the 3'UTR of BACE1. Another study found that mR-107 expression is decreased following traumatic brain injury but whether or not this decreased expression is related to an increased risk of developing Alzheimer's disease is unknown (Redell et al., 2009; Wang et al., 2010a). A 2010 study identified Granulin as a target for miR-107 in the brain following co-IP analysis used to find miR-107 targets. Granulin has been implicated in a number of human diseases including cancers and neurodegenerative diseases and it is a critical modulator of cell growth Cells that were supplemented with glucose exhibited increased miR-107 expression and decreased granulin expression. The cells also exhibited decreased secretion of the granulin protein (Wang et al., 2010a).

A general trademark of cancer in the human system is a global downregulation of miRNAs. One of the big questions in cancer research is how the cancer cell loses miRNA activity while retaining their basal cellular functions (Martello et al., 2010). A study from this year has discovered that breast cancer cells have found a way to alleviate this problem. Elevated levels of miR-107 expression are found in human breast cancer and these cells target Dicer mRNA resulting in global

miRNA downregulation. Low levels of Dicer are associated with poor survival in lung and ovarian cancer patients. This study speculates that the use of miR-107 as a treatment for breast cancer may be preferential over genetic therapies because it is a reversible means of affecting Dicer protein expression. miR-107 has also been implicated in metabolism. A bioinformatics study found that a large portion of the target mRNA for miR-107 have a role in lipid and energy metabolic pathways (Wilfred et al., 2007).

Other cells used in this study were the murine immortalized BMDM, murine J774 macrophages, murine Raw264.7 macrophages, and primary murine bone marrow derived macrophages and dendritic cells. Human cells were also used in the study including human THP1 monocytes, HEK293 human embryonic kidney cells, HEK293 cells stably transfected with TLR4, Caco2 gut epithelial cells, A172 a human glioblastoma cell line and primary human peripheral blood mononuclear cells (PBMC). Our results have identified a miRNA, miR-107 that is downregulated specifically in many cell types including primary mouse and human cells in response to the TLR4 ligand LPS. LPS stimulation limits miR-107 expression thus releasing its "brake" on its target gene to allow for cellular processes to occur.

Cell Type	Ligand	↑ OR ↓	Time of ↑ OR ↓
DC2.4	LPS	↓	4-18 hours (h)
	TNF-α	↓	4-18 h
J774	LPS	↓	4 h
Raw264.7	LPS	↓	2-24 h
I-BMDM	LPS	↓	18-24 h
	Heat-killed *E. coli*	↓	1 h
Primary BMDM	LPS	↓	4-18 h
Primary BMDC	LPS	↓	4-22 h
THP1	LPS	↑	4 h
HEK293	LPS	---	---
HEK293-TLR4	LPS	↓	8-18 h
A172	LPS	↓	4-24 h
	TNF-α	↓	2-8 h
Caco2	LPS	---	---
PBMC	LPS	↓	4-8 h

Table 3.1. **miR-107 expression in various mouse and human cell types**. The table depicts the cell type used, the immune stimuli used and the time at which miR-107 expression is at its minimum or maximum.

Cell Type	Ligand	↑ OR ↓	Time of ↑ OR ↓
DC2.4	LPS	↑	2-24 h
	TNF-α	---	---
J774	LPS	↑	4-18 h
Raw264.7	LPS	↑	2-24 h
I-BMDM	LPS	↑	4-24 h
	Heat-killed *E. coli*	↑	1 h
Primary BMDM	LPS	↑	4-24 h
Primary BMDC	LPS	↑	18 h
THP1	LPS	↑	18-24 h
HEK293	LPS	↑	4-24 h
HEK293-TLR4	LPS	↑	4-8 h
A172	LPS	---	---
	TNF-α	↑	4-24 h
Caco2	LPS	---	---
PBMC	LPS	↑	4-24 h

Table 3.2. **miR-146a expression in various mouse and human cell types**. The table depicts the cell type used, the immune stimuli used and the time at which miR-146a expression is at its minimum or maximum.

.

Cell Type	Ligand	↑ OR ↓	Time of ↑ OR ↓
DC2.4	LPS	↑	4-24 h
Raw264.7	LPS	↑	18-24 h
Primary BMDC	LPS	---	---
HEK293-TLR4	LPS	↑	2 h
PBMC	LPS	↑	2 h

Table 3.3. **miR-21 expression in various mouse and human cell types**. The table depicts the cell type used, the immune stimuli used and the time at which miR-21 expression is at its minimum or maximum.

CHAPTER 4

MECHANISM OF miR-107 EXPRESSION

4.1. **Introduction**

4.1.1. *Biogenesis of small regulatory non-coding miRNA molecules*

The human genome is comprised of approximately 97% non-coding DNA. According to the miRBase database, the non-coding DNA contains the sequences for 940 identified human non-coding regulatory miRNA sequences and the mouse genome consists of 590 sequences. These hundreds of miRNAs are estimated to post-transcriptionally regulate 30% of the protein-coding genes.(Lewis et al., 2005; Nilsen, 2007). miRNAs were originally thought to only be found within intergenic portions of the genome, acting as their own transcriptional unit (Kim, 2005). It is now known that the majority of miRNAs are found within introns of non-coding and protein-coding genes. In most cases, the transcription of an intronic miRNA corresponds with the transcription of its host gene and at the same level whereas intergenic miRNA are transcribed in a cluster of other miRNAs. However, a study from 2008 identified that one-third of intronic miRNAs have transcription start sites that are independent of their host gene's promoter (Ozsolak et al., 2008). As described in section (1.1), the mature miRNA is produced from a genome encoded primary-miRNA (pri-miRNA) transcript through a series of steps (Kim and Kim, 2007; Rodriguez et al., 2004). The pri-miRNA transcript is spliced from the genome as a complicated double-strand stem-loop structure. Within the nucleus it is cleaved by the Microprocessor complex consisting of the RNase II enzyme Drosha and its cofactor DGCR8 into the precursor-miRNA (pre-miRNA). The pre-miRNA transcript is exported into the cytoplasm of the cell by the Exportin 5 protein and in the cytoplasm it is further cleaved by the RNase III endonuclease Dicer into a double strand miRNA complex consisting of the mature miRNA and the miRNA*. Based on thermodynamic properties one strand (mature miRNA) is favored over the other (miRNA* strand) and escorted into the Argonaute containing RNA-induced silencing complex (RISC) complex where the miRNA will meet its mRNA target sequence resulting in the degradation of the mRNA or its translational inhibition.

This study investigated a novel miRNA that is downregulated in response to LPS stimulation, so I next examined the mechanism underlying this downregulation. It is important to understand how intronic miRNAs are spliced from the genome to

become regulators of mRNA expression if their therapeutic potential is to be fully realized. Several recent studies have examined how pri-miRNA transcripts are spliced from the host intron. During the pre-mRNA process, a complex called the spliceosome splices out introns and the remaining exons are joined together forming a mature mRNA product (Jaillon et al., 2008; Siomi and Siomi, 2010; Sperling et al., 2008). There is thought to be coordinated crosstalk between the spliceosome and the microprocessor complex that cleaves the pri-miRNA transcript into the pre-miRNA. Proteins have been identified that associate with the microprocessor that act as splicing factors. Three possible mechanisms of miRNA-mRNA splicing have been described (Brown et al., 2008). Post-splicing cleavage occurs when the pri-miRNA and mRNA are spliced together and the pri-miRNA is released after splicing. Pre-splicing cleavage occurs when the microprocessor cleaves the pre-miRNA from the mRNA. Co-splicing cleavage occurs when the microprocessor cleaves the pri-miRNA from the mRNA while cleaving the intron resulting in the splicing of the mRNA (Brown et al., 2008). miRNA processing and mRNA splicing are thought to be coordinated processes where the microprocessor and the spliceosome interact with each other in what seems to be a tightly regulated process.

In cancer, miRNAs are often aberrantly expressed and an extensive study of miRNAs in primary tumors found that the downregulation of miRNAs is due to a malfunctioning microprocessor in particular the Drosha enzyme and because of this failure, discrepancies between levels of pri-miRNA and mature miRNA have been found (Thomson et al., 2006). Plant studies have shown that miRNAs undergo post-transcriptional modulation that affect their maturation and stabilization. These include modifications at the 3`terminal end by RNA methyltransferases that protect miRNAs from degradation and uridylation where the miRNA is destabilized. Post-transcriptional adenylation at the 3`end results in a more stabilized miRNA. Another regulatory mechanism is found in the stem-loop of the pri-miRNA. It must possess a certain structure, a terminal loop, an upper stem, a lower stem and basal segments and the terminal loop has been shown to be a major RNA-binding protein site of recognition. Depending on the RNA-binding protein present, the conformation of the stem-loop will change and its interactions with the microprocessor complex will also change. RNA-binding

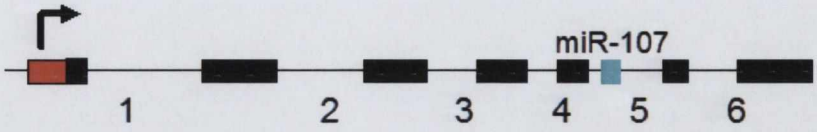
proteins can also recruit other proteins that act as modifying enzymes that may lead to the degradation or destabilization of the pre-miRNA transcript. Another post-transcriptional regulatory element used by the cell to regulate the levels of miRNAs is the presence of exoribonuclease. A study in *Arabidopsis* showed that a gene called small RNA degrading nuclease (SDN) degrades mature miRNA (Ramachandran and Chen, 2008). For normal plant development to occur it is essential that there is efficient miRNA turnover. This could also be the case with the mammalian system. RNase enzymes could be encoded within the genome and are transcribed in host defense situations leading to the degradation of certain miRNA and the upregulation of target genes. There is a tremendous level of regulation over the transcription and post-transcriptional activity of miRNAs indicating that their expression is extremely vital for many cellular functions.

4.1.2. *PanK1α, PPARα and the immune response*

The primary miR-107 sequence is found in intron five of the pantothenate kinase1-alpha (PanK1α) gene on chromosome 10 in the human genome and on chromosome 19 in the mouse (figure 4.1A and B). A recent paper used bioinformatics to suggest that there is a discordant expression between miR-107 and PanK1α based on their expression in different mouse tissues (Polster et al., 2010). Two other studies showed that the activation of the tumor suppressor p53 upregulated miR-107 expression and that miR-107 and PanK1α are co-regulated by p53 (Bohlig et al., 2010). p53 is recruited to the PanK1α promoter after the cell senses there is damage to the DNA. The authors speculate that this increase would lead to a decrease in the cell cycle through the identification of the target genes cyclin-dependent kinase 6 and p130. A similar approach could be used to examine miR-107 promoter expression in response to LPS.

The PanK1α gene is under the control of the transcription factor PPARα (peroxisome proliferator-activated receptor-alpha) (Ramaswamy et al., 2004). The PanK1α promoter region contains binding sites for the transcription factor PPARα as well as a carbohydrate response element, a sterol-regulatory element binding protein site (SREBP) and a glucose response element (GIRE) (Leonardi et al., 2005). Four PPRE are found in the PanK1α promoter region (figure 4.2). PanK1α acts as the key regulatory enzyme in the synthesis of Coenzyme A (CoA) an

A



B

CCTCAACTCCTCTTTCCTGTCTTTCTAATATACCTCAGTGTGAAGAGTTCTACTTTATACACCTTGTATT
TCAGAAAAGGTTCAATTTTTTCCAAACGAATCTTGCAATGCTTCAAAACATGTTAATACAACTTTGTATG
TCACCAGCTCCACCCCTTTTTGTGCCTGGGACTCTGGCTGGCCTTGGCTGTAGCAAGCTCTCTGTGCTTT
GATAGCCCTGTACAATGCTGCTTGAACTCCATGCCACAAGGCAACACTGTAAAGAAGCTGAAAGCAGAGA
GAATATCGAATATTGCAAGTCGAGCATTTTACCTGCAGTTATGTGCAAGGATGCTCAGACCTTTTCCTCA
CATTTCAGTGGACACATGGCAATAATGATGGTTAGAGAGACTATGACATGGGTTGTAATTGTATCCTGTT
TCCACAGGTGAATGGTTTATCATTCATTATCATCCAGTGCCTTCTTAAAAATAAAGCATATATTCCTCCC
CCTCCCCCAACACACACCCCTCCTGTTCTGTAAAGTGTGACTAGAGTAAAGGGAAGCTTTCCTAAGGATA
TGTAGTTGTGTAAGAGTCAACAGGTGTTGCACTGCCAAGATGATGTATATGATGACACACAGCTTTCACC
GGGTTGAGTAAGGCCTTAC

Figure 4.1. **The precursor miR-107 sequence is found in intron 5 of the PanK1α gene**. The precursor sequence is underlined and the mature 23 nucleotide miR-107 sequence is surrounded by a box.

The human PPRE consensus sequence is as follows:

```
      TCACA
AGGNCACAGGTCA
G  A  AGGGTTGGC
      G  T
```

TGAATTTGTGTTGGGCCGTATTCAAAGCCGTCCTGAGCCGCATGCAGGCTGTGGGCCACAGGCTAGACAA
GCTTGATATAAGTCATTTATCCAGTCACAAATAATTACCAAGTGCCTCCT**AGGGATAGAGTGA**TGAACAA
GTCATCTGCCTTAAAGATGCTTACAGTGAAGTGGGGTAAGATGGGCAATCAAATAATAATAATGTCTTTT
TCTAGCACTTACAATGTGCTGGACACTTTACATATGTTAACCTTAAATAATGAGATTTAGAGAACATGAT
TAAGTATGAAGTTTGAGTGCAAAGCTTGAGGATAGCCACCTGGAAACACTAACTCCAAATGAGTGGGATC
AGTGCTCCAAAGTGGAGAAGTTAAGATTTCACTTATACTGGCAGAGATGGAGAAGTTCCAGCAGAATTAC
ATTTTCCATACAAGACCAATGCATATGCCACAGCGATTTGATTGGTTGCAGACTGCTGCATTCCAAGGAA
GATTATTACTCTGTGAGGAGAGGCAGTGATCCAAGGGATTAGTATCTCTGGCCCTGCTCGGTCTTCCTAA
TTATTTACAAGGAAAAAAGGCAAGCCCAGGCATGGTGGCTCATTCCTATAATTCCAATACTTTGGGAGGC
CAAGGTGGGAGGATCGCTTGAGCCCAGGAGTTGGAGGCTACAGTAAGCTACGACTGTGCCACTGCACTCC
AGCCTGGGTGAAGGAGTGAGACCTTGTCTTAAAAAAAAAAAAAAAAAAAAGCAGAAGTTGTAGCTGCATAG
CCACATTTCTCTCAAGTCTCACAAAAAAGTTCCAATAGCTTGAAGTTTGAATTAATTTTACGCATGTGTT
ATGCATTTCATCAGTCTAACAACTCAGTGATGTCCTATTATTCTCAAGTTACAAATGA**GGGAACAGATGC**
ATGGTATAGTTACAAAATGATAA**GGAGTCATAAACAGA**GTACAAGGAGTAGGAAGAGGGTATGGCAGGGA
GACCTAATGTAGCCCTAAGGGTCAGGGAACATTTCTCTAAATATGAGAAGTTAAAGAGGAGATCTAAAGT
TGGAGTCTAGTAGACAAAAGAGGTCTTAGAGAAGAGACTTCTCTAAGGCAATGGAAACAGCAGAATGTTG
TTTAAGGAATTGAAGGCAGCACAGGGAGCCCCTGATGAGGCAGGAGAGGTAGGGAGGGGCCAGATCACCT
GGGTTTTTTTCTCTGTCTTTAAATAGCATAAGGTTAGGGAAGCTAAGAGAGTTGAGATTTGGAGTTTAGT
CCCACCTTTGCTCTTAATAACCTCAGCCATCTGTCTGCAGCTCAGTTTCCTGATACGAAAAAAGTATGCA
AGAGTGGATAGACCAGAGTGCTCCAGTGGCCCCCATGGTTCTCAAGCTCTGATTCTAGGTAAGGCTCTGC
TGGAAGGAATTGCCAGATGCAAGCCCTAGATGCTGCTGAATGCACTGAAGCCCAGGGGCCCAGCAACCCA
GTAGCCAGCCAGCACCTGCC**AGACTCTGACTCC**TCTGTAGATTAATTGCAAATCACGGAGAATATCACAA

Figure 4.2. **Four PPRE are found in the promoter of PanK1α**. The second underlined consensus sequence is found 1370 basepairs from the PanK1α transcription start site and it matches 100% with the human consensus sequence whereas the other three deviate by 1 basepair (Chinetti et al., 2000; Ramaswamy et al., 2004).

essential cofactor in the metabolism of carboxylic acids which includes short and long chain fatty acids (Leonardi et al., 2005). PPARα is ligand induced and belongs to the nuclear receptor family. It is activated in response to fatty acids and eicosanoids, WY14643 (Pirinixic acid), fibrates such as Bezafibrate and fish oils and herbicides. Activated PPARα binds to RXR, and this complex binds to PPRE located in the promoter regions of target genes like PanK1α leading to upregulation of gene expression. Studies have shown that the addition of fibrates to cells increases PPARα mRNA levels and PanK1α promoter activity as well as CoA levels indicating the PPARα-dependent regulation of PanK1α which controls CoA concentrations intracellularly (Ramaswamy et al., 2004).

Both PanK1α and PPARα have known roles in lipid metabolism in the cell but little is known about their possible roles in TLR and immune signaling. PPARα ligands have been shown to inhibit the activation of inflammatory genes including IL-2, IL-6, IL-8 and TNF-α by interfering with NF-κB and AP-1 signaling in a DNA-binding independent manner (Chinetti et al., 2000). When the synthetic PPARα ligand WY14643 was added to cultured Raw264.7 mouse macrophages then stimulated with LPS, nitric oxide and TNF-α production in the cells was reduced (Murakami et al., 2007; Paukkeri et al., 2007). Cells taken from PPARα null mice exhibited enhanced IL-6 production in response to LPS (Delerive et al., 1999). There is evidence that PPARα activation represses both c-Jun and p65 induced transcription of the IL-6 promoter. Through the use of glutathione *S*-transferase pull-down experiments it was demonstrated that PPARα physically interacts with c-Jun and p65. PPARα also prevents the binding of NF-κB and AP-1 to their target gene sequences possibly by preventing the phosphorylation of p65 and inhibiting the degradation of IκBα (Murakami et al., 2007). The transcriptional interference between PPARα and both c-Jun and p65 occurs reciprocally with bidirectional anatagonism, since c-Jun and p65 also inhibit PPARα mediated activation of PPAR response element-driven promoters like PanK1α.

In silico analysis revealed the PanK1α promoter region is hypermethylated leading to transcriptional silencing of the gene (Lee et al., 2009). A recent study identifying epigenetically modified miRNA identified miR-107 as a miRNA that

is methylated in cancer situations leading to its repression. About 10% of miRNAs are epigenetically modified and have methylated promoter regions (Han et al., 2007). Overexpression of miR-107 in pancreatic cancer cells inhibits *in vitro* growth resulting in the repression of cyclin-dependent kinase 6 (CDK6) levels. Epigenetic inactivation of miR-107 has been linked with cell growth (Lee et al., 2009). There is strong evidence that PPARα may be regulating miR-107 expression in TLR4 signaling. In this chapter, I explore PanK1α and PPARα expression in response to LPS in order to help define the mechanism of miR-107 downregulation in response to LPS stimulation.

4.2. **Results**

4.2.1. *Analysis of PanK1α and PPARα expression in DC2.4 cells following treatment with LPS over time*

Because the miR-107 sequence is found in intron 5 of the PanK1α gene, mRNA levels of PanK1α and the transcription factor known to regulate its expression PPARα were analyzed to see if they are also downregulated in response to LPS. This would possibly provide evidence regarding the mechanism of miR-107 regulation. Following LPS treatment at various times, RNA was extracted from DC2.4 cells and analyzed for expression of PanK1α and PPARα. Figure 4.3A shows the downregulation of PanK1α from 2 to 4 hours of about 4 fold but its expression returns to basal levels at 8 hours post stimulation and is downregulated again from 18 to 24 hours. Figure 4.3B shows the downregulation of PPARα following the same trend as PanK1α. It is down about 10 fold at 2 hours and returns to basal levels at 8 hours post stimulation and returns to levels seen at 2 hours at 18 hours.

4.2.2. *Analysis of PanK1α and PPARα expression in Raw264.7 macrophages following treatment with LPS over time*

Raw264.7 macrophages were treated with LPS over a 24 hour period and assessed for PanK1α and PPARα expression. Similar to the DC2.4 cells, PanK1α expression decreased 6 fold from 2 to 8 hours and returned to basal levels at 18 hours post-stimulation as demonstrated in figure 4.4A. PPARα is shown in figure 4.4B and it also decreases 5 fold in response to LPS at 2 hours but remains decreased through 24 hours.

4.2.3. *Analysis of PanK1α and PPARα expression in I-BMDM following treatment with LPS over time*

I-BMDM were treated with LPS over a 24 hour period and assessed for PanK1α and PPARα expression. Similar to the DC2.4 cells and the Raw264.7 cells, PanK1α expression decreased 4 fold from 4 to 8 hours but unlike in the DC2.4 cells, remained decreased through 24 hours as demonstrated in figure 4.5A. PPARα is shown in figure 4.5B and it also decreases 5 fold in response to LPS at

4 hours and remains decreased through 18 hours, but returns to basal levels after 24 hours.

4.2.4. *Analysis of PanK1α and PPARα protein expression following treatment with LPS using SDS-PAGE and western blotting*

I-BMDM and primary BMDM were treated with LPS over time and cell lysates were analyzed on a 12% SDS-PAGE gel and assessed for PanK1α or PPARα protein expression. Figure 4.6A shows PanK1α expression in I-BMDM in response to LPS and figure 4.6B shows its expression in primary BMDM. Starting at 4 hours, its expression begins to decrease and by 24 hours it is gone. Figure 4.4C shows PPARα expression in I-BMDM and similar to PanK1α, its expression also decreases over the 24 hour LPS treatment, beginning at 1 hour post-stimulation.

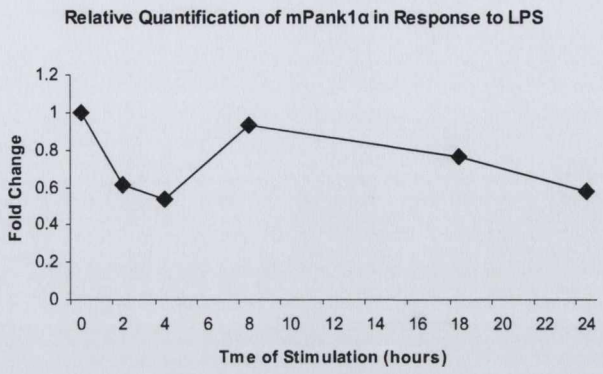
4.2.5. *Analysis of the expression levels of PanK1α and PPARα following infection with heat-killed E. coli in I-BMDM*

I next examined the expression of PanK1α and PPARα in response to a heat-killed *E. coli* infection in the I-BMDM to observe if like miR-107, their expression would decrease and then increase. Figure 4.7A shows PanK1α expression decreases immediately 2 fold at 2 hours post-infection and continue to decrease 8 fold through 4 hours, but level off at 8 hours. PPARα expression did not change drastically in response to the heat-killed *E. coli* infection, only decreasing about 2 fold as shown in figure 4.7B. These decreases are similar to the decrease seen in the expression of miR-107 suggesting that the whole gram-negative bacterium can cause a decrease in miR-107, PanK1α and PPARα.

4.2.6. *Analysis of primary and precursor-miR-107 transcript expression in I-BMDM following LPS stimulation*

To determine if miR-107 downregulation in response to LPS is transcriptionally regulated the expression of the primary and the precursor-miR-107 transcripts were measured. Figure 4.8A shows that after 1 hour of LPS stimulation, primary-miR-107 is downregulated nearly 8 fold and remains decreased through 24 hours. Figure 4.8B shows that the precursor-miR-107 transcript is not downregulated until 8 hours post-LPS stimulation.

A



B

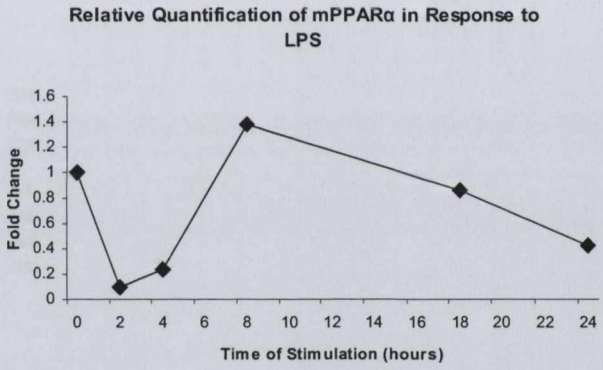
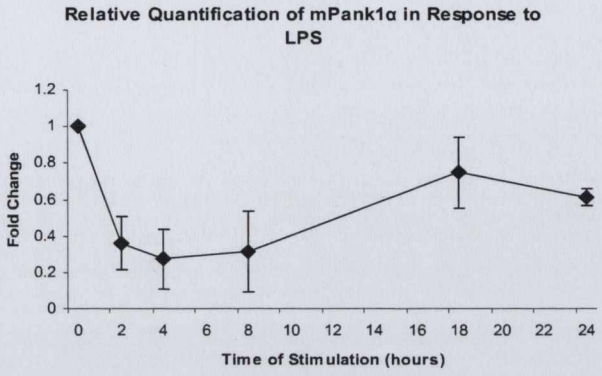


Figure 4.3. **Expression levels of PanK1α and PPARα in murine dendritic cell line DC2.4 in response to LPS.** DC2.4 ($3x10^5$ cells/mL) were plated and incubated with LPS (0.1μg/mL) over time or left unstimulated. RNA was extracted and analyzed using SYBR green PCR with primers specific to PanK1α (A) or PPARα (B). Fold changes in mRNA expression were calculated using ΔΔCt method with RNA from unstimulated cells as a calibrator and GAPDH as an endogenous control. The shown is from a single experiment done in triplicate and is representative of three separate experiments.

A



B

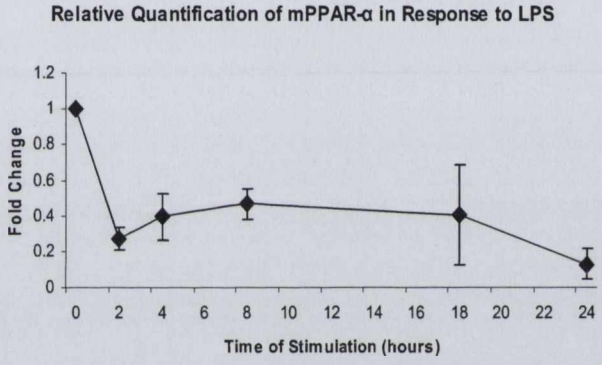
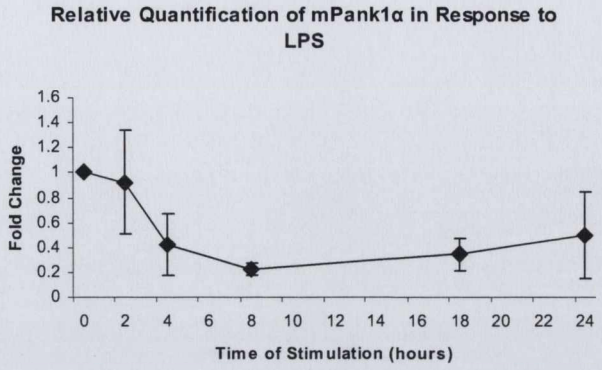


Figure 4.4. **Expression levels of PanK1α and PPARα in murine macrophage cell line Raw264.7 in response to LPS.** Raw264.7 ($3x10^5$ cells/mL) were plated and incubated with LPS (0.1μg/mL) over time or left unstimulated. RNA was extracted and analyzed using SYBR green PCR with primers specific to PanK1α (A) or PPARα (B). Fold changes in mRNA expression were calculated using ΔΔCt method with RNA from unstimulated cells as a calibrator and GAPDH as an endogenous control. The data shown is the mean expression ± S.E.M. of three separate experiments, each carried out in triplicate.

A



B

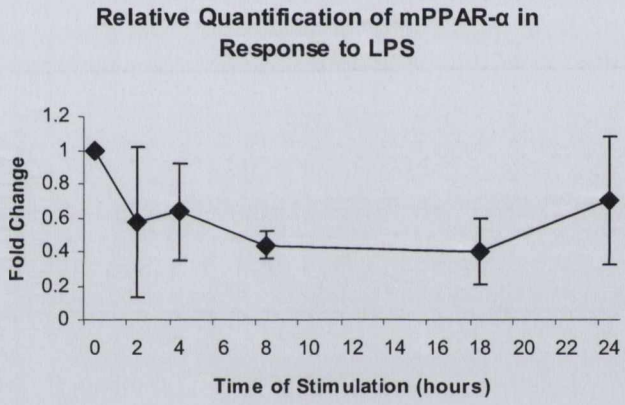


Figure 4.5. **Expression levels of PanK1α and PPARα in murine macrophage cell line I-BMDM in response to LPS.** I-BMDM ($3x10^5$ cells/mL) were plated and incubated with LPS (0.1μg/mL) over time or left unstimulated. RNA was extracted and analyzed using SYBR green PCR with primers specific to PanK1α (AB) or PPARα (B). Fold changes in mRNA expression were calculated using ΔΔCt method with RNA from unstimulated cells as a calibrator and GAPDH as an endogenous control. The data shown is the mean expression ± S.E.M. of three separate experiments, each carried out in triplicate.

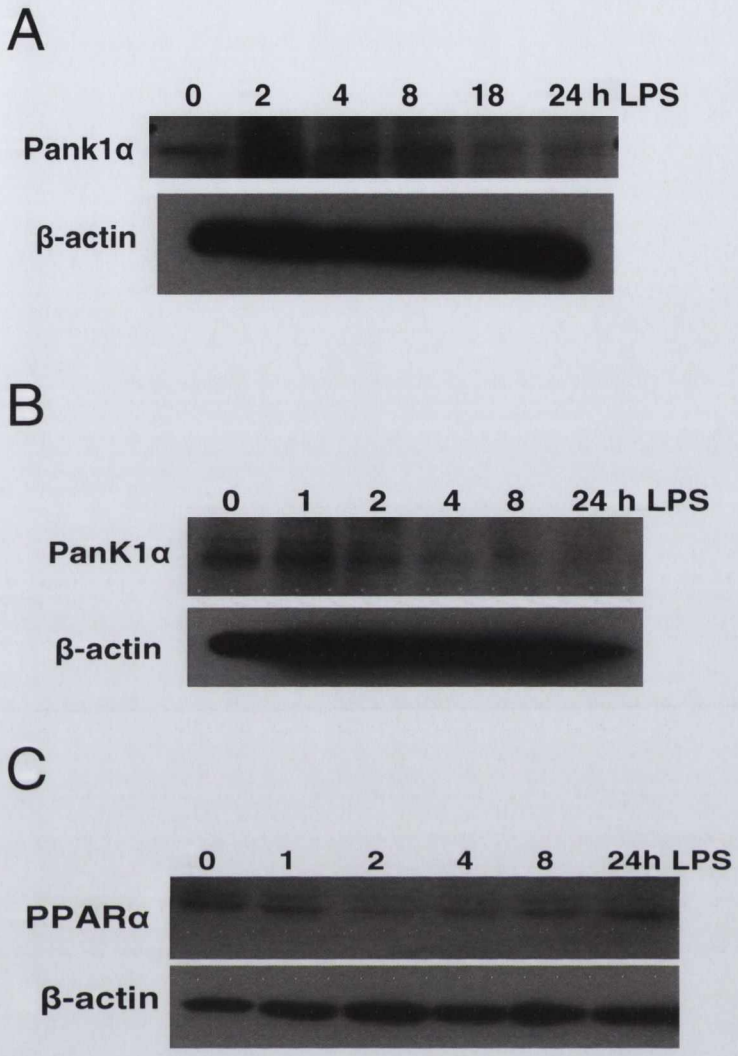
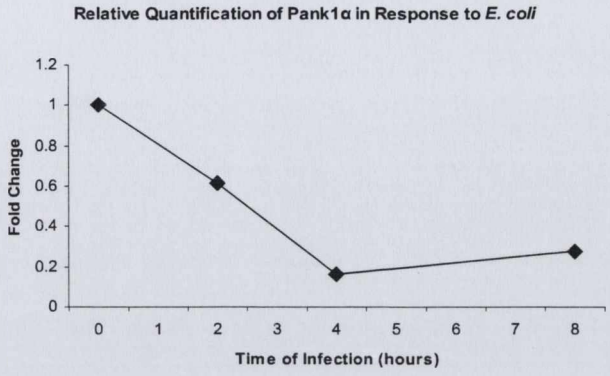


Figure 4.6. **Western blot analysis of PanK1α and PPARα protein expression in I-BMDM in response to LPS**. Immortalized and primary BMDM cells ($3x10^5$ cells/mL) were plated and incubated with LPS (0.1μg/mL) for various times or left unstimulated. Cells were lysed and SDS-PAGE/western blot analysis was used with a primary PanK1α anti-rabbit antibody or primary PPARα anti-rabbit antibody. Figure A shows PanK1α expression in I-BMDM and figure B shows expression in primary BMDM. PPARα protein expression in I-BMDM is shown in figure C in response to LPS.

A



B

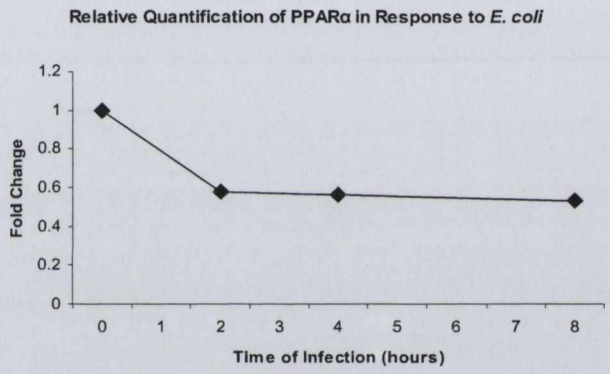
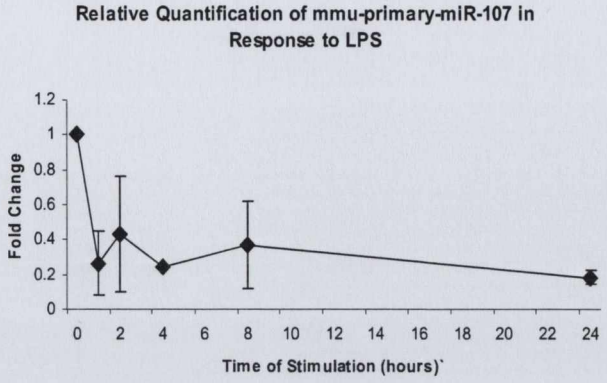


Figure 4.7. **Expression levels of PanK1α and PPARα in I-BMDM in response to *E. coli*.** I-BMDM ($3x10^5$ cells/mL) were plated and incubated with heat-killed (MOI of 40:1) or left unstimulated. RNA was extracted and analyzed using SYBR green PCR with primers specific to PanK1α (A) or PPARα (B). Fold changes in mRNA expression were calculated using ΔΔCt method with RNA from unstimulated cells as a calibrator and GAPDH as an endogenous control. The data shown is representative of an experiment done in duplicate.

A



B

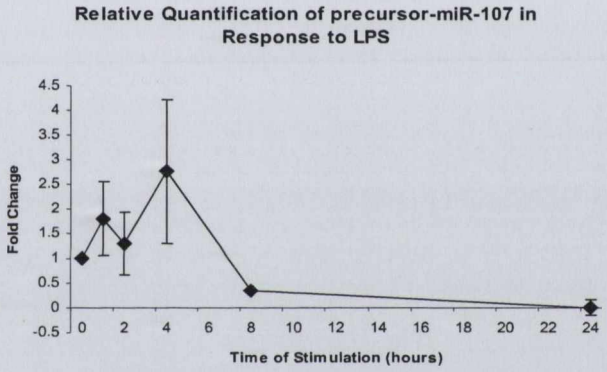


Figure 4.8. **Expression levels of primary-miR-107 and precursor-miR-107 transcripts in murine macrophage cell line I-BMDM in response to LPS.** I-BMDM ($3x10^5$ cells/mL) were plated and incubated with LPS (0.1μg/mL) over time or left unstimulated. RNA was extracted and analyzed using TaqMan PCR for analysis of the primary-miR-107 transcript (A) or SYBR green PCR with primers specific to pre-miR-107 (B). Fold changes in gene expression were calculated using ΔΔCt method with RNA from unstimulated cells as a calibrator and GAPDH as an endogenous control. The data shown is the mean expression ± S.E.M. of three separate experiments, each carried out in triplicate.

4.2.7. *Analysis of miR-107, PanK1α and PPARα expression in adaptor deficient I-BMDM following LPS stimulation*

I next examined miR-107 downregulation in response to LPS in MyD88 and Trif deficient BMDM. RNA was extracted from the adaptor deficient and wild-type BMDM following LPS stimulation and analyzed for expression of miR-107, PanK1α and PPARα. Figure 4.9A shows that after 8 and 24 hours of LPS stimulation, miR-107 is downregulated nearly 8 fold in both the wild-type cells and the Trif deficient cells, but not in the MyD88-deficient cells meaning that miR-107 downregulation is MyD88 dependent. Like miR-107, PanK1α is also downregulated in the wild-type and the Trif-deficient cells at both 8 and 24 hours post-stimulation as shown in figure 4.9B. Similar to miR-107 and PanK1α, figure 4.9C shows that PPARα is downregulated in the wild-type BMDM and Trif deficient cells but is actually increased 2.5 fold following 8 hours of LPS stimulation. Its expression remains decreased about 2 to 3 fold following 24 hours of LPS stimulation.

4.2.8. *Analysis of primary and precursor-miR-107 transcripts in adaptor deficient I- BMDM following LPS stimulation*

Having observed that both the primary-miR-107 and precursor-miR-107 transcripts are downregulated in response to LPS I next examined if the primary transcript is downregulated in MyD88 or Trif deficient BMDM. Figure 4.10A shows that after 8 and 24 hours of LPS stimulation, primary-miR-107 is downregulated nearly 8 fold in both the wild-type cells and the Trif deficient cells, but not in the MyD88-deficient cells meaning that the processing of miR-107 from the genome is MyD88 dependent. Like the primary-miR-107 transcript the precursor-miR-107 transcript is also MyD88-dependent. Figure 4.10B shows that it is decreased in both the wild-type BMDM and the Trif-deficient cells following 8 and 24 hours of LPS stimulation.

4.2.9. *Rantes cytokine production is impaired in Trif deficient BMDM and TNF-α production is impaired in MyD88 deficient BMDM*

To ensure that the adaptor deficient BMDM were behaving as they should Rantes and TNF-α was measured. The activation of the Trif pathway following LPS stimulation results in the activation of IRF and Rantes cytokine production. The

activation of the MyD88 pathway leads to activation of NF-κB and the production of TNF-α. Figure 4.11A and C shows wild-type BMDM produced both Rantes and TNF-α in a time dependent. Trif deficient BMDM were unable to produce Rantes over time as seen in figure 4.11B but were able to produce TNF-α at 24 hours post-stimulation as seen in figure 4.11D. MyD88 deficient BMDM were able to produce Rantes at 24 hours as shown in figure 4.11B but were unable to produce TNF-α in response to LPS as expected.

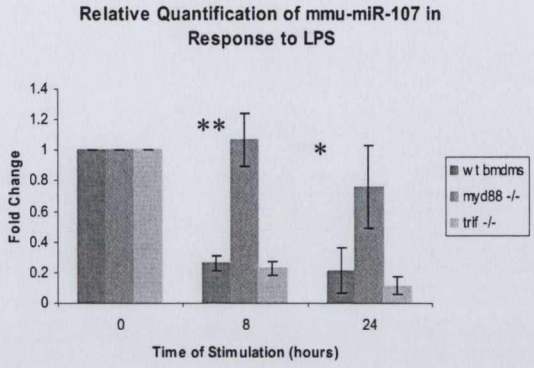
4.2.10. *Analysis of miR-107, PanK1α and PPARα expression in p65 deficient MEF following LPS stimulation*

Previous studies have indicated the expression of the transcription factor PPARα is dependent upon NF-κB signaling. To investigate this further I used wild-type and P65 deficient mouse embryonic fibroblasts (MEF) stimulated with LPS over time and measured miR-107, PanK1α and PPARα expression. Figure 4.12A illustrates that miR-107 is not downregulated in the p65 deficient cells but is still downregulated in the wild-type cells. Figure 4.12B illustrates that PanK1α expression decreases in wild-type cells by 2 fold over 2 to 8 hours post-LPS stimulation, whereas it does not decrease in the p65 deficient cells. Similarly, PPARα expression is shown in figure 4.12C and it decreases in the wild-type cells 4 fold over 1 to 4 hours post-stimulation but does not decrease in the p65 deficient cells. These experiments provide further evidence that miR-107 is regulated by PPARα in a MyD88 and NF-κB dependent manner.

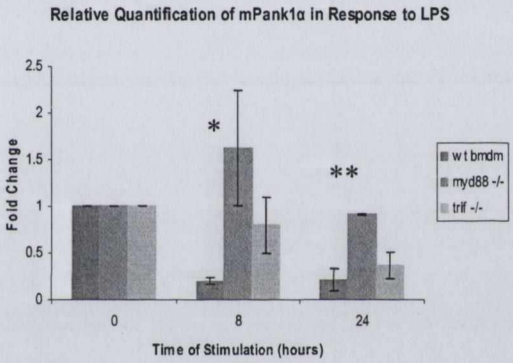
4.2.11. *Analysis of primary and precursor-miR-107 transcript expression in p65 deficient MEF following LPS stimulation*

Based on the evidence obtained in the previous few experiments, I wanted to see if the primary and precursor miR-107 transcripts were p65 dependent. Figure 4.13A illustrates that primary-miR-107 is not downregulated in the p65 deficient cells but is still downregulated 4 fold in the wild-type cells in response to 4 hours of LPS stimulation. Figure 4.13B shows that precursor-miR-107 is not downregulated in the wild-type cells but it is actually increased slightly in the p65 deficient cells. The difference in expression of the primary and the precursor-miR-107 transcripts in response to LPS is due to the lack of p65 in the deficient cells.

A



B



C

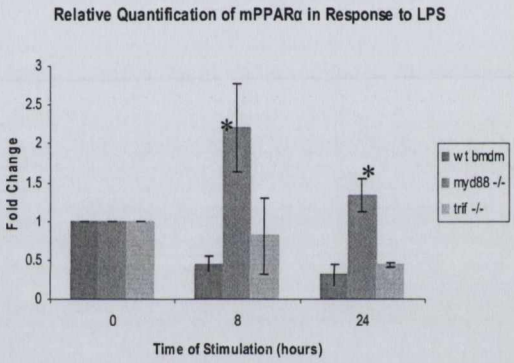
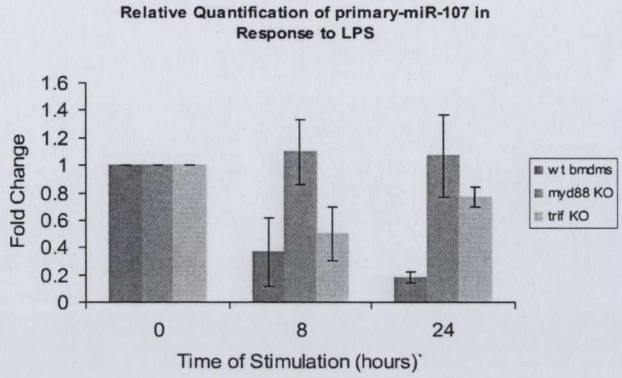


Figure 4.9. **Expression levels of miR-107, PanK1α and PPARα in adaptor deficient I-BMDM in response to LPS.** Wild-type and adaptor deficient I-BMDM ($3x10^5$ cells/mL) were plated and incubated with LPS (0.1μg/mL) for 8 or 24 hours or left unstimulated. RNA was extracted and analyzed using miRNA TaqMan PCR with probes specific to miR-107 (A), SYBR green PCR with primers specific to PanK1α (B) or PPARα (B). Fold changes in miRNA or gene expression were calculated using ΔΔCt method with RNA from unstimulated cells as a calibrator and U6 rRNA or mGAPDH as an endogenous control. The data shown is the mean expression ± S.E.M. of three separate experiments, each carried out in triplicate.

A



B

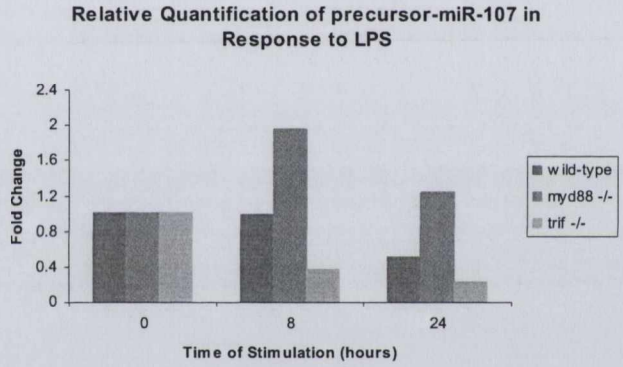


Figure 4.10. **Expression levels of primary-miR-107 and precursor-miR-107 transcripts in adaptor deficient I-BMDM in response to LPS.** Wild-type and adaptor deficient I-BMDM ($3x10^5$ cells/mL) were plated and incubated with LPS (0.1μg/mL) or left unstimulated. RNA was extracted and analyzed using TaqMan PCR for analysis of the primary-miR-107 transcript (A) or SYBR green PCR with primers specific to pre-miR-107 (B). Fold changes in gene expression were calculated using ΔΔCt method with RNA from unstimulated cells as a calibrator and U6 rRNA or mGAPDH as an endogenous control. The data shown in part A are the mean expression ± S.E.M. of three separate experiments, each carried out in triplicate. Data in part B is representative from an experiment done in duplicate.

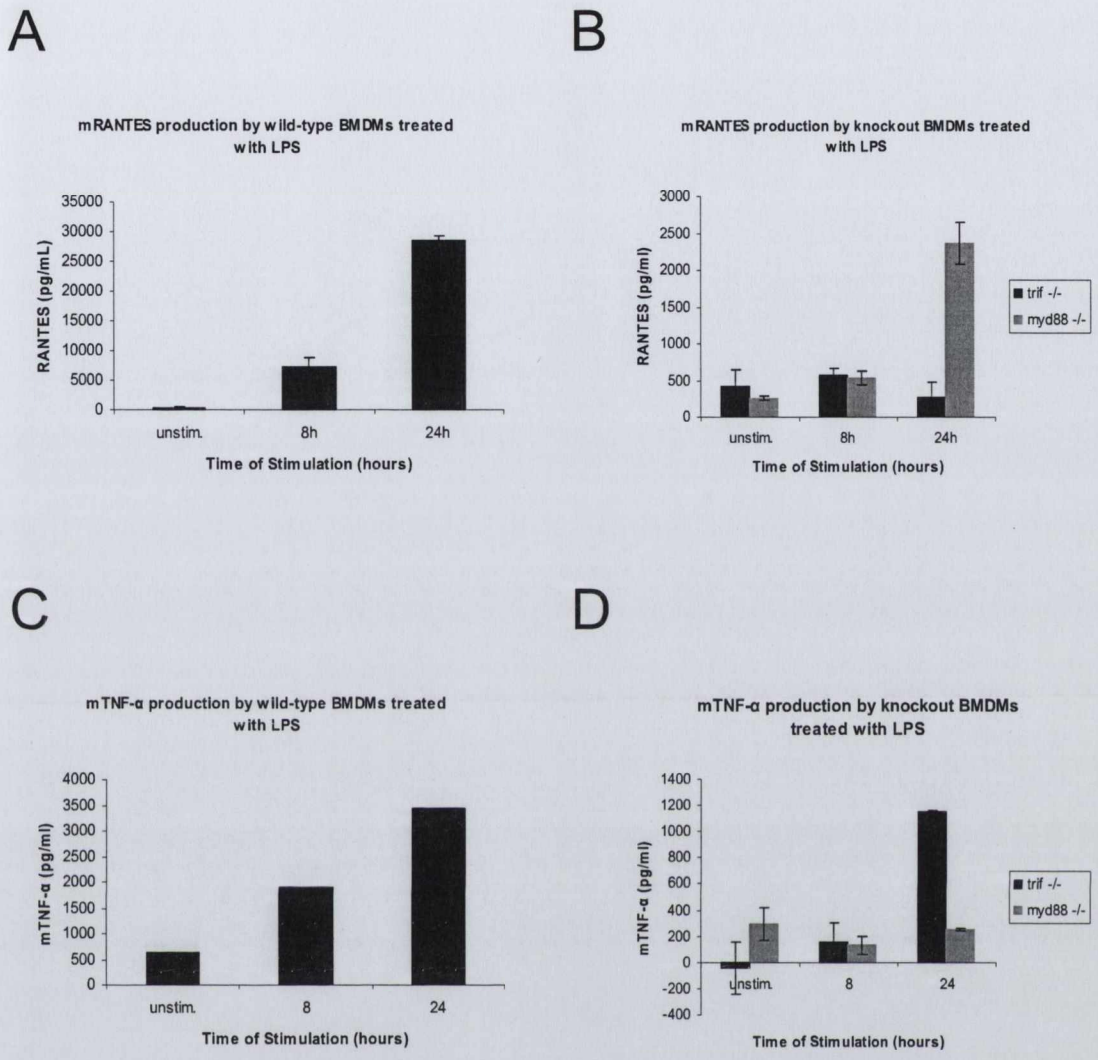
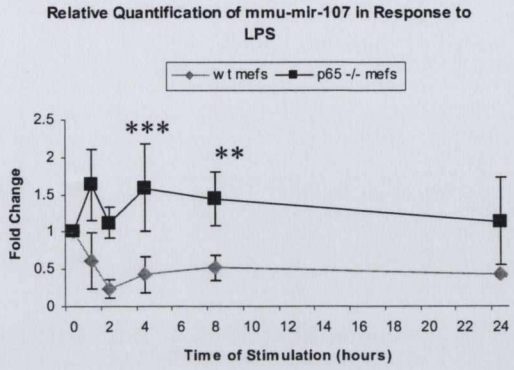
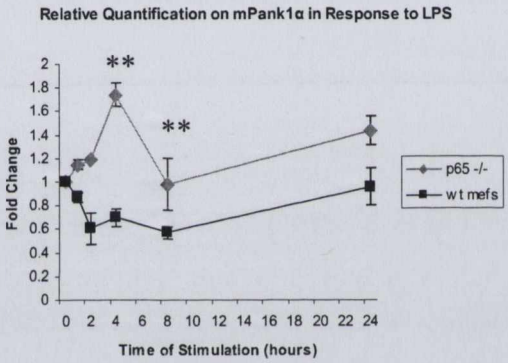


Figure 4.11. **TNF-α and Rantes production in adaptor deficient I-BMDM in response to LPS.** Wild-type and adaptor deficient I-BMDM ($3x10^5$ cells/mL) were plated and incubated with LPS (0.1μg/mL) or left unstimulated. Supernatants were collected at various time points and analyzed by ELISA for Rantes (A and B) or TNF-α (C and D) production. The data shown is the mean cytokine level ± S.E.M. of three separate experiments, each measured in triplicate.

A



B



C

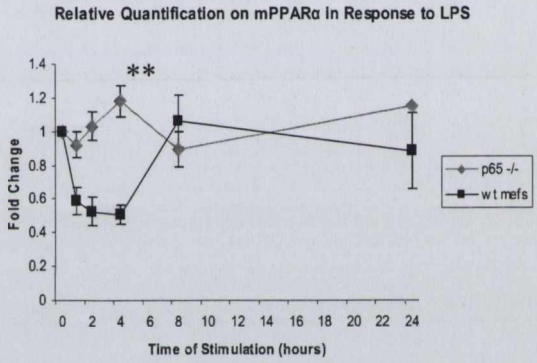
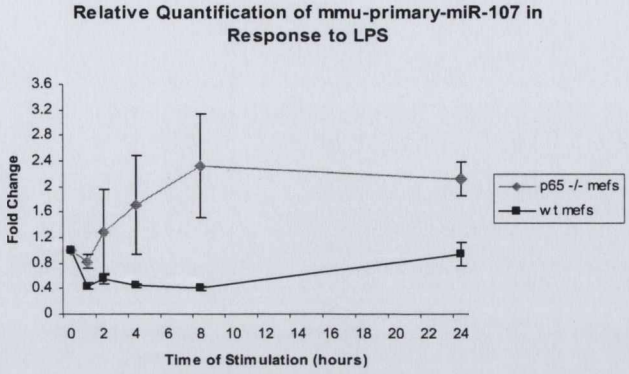


Figure 4.12. **Expression levels of miR-107, mPanK1α and mPPARα in wild-type and p65 deficient mouse embryonic fibroblasts in response to LPS.** MEF ($3x10^5$ cells/mL) were plated and incubated with LPS (0.1μg/mL) or left unstimulated. RNA was extracted and analyzed using miRNA TaqMan PCR with probes specific to miR-107 (A), SYBR green PCR with primers specific to PanK1α (B) or PPARα (C). Fold changes in gene expression were calculated using ΔΔCt method with RNA from unstimulated cells as a calibrator and U6 rRNA or mGAPDH as an endogenous control. The data shown is the mean expression ± S.E.M. of three separate experiments, each carried out in triplicate.

A



B

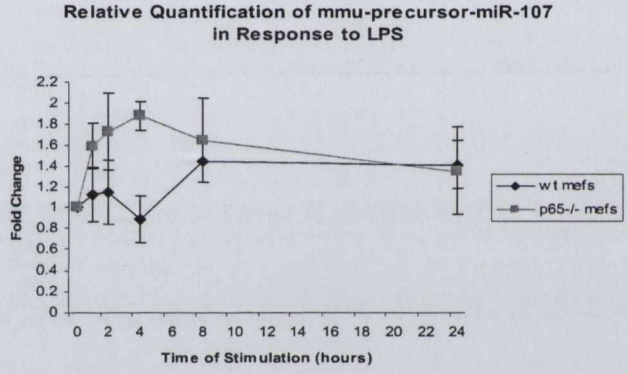


Figure 4.13. **Expression levels of primary-miR-107 and precursor-miR-107 transcripts in wild-type and p65 deficient mouse embryonic fibroblasts in response to LPS.** MEF ($3x10^5$ cells/mL) were plated and incubated with LPS (0.1μg/mL) for various times or left unstimulated. RNA was extracted and analyzed using TaqMan PCR for analysis of the primary-miR-107 transcript (A) or SYBR green PCR with primers specific to pre-miR-107 (B). Fold changes in gene expression were calculated using ΔΔCt method with RNA from unstimulated cells as a calibrator and mGAPDH as an endogenous control. The data shown is the mean expression ± S.E.M. of three separate experiments, each carried out in triplicate.

This data suggests that the downregulation of miR-107 is transcriptionally regulated and it is dependent upon NF-κB signaling.

4.2.12. *Rantes cytokine production is elevated in the p65 deficient MEF but TNF-α production is impaired*

TNF-α and Rantes cytokine production were measured using ELISA to determine if the wild-type and p65 deficient cells were behaving accordingly. Figure 4.14A shows the production of TNF-α by wild-type cells at 24 hours in response to LPS. Figure 4.14B illustrates the enhanced production of Rantes cytokine by the p65 deficient cells from 1 hour to 24 hours compared to the wild-type cells.

4.2.13. *Analysis of PPARα, PanK1α and miR-107 in murine macrophage cell line Raw264.7 following treatment with various doses of the PPARα specific agonist WY14643*

RNA was extracted from Raw264.7 cells treated with various concentrations of the PPARα specific agonist WY14643 (10μM - 100μM) which binds to the ligand binding domain of PPARα. Figure 4.15A shows PPARα expression increased dramatically over 40 fold in response to 10μM of the compound and decreased dose-dependently. PanK1α expression is shown in figure 4.15B and it only increased 2 fold following treatment with the high dose of 100μM for 24 hours. Figure 4.15C shows the expression of miR-107 increased 3 fold following treatment with the low dose of 10μM of the compound and expression decreased in a similar manner as PPARα. It seems that PPARα becomes desensitized to high doses of the compound. The dissimilar expression of PPARα and PanK1α suggests that there may be different pathways for LPS signalling and WY14643 induction. A recent paper described the discordant expression between miR-107 and PanK1α in different tissues like the brain and the liver and the results from this experiment suggest that in different tissues miR-107 may be transcribed independently of PanK1α and because the expression of a single miRNA can vary from cell type to cell type this could be true with the expression of PanK1α and the intronically encoded miR-107 in response to different treatments like WY14643 (Polster et al., 2010).

4.2.14. *Analysis of miR-107 and PPARα expression in I-BMDM following treatment with various doses of the PPARα specific agonist WY14643 for 8 or 24 hours*

RNA was extracted from cells treated with various concentrations of the PPARα specific agonist WY14643 (10μM - 100μM) for 8 or 24 hours and assessed for miR-107 expression. Figure 4.16A shows a dose-dependent increase in miR-107 expression following treatment of I-BMDM with the compound. Its expression reaches it maximum with the high dose of 100μM following 8 hours of treatment. Figure 4.16B illustrates the protein expression of PPARα in response to doses of WY14643 for either 8 hours or 24 hours. Treatment of cells for 8 hours with the higher doses of 10-100μM of WY14643 resulted in an increase in protein expression. Treatment of cells for 24 hours with these higher doses resulted in decreased expression of PPARα compared to the DMSO vehicle control.

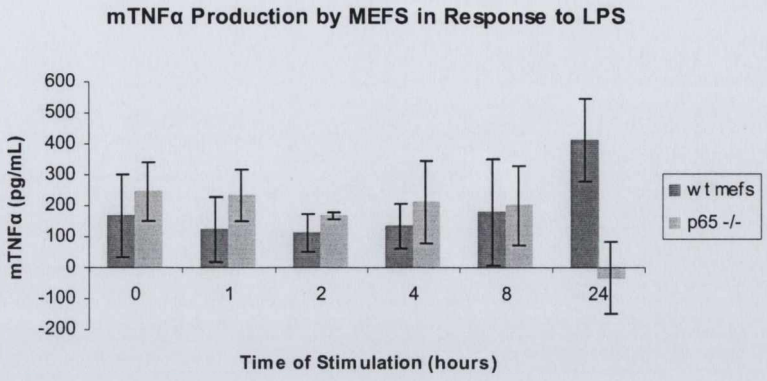
4.2.15. *Production of TNF-α by macrophages pretreated with WY14643 before stimulation with LPS for 6 hours*

Previous studies have shown that the PPARα specific agonist WY14643 can inhibit the production of TNF-α. Figure 4.17A shows that pre-treating cells with higher doses of WY14643, 50μM and 100μM for 1 hour before stimulating with LPS for 6 hours returned TNF-α levels to unstimulated levels in Raw264.7 macrophages. Figure 4.17B shows an opposite dose-dependent effect in I-BMDM. The lower doses of WY14643 inhibited TNF-α greater than the higher doses, but all doses reduced TNF-α production from cells treated with LPS alone.

4.2.16. *Analysis of miR-107, PanK1α and PPARα expression in macrophages pretreated with WY14643 before stimulation with LPS for 6 hours*

Raw264.7 macrophages were pre-treated with either10μM, 50μM or 100μM of WY14643 for 1 hour before the addition of LPS for 6 hours. Expression levels of miR-107, PanK1α and PPARα were then quantified. Figure 4.18A shows the expression of miR-107 decreasing in response to LPS but increasing in response to pre-treatment with 50μM of WY14643 followed by LPS. A similar pattern of expression was seen with PanK1α and PPARα. Figure 4.18B illustrates PanK1α expression and it increases nearly 2 fold in response to pre-treatment with 50μM of WY14643 followed by LPS. Figure 4.18C also shows that PPARα increases in

A



B

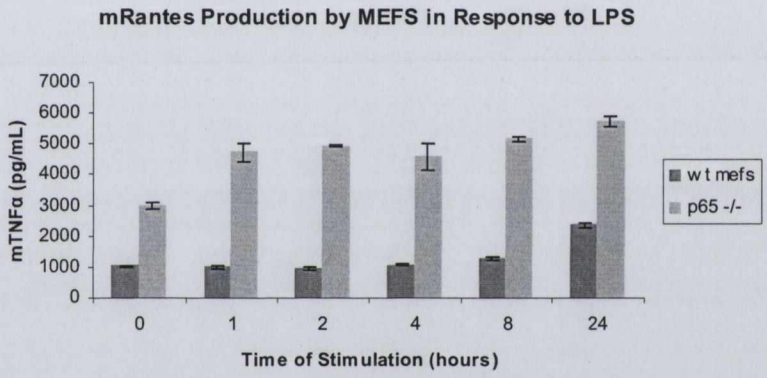
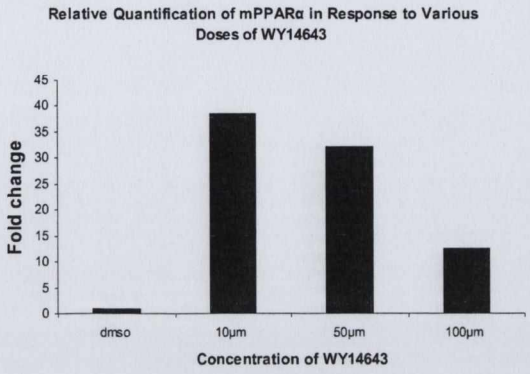
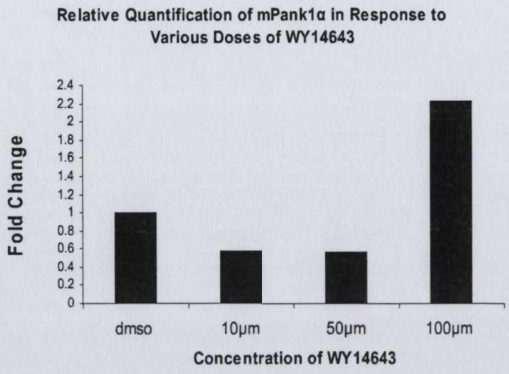


Figure 4.14. **TNF-α and Rantes production by wild-type and p65 deficient mouse embryonic fibroblasts in response to LPS.** MEF ($3x10^5$ cells/mL) were plated and incubated with LPS (0.1μg/mL) for various times or left unstimulated. Supernatants were collected at various time points and analyzed by ELISA for TNF-α (A) and Rantes (B) production. The data shown is the mean cytokine level ± S.E.M. of three separate experiments, each measured in triplicate.

A



B



C

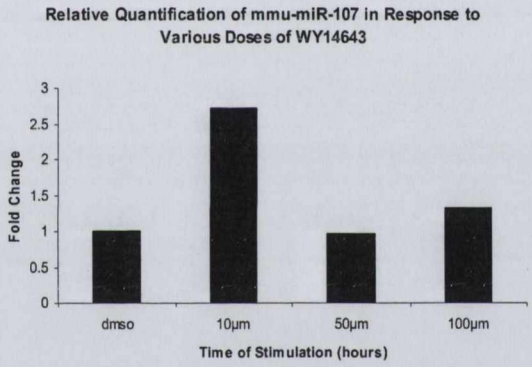
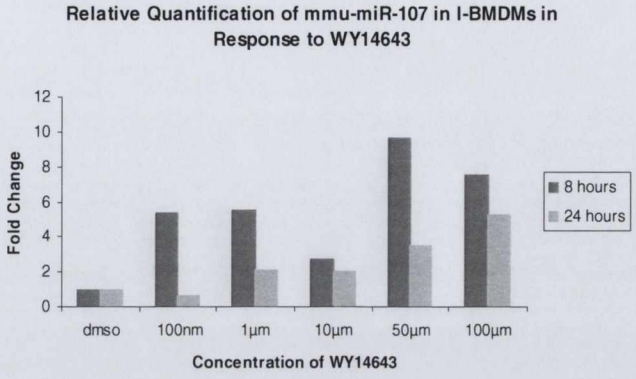


Figure 4.15. **Expression levels of PPARα, PanK1α and miR-107 in murine macrophage cell line Raw264.7 in response to WY14643.** Raw264.7 ($3x10^5$ cells/mL) were plated and incubated with different concentrations of the PPARα specific agonist WY14643 (1μM - 100μM) or the vehicle control DMSO for 24 hours. RNA was extracted and analyzed using SYBR Green PCR with primers specific to PPARα (A), PanK1α (B) or miR-107 (C). Fold changes in gene expression were calculated using ΔΔCt method with RNA from DMSO stimulated cells as a calibrator and mGAPDH or U6 rRNA as an endogenous control. Data shown is representative of data obtained in three individual experiments.

A



B

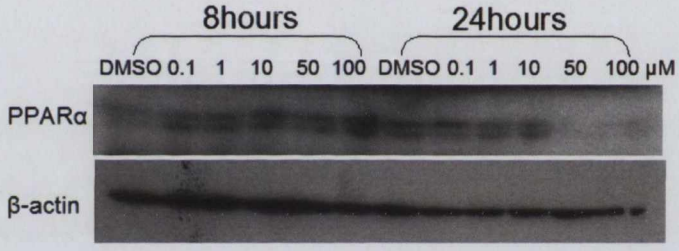
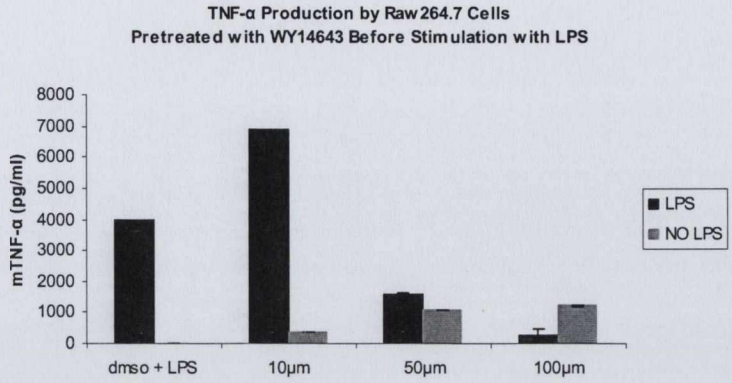


Figure 4.16. **Expression levels of PPARα and western blot analysis of PPARα protein expression in I-BMDM in response to WY14643.** I-BMDM ($3x10^5$ cells/mL) were plated and incubated with doses of WY14643 for 8 or 24 hours or the vehicle control DMSO. RNA was extracted and analyzed using miRNA TaqMan PCR with probes specific to miR-107 (A). Fold changes in miRNA expression were calculated using ΔΔCt method with RNA from DMSO stimulated cells as a calibrator and U6 rRNA as an endogenous control. Data shown is representative of data obtained in two individual experiments. Cells were also lysed and SDS-PAGE/western blot analysis was used with a primary PPARα anti-rabbit antibody (B).

A



B

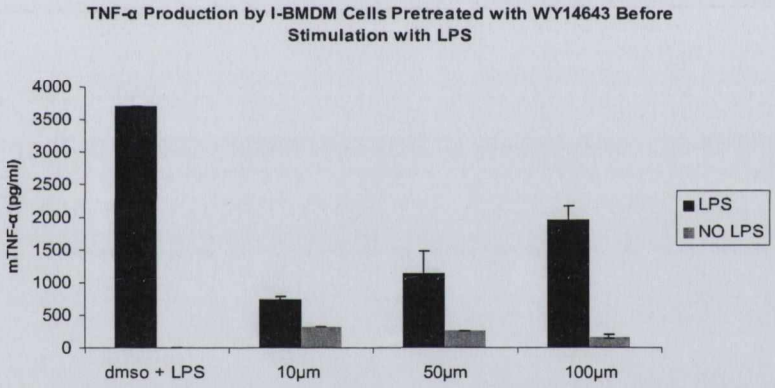
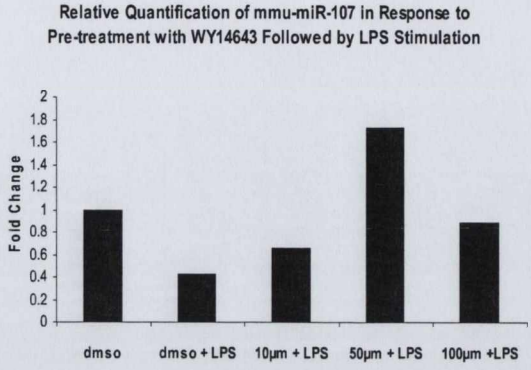
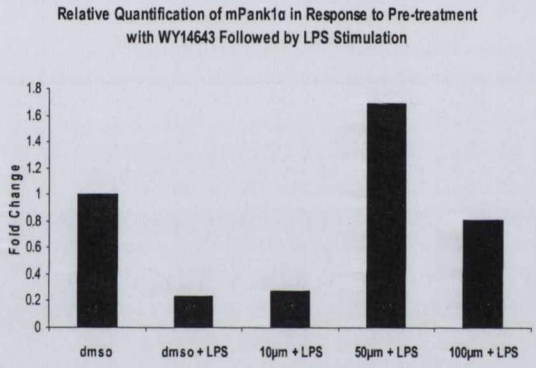


Figure 4.17. **Production of TNF-α Cytokine in Raw264.7 and I-BMDM in response to pre-treatment with WY14643 before LPS stimulation.** Raw264.7 and I- BMDM ($3x10^5$ cells/mL) were plated and pretreated with varying doses of WY14643 for 30minutes before the addition of LPS (0.1μg/mL) for 6 hours or left unstimulated by LPS or treated with the vehicle control DMSO. Supernatants were collected at various time points and analyzed by ELISA for TNF-α production. Figure A shows TNF-α by Raw264.7 and figure B shows TNF-α by I-BMDM. The data shown represent mean cytokine level $\pm$ S.E.M. for three separate measurements of each sample, data is representative of two experiments.

A



B



C

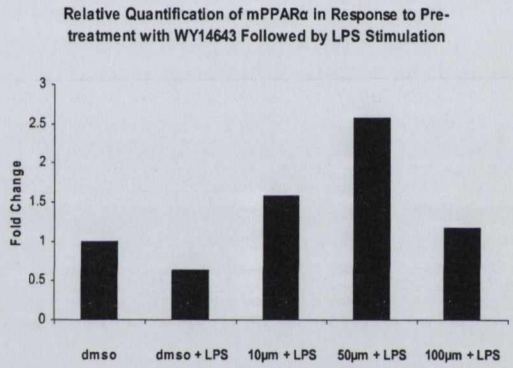


Figure 4.18. **Expression levels of miR-107, PanK1α and PPARα in Raw264.7 in response to pre-treatment with WY14643 before LPS stimulation.** Raw264.7 ($3x10^5$ cells/mL) were plated and pretreated with varying doses of WY14643 for 30 minutes before the addition of LPS (0.1µg/mL) for 6 hours or treated with the vehicle control DMSO. RNA was extracted and analyzed using miRNA TaqMan PCR or SYBR Green PCR with probes or primers specific to miR-107 (A), PanK1α (B) and PPARα (C). Fold changes in expression were calculated using ΔΔCt method with RNA from DMSO stimulated cells as a calibrator and U6 rRNA or GAPDH as an endogenous control. The data shown is representative of data obtained in two separate experiments.

response to pre-treatment with 50μM of WY14643 followed by LPS. Because WY14643 is specific to PPARα, the upregulation of miR-107 in response to it signifies that the upregulation and downregulation of miR-107 is dependent on PPARα expression and regulation.

4.3. **Discussion**

This study confirmed that miR-107 is downregulated in many cell types in response to LPS primarily from 4 to 8 hours post-stimulation. Through the use of MyD88 and Trif adaptor deficient BMDM and p65 deficient MEF, I have found that miR-107 expression is MyD88 and p65-dependent meaning that its expression depends on MyD88 signaling of TLR4 and the activation of the NF-κB signaling pathway. The primary miR-107 transcript is found in intron five of the PanK1α gene and I have found that both the primary and the cleaved precursor miR-107 transcripts are downregulated in response to LPS dependent on MyD88 indicating that the downregulation is transcriptionally regulated. PanK1α mRNA and protein expression are also decreased in a MyD88 and p65-dependent manner in response to LPS in a similar trend as miR-107 suggesting a level of co-regulation. Previous studies have shown that PanK1α is regulated by the transcription factor PPARα. This transcription factor plays an anti-inflammatory role in LPS signaling. I have found that PPARα is also downregulated in response to LPS stimulation along a similar time line as miR-107 and PanK1α and its expression is also dependent upon MyD88 and p65. Through the use of the chemical ligand WY14643 which acts as a specific agonist towards PPARα, miR-107 expression increased in the same manner as PPARα in response to treatment with this compound in Raw264.7 macrophages and I-BMDM. PanK1α mRNA expression only increased in response to the highest dose of WY14643 suggesting that PPARα is regulating its expression in response to the compound but perhaps only when it becomes desensitized. Macrophages that were pre-treated with the compound prior to LPS stimulation exhibited an inhibition in TNF-α cytokine secretion and an increase in miR-107 levels following treatment with the same dose of WY14643 possibly signifying two competing pathways of signaling.

Both PanK1α and PPARα have known roles in lipid metabolism in the cell but little is known about their possible roles in TLR and immune signaling. PanK1α is involved in the first and most highly regulated step in the synthesis of CoA an essential cofactor in the metabolism of carboxylic acids which includes short and long chain fatty acids (Leonardi et al., 2005). The biosynthesis of CoA from pantothenic acid is a universal pathway in both prokaryotes and eukaryotes and

the activation of PanK is the rate limiting step. PanK phosphorylates pantothenate (vitamin B5) into 4'-phosphopantothenate. A study examining the effect of PanK expression on CoA concentration revealed that an increase in PanK protein resulted in a 14-fold increase in CoA levels and 3-fold increase in 4'-phosphopantetheine (Rock et al., 2000). Metabolic state, disease, and use of hypolipidemic drugs all have an effect on the expression of PanK which leads to modifications of CoA levels (Ramaswamy et al., 2004). Intracellular CoA levels decrease in response to glucose and insulin. CoA levels increase in response to glucagon which leads to the process of gluconeogenesis, or the conversion of non-carbohydrate substrates like pyruvate and lactate into glucose (Robishaw et al., 1982). Feedback inhibition of PanK by CoA is needed to control levels of CoA and the level of PanK expression maintains the level of CoA through feedback regulation (Ramaswamy et al., 2004). In mammals there are four genes encoding PanK, PanK1-4. Both mouse and human PanK1 have two isoforms due to an alternative splicing event, PanK1α (60 kilodaltons) and PanK1β (41.6 kilodalotons). However, the human PanK1α differs from the mouse in that its N-terminus has an additional 38 amino acids (Ramaswamy et al., 2004).

The different tissue-specific isoforms of PanK represent the tissue-specificity of CoA production (Leonardi et al., 2010). PanK1 is highly expressed in the liver, PanK2 is most highly expressed in the brain, PanK3 is found in most tissues and there is little information on PanK4 expression although it is known to increase in response to glucose and plays a role in inhibiting pancreatic β-cell apoptosis (Li et al., 2005; Xiang et al., 2007). PanK expression is found primarily in the mitochondria of the cell and most of the CoA in the cell is found in the mitochondria, but CoA biosynthesis occurs in the cytosol. PanK2 mutations result in a decrease in CoA in the brain and have been linked to Pantothenate kinase-associated neurodegeneration (PKAN) disease. There is speculation that like PanK2, the inactivation of PanK1 would have a detrimental effect on CoA synthesis and lead to the progression of diseases like Alzheimer's and Parkinson's diseases which are caused by damage to the mitochondria (Atamna and Frey, 2007; Leonardi et al., 2010). CoA biosynthesis is vital for metabolic function. This was shown in a 2007 study where a pantothenate antimetabolite was used to inhibit all of the PanK isoforms in the cell. Mice treated with the inhibitor

exhibited reduced CoA levels, defective fatty acid oxidation and hypoglycemia (Zhang et al., 2007). Fatty acid oxidation occurs in the mitochondria where fatty acyl-carnitine reacts with CoA to release the fatty acid and produce acetyl-CoA. The liver of the PanK1 knockout mouse contains 40% less CoA in their livers and during starvation, fatty acid oxidation and gluconeogenesis were impaired resulting in hypoglycemia (Leonardi et al., 2010). Serum triglycerides in the knockout mice were elevated and the mice were 10-15% larger than the wild-type controls. This 40% reduction in CoA was not lethal to the mice but it reduced the ability of the liver to produce glucose from pyruvate during gluconeogenesis (Leonardi et al., 2010). LPS may decrease gluconeogenesis and fatty acid oxidation as a way to conserve glucose during infection but this decrease can be detrimental in some tissues and beneficial in other tissues like the heart (Kantor et al., 2000). There is more evidence emerging regarding the interface between metabolism and the immune system. Several cytokines and transcription factors play roles in both functions. So called adipokines, or cytokines that derive from adipose tissue include IL-1 and TNF-α. A rapid increase in metabolic rate and glycolysis is required to support proliferation, and differentiation of T lymphocytes (Atamna and Frey, 2007; Zhang et al., 2007).

A study in 1986 showed that gangliosides cultured with LPS exhibited a decrease in glucose in the media (Ryan et al., 1986). They described it as a decrease in glucose metabolism but only measured glucose remaining in the media so I believe it is actually a decrease in gluconeogenesis due to a decrease in PanK1α expression. Increasing the supply of CoA is vital for the transition from glucose consumption and fatty acid synthesis to gluconeogenesis and fatty acid oxidation. LPS stimulation has been shown to induce hypoglycemia and decrease liver gluconeogenesis in rats (Goto et al., 1994; Lang et al., 1993). LPS is also known to decrease fatty acid oxidation during sepsis (Feingold et al., 2009; Feingold et al., 2008; Memon et al., 1999; Memon et al., 1998). Hepatocytes from rats were isolated and incubated with recombinant TNF-α to evaluate its effects on gluconeogenesis and glucose uptake (Goto et al., 2001). There was a decrease in gluconeogenesis and an increase in glucose uptake indicating a mutual inhibition between TNF-α stimulation and gluconeogenesis. A study using IRAK1 knockout mice showed that wild-type mice exposed to LPS exhibit a dramatic increase in

plasma fatty acids and triglycerides whereas the IRAK1 knockout mice do not accumulate fatty acids. This study showed that the accumulation was due to LPS suppression of fatty acid oxidation genes such as CPT-1 and MCAD. It was also observed that LPS suppresses the expression of the transcription factor PPARα in wild-type mice but not in the IRAK1 knockout mice (Maitra et al., 2009).

The PanK1α promoter region contains binding sites for the transcription factor PPARα (Leonardi et al., 2005). PPARα is ligand induced and belongs to the nuclear receptor family (Chinetti et al., 2000). It is highly expressed in the liver and has a role in regulating the expression of fatty acid oxidation genes (Ramaswamy et al., 2004). The function of PPARα is modified by the shape of its ligand-binding domain which is affected by a number of coactivator and corepressor proteins. It is activated in response to fatty acids and synthetic ligands such as WY14643 and fibrates. These compounds are used to treat diabetes, obesity, dyslipidemia, and recently have been shown to regulate cell growth, survival, migration, and invasion of tumor cells (Pozzi and Capdevila, 2008). The addition of polyunsaturated fatty acids (PUFAs) and fibrates to cells increases PPARα mRNA levels, PanK1α promoter activity and CoA levels indicating the PPARα-dependent regulation of PanK1α which controls CoA concentrations intracellularly (Ramaswamy et al., 2004). The decrease observed in PanK1α expression in response to LPS could be transcriptionally regulated but the mRNA could also be degraded over time. A proteasome blocker like lactocystin or MG132 could potentially interfere with the decrease in PanK1α and establish that it is degradation of the protein.

The main function of PPARα is as a transcription factor functioning to modulate the expression of specific target genes including many inflammatory genes (Moraes et al., 2006). I have found that LPS stimulation leads to a decrease in PPARα mRNA and protein expression. Previous studies have shown that recombinant TNF-α stimulation led to a decrease in PPARα mRNA expression in rat liver hepatocytes. The precise mechanism of PPARα downregulation by TNF-α is not known but TNF-α stimulates the expression of c-Jun a component of the AP-1 signaling pathway and c-Jun and PPARα are known to mutually inhibit each other. A 1999 study demonstrated that activation of PPARα with fibrate treatment

repressed both c-Jun- and p65-induced transcription of the IL-6 promoter. c-Jun and p65 were also shown to inhibit PPARα mediated activation of a PPRE-driven promoter similar to PanK1α. A glutathione S-transferase pull-down experiment demonstrated that PPARα physically interacts with c-Jun and p65 (Delerive et al., 1999). Injection of hypertensive rats with fenofibrates which would increase PPAR-α led to a protective effect on cardiac remodeling by decreasing the expression of c-jun leading to the decrease in the transcription of AP-1 responsive genes (Li et al., 2009a). A 2002 study showed that PPARα positively autoregulates its own expression (Pineda Torra et al., 2002). They demonstrated that the PPARα/RXR complex directly binds to the PPARα promoter. Through the use of the p65 adaptor deficient cells I have shown that the decrease in PPARα mRNA in response to LPS is p65 dependent. This suggests that p65 plays a role in the inhibition of the formation of the PPARα/RXR complex directly or it is interacting directly at the PPARα promoter preventing its transcription. There may also be an unknown factor involved and p65 is affecting this cofactor resulting in the inhibition of either the formation of the complex or the transcription of PPARα leading to a decrease in PPARα, PanK1α and miR-107 expression.

I have used the PPARα specific ligand WY14643 in this study to show the coregulation between PPARα, PanK1α and miR-107 expression. The mRNA expression levels of miR-107, PanK1α and the protein and mRNA of PPARα all increased in macrophage cells in response to the high dose of 100μM of the compound. I also pre-treated macrophages with the compound before stimulating cells with LPS to see if one pathway could suppress the other and I found that treating cells with the 50μM resulted in an increase in mRNA expression of miR-107 and PPARα but only a minor increase in PanK1α suggesting that if the dose is high enough PPARα will not be suppressed by LPS but will be activated and result in an inhibition of TNF-α (Marx et al., 2001). PPARα activating ligands have been shown to inhibit the activation of inflammatory genes by interfering with NF-κB and AP-1 signaling in a DNA-binding independent manner (Chinetti et al., 2000). PPARα prevents the binding of NF-κB and AP-1 to their target gene sequences possibly by preventing the phosphorylation of p65 and inhibiting the degradation of IκBα (Murakami et al., 2007). This is interesting because I have shown that the downregulation of PPARα in response to LPS is dependent upon

the p65 subunit which is required for NF-κB signaling so there seems to a type of feedback inhibition. The p65 subunit is phosphorylated in response to TLR4 signaling leading to the decrease in PPARα mRNA and protein expression. A potential mechanism of PPARα activation by its ligands is via its phosphorylation by p38 MAPK. Previous studies have demonstrated that PPARα is a phosphoprotein and its phosphorylation is increased in the presence of fibrates, insulin and metabolic stress stimuli (Barger et al., 2001; Passilly et al., 1999; Shalev et al., 1996). p38 MAPK activation significantly enhances the phosphorylation of PPARα indicating a level of crosstalk between the two pathways. It has been suggested that the capacity of PPARα to activate target gene transcription is dependent on p38 MAPK but this study used a constitutively active MKK6 to activate p38 which could result in a false positive result. This could be addressed by using the p38 specific inhibitor and observing its effect on PPARα.

PPARα is expressed in differentiated human and mouse macrophages and is thought to have a protective role in the inflammatory response (Chinetti et al., 2000). An anti-inflammatory response resulted when synthetic ligands specific for PPARα activation such as WY14643 were added to cultured Raw264.7 mouse macrophages stimulated with LPS (Murakami et al., 2007; Paukkeri et al., 2007). In another study, agonists of PPARα inhibited the production of cytokine and LPS induced vascular cell adhesion molecule-1 (VCAM-1) and monocyte chemoattractant protein-1 (MCP-1) in LPS treated cells (Xu et al., 2005). Both of these molecules are involved in monocyte recruitment and their reduction by PPARα specific ligands suggests a potent anti-inflammatory role for PPARα (Marx et al., 1999; Murakami et al., 2007). In mice exposed to TNF-α or LPS, PPARα mRNA in the lungs was decreased by 50-60% (Becker et al., 2008). The downregulation of PPARα was maximal at 4 hours post LPS challenge. In mice exposed to LPS and then treated with fibrates or dexamethasone, the downregulation of PPARα was suppressed and lung inflammation was eliminated. A study in 2000 speculated that the decrease in PPARα mRNA in response to LPS is due to mRNA degradation of RXR (Beigneux et al., 2000).

PPARα expression has been linked to the regulation of several miRNA (Shah et al., 2007; Yang et al., 2008b). A study examining the expression of miRNA in hepatic liver cells following the addition of the ligand WY14643 showed that PPARα is a major regulator of miRNA and it regulates hepatocellular proliferation. miR-107 was one of the 27 miRNAs identified in the study as being regulated by PPARα. Its expression increased two fold in response to WY14643. The expression of miRNA let-7c was inhibited following a 4 hour treatment with the ligand. The transcription factor c-myc is a direct target of let-7c. C-myc is a proto-oncogene and its overexpression is linked to many cancers. It is thought the downregulation of let-7c in response to the ligand leads to the upregulation of c-myc and proliferation of liver cells and tumorigenesis. The direct mechanism for the development of tumors following treatment with PPARα ligands remains unknown but they have been shown to increase oxidative stress and DNA synthesis. PPARα-null mice fed WY14643 did not exhibit uncontrolled hepatocellular growth or liver tumors while all wild-type mice developed tumors signifying the requirement for PPARα. Some PPARα agonists have been used for over 30 years to lower triglyceride levels without elevated incidence of cancer, however cancers can take over 20 years to develop following exposure to carcinogens (Shah et al., 2007). So before ligands like WY14643 can be used as a long-term treatment in humans the mechanism of its regulation on miRNA and proliferation need to be understood. This is the first study to show that PPARα downregulation in response to LPS is MyD88 and NF-κB dependent and that PanK1α is downregulated in response to LPS in the same MyD88/ NF-κB-dependent manner. This study has discovered that the MyD88/NF-κB/PPARα-dependent miRNA, miR-107 may play a role in regulating the pro or anti-inflammatory responses depending on the treatment. If its expression is induced it acts in an anti-inflammatory manner, whereas when cells are stimulated with LPS, miR-107 expression decreases leading to an enhanced pro-inflammatory response. I next explored the functional consequences of miR-107 expression to determine exactly how miR-107 affects the inflammatory response.

CHAPTER 5

miR-107 FUNCTION

5.1. **Introduction**

5.1.1. *Functional Consequences of miR-107 Downregulation*

The most challenging aspect of miRNA research is the identification of target mRNA and the functional relevance of that interaction. In recent years, the detection of a target mRNA has relied primarily on the use of miRNA target prediction databases and microarray profiling. It remains unclear if many miRNAs can target a single mRNA but it is obvious now that a single miRNA can target many mRNA. Bioinformatic programs are used routinely to obtain lists of potential target mRNA. A study in 2002 showed that a seed sequence in the 3' UTR of a mRNA of 7-8 nucleotides is sufficient enough for a miRNA to recognize and repress its translation or degrade it (Lai, 2002). The seed sequence can be highly conserved or not very conserved between species. Some computer miRNA databases refer to a context score which is calculated by taking into consideration several "rules" (Grimson et al., 2007b; Lewis et al., 2005). First the site-type contribution or seed match is considered. A single 8mer seed (miRNA positions 1-8) is sufficient to confer strong gene regulation by the miRNA. A single 7mer seed (positions 2-8) is also functional, although less effective. However, the magnitude of regulation for 8mer and 7mer seeds is strongly increased when two or more copies of the site are found in the 3` UTR of the mRNA. This leads to a cooperative repression. Secondly, 3' pairing contribution is taken into account. This reflects the sequence that surrounds the seed region. Thirdly, the AU content 30 nucleotides upstream and downstream of the predicted site of the transcript are considered. The greater the AU content the more effective the match is. Lastly, the position contribution of the seed sequence is important and this reflects the distance to nearest end of the 3`UTR of the target mRNA. The context score is the sum of the scores based on these four criteria (Friedman et al., 2009; Lewis et al., 2003).

Having established that miR-107 expression is downregulated in response to TLR4 stimulation, I next investigated the functional relevance of this downregulation by investigating miR-107 target genes. miR-107 has several published targets including Dicer1, Bace1, NF1-A, HIF-1α and CDK6 (Dolt et al., 2007; Garzon et al., 2007; Martello et al.; Nelson and Wang, 2010; Wang et al.,

2008; Wang et al., 2010a; Yamakuchi et al., 2010). I approached this study by first examining the TargetScan database which revealed a list of hundreds of genes so I found the genes that had already been experimentally validated. The focus of my study became CDK6 which has been shown to be a target for many miRNAs including miR-107 in the context of cancer (Furuta et al., 2010; Johnson et al., 2007; Lee et al., 2009; Li et al., 2009b; Liu et al., 2008; Shi et al., 2010; Wu et al., 2010; Xu et al., 2009; Yang et al., 2009; Zhao et al., 2010).

This study centered on the role of CDK6 in LPS signaling. Cell cycle progression is regulated by a series of CDKs. CDK6 is a subunit in a protein kinase complex that is important for cell cycle G1 phase progression and the G1 to S transition. The activity of this kinase first appears in mid-G1 phase, and it is controlled by regulatory subunits including D-type cyclins. CDK6, as well as its functional analog CDK4, has been shown to phosphorylate and inactivate the tumor suppressor protein retinoblastoma (Rb) and this phosphorylation releases the transcriptional repression on many genes involved in proliferation (Vadiveloo, 1999). CDK6 and CDK4 are expressed ubiquitously in the cell (Grossel and Hinds, 2006a; Meyerson and Harlow, 1994). Certain types of cancer have been shown to preferentially express CDK6 or CDK4 signifying non-redundant functions. CDK6 localizes to the cytoplasm and the ruffling edge of spreading fibroblasts, implicating CDK6 in migration and motility of cells (Fahraeus and Lane, 1999). CDK6 has also been linked to cellular differentiation and the cytoskeletal changes that occur during the process (Slomiany et al., 2006). Overexpression of CDK6 in mouse astrocytes resulted in a lack of stress fibers and differences in cytoskeletal arrangement as well as a greater ability to migrate into a "wounded" monolayer of cells.

CDK inhibitors have demonstrated pro-apoptotic potential (Rossi et al., 2006). Immune cells such as neutrophils undergo apoptosis during the resolution phase of inflammation leading to the recognition and removal of the apoptotic bodies by macrophages. However, if macrophage phagocytosis or neutrophil apoptosis is impaired, chronic inflammation may occur. CDK inhibitors such as R-roscovitine and PD0332991 are undergoing clinical trials as anti-cancer therapies and they have the therapeutic potential to treat inflammatory diseases by targeting

neutrophils for apoptosis. It is suggested that key endogenous survival proteins are the targets of these CDK inhibitors and may be of critical importance in the resolution of inflammation (Leitch et al., 2010). CDK6 has not been linked directly to immune function but based on the evidence provided from previous studies it seems to have the potential to play a role in regulating the proliferation and migration of cells that have been exposed to TLR ligands such as LPS. In this chapter, I examined whether CDK6 is a target of miR-107 in TLR4 signaling and the functional significance of its expression.

5.2. **Results**

5.2.1. *Identifying immunomiRs and target genes using in silico methods*

I first attempted to identify possible target genes for miR-107. The most widely used database for identifying potential target genes is the Massachusetts Institute of Technology (MIT) based site, TargetScan.org. Upon entering miR-107 into TargetScan, 360 conserved mouse genes and 471 conserved human target genes are found. Many of these predicted target genes have a role in the immune response. Table 5.1 lists 43 of the mouse genes identified through TargetScan and table 5.2 lists 56 of the human genes. The lists of predicted targets were entered into the G-profiler database which is used to identify common functions amongst large subsets of genes. Some of the common functions identified for these genes includes regulation of metabolic processes, cell development, formation of membrane bound organelle (endosome), and protein binding; these are shown in figure 5.1.

Some of the predicted targets include four Rab-GTPase family proteins including Rab11FIP2 (family interacting protein 2), Rab1b and Rab11FIP4 (family interacting protein 4) and Rab15. This suggests that miR-107 might have a role in phagosome maturation and trafficking of particles through the cell. Other predicted target genes involved in vesicle trafficking were identified including Vamp1, Vamp4 and Vamp8 (vesicle-associated membrane protein). miR-107 also has several potential target genes with functions related to the actin cytoskeleton and polymerization of filamentous actin (F-actin) including ephrinA7, myosin9, vinculin, Thy-1, and ankyrin1. Genes that have previously been published as miR-107 targets were also on the TargetScan lists. These include NF1-A (Nuclear factor 1 A-type), Bace1, HIF-1β, HIF-1α, Dicer1, and CDK6.

5.2.2. *Quantifying mRNA expression of miR-107 predicted target genes in response to LPS*

RNA was isolated from I-BMDM that had been stimulated with LPS for a 24 hour period and analyzed for expression of various predicted target genes. cDNA was synthesized and primers specific to the sequences of possible target genes of miR-107 were used to quantify mRNA levels in cells stimulated with LPS (See table

2.1 for primer sequences). Figure 5.2 illustrates the expression of EphA7 (A), Myosin9 (B), Vinculin (C), Thy-1 (D) and Ankyrin1 (E). Because miR-107 expression decreases from 4-8 hours post-LPS stimulation I was looking for target mRNA expression that would increase during the same time period as miR-107 downregulation. Myosin9, Vinculin and Ankyrin1 each increased at least 2 fold during the time period of 2-18 hours post-LPS stimulation. I next examined the mRNA expression of Rab11FIP2, Rab11FIP4, Vamp1, Vamp4 and Vamp8 to see if there is an increase in mRNA expression of these genes in response to LPS and this is shown in figure 5.3. None of these genes exhibited an increase in expression in response to LPS stimulation. I then examined genes that had previously been published with a link to miR-107 and this is shown in figure 5.4, these include Bace1 (A) and NF1-A (B) HIF-1β (C) and HIF-1α (D) (Dolt et al., 2007; Nelson and Wang, 2010; Wang et al., 2008; Yamakuchi et al.). HIF-1α protein has previously been shown to increase in response to LPS stimulation (Rius et al., 2008; Westra et al., 2010). Figure 5.4C illustrates that HIF-1α mRNA increases nearly 3 fold following 8 hours of LPS stimulation.

5.2.3. *Quantifying mRNA expression of published targets of miR-107 in response to LPS*

Other potential target genes examined were Dicer1 and CDK6 which have previously been identified as target genes of miR-107 (Lee et al., 2009; Martello et al., 2010; Takahashi et al., 2009). Figure 5.5A shows Dicer1 mRNA expression increasing over 2 fold following 1 hour of LPS stimulation and then its expression decreases to basal levels by 24 hours post-stimulation. Dicer1 expression was also examined in the adaptor deficient I-BMDM to determine if it is dependent upon the MyD88 or the Trif signaling pathways. Figure 5.5B demonstrates that the induction of its expression is MyD88 dependent. p65 deficient MEF were examined next to determine if the upregulation of Dicer1 in response to LPS is dependent on NF-κB signaling. Figure 5.5C shows that its expression is p65-dependent.

Cdk6 expression in response to LPS was investigated next in the I-BMDM cell line. Figure 5.6A illustrates that its expression increases over 2.5 fold after 2 to 4 hours of LPS stimulation followed by a return to basal levels from 8 to 24 hours

Human ortholog of target gene	Gene name	Conserved sites				Total context score
		total	8mer	7mer-m8	7mer-1A	
PDCD10	programmed cell death 10	1	1	0	0	-0.48
RAB11FIP2	RAB11 family interacting protein 2 (class I)	1	1	0	0	-0.46
PHACTR2	phosphatase and actin regulator 2	1	1	0	0	-0.46
RAI14	retinoic acid induced 14	1	1	0	0	-0.39
VAMP4	vesicle-associated membrane protein 4	1	0	0	1	-0.38
ANK1	ankyrin 1, erythrocytic	1	1	0	0	-0.35
RAB1B	RAB1B, member RAS oncogene family	1	1	0	0	-0.31
DICER1	dicer 1, ribonuclease type III	1	0	0	1	-0.28
LRP2	low density lipoprotein-related protein 2	1	0	1	0	-0.27
CORO2B	coronin, actin binding protein, 2B	1	0	1	0	-0.26
VCL	vinculin	1	0	0	1	-0.26
TNPO1	transportin 1	1	1	0	0	-0.26
CDK8	cyclin-dependent kinase 8	1	1	0	0	-0.26
CAPZA2	capping protein (actin filament) muscle Z-line, alpha 2	1	0	1	0	-0.25
BDNF	brain-derived neurotrophic factor	1	0	1	0	-0.25
TGFBR3	transforming growth factor, beta receptor III	1	0	1	0	-0.24
LRP1B	low density lipoprotein-related protein 1B (deleted in tumors)	1	0	1	0	-0.23
SCAMP5	secretory carrier membrane protein 5	1	1	0	0	-0.23
ACTG1	actin, gamma 1	1	0	0	1	-0.23
RIMS3	regulating synaptic membrane exocytosis 3	2	0	1	1	-0.21
VAMP1	vesicle-associated membrane protein 1	1	0	1	0	-0.2
CDK6	cyclin-dependent kinase 6	1	0	1	0	-0.2
ANKRD52	ankyrin repeat domain 52	1	1	0	0	-0.19
CDK5R1	cyclin-dependent kinase 5, regulatory subunit 1 (p35)	1	0	1	0	-0.19
ANKFY1	ankyrin repeat and FYVE domain containing 1	1	0	0	1	-0.18
EFNB2	ephrin-B2	1	0	0	1	-0.18
CDC27	cell division cycle 27 homolog (S. cerevisiae)	1	0	1	0	-0.17
MMP24	matrix metallopeptidase 24 (membrane-inserted)	1	1	0	0	-0.17
ANK3	ankyrin 3, node of Ranvier (ankyrin G)	1	0	0	1	-0.16
TMEM184B	transmembrane protein 184B	1	1	0	0	-0.15
CCNJL	cyclin J-like	1	0	1	0	-0.13
RAB11FIP4	RAB11 family interacting protein 4 (class II)	1	1	0	0	-0.11
CCNJ	cyclin J	1	0	0	1	-0.11
APBA1	amyloid beta (A4) precursor protein-binding, family A, member 1	1	0	0	1	-0.11
PI4KB	phosphatidylinositol 4-kinase, catalytic, beta	1	0	1	0	-0.07
IGSF3	immunoglobulin superfamily, member 3	1	0	0	1	-0.06
RASL12	RAS-like, family 12	1	0	1	0	-0.06
TGIF2	TGFB-induced factor homeobox 2	1	0	1	0	-0.06
LRP1	low density lipoprotein-related protein 1 (alpha-2-macroglobulin receptor)	1	0	1	0	-0.06
THY1	Thy-1 cell surface antigen	1	0	0	1	-0.04
MAP4	microtubule-associated protein 4	1	0	0	1	-0.03
SYT6	synaptotagmin VI	1	1	0	0	N/A
RAB15	RAB15, member RAS onocogene family	1	0	0	1	N/A

Table 5.1. **Selection of the predicted mouse genes targeted by miR-107 with a role in the immune response.** Targetscan.org database was used to predict target mRNAs for miR-107. Fifty-three genes with role in immune response are listed above along with the number a conserved seed sequences and context score.

Target gene	Gene name	Conserved sites				Total context score
		total	8mer	7mer-m8	7mer-1A	
DICER1	dicer 1, ribonuclease type III	**5**	3	1	1	-1.54
TWF1	twinfilin, actin-binding protein, homolog 1 (Drosophila)	**1**	1	0	0	-0.56
MYH9	myosin, heavy chain 9, non-muscle	**1**	1	0	0	-0.53
PDCD10	programmed cell death 10	**1**	1	0	0	-0.48
RAB11FIP2	RAB11 family interacting protein 2 (class I)	**1**	1	0	0	-0.46
IGSF3	immunoglobulin superfamily, member 3	**1**	1	0	0	-0.45
ACTR2	ARP2 actin-related protein 2 homolog (yeast)	**1**	0	1	0	-0.42
TGFBR2	transforming growth factor, beta receptor II (70/80kDa)	**1**	1	0	0	-0.4
RAI14	retinoic acid induced 14	**1**	1	0	0	-0.39
CRKRS	Cdc2-related kinase, arginine/serine-rich	**1**	1	0	0	-0.39
PRKCE	protein kinase C, epsilon	**3**	1	0	2	-0.39
BDNF	brain-derived neurotrophic factor	**1**	0	1	0	-0.36
VCL	vinculin	**1**	1	0	0	-0.36
ANK1	ankyrin 1, erythrocytic	**1**	1	0	0	-0.35
LRP2	low density lipoprotein-related protein 2	**1**	0	1	0	-0.35
IRF2BP2	interferon regulatory factor 2 binding protein 2	**1**	1	0	0	-0.33
RIMS3	regulating synaptic membrane exocytosis 3	**3**	0	2	1	-0.33
CDK8	cyclin-dependent kinase 8	**1**	1	0	0	-0.31
SYT10	synaptotagmin X	**1**	0	1	0	-0.31
TGIF2	TGFB-induced factor homeobox 2	**1**	0	1	0	-0.29
GSTCD	glutathione S-transferase, C-terminal domain containing	**1**	0	1	0	-0.29
RAB1B	RAB1B, member RAS oncogene family	**1**	1	0	0	-0.28
ANKFY1	ankyrin repeat and FYVE domain containing 1	**1**	0	0	1	-0.27
TGFBR3	transforming growth factor, beta receptor III	**1**	0	1	0	-0.26
CORO2B	coronin, actin binding protein, 2B	**1**	0	1	0	-0.26
EXOC5	exocyst complex component 5	**1**	0	1	0	-0.24
LRP1B	low density lipoprotein-related protein 1B	**1**	0	1	0	-0.24
ANK3	ankyrin 3, node of Ranvier (ankyrin G)	**1**	0	0	1	-0.22
CDK6	cyclin-dependent kinase 6	**1**	0	1	0	-0.22
CDC14A	CDC14 cell division cycle 14 homolog A (S. cerevisiae)	**1**	0	1	0	-0.21
VAMP4	vesicle-associated membrane protein 4	**1**	0	0	1	-0.21
VAMP1	vesicle-associated membrane protein 1	**1**	0	1	0	-0.2
SYT6	synaptotagmin VI	**1**	1	0	0	-0.2
SCAMP5	secretory carrier membrane protein 5	**1**	1	0	0	-0.2
SIPA1L2	signal-induced proliferation-associated 1 like 2	**1**	0	1	0	-0.2
CDC23	cell division cycle 23 homolog (S. cerevisiae)	**1**	0	1	0	-0.19
EFNB2	ephrin-B2	**1**	0	0	1	-0.18
IRS2	insulin receptor substrate 2	**1**	0	1	0	-0.17
CDK5R1	cyclin-dependent kinase 5, regulatory subunit 1 (p35)	**1**	0	1	0	-0.17
CNNM2	cyclin M2	**1**	0	1	0	-0.16
VAMP8	vesicle-associated membrane protein 8 (endobrevin)	**1**	0	1	0	-0.15
BAI3	brain-specific angiogenesis inhibitor 3	**1**	0	0	1	-0.15
MMP24	matrix metallopeptidase 24 (membrane-inserted)	**1**	1	0	0	-0.14
RAB11FIP4	RAB11 family interacting protein 4 (class II)	**1**	1	0	0	-0.13

ACTG1	actin, gamma 1	1	0	0	1	-0.12
CCNJ	cyclin J	1	0	0	1	-0.11
CCNE1	cyclin E1	1	0	1	0	-0.1
PELI2	pellino homolog 2 (Drosophila)	1	1	0	0	-0.1
APBA1	amyloid beta (A4) precursor protein-binding, family A, member 1	1	0	0	1	-0.1
IGSF9B	immunoglobulin superfamily, member 9B	1	1	0	0	-0.09
MAP4	microtubule-associated protein 4	1	0	0	1	-0.07
THY1	Thy-1 cell surface antigen	1	0	0	1	-0.07
SYT2	synaptotagmin II	1	0	0	1	-0.06
IPO9	importin 9	1	0	1	0	-0.06
LRP1	low density lipoprotein-related protein 1 (alpha-2-macroglobulin receptor)	1	0	1	0	-0.03
RAB15	RAB15, member RAS onocogene family	1	0	0	1	N/A

Table 5.2. **Selection of the predicted human genes targeted by miR-107 with a role in the immune response.** Targetscan.org database was used to predict target mRNAs for miR-107. Fifty-six genes with role in immune response are listed above along with the number a conserved seed sequences and context score.

Number

of genes			Function
134	GO:0007154	BP	cell communication (1)
112	GO:0051179	BP	localization (1)
103	GO:0051234	BP	establishment of localization (1)
101	GO:0006810	BP	transport (2)
71	GO:0048731	BP	system development (1)
41	GO:0007399	BP	nervous system development (2)
248	GO:0065007	BP	biological regulation (1)
233	GO:0050789	BP	regulation of biological process (2)
60	GO:0048519	BP	negative regulation of biological process (3)
135	GO:0019222	BP	regulation of metabolic process (3)
106	GO:0009889	BP	regulation of biosynthetic process (4)
103	GO:0051171	BP	regulation of nitrogen compound metabolic process (4)
121	GO:0080090	BP	regulation of primary metabolic process (4)
122	GO:0060255	BP	regulation of macromolecule metabolic process (4)
102	GO:0010556	BP	regulation of macromolecule biosynthetic process (5)
105	GO:0010468	BP	regulation of gene expression (5)
224	GO:0050794	BP	regulation of cellular process (3)
56	GO:0048523	BP	negative regulation of cellular process (4)
124	GO:0031323	BP	regulation of cellular metabolic process (4)
106	GO:0031326	BP	regulation of cellular biosynthetic process (5)
103	GO:0019219	BP	regulation of nucleobase, nucleoside, nucleotide and nucleic acid metabolic... (5)
93	GO:0051252	BP	regulation of RNA metabolic process (6)
97	GO:0045449	BP	regulation of transcription (6)
93	GO:0006355	BP	regulation of transcription, DNA-dependent (7)
22	GO:0045595	BP	regulation of cell differentiation (1)
13	GO:0045596	BP	negative regulation of cell differentiation (2)
64	GO:0043412	BP	biopolymer modification (1)
62	GO:0006464	BP	protein modification process (2)
52	GO:0043687	BP	post-translational protein modification (3)
160	GO:0044260	BP	cellular macromolecule metabolic process (1)
160	GO:0034960	BP	cellular biopolymer metabolic process (2)
21	GO:0045202	CC	synapse (1)
28	GO:0030054	CC	cell junction (1)
38	GO:0044430	CC	cytoskeletal part (1)
397	GO:0005623	CC	cell (1)
397	GO:0044464	CC	cell part (2)
324	GO:0005622	CC	intracellular (3)
312	GO:0044424	CC	intracellular part (3)
217	GO:0005737	CC	cytoplasm (4)
265	GO:0043226	CC	organelle (1)
232	GO:0043227	CC	membrane-bounded organelle (2)
265	GO:0043229	CC	intracellular organelle (2)
232	GO:0043231	CC	intracellular membrane-bounded organelle (3)
169	GO:0005634	CC	nucleus (4)
20	GO:0005768	CC	endosome (1)

Figure 5.1. **Common biological functions of miR-107 according to GProfiler.** The list of miR-107 potential target genes obtained from the Targetscan.org database was inputted into the Gprofiler database to find potential common functions of the gene subsets. The image above lists the number of TargetScan genes involved in the function and the gene ontology database function number.

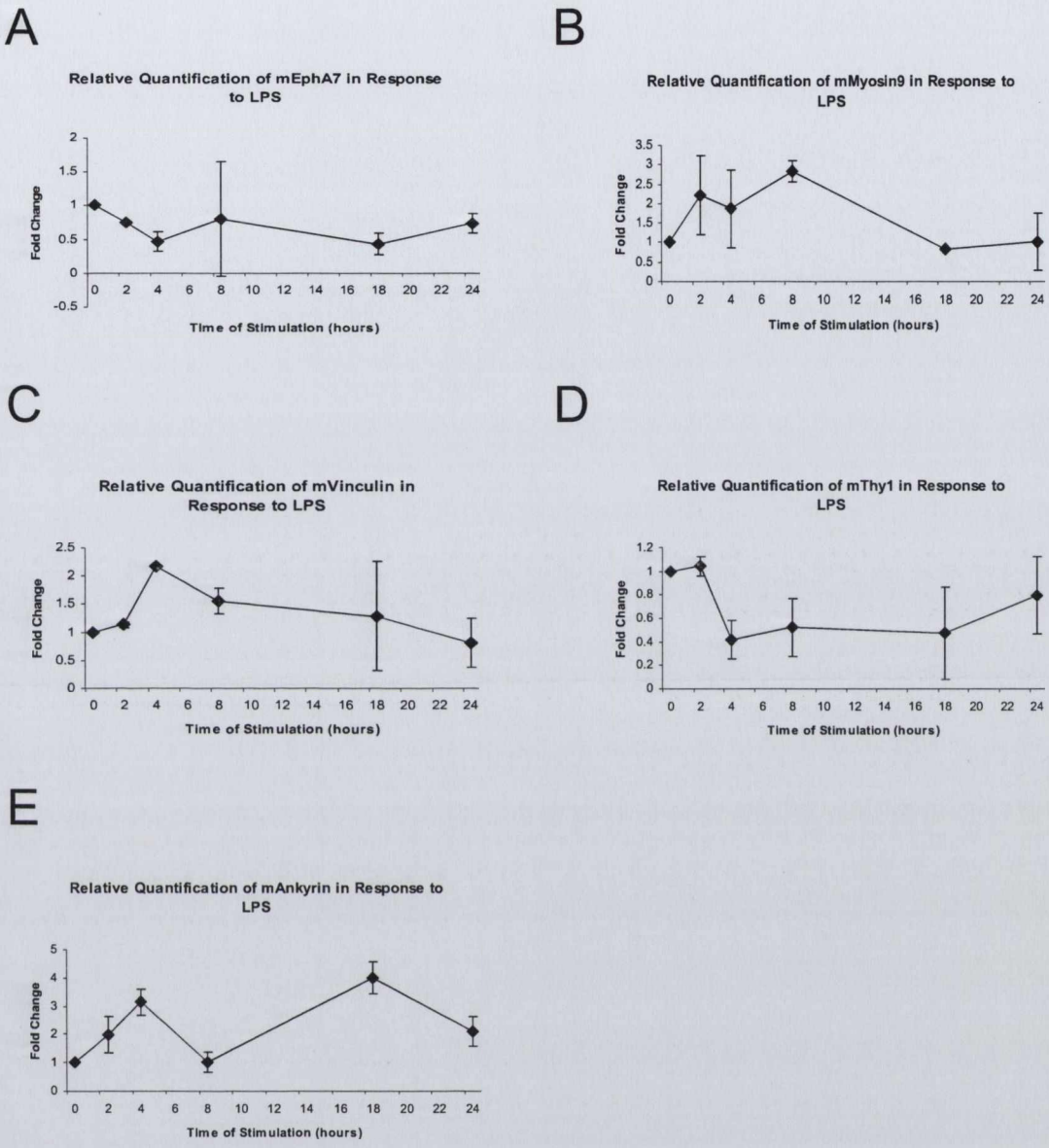


Figure 5.2. **Expression of potential target genes in murine macrophage cell line I-BMDM in response to LPS.** I-BMDM ($3x10^5$ cells/mL) were plated and incubated with LPS (0.1μg/mL) over time or left unstimulated. RNA was extracted and analyzed using SYBR green PCR with primers specific to mEphrinA7(A) mMyosin9 (B) mVinculin (C) mThy-1 (D) and mAnkyrin1 (E). Fold changes in mRNA expression were calculated using ΔΔCt method with RNA from unstimulated cells as a calibrator and GAPDH as an endogenous control. The data shown is the mean expression ± S.E.M. of three separate experiments, each carried out in triplicate.

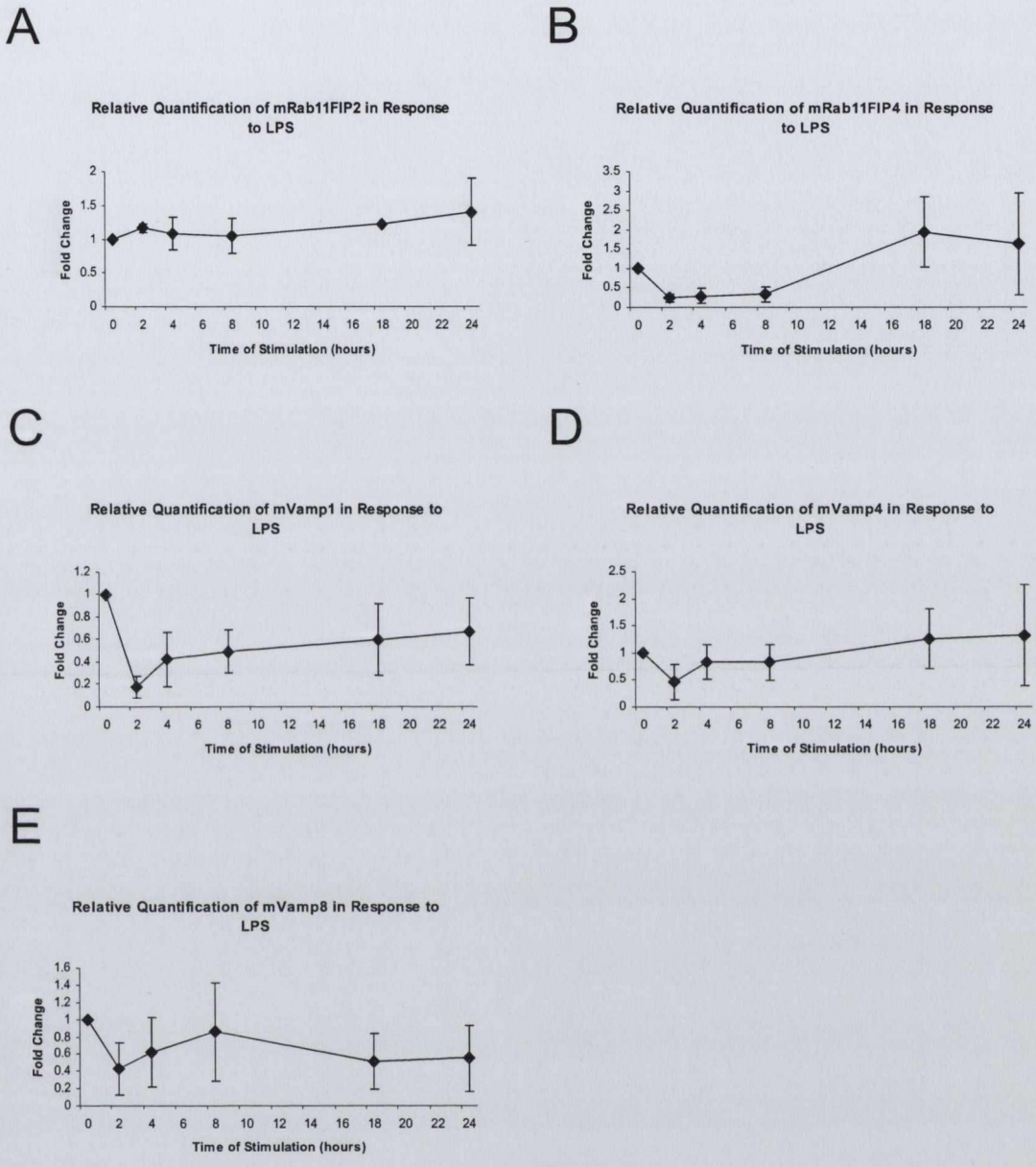


Figure 5.3. **Expression of potential target genes in murine macrophage cell line I-BMDM in response to LPS.** I-BMDM ($3x10^5$ cells/mL) were plated and incubated with LPS (0.1μg/mL) over time or left unstimulated. RNA was extracted and analyzed using SYBR green PCR with primers specific to mRab11FIP2 (A) mRab11FIP4 (B) mVamp1 (C) mVamp4 (D) and mVamp8 (E). Fold changes in mRNA expression were calculated using ΔΔCt method with RNA from unstimulated cells as a calibrator and GAPDH as an endogenous control. The data shown are the mean expression ± S.E.M. of three separate experiments, each carried out on triplicate.

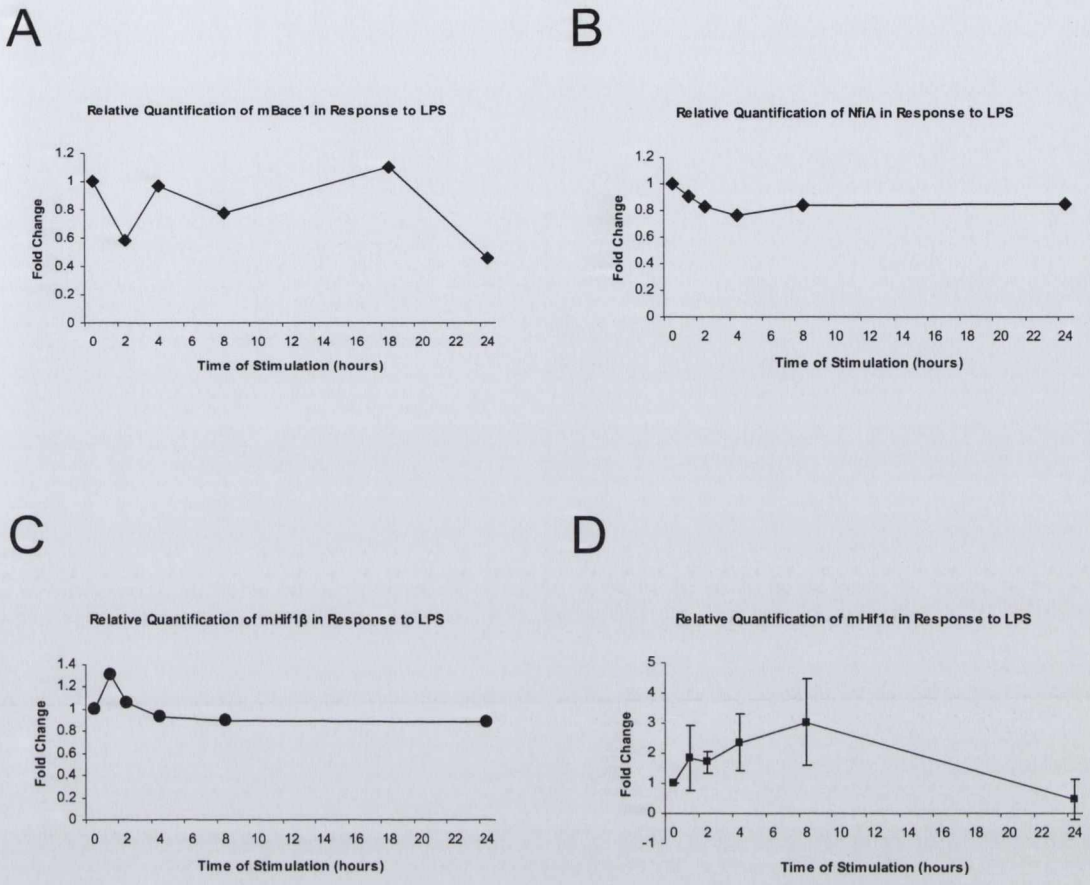
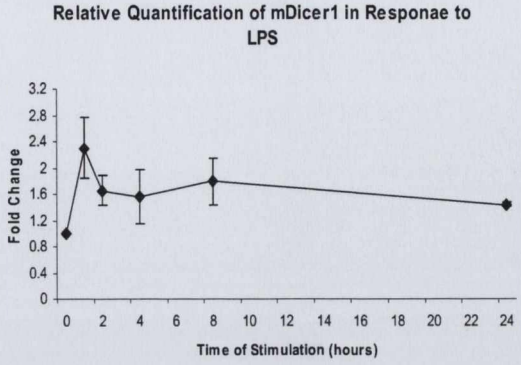
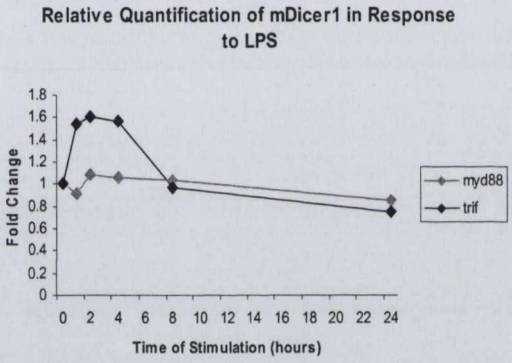


Figure 5.4. **Expression levels of potential known target genes in murine macrophage cell line I-BMDM in response to LPS.** I-BMDM ($3x10^5$ cells/mL) were plated and incubated with LPS (0.1μg/mL) over time or left unstimulated. RNA was extracted and analyzed using SYBR green PCR with primers specific to mBace1 (A), mNF1-A (B), mHif1β (C) and mHif1α (D). Fold changes in mRNA expression were calculated using ΔΔCt method with RNA from unstimulated cells as a calibrator and GAPDH as an endogenous control. The data shown in figure A, B and C are representative of a single experiment done in triplicate. The data shown in figures D are the mean expression ± S.E.M. of three separate experiments, each carried out on triplicate.

A



B



C

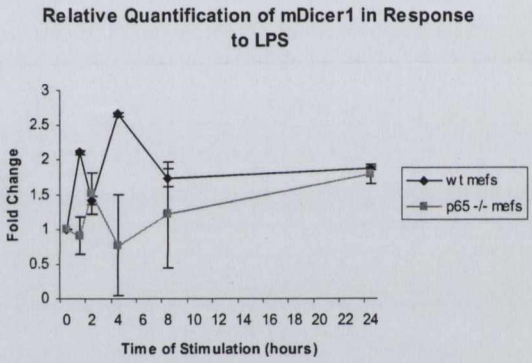
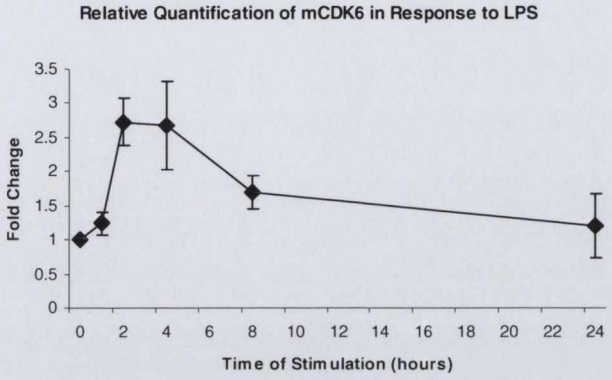


Figure 5.5. **Expression levels of mDicer1 in murine macrophage cell line I-BMDM and MEF in response to LPS.** I-BMDM ($3x10^5$ cells/mL) or MEF were plated and incubated with LPS (0.1μg/mL) over time or left unstimulated. RNA was extracted and analyzed using SYBR green PCR with primers specific to mDicer1. Figure A shows expression in wild-type BMDM, figure B shows expression in MyD88 and Trif deficient BMDM and figure C shows expression in p65 deficient MEF. Fold changes in mRNA expression were calculated using ΔΔCt method with RNA from unstimulated cells as a calibrator and GAPDH as an endogenous control. The data shown in A and C are the mean expression ± S.E.M. of three separate experiments, each carried out in triplicate.

A

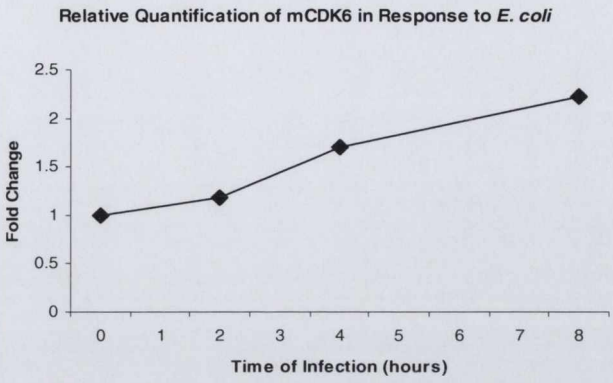


B



Figure 5.6. **Expression level of CDK6 in murine macrophage cell line I-BMDM in response to LPS.** I-BMDM ($3x10^5$ cells/mL) were plated and incubated with LPS (0.1μg/mL) over time or left unstimulated. RNA was extracted and analyzed using a TaqMan probe specific to mCDK6. Figure A shows mRNA expression in I- BMDM and figure B shows CDK6 protein expression in I-BMDM. Fold changes in mRNA expression were calculated using ΔΔCt method with RNA from unstimulated cells as a calibrator and GAPDH as an endogenous control. The data shown in figure A are the mean expression ± S.E.M. of three separate experiments, each carried out in triplicate

A



B

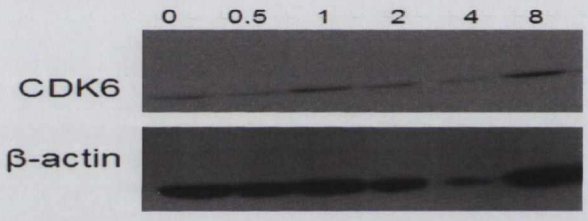
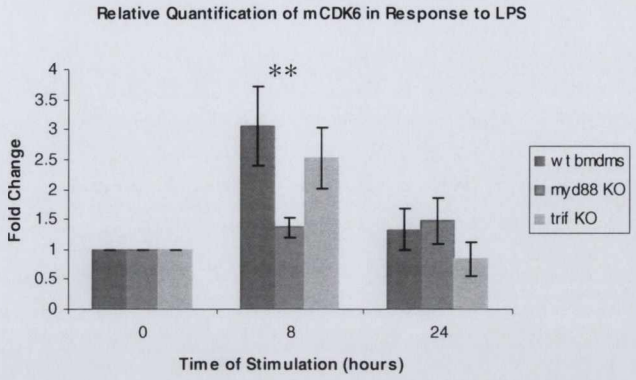


Figure 5.7. **Expression level of CDK6 in murine macrophage cell line I-BMDM in response to *E. coli*.** I-BMDM ($3x10^5$ cells/mL) were plated and incubated with heat-killed (MOI of 40:1) *E. coli* or left unstimulated. RNA was extracted and analyzed using a TaqMan probe specific to mCDK6. Figure A shows mRNA expression in I-BMDM and figure B shows CDK6 protein expression in I-BMDM. Fold changes in mRNA expression were calculated using ΔΔCt method with RNA from unstimulated cells as a calibrator and GAPDH as an endogenous control.

A



B



C

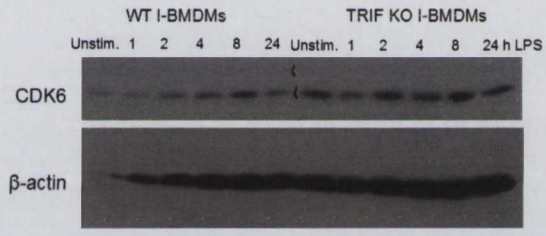
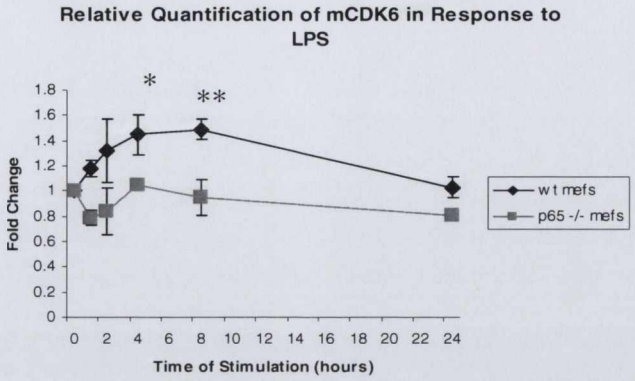


Figure 5.8. **Expression levels of mCDK6 in adaptor deficient murine macrophage cell line in response to LPS.** Wild-type and adaptor deficient I-BMDM ($3x10^5$ cells/mL) were plated and incubated with LPS (0.1μg/mL) over time or left unstimulated. RNA was extracted and analyzed using a TaqMan probe specific to mCDK6. Figure A shows mRNA expression in adaptor deficient BMDM and figure B shows protein expression MyD88 deficient I-BMDM and figure C shows CDK6 protein expression in Trif knockout I-BMDM. Fold changes in mRNA expression were calculated using ΔΔCt method with RNA from unstimulated cells as a calibrator and GAPDH as an endogenous control. The data shown in figure A are the mean expression ± S.E.M. of three separate experiments, each carried out in triplicate

A



B

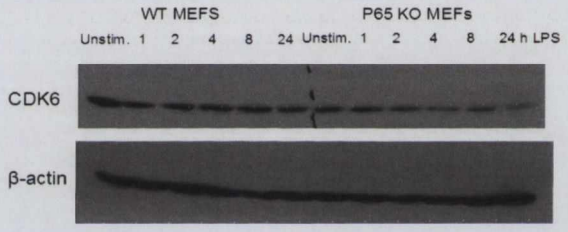


Figure 5.9. **Expression levels of mCDK6 in p65 deficient mouse embryonic fibroblasts in response to LPS.** MEF ($3x10^5$ cells/mL) were plated and incubated with LPS (0.1μg/mL) over time or left unstimulated. RNA was extracted and analyzed using a TaqMan probe specific to mCDK6. Figure A shows mRNA expression in p65 knockout MEF and figure B shows protein expression wild-type and p65 knockout MEF in response to LPS. Fold changes in mRNA expression were calculated using ΔΔCt method with RNA from unstimulated cells as a calibrator and GAPDH as an endogenous control. The data shown in figure A are the mean expression ± S.E.M. of three separate experiments, each carried out in triplicate.

of stimulation. Figure 5.6B shows that CDK6 protein expression also increases over-time in response to LPS with the greatest increase occurring at 4 to 8 hours or stimulation. The difference in peak time points of CDK6 expression is probably because of the delay in turn-over from mRNA to protein.

Cdk6 mRNA also increases 2 fold in response to infection with heat-killed *E. coli* as shown in figure 5.7A. Protein expression in response to heat-killed *E. coli* is shown in figure 5.7B. CDK6 increases 4 to 8 hours post-infection in response to heat-killed *E. coli*. Cdk6 expression was next examined in the adaptor deficient I-BMDM to determine if its expression is dependent upon the MyD88 signaling pathway or the Trif signaling pathway. Figure 5.8A shows that Cdk6 mRNA does not increase in the MyD88 deficient cells but it increases in the wild-types and the Trif deficient cells. CDK6 protein expression increases in response to LPS occurs in the wild-type and Trif deficient cells but not in the MyD88 deficient cells as shown in figure 5.8B and C. p65 deficient MEF were then used to determine if the increase in CDK6 is dependent upon NF-κB. Figure 5.9A shows that Cdk6 mRNA expression does not increase in the p65 MEF but does increase in the wild-type MEF. Similarly Figure 5.9B shows that CDK6 protein levels do not increase in the wild-type MEF because the protein is highly expressed at all time points, but expression actually decreases in the p65 deficient MEF signifying the dependency of the maintenance of CDK6 expression on the activity of NF-κB.

5.2.4. *Optimizing transfection efficiency of DC2.4 cells using two transfection reagents*

Small RNA molecules that manipulate levels of miR-107 were next transfected into cells. The antisense-miR-107 (anti-107) is used to knockdown expression of miR-107 similarly to the effect of LPS on cells. It is an antisense sequence that is complementary to the 23 nucleotide sequence of miR-107. A fluorescent tagged anti-miR negative control oligonucleotide was used as a transfection control and cells were measured using FACS following transfection. Figure 5.10 shows the different transfection reagents used to optimize transfection efficiency and it was found that Lipofectamine RNAiMAX and Lipofectamine2000 are more efficient than the SiPort NeoFx reagent, giving nearly 90% transfection 24 hours post-transfection. Figure 5.10B illustrates cells transfected with the pre-107 displaying

enhanced miR-107 which decreases when cells are treated with LPS. Figure 5.10C shows the anti-107 molecule not affecting miR-107 expression until LPS is added to the cells leading to a decrease in the expression of miR-107. This suggests that the anti-sense molecule is not efficient at silencing miR-107 expression.

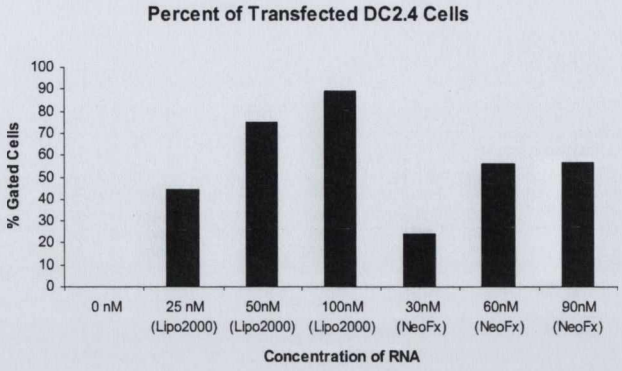
5.2.5. *Quantifying Cdk6 mRNA expression in I-BMDM transfected with antisense-miR-107 or precursor-miR-107 in response to LPS*

To determine if Cdk6 expression is affected by miR-107 expression, I-BMDM were transfected with anti-107 or pre-107 and cells were stimulated with LPS for 24 hours. Figure 5.11A illustrates the upregulation of Cdk6 mRNA in cells transfected with the anti-control at 2 hours of LPS stimulation and cells transfected with the anti-107 show an enhanced expression of Cdk6 in response to LPS at 8 hours of stimulation. CDK6 protein is shown in figure 5.11B and it is also enhanced in cells transfected with anti-107. This enhancement is because all of the miR-107 that was endogenously expressed was eliminated with the anti-107 releasing any repression miR-107 may have had on CDK6. It is interesting to note that the anti-107 is not sufficient to alone to enhance Cdk6 expression, LPS is required to enhance expression. This could be because the anti-107 molecule is stable until LPS is added to the cell affecting its interaction with RISC. Figure 5.11C demonstrates the effect of pre-107 on Cdk6 mRNA expression. In cells transfected with the pre-control there is an increase in Cdk6 expression after 2 hours of LPS stimulation but in cells transfected with pre-107 this increase is inhibited. Transfection of cells with the pre-107 results in decreased CDK6 protein expression in response to LPS compared to cells transfected with the pre-control as shown in figure 5.11D. These results provide evidence that CDK6 is a target for miR-107 in TLR4 signaling.

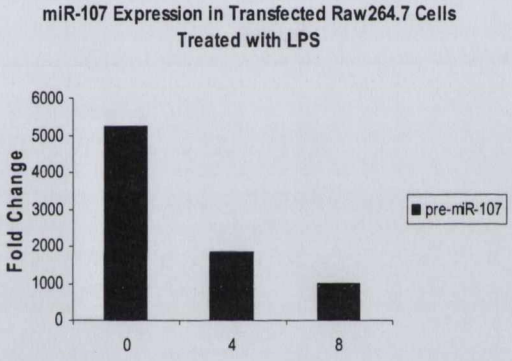
5.2.6. *miR-107 directly binds to CDK6 as shown using the 3`UTR luciferase reporter construct*

To determine if miR-107 is directly binding to CDK6 resulting in its downregulation, a luciferase reporter construct containing the 3`UTR of murine CDK6 was obtained. It is illustrated in figure 5.12. When the construct is transfected into cells, the SV40 enhancer promoter on the plasmid turns on the

A



B



C

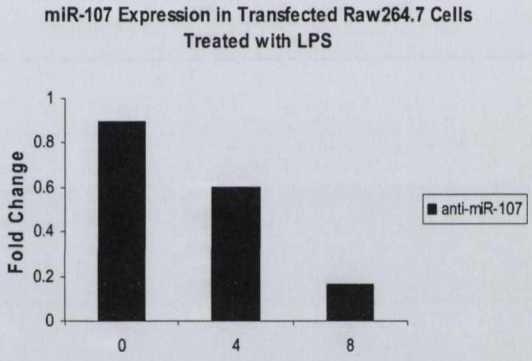


Figure 5.10. **Optimizing Transfection Efficiency**. DC2.4 ($3x10^5$ cells/mL) were plated and transfected with two different transfection reagents according to manufacturer's protocol with FAM-anti-miR-control transfection RNA. Cells were assayed for fluorescence 24 hours post-transfection using FACS. Figure A shows values that are representative of percent fluorescent cells of the total cell population. Figure B shows the expression of miR-107 in Raw264.7 cells transfected with 50nM precursor-miR-107 followed by stimulation with 0.1μg/mL LPS and figure C shows miR-107 expression in cells transfected with 50nM antisense-miR-107 and stimulated with LPS. Fold changes in miRNA expression were calculated using ΔΔCt method with RNA from unstimulated PBMC as a calibrator and U6 rRNA as an endogenous control. Data shown is representative of data obtained in triplicate experiments.

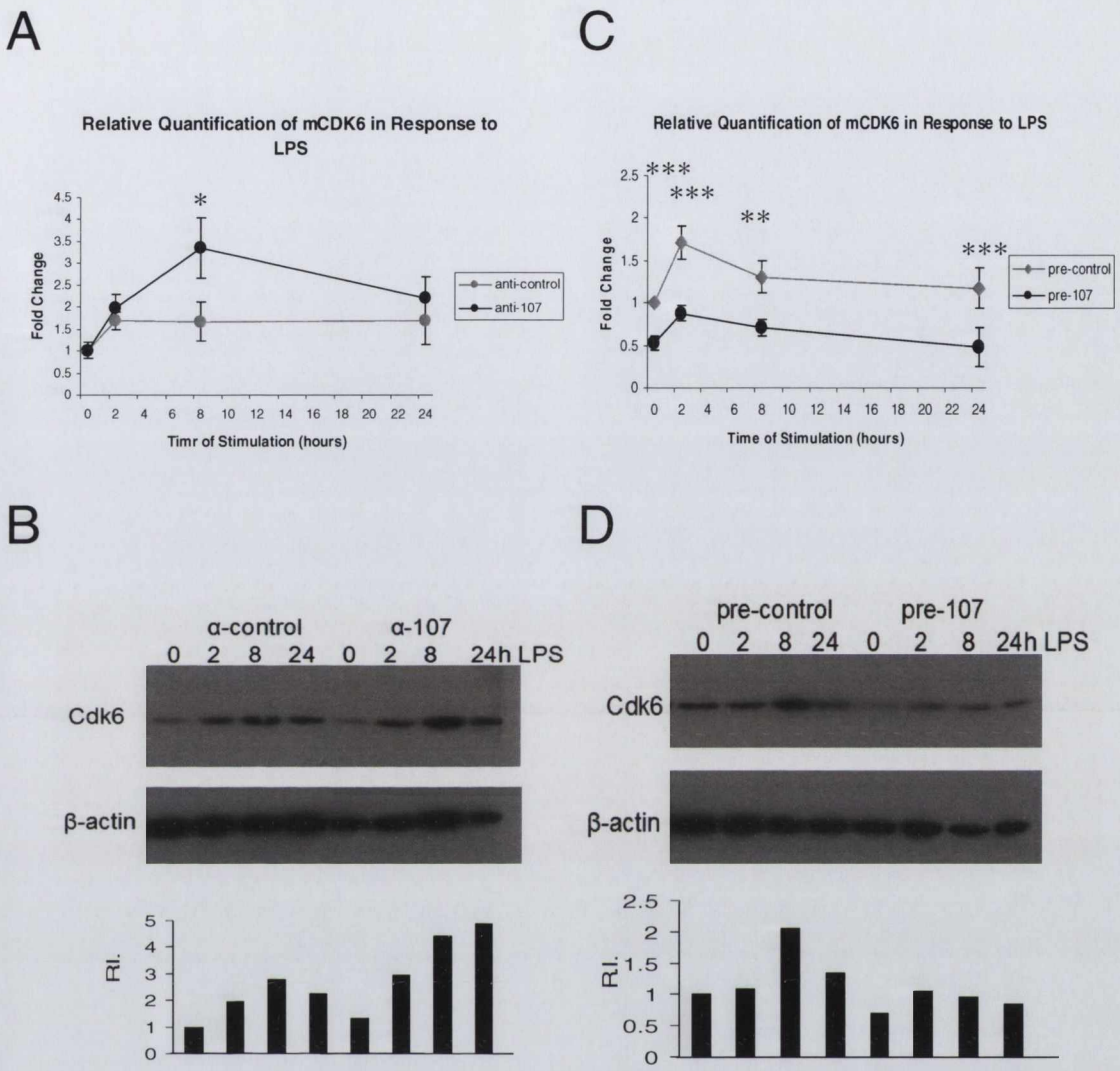


Figure 5.11. **Expression levels of mCDK6 in murine macrophage cell line I-BMDM in response to LPS.** I-BMDM ($3x10^5$ cells/mL) were plated and transfected with 50nM anti-sense (A and B) or precursor miRNA (C and D) molecules for 24 hours. Following transfection cells were incubated with LPS (0.1μg/mL) over time or left unstimulated. RNA was extracted and analyzed using TaqMan PCR with a primer/probe specific to mCDK6. Fold changes in mRNA expression were calculated using ΔΔCt method with RNA from unstimulated cells as a calibrator and GAPDH as an endogenous control. The data shown is the mean expression ± S.E.M. of three separate experiments, each carried out in triplicate. Cells were also lysed and SDS-PAGE/western blot analysis was used with a primary CDK6 anti-mouse antibody. The CDK6 isoform is shown at 36 kDa.

promoter and the luciferase activity so there is no requirement to add additional stimulation to turn on the promoter. A point mutation was made in the miR-107 seed sequence site in the CDK6 3`UTR at position 308. HEK293T cells were co-transfected with the luciferase plasmid and either the anti-107 or pre-107. Figure 5.13A illustrates that cells transfected with the anti-107 had no change in luciferase expression. Cells transfected with the pre-107 had significantly reduced luciferase expression whereas cells transfected with mutant CDK6 luciferase also had reduced expression but not nearly as great a reduction as shown in figure 5.13B. The reason for the slight decreased luciferase in the mutant expression is probably due to the second seed sequence in the 3`UTR that the pre-107 is still able to recognize. This result signifies the direct binding of miR-107 to the 3`UTR of CDK6.

5.2.7. *Secreted TNF-α cytokine production is affected by transfection of miRNA molecules into DC2.4 and Raw264.7 cells*

Cells were transfected with the miRNA oligonucleotides and stimulated with LPS then analyzed for TNF-α production to examine if the effect on TNF-α production seen using the WY14643 compound was acting via miR-107. Figure 5.14A shows DC2.4 cells transfected with anti-107 produced more secreted TNF-α when stimulated with LPS than cells transfected with the anti-control molecule. DC2.4 cells transfected with pre-107 displayed significantly decreased TNF-α production in response to LPS stimulation over time following LPS stimulation compared to cells transfected with the pre-control molecule as illustrated in figure 5.14B. A similar trend was seen in Raw264.7 cells transfected with RNA molecules. Figure 5.14C shows transfection of cells with anti-107 resulted in more TNF-α secretion compared to cells transfected with anti-control and cells transfected with pre-107 secreted less TNF-α following 4 hours of LPS stimulation as shown in figure 5.14D.

5.2.8. *Fluorescence Microscopy shows that DC2.4 Cells Transfected with Pre-miR-107 show decrease in F-actin*

I next examined the effect of knocking down miR-107 or over-expressing it would have on cellular morphology because of the link between CDK6 and the actin cytoskeleton (Slomiany et al., 2006). Overexpression of CDK6, which would be

similar to adding the anti-107 resulted in enhanced motility and decreased stress fibers of mouse astrocytes. I used dendritic cells to observe morphological changes in response to knocking down or overexpressing miR-107 because it is well characterized that dendritic cells undergo vast cytoskeletal changes when maturing in response to TLR ligands including LPS (West et al., 2004). Only basic cellular observations can be made from this experiment because changes in morphology were not quantified. To do this, high-context analysis of a large number of cells could be used to count protrusions from cells and actin polymerization. Cells were transfected and the filamentous actin was stained with Phalloidin. DC2.4 transfected with the anti-miR-control are shown in figure 5.15A. DC2.4 transfected with the anti-miR-control and stimulated with LPS for 18 hours are shown in figure 5.15B. Changes are seen in the cells, including more intense red color indicating more actin polymerization, more protrusions and filaments are also evident. Part C shows unstimulated cells transfected with the anti-107 molecule and D shows these cells stimulated with LPS for 18 hours. Pools of actin are visible and these pools appear denser than in the control transfected cells. Part E shows unstimulated cells transfected with the pre-miR-control molecule and F shows these cells stimulated with LPS for 18 hours. As evident in the anti-miR-control cells, the pre-miR-control transfected cells exhibit more polymerized f-actin and more cellular protrusions. Part G shows unstimulated cells transfected with the pre-107 molecule and H shows these cells stimulated with LPS for 18 hours. When comparing these cells to the pre-miR-control cells there appears to be less actin polymerization following stimulation with LPS and there appears to be less filament extension and protrusions. This experiment is flawed in that a fluorescent marker should have been co-transfected with the anti-107 and pre-107 so I would know what cells were actually transfected. However, what I can say based on these basic observations without quantifying is that the pre-107 molecule is potentially targeting the mRNA of genes involved in maintenance of the actin cytoskeleton like myosin9.

5.2.9. *Cells over-expressing miR-107, knocked down for CDK6 or CDK6 deficient BMDM exhibit less cellular proliferation*

Following verification that CDK6 is a direct target of miR-107 I explored the functional consequences of CDK6 expression. CDK6 has a known role in

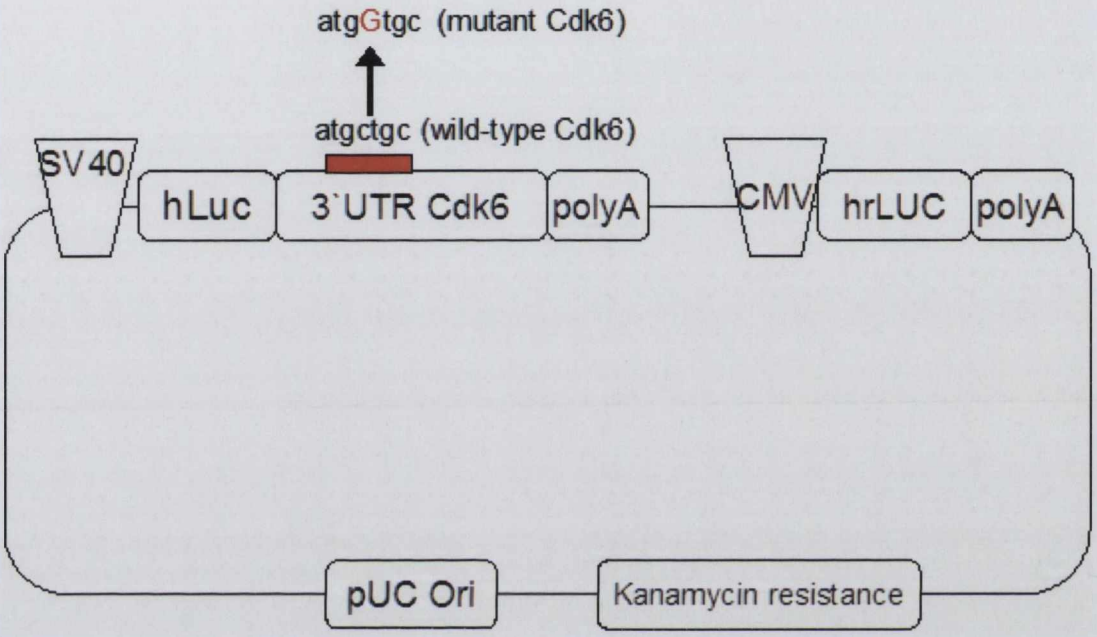
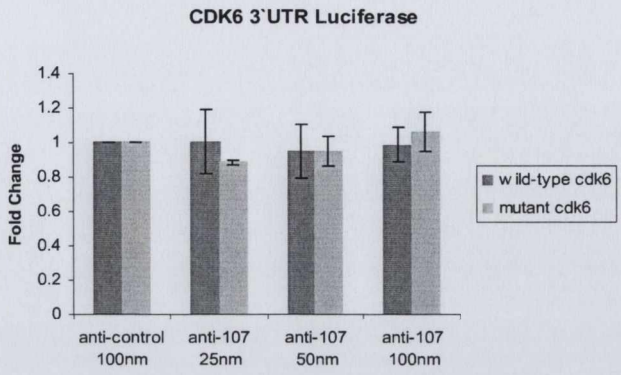


Figure 5.12. **Illustration of luciferase construct containing 3`UTR of mouse Cdk6.** The early SV40 enhancer/promoter region and the CMV immediate early enhancer/promoter region typically provide high-level transcription.

A



B

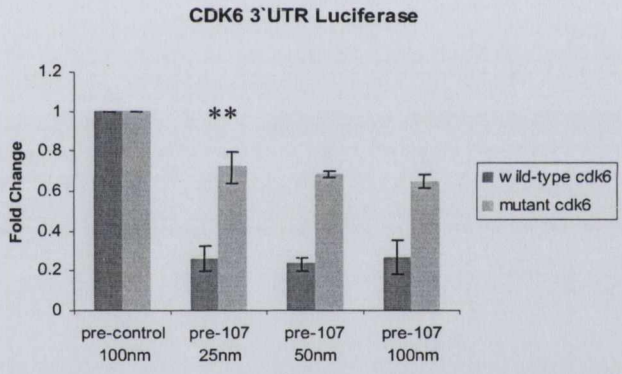


Figure 5.13. **CDK6 3`UTR luciferase expression in I-BMDM transfected with miRNA.** I-BMDM ($3x10^5$ cells/mL) were plated and co-transfected with doses of anti-sense (A) or precursor miRNA (B) molecules (25-100nM) and either the wild-type Cdk6 luciferase or mutant luciferase plasmid as well as the TK renilla control plasmid for 24 hours. Cells were lysed in passive lysis buffer and assessed for either luciferase activity or TK renilla activity. The data shown is the mean luciferase relative to TK renilla $\pm$ S.E.M. of three separate experiments, each carried out in triplicate.

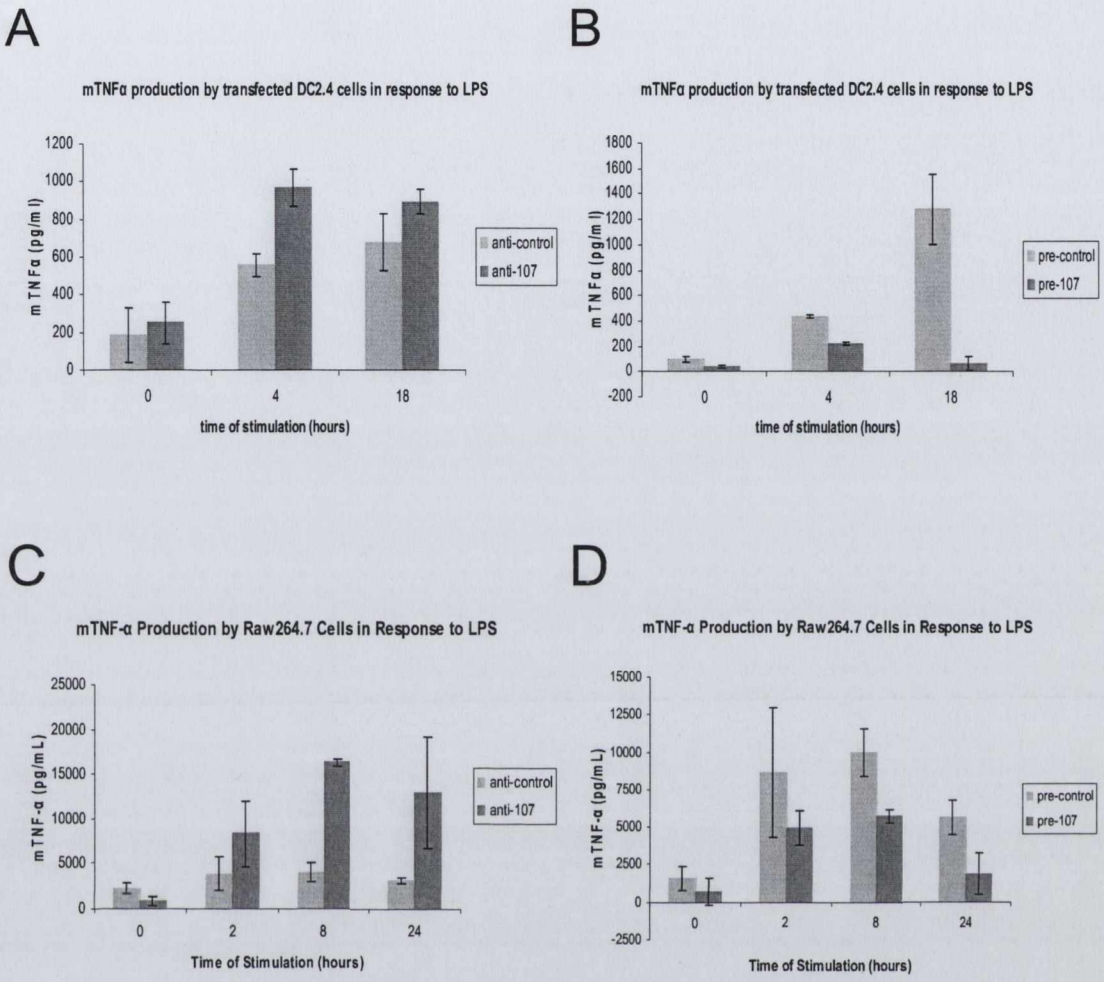


Figure 5.14. **Production of TNF-α in transfected mouse DC2.4 cells and Raw264.7 cells in response to LPS.** DC2.4 (A and B) and Raw264.7 cells (C) ($3x10^5$ cells/mL) were plated and transfected with 50nM various miRNA molecules for 24 hours. Media was changed and cells were incubated with LPS (0.1μg/mL for the times indicated) or left unstimulated. Supernatants were collected at various time points and analyzed by ELISA for TNF-α production. The data shown represent mean cytokine level ± S.E.M. for three separate experiments, each carried out in triplicate

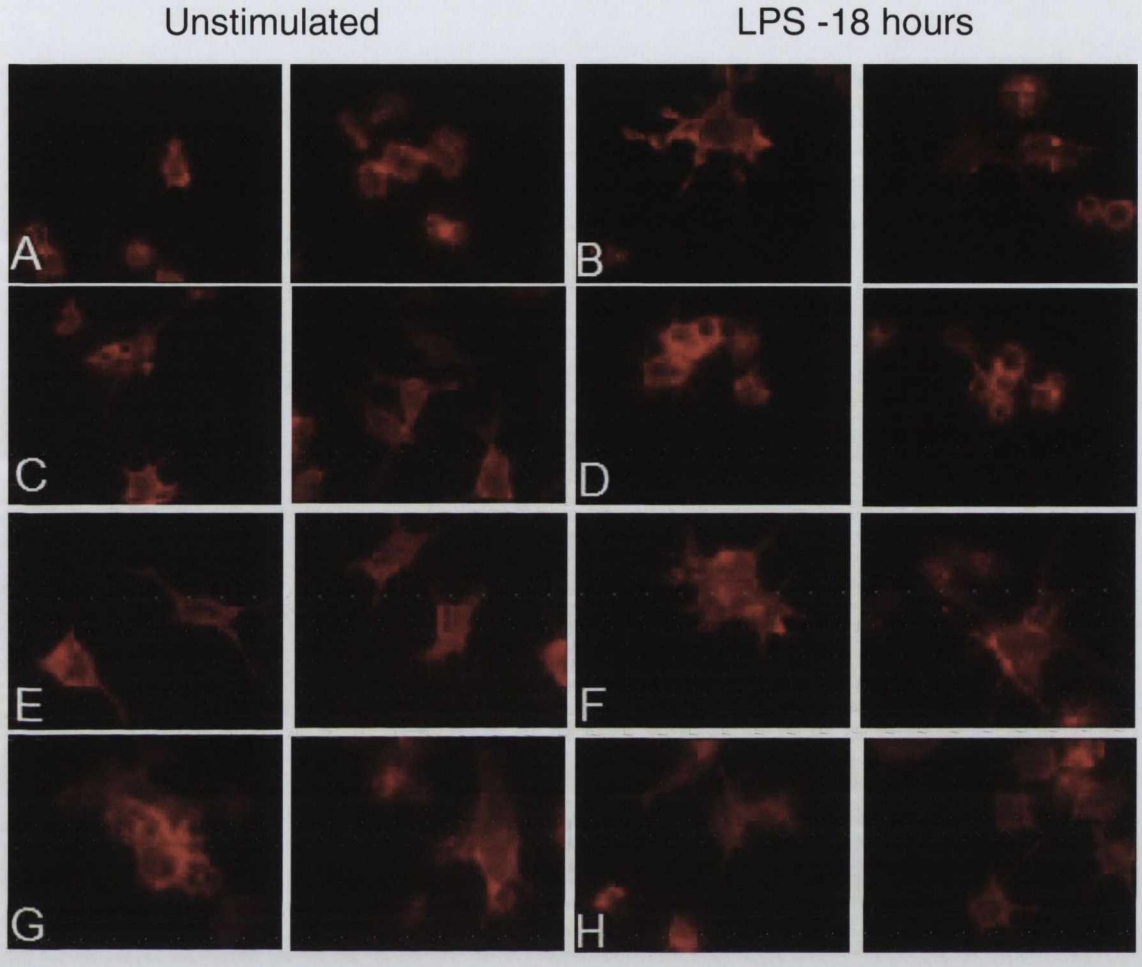


Figure 5.15. **Fluorescence microscopy of DC2.4 Cells Transfected with anti-miR-107 or pre-miR-107 in response to LPS.** DC2.4 ($3x10^5$ cells/mL) were plated and transfected with anti or pre control miR molecules or anti-miR-107 or pre-miR-107 on coverslips. 24 hours post-transfection, cells were either left unstimulated or stimulated for 18 hours with 0.1μg/mL LPS. Cells were then fixed with paraformaldehyde, lysed with 20% triton x-100 and stained with Phalloidin alexa fluor 594. Two images are shown for each treatment. A shows anti-control transfected cells and B shows anti-control transfected cells stimulated with LPS. C shows unstimulated anti-107 transfected cells and D shows those cells stimulated with LPS for 18 hours. E shows unstimulated cells transfected with pre-control and F shows those cells stimulated with LPS for 18 hours. Figure G illustrates unstimulated cells transfected with pre-107 while H shows those cells stimulated with LPS.

proliferation of cells but it has not been implicated in TLR signaling. I next examined cellular proliferation through the use of the reagent MTT. This compound is only taken up by living cells that are dividing. The compound is metabolized by the mitochondria of the cell, so this assay can also be a measurement of metabolism of the cell, I will call it proliferation for the sake of simplicity but this experiment could signify a more complicated mechanism. Figure 5.16A illustrates that I-BMDM transfected with anti-107 show enhanced proliferation in response to LPS over-time compared to cells transfected with the anti-control. Figure 5.16B shows that cells transfected with pre-107 exhibit reduced proliferation in response to LPS compared to cells transfected with pre-control. I-BMDM were transfected with siRNA to CDK6 to observe the effect knocking down CDK6 has on cell growth, similar to over-expressing miR-107 with pre-107, siRNA to CDK6 reduces cell proliferation compared to cells transfected with control siRNA which show an increased ability to grow in response to LPS as shown in figure 5.17.

I next obtained primary BMDM from CDK6 deficient mice and figure 5.18A shows that when they were stimulated with LPS the wild-type control BMDM displayed enhanced growth after 4 hours of LPS stimulation whereas the CDK6 deficient cells proliferated half as well. I measured cytokine production from the knockout cells to observe if there was decreased cytokine because there are fewer cells. Figure 5.18B demonstrates that over a 24 hours period, CDK6 deficient BMDM produce half the amount of TNF-α cytokine following 4 to 8 hours of LPS stimulation compared to wild-type BMDM. The anti-inflammatory cytokine IL-10 was also measured and is shown in figure 5.18C. Like TNF-α, IL-10 was also decreased following 4 to 8 hours of LPS stimulation suggesting that either because CDK6 deficient cells do not grow as well as wild-type cells in response to LPS, the cells that are present do not produce as much cytokine as wild-type BMDM or there is something physiologically wrong with the deficient cells that causes them to produce less cytokine. I suggest this second explanation because at the 2 hour post-stimulation time point there is no difference in either TNF-α or IL-10 compared to wild-type cells implying that at this time point the cells are still able to produce equivalent amounts of cytokine and that it is not until 4 and 8 hours post-stimulation that less cytokine is produced by the deficient cells. I also

wanted to ensure that miR-107 was being downregulated in the CDK6 deficient cells so I measured its expression in response to LPS as illustrated in figure 5.19. I found that like in the wild-type BMDM, miR-107 is downregulated over 5 fold following 2 hours of LPS stimulation, in the deficient BMDM then returns to just below basal levels at 8 hours then returns to 5 fold downregulated by 24 hours. Because of the earlier time points of LPS induction of proliferation observed in these experiments this could also be a burst of metabolic activity at the earlier time point and not be solely due to an increase in cell growth.

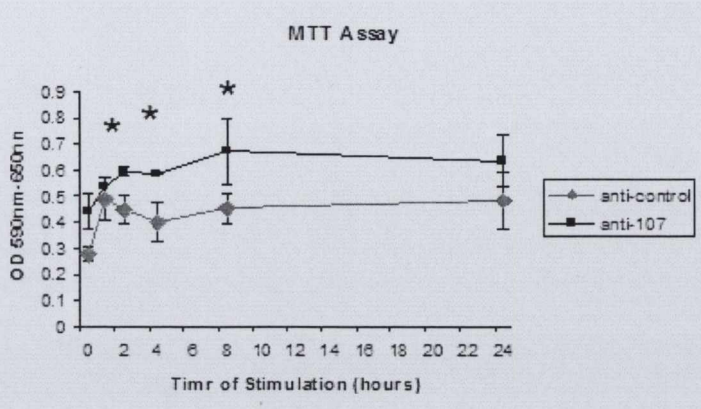
5.2.10. *Mice deficient for CDK6 were less susceptible to the lethal effect of LPS and produced less TNF-α and enhanced IL-10*

To examine the role of CDK6 in TLR signaling and inflammation further, we injected CDK6-deficient and wild-type control mice with LPS and monitored their survival. CDK6-deficient mice were less susceptible to LPS, with lower mortality than wild-type mice. Figure 5.20A shows that mice lacking CDK6 are less susceptible to the lethal effect of LPS. Figure 5.20B shows analysis of circulating cytokine concentrations 1 h after LPS injection and TNF-α concentrations were lower in CDK6-deficient mice treated with LPS consistent with lower susceptibility. Figure 5.20C shows analysis of IL-10 concentrations at 4 h after LPS injection and serum concentrations in CDK6-deficient mice were greater than those in wild-type mice. These data indicate that CDK6 has a pro-inflammatory role in LPS signaling.

5.2.11. *Cells transfected with miR-107 molecules exhibited no differences in amount of apoptotic cells*

Because of the decrease in proliferating cells when I-BMDM were transfected with the pre-107 or siRNA to CDK6, I next examined apoptosis using the annexin V assay to ensure that the differences were not simply due to more cells dying. During apoptosis, phosphatidylserines are translocated from the inner leaflet of the plasma membrane to the outer leaflet soon after the induction of apoptosis. The annexin V protein has a specific affinity for phosphatidylserines and binds to FITC-labeled annexin V which is then detected by FACS analysis. Propidium iodide is used alongside the annexin v stain to detect extracellular DNA from necrotic cells. This assay does not distinguish between the two pathways but is

A



B

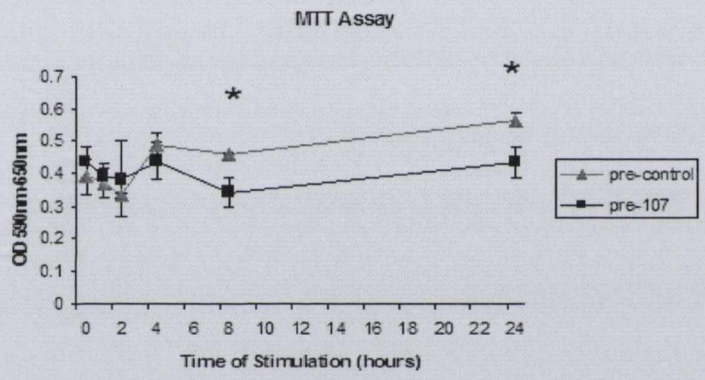


Figure 5.16. **Cell Proliferation of I-BMDM in response to LPS.** I-BMDM cells ($3x10^5$ cells/mL) were plated and transfected with 50nM various miRNA molecules for 24 hours. Media was changed and cells were incubated with LPS (0.1μg/mL) for the times indicated or left unstimulated. 5mg/mL MTT reagent was added to the cells and left to incubate for 4 hours. The supernatant was then removed and the substrate was cleaved releasing a purple color. Samples were read at OD_{590nm}. Figure A shows cell proliferation of cells transfected with the anti-miR-control or anti-miR-107 in response to LPS. Figure B shows cells transfected with pre-miR-control or pre-miR-107 in response to LPS. Data shown is the mean $\pm$ S.D. from a single experiment done in triplicate but is representative of three separate experiments.

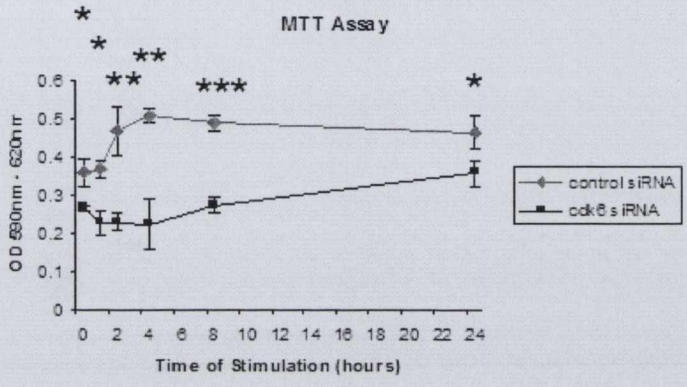
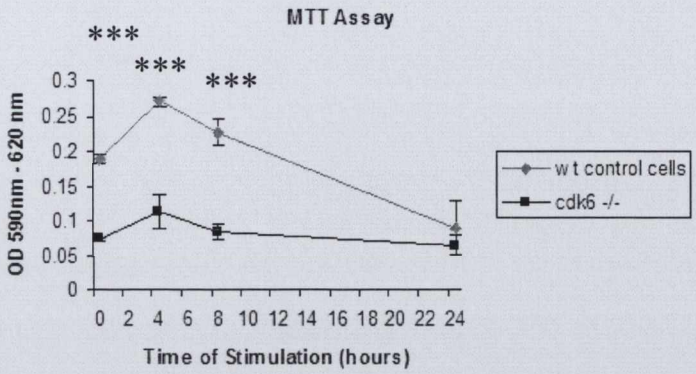
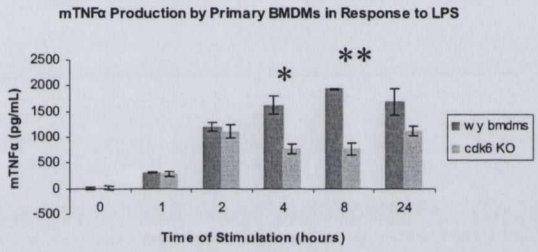


Figure 5.17. **Cell Proliferation of I-BMDM in response to LPS.** I-BMDM ($3x10^5$ cells/mL) were plated and transfected with 100nM control siRNA molecule or CDK6 siRNA for 24 hours. Media was changed and cells were incubated with LPS (0.1μg/mL) for the times indicated or left unstimulated. 5mg/mL MTT reagent was added to the cells and left to incubate for 4 hours. The supernatant was then removed and the substrate was cleaved releasing a purple color. Samples were read at OD_{590nm}. Data shown is the mean ± S.D. from a single experiment done in triplicate but is representative of three separate experiments.

A



B



C

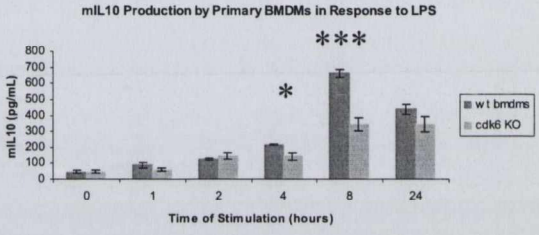


Figure 5.18. **Cell Proliferation and TNF-α and IL-10 production of Primary BMDM in response to LPS.** Primary wild-type and CDK6 deficient BMDM ($3x10^5$ cells/mL) were plated and incubated with LPS (0.1μg/mL) for the times indicated or left unstimulated. 5mg/mL MTT reagent was added to the cells and left to incubate for 4 hours. The supernatant was then removed and the substrate was cleaved releasing a purple color. Samples were read at OD_{590nm}. Data shown is the mean ± S.D. from a single experiment done in triplicate but is representative of three separate experiments from three individual mice. Supernatants were collected at various time points and analyzed by ELISA for TNF-α (B) and IL-10 (C) production. The data shown is the mean ± S.E.M. of three separate experiments, each carried out in triplicate.

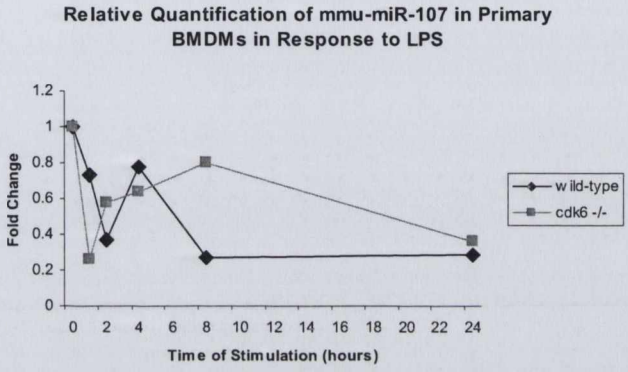


Figure 5.19. **Expression level of miR-107 in CDK6 deficient BMDM in response to LPS.** CDK6 deficient BMDM and wild-type BMDM ($3x10^5$ cells/mL) were plated and incubated with LPS (100ng.mL) for various time points or left unstimulated. RNA was extracted and analyzed using miRNA TaqMan PCR with probes specific to miR-107. Fold changes in miRNA expression were calculated using ΔΔCt method with RNA from unstimulated cells as a calibrator and U6 rRNA as an endogenous control.

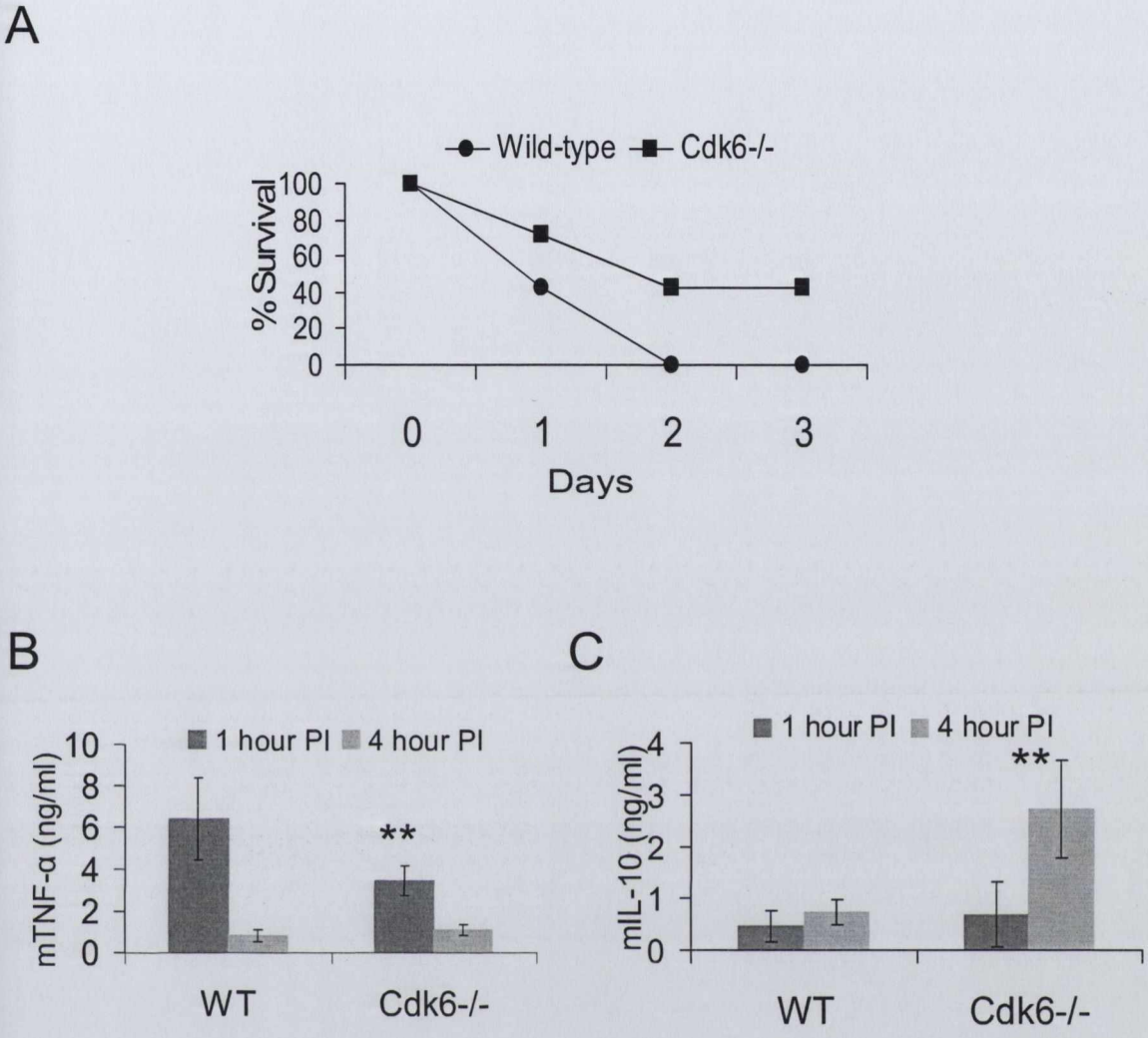
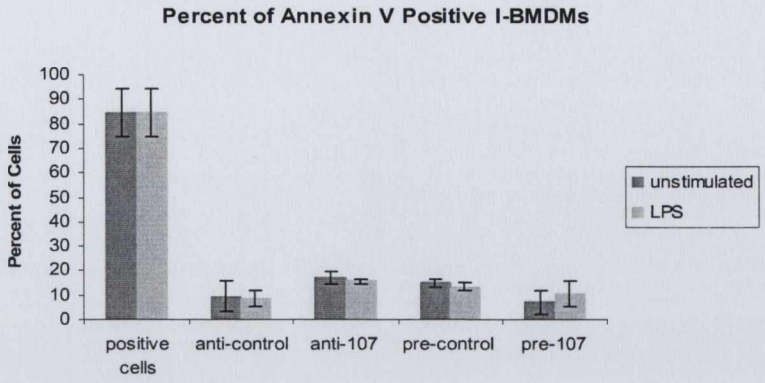


Figure 5.20. **Survival of wild-type and CDK6 deficient mice in response to LPS injection and TNF-α and IL-10 in the serum of these mice.** Wild-type (WT) control mice and CDK6-deficient (Cdk6-/-) mice 8 weeks of age were injected intraperitoneally with LPS (30 mg/ml), and monitored over a period of 3 d; Figure A shows results plotted as a percentage of total numbers (n = 7 mice per group). Serum were collected at various time points and analyzed by ELISA for TNF-α (B) and IL-10 (C) production. Data are representative of one independent experiment. In all cases, results are expressed as mean ± S.E.M. of triplicate determinations from three separate experiments

A



B

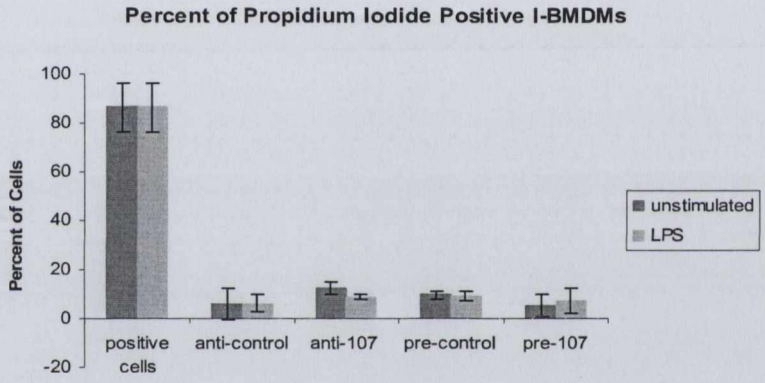


Figure 5.21. **Percent of apoptotic I-BMDM in response to LPS.** I-BMDM ($3x10^5$ cells/mL) were plated and transfected with 50nM miRNA molecules for 24 hours. Media was changed and cells were incubated with LPS (0.1μg/mL) for 8 hours or left unstimulated. Annexin V-fitc and Propidium Iodide was added to the cells to stain phosphatidylserines and DNA. A sample of cells was boiled to induce cell death and use as a positive control. FACS analysis was conducted. Figure A shows the percent of cells positive for annexin V compared to the positive cell sample. Figure B shows the percent of cells positive for propidium iodide compared to the positive cell sample. Data shown is the mean ± S.D. from a single experiment done in triplicate but is representative of three separate experiments.

useful to assess the amount of overall cell death. As a positive control for cell death, a sample of cells was boiled which results in both apoptosis and necrosis. Figure 5.21A illustrates that the sample of cells that was boiled resulted in nearly 100% apoptosis or cell death. The transfected samples displayed an average of 10% annexin V positive cells and figure 5.21B shows a similar result using the propidium iodide stain for DNA. The boiled cell sample resulted in nearly 100% positive for propidium iodide but transfected cells showed an average of 8% positive for propidium iodide.

5.2.12. *Cells over-expressing miR-107 exhibit less migration*

CDK6 has been implicated in cell migration so I next measured migration of I-BMDM transfected with anti-107 or pre-107 and stimulated with LPS. A monolayer of I-BMDM was grown and then a "wound" was introduced to the monolayer using a p10 pipette tip. Cells were then stimulated with LPS and the cells that had migrated into the "wound" were counted. Figure 5.22 demonstrates that cells transfected with anti-107 exhibit greater migration towards the wound and migrate more when stimulated with LPS. Figure 5.23 illustrates that cells transfected with pre-107 have significantly decreased ability to migrate towards the wound compared to control transfected cells. Percent wound closure was calculated after a grid was placed over the photograph and empty grid were counted and subtracted from the total number of grids and plotted.

5.2.13. *Cells over-expressing miR-107 exhibit less internalization of live E. coli*

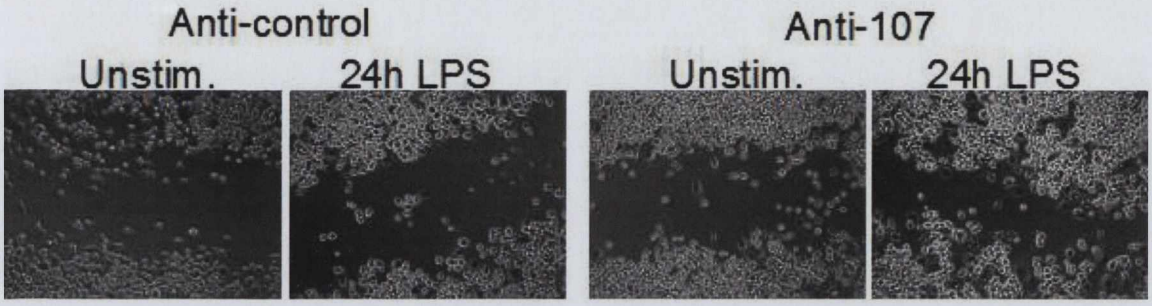
Because of the differences seen in the cell morphology and levels of actin polymerization in transfected cells using fluorescence microscopy, cells transfected with the anti or precursor form of miR-107 were incubated with live bacteria to assess if there are also differences in phagocytosis because it is an actin-dependent process. *E. coli* was used as a positive control because it is a gram negative bacterium covered in LPS. Figure 5.24A demonstrates that there are no differences in the amount of phagocytosed *E. coli* in cells transfected with the anti-miR-107. Whereas figure 5.24B shows cells transfected with the pre-miR-107 molecule exhibit less phagocytosis of live *E. coli*. The internalization index is a ratio of the amount of bacteria that were initially introduced to the cells to the amount of bacteria that were recovered following the gentamicin protection assay.

All physiological differences observed seem to be enhanced when miR-107 is overexpressed perhaps because LPS is decreasing miR-107 levels and transfecting cells with the anti-sense for miR-107 only results in marginal effects.

5.2.14. *Effect on TNF-α and IL-6 cytokine secretion by cells transfected with miRNA molecules following infection with live E. coli*

Supernatants were collected from the Raw264.7 cells transfected with miRNA molecules and infected with live *E. coli* and analyzed for TNF-α and IL-6 production. Figure 5.25A shows that TNF-α is decreased in cells transfected with pre-miR-107 and infected with *E. coli*. This result corresponds with data obtained using LPS on transfected cells. Figure 5.25B shows that IL-6 production is also impaired in cells transfected with pre-miR-107 so the effect on cytokine production is not specific to TNF-α secretion.

A



B

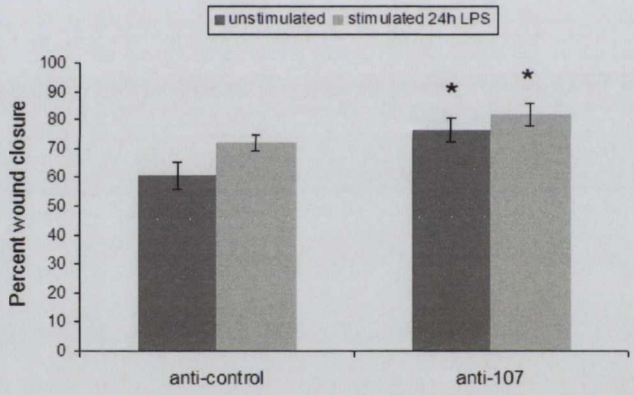
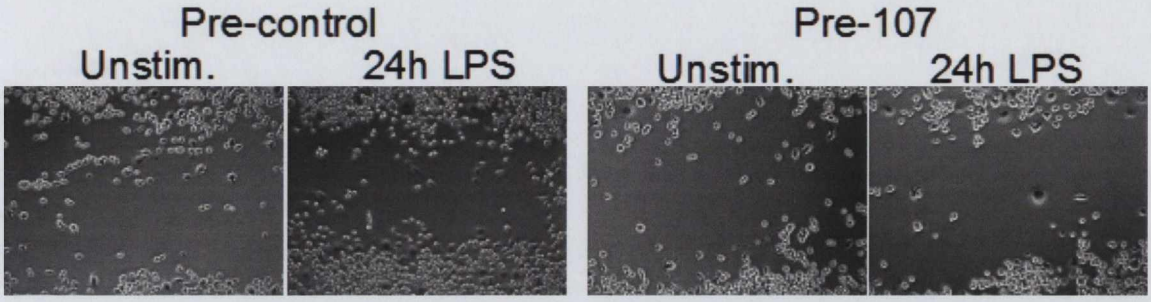


Figure 5.22. **Cell migration of I-BMDM in response to LPS.** I-BMDM ($3x10^5$ cells/mL) were plated and transfected with 50nM anti-control or anti-107 for 24 hours. Media was changed and cells were incubated with LPS (0.1μg/mL) for 24 hours or left unstimulated. Cells were then observed through the Olympus IX-81 Fluorescent microscope. The data shown is the mean percent wound closure ± S.D. of triplicate transfections and is representative of an experiment done in triplicate.

A



B

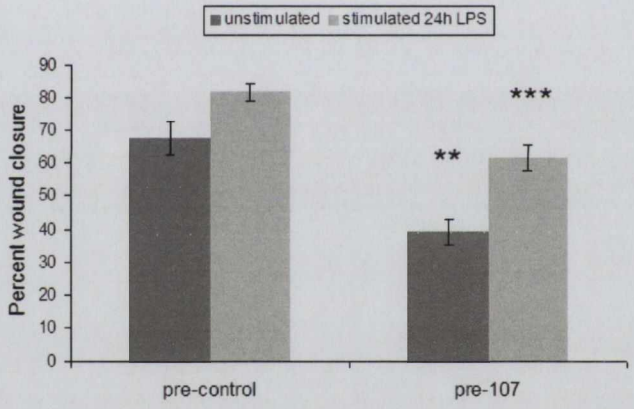
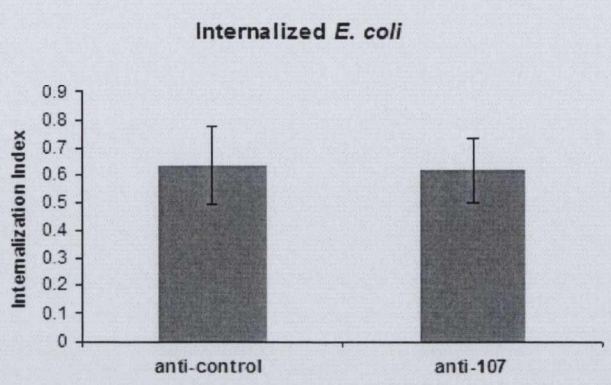


Figure 5.23. **Cell migration of I-BMDM in response to LPS.** I-BMDM ($3x10^5$ cells/mL) were plated and transfected with 50nM pre-control or pre-107 for 24 hours. Media was changed and cells were incubated with LPS (0.1μg/mL) for 24 hours or left unstimulated. Cells were then observed through the Olympus IX-81 Fluorescent microscope. The data shown is the mean percent wound closure ± S.D. of triplicate transfections and is representative of an experiment done in triplicate.

A



B

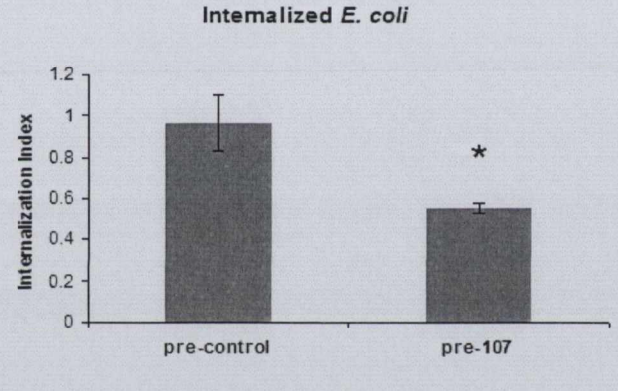
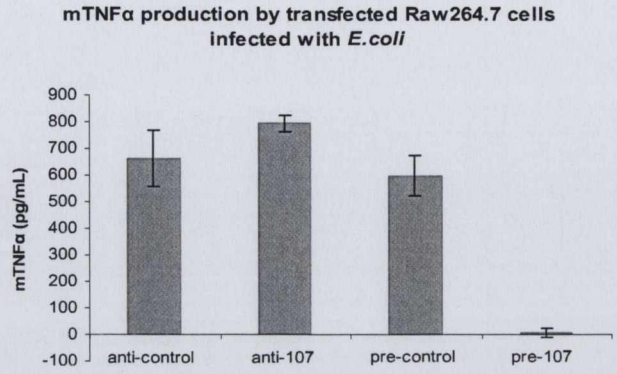


Figure 5.24. **Intracellular bacteria counts of Raw264.7 cells infected with wild-type *E. coli*.** Raw264.7 ($3x10^5$ cells/mL) were plated and transfected with 50nM various miRNA molecules for 24 hours. Media was changed and cells were infected with *E. coli* at an MOI of 10:1 or left uninfected for 1 hour. Cells were treated with 100ng/mL gentamicin for 1 hour and lysed with water. Lysates were than spot plated on LP agar plates and incubated at 37°C overnight and CFUs were counted the following day. Figure A shows internalization index collected from Raw264.7 cells transfected with anti-107 molecules and the control and infected with *E. coli*. Figure B shows internalization index from cells transfected with pre-107 molecules and the control and infected with *E. coli*. Data shown is representative of an experiment done in triplicate.

A



B

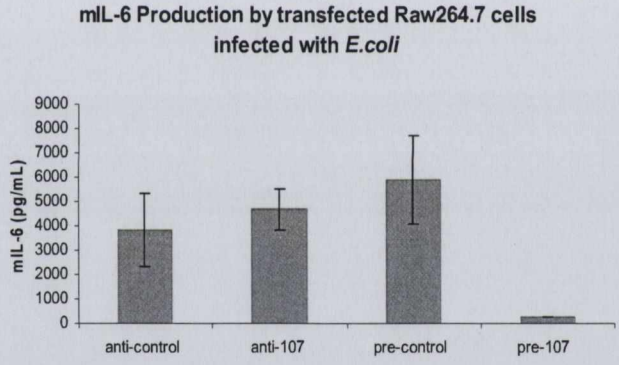


Figure 5.25. **TNF-α and IL-6 cytokine production of Raw264.7 cells transfected with miRNA RNA molecules and infected with *E. coli*.** Raw264.7 ($3x10^5$ cells/mL) were plated and transfected with 50nM various miRNA molecules for 24 hours. Media was changed and cells were infected with *E. coli* at an MOI of 10:1 or left uninfected for 1 hour. Supernatants were collected at various time points and analyzed by ELISA for TNF-α or IL-6 production. Figure A shows TNF-α production by cells transfected with precursor-miR and anti-sense-miR molecules and infected with *E. coli* while B shows the production of IL-6 from these cells. The data shown represent mean cytokine level $\pm$ S.E.M. for three separate experiments

5.3. **Discussion**

One of the most elusive aspects of miRNA research is the identification of valid targets and the functional consequences associated with the target. The downregulation of miR-107 in response to LPS is releasing the brake on target gene expression in response to LPS and will result in the post-transcriptional upregulation of its target genes and will contribute to the immune response in some way. This study began with a comparison of the different miRNA target gene prediction databases. TargetScan is the database that is the most user friendly while providing the most comprehensive list of genes using the most stringent set of rules to calculate a context score. The list of genes found using TargetScan was entered into the GProfiler database to find common functions amongst the large list of potential genes. The list of genes was sorted into genes with a role in the immune response as listed in table 5.1 and table 5.2. These genes have roles in processes like maintenance of cell shape, migration, proliferation, cell cycle and phagocytosis. Some of these genes were selected for analysis of their expression following LPS stimulation. If these were valid targets of miR-107 their mRNA expression would increase in response to LPS from 2 to 8 hours post-stimulation.

The genes that were measured in response to LPS include EphrinA7, a member of the ephrin family of proteins. It has a role in monocyte recruitment to a site of infection. Its mRNA expression did not change from basal levels of expression following stimulation with LPS. Myosin, heavy chain 9 is involved in cytoskeleton rearrangement and maintenance of cell shape. Myosin mRNA expression increased 3 fold at 8 hours post-stimulation indicating that it may be a potential target of miR-107. Vinculin mRNA expression increased 2 fold 4 hours post-stimulation also signifying its potential as a target of miR-107. Vinculin is a cytoskeletal protein associated with cell-cell junctions, where it is thought to be involved in anchoring f-actin to the membrane. Ankyrin1 also increased approximately 2 fold from 2 hours to 18 hours after cells were stimulated with LPS. Ankyrin1 is mainly found in erythrocytes but has also been found in brain and muscle tissue. It is thought to play a key role in cell motility, proliferation, contact and the maintenance of specialized membrane domains (Kontrogianni-Konstantopoulos et al., 2003). Thy1 was examined next and its expression did not

change in response to LPS. Rab11FIP2 and Rab11FIP4 were assessed next for mRNA expression post-stimulation with LPS. Neither of these genes increased in expression from basal levels. Three of the Vamp protein members were analyzed next, Vamp1, Vamp4 and Vamp8 and none of their mRNA expression levels changed from basal levels.

Published targets of miR-107 were examined next and the first to be analyzed was NF1-A. The expression of this gene did not change following stimulation with LPS. Bace1 was the next gene analyzed and its expression also did not change in response to LPS. HIF-1β and HIF-1α mRNA expression were next examined based on the previous publications stating that they are targets of miR-107 (Dolt et al., 2007; Yamakuchi et al., 2010). HIF-1β expression did not change in response to LPS stimulation whereas HIF-1α expression increased 3 fold following 8 hours of LPS stimulation signifying its potential as a valid miR-107 target. HIF-1α is a known LPS responsive gene as described in chapter 3 section 4 (Blouin et al., 2004; Rius et al., 2008). Dicer1 mRNA expression was examined next and it increased 2 fold following 1 to 2 hours of LPS stimulation. CDK6 expression was the last mRNA examined and it increased 3 fold from 2 to 8 hours following LPS stimulation. Following my analysis of potential target genes, the only genes to increase in expression in response to LPS were Myosin9, Vinculin1, Ankyrin1, HIF1-α, Dicer1, and CDK6. Table 5.3 illustrates these genes and lists their role in cancer and diseases associated with their altered expression. I chose to focus the remainder of this study on examining CDK6 as a target for miR-107 based on consistency of upregulation in response to LPS and its ability to be affected by the anti-sense and precursor oligonucleotides for miR-107.

This study is the first to directly link any of the cyclin-dependent kinases as LPS responsive genes. I have found that CDK6 is MyD88 dependent through the use of adaptor deficient macrophages. Both its mRNA and protein expression levels failed to increase in the MyD88 deficient cells whereas the mRNA and protein both increased in the wild-type and the Trif deficient macrophages. I have also found through use of the p65 deficient MEF that CDK6 is NF-κB dependent. Cdk6 mRNA and protein levels in the wild-type MEF increased only marginally compared to the unstimulated cells and its protein expression in the wild-type

MEF did not change at all compared to the unstimulated wild-type cells. This is because CDK6 is expressed very high basally in MEF so the increase in response to LPS is difficult to observe. However, in the p65 deficient MEF CDK6 protein expression decreased signifying the requirement of NF-κB signaling for its upregulation in response to LPS.

To determine if CDK6 is a target of miR-107 I transfected I-BMDM with the anti-sense or the precursor miR-107 oligonucleotides and the cells were then stimulated with LPS and I measured Cdk6 mRNA and protein expression. I found that in cells overexpressing miR-107, Cdk6 mRNA and protein were inhibited and cells where miR-107 was knocked down CDK6 expression was enhanced. To establish if this effect is directly due to miR-107 expression I obtained a luciferase construct that contained the 3'UTR of CDK6 and transfected it into cells along with either the anti-sense or precursor miR-107 oligonucleotides. I also made a mutant construct where a single base pair in the predicted miR-107 seed sequence was changed. I observed that CDK6 is a direct target of miR-107 through the inhibition of luciferase activity in cells transfected with pre-107 compared to cells transfected with the pre-control. Pre-miR-107 was able to slightly inhibit the mutant CDK6 construct because there are two conserved seed sequences in the 3'UTR of CDK6 for miR-107 recognition.

Based on the effect on TNF-α secretion I observed following the pre-treatment of macrophages with WY14643 before stimulation with LPS I next examined the effect of overexpressing or knocking down miR-107 on TNF-α secretion to see if the effect with the compound was occurring via miR-107. In DC2.4 and Raw264.7 cells stimulated with LPS and lacking miR-107, TNF-α cytokine secretion was enhanced. Cells overexpressing miR-107 exhibited significantly decreased TNF-α cytokine secretion. This suggests that miR-107 is having an effect on TNF-α secretion. TNF-α molecules must be actively exported from the cell through the process of exocytosis. Molecules are transported to the surface of the cell in recycling endosomes and following a series of fusion events involving the Vamp proteins, TNF-α accumulates in phagocytic cups where it is cleaved by TNF-α converting enzyme (TACE) and released into the extracellular

environment (Murray et al., 2005). miR-107 potentially targets the mRNA of the Vamp proteins so could potentially be affecting the process of exocytosis.

LPS stimulation of dendritic cells results in an increase in f-actin, membrane ruffling, lamellipodia and filopodia formation, and migration (West et al., 2000; Williams and Ridley, 2000). I used DC2.4 cells to observe changes in the actin cytoskeleton because of the dynamic changes LPS induces in these cells. DC2.4 cells were transfected with anti-miR-107 and pre-miR-107 and observed for morphological and cytoskeletal changes before and after LPS stimulation. Dendritic cells transfected with either the anti-control or the pre-control appeared similar before and after LPS stimulation. The cells appeared to be more activated with more protrusions, filipodia and pools of f-actin following the addition of LPS. Cells transfected with anti-miR-107 appeared to have more f-actin pooled along the plasma membrane compared to the anti-control transfected cells while dendritic cells overexpressing miR-107 exhibited less polymerized f-actin and the cells appeared to have fewer protrusions indicating they are less activated. The microscopy was not quantified so these observations are not concrete and must be taken with due consideration. In a previous study examining the role of CDK6 in cellular differentiation, CDK6 expression was associated with changes in the actin cytoskeleton (Slomiany et al., 2006). Differentiation of cells is dependent on the coordinated regulation of the actin cytoskeleton. Cells overexpressing CDK6 displayed morphological changes and an alteration in polarity, moving from multipolar to bipolar (Ericson et al., 2003). These changes correlated with less cellular differentiation. CDK6 overexpressing mouse astrocytes displayed changes in the expression of proteins that regulate actin dynamics, they lack stress fibers and exhibit enhanced motility.

CDK6 has a known role in cellular proliferation and LPS induces cellular proliferation (Fiaschi-Taesch et al., 2010; Moore et al., 1980; Peavy et al., 1978; Pedersen et al., 1995; Vos, 1978; Williams and Ridley, 2000). LPS stimulation was shown to enhance the proliferation of the B9 cell line in a dose-dependent manner through use of thymidine incorporation and the MTT assay. A study examining the effect of arsenic on proliferation of mouse liver hepatocytes showed that arsenic exposure inhibited LPS induced proliferation through changes

in mediators of cell cycle progression like CDK6 (Arteel et al., 2008). I wanted to examine the effect of miR-107 and CDK6 expression on proliferation along with LPS. I measured cell growth of I-BMDM transfected with anti-miR-107, pre-miR-107 or the control oligonucleotides, as well as I-BMDM transfected with siRNA for CDK6 or control siRNA. There was a significant increase in proliferation of cells lacking miR-107 following LPS stimulation compared to anti-control transfected cells. While LPS stimulated cells overexpressing miR-107 exhibited a significant decrease in proliferation compared to the pre-control transfected cells. Cells transfected with siRNA for CDK6 demonstrated a similar trend as cells transfected with pre-107, an enhanced decrease in cellular proliferation in response to LPS compared to control transfected cells. I was also able to obtain CDK6 deficient BMDM and like cells transfected with siRNA for CDK6 these cells displayed an even greater reduction in their ability to proliferate in response to LPS stimulation compared to wild-type BMDM. As I mentioned earlier in this section, the assay used to determine cell proliferation is also a measure of metabolism so these results could also signify the effect of miR-107 on metabolism of cells in response to LPS. When miR-107 is over-expressed, cells exhibit a decrease in metabolism, and similarly when CDK6 is knocked down, there is potentially a decrease in metabolism.

CDK6 has a prominent role in the cell cycle. It is required to progress cells from G1 to S phases of the cell cycle. The cell cycle is divided into four main phases, G1, S, G2 and M phase. The tightly regulated transition between G1 and S requires a change in gene expression to allow for DNA replication. To regulate the onset of DNA replication, CDKs like CDK6 and CDK4 partner with cyclins to phosphorylate Rb protein (Grossel and Hinds, 2006a, b). Once phosphorylated, pRb releases its binding partner E2F to activate genes necessary for DNA replication. Two families of CDK inhibitor proteins function to control the progression of cells into S phase. The INK family contains $p16^{INK4a}$, $p18^{INK4c}$ and $p19^{INK4d}$, and the CIP/KIP family contains $p21^{Cip1/Waf1}$, $p27^{Kip1}$ and $p57^{Kip2}$. These inhibitors will bind to CDKs so that they can no longer bind to cyclins and phosphorylate pRb. A future experiment would be to observe the role of miR-107 and LPS in the cell cycle. Based on the inhibition of proliferation of cells overexpressing miR-107, the cell cycle should be affected.

CDK expression has been linked to migration and motility of cells (Zhong et al., 2010). A recent study showed that decreasing the activity of cyclin D1 decreased the kinase activity of CDK4/6 resulting in decreased motility of a breast cancer cell line. Overexpression of CDK6 suppressed the inhibitor protein $p16^{INK4a}$ resulting in a decrease in cell spreading (Fahraeus and Lane, 1999). CDK6 was also shown to localize to the ruffling edge of spreading cells, indicating a function for CDK6 in controlling matrix-dependent cell spreading. Several studies have shown that stimulation of cells with LPS results in an increase in cellular motility and in some cases an increase in wound repair (Maa et al., 2008; Williams and Ridley, 2000). Migration of cells is essential for proper wound healing so I next observed the effect of overexpressing miR-107 or inhibiting miR-107 expression on migration of I-BMDM stimulated with LPS (Slomiany et al., 2006). I have shown that cells overexpressing miR-107 exhibited a decreased ability to migrate into a wounded area whereas cells lacking miR-107 displayed an enhanced capacity to move into the wounded area. All cells exhibited an enhanced ability to migrate following LPS stimulation for 24 hours.

The consequence of having decreased cellular proliferation and motility are a decrease in the overall immune response including decreased phagocytosis as well as decreased cytokine secretion. Microbes, apoptotic cells, necrotic cells and cellular debris are all recognized by receptors like TLRs and they are internalized through a cytoskeleton-dependent process of engulfment called phagocytosis (Janeway and Medzhitov, 2002). Yeast studies have demonstrated that phagocytosis in mammalian cells requires a properly functioning actin cytoskeleton (Lamaze et al., 1997). I next examined the effect of miR-107 expression on phagocytosis. Macrophages exhibited a decreased ability to phagocytose live *E. coli* when miR-107 was overexpressed compared to control transfected cells. Cells lacking miR-107 displayed no difference in their ability to phagocytose live *E. coli* compared to anti-control transfected cells. TNF-α secretion was also measured and it was reduced in cells overexpressing miR-107 and infected with live *E. coli*. This effect could be due to a more direct mechanism involving the metabolism of the cell increasing in response to LPS and when miR-107 is over-expressed there is less cytokine secretion because there

is a decrease in metabolism. A possible mechanism for the massive decrease in TNF-α secretion by cells infected with live *E. coli* and over-expressing miR-107 could be due to a functioning miR-107* sequence targeting an mRNA in this situation and not when only LPS is present. In fact, the miR-107* strand should always be considered and in future experiments should be assessed for its function.

A BLAST search was conducted using both the precursor miR-107 transcript sequence and the mature sequence to observe if other genes are homologous to the sequence. A partial match with sequence similarity of 16 of 22 nucleotides was found within the *Yersinia enterocolitica* 8081 bacterial genome. No studies have shown the ability of bacteria to exploit a cellular mechanism like the regulation of miRNA but they do take advantage of other mechanisms. *Y. enterocolitica* is a gram-negative bacterium and signals through TLR4. It replicates within the host in alternative phagosomes where it can live and avoid the acidic environment of traditional phagosomes. The partial miR-107 sequence found in the *Yersinia* genome is flanked by transposable insertion elements on either side. Transposable elements make it possible for a sequence to move within its own genome, to a plasmid or the genomes of other organisms. It may be possible that a strain of *Y. enterocolitica* was able to "steal" the sequence of miR-107 and insert it into its own genome. Why a bacterium would want to have the miR-107 sequence in its own genome remains a mystery, but it could be possible that it is able to manipulate an infected host cell into thinking that miR-107 is being expressed and its target genes like CDK6 will be downregulated leading to a decrease in actin polymerization and proliferation and enable an internalized *Y. enterocolitica* bacterium to remain undetected by host defense mechanisms.

In data not shown, I infected macrophages overexpressing or lacking miR-107 with *Y. enterocolotica*. Cells overexpressing miR-107 exhibited an enhanced ability to phagocytose live *Y. enterocolitica* compared to control transfected cells, whereas cells lacking miR-107 displayed a decreased ability to phagocytose live bacteria. It is possible that the miR-107 sequence found in the *Y. enterocolotica* genome is expressed by the bacterium and targets the precursor miR-107 sequence for degradation similar to RNAi resulting in an upregulation of miR-107

target genes like CDK6 and thus an increase in cellular proliferation and migration. This would allow for more phagocytosis and more *Y. enterocolotica* to be found within host cells. Many more experiments need to be done to further this hypothesis. For instance the miR-107 sequence could be deleted from the *Y. enterocolotica* genome and the mutant bacteria could be assessed for rate of uptake by macrophages.

Each of the functional experiments shown in this study has resulted in more evidence to support a key role for miR-107 in the immune response. I have found that miR-107 expression impacts several cellular functions and most likely many more. I have demonstrated that increased miR-107 expression leads to decreased CDK6 expression and this leads to decreased polymerization of filamentous actin, decreased TNF-α cytokine secretion, decreased cellular proliferation, decreased migration and decreased phagocytosis of live *E. coli*. As more miR-107 targets are validated more functional consequences related to the expression of miR-107 will be established. The more that is understood regarding the role miR-107 in TLR signaling, the greater the therapeutic potential to be used as a small molecule inhibitor to treat inflammatory diseases and sepsis where there is excessive inflammation that needs to controlled.

Potential miR-107 target	Pro or anti-inflammatory	Tumor suppressor or oncogenic	Associated Disease
Myosin9	Pro-inflammatory	Oncogenic	Epstein syndrome, May-Hegglin anomal, glomerulosclerosis
Vinculin	Pro-inflammatory	Tumor suppressor	Dilated cardiomyopathy
Ankyrin1	Pro-inflammatory	Tumor suppressor	Spherocytosis
HIF-1α	Pro-inflammatory	Oncogenic	Hypoxia, leukemia
Dicer1	Pro-inflammatory	Haploinsufficient tumor suppressor, Oncogenic	Ovarian, gastric cancer, pleuropulmonary blastoma
CDK6	Pro-inflammatory	Tumor suppressor	Retinoblastoma, medulloblastoma

Table 5.3. **Potential miR-107 target genes that are induced in response to LPS**. The table depicts if expression of the potential target gene is pro or anti-inflammatory, if it progresses or prevents the development of cancer, and the diseases associated with the irregular expression of the gene.

CHAPTER 6

FINAL DISCUSSION

The first aim of this study was to validate previous data obtained in a screen of 158 miRNAs following stimulation with various TLR ligands in a murine dendritic cell line. The data from the screen showed that five miRNAs are upregulated and four miRNAs are downregulated in response to three different TLR ligands. Both sets of miRNAs were examined in this study but based on the preliminary data obtained I focused on one particular miRNA, miR-107 and its response to TLR stimulation over time and in different cell types. By using *in vitro* and *in silico* methods, I have explored the role of miR-107 in TLR signaling as well as its role and function in host defense mechanisms. Figure 6.1 depicts the findings from this study. Following activation of TLR4 by LPS, NF-κB is activated which I have shown is required for the decrease in PPARα expression. A previous study has shown that p65 directly interacts with PPARα. I believe that this interaction is required for the downregulation of PPARα mRNA expression either through the inhibition of transcription of PPARα at the promoter level or p65 is inhibiting the formation of the PPARα/RXR complex. Two studies demonstrated that addition of WY14643 resulted in decreased proliferation of smooth muscle cells and also interfered with cellular migration through the inhibition of matrix metalloproteinase 9. Splenocytes harvested from mice fed WY14643 demonstrated impaired production of IFNγ, IL-6, and TNF-α (Cunard et al., 2002; Zahradka et al., 2006). I have found that the decrease in PPARα leads to the subsequent downregulation of both PanK1α and miR-107 expression which results in the upregulation of CDK6 and the proliferative and migratory ability of cells is enhanced.

In the past, the majority of miRNA studies began with *in silico* analysis to find target genes of the selected miRNAs. Currently, lists of target genes are obtained through microarray analysis where the use of anti-miR oligonucleotides to knockdown a miRNA and precursor oligonucleotides to overexpress a miRNA are used to find genes affected by both. There is speculation surrounding the many miRNA databases and at times there is difficulty in finding consistency between databases (Grimson et al., 2007a). Other methods need to be developed to find and validate potential targets of miRNAs. A recent study described a novel technique for revealing miRNA targets by transfecting cells with a biotinylated

miRNA which is used to pull down all the mRNA that binds to it (Orom and Lund, 2007; Orom et al., 2008). The RNA was then isolated and subjected to microarray technology to identify the mRNA that has bound to the miRNA. A list of direct targets for the miRNA is revealed and this list can be compared to the databases.

Through the use of microarray analysis and the generation of knockout mice more evidence has been generated to support the idea that miRNAs have a direct role in the immune response. miR-146a is a negative regulator of innate immune signaling and miR-155 is needed for the correct development of adaptive immunity and in regulating the pro-inflammatory response (McCoy et al., 2010; O'Connell et al., 2007; Rodriguez et al., 2007; Taganov et al., 2006; Thai et al., 2007). miR-21 induction is required for the anti-inflammatory response to be initiated following stimulation with LPS (Sheedy et al., 2010). Let-7i displayed a degree of regulation over TLR4 signaling (Chen et al., 2007). miR-9 plays a role in neutrophil response to LPS and has been shown to target translation of p65 (Bazzoni et al., 2009). miR-147 is induced in macrophages in response to TLR2, 3 and 4 stimuli resulting in the negative regulation of pro-inflammatory cytokine production (Liu et al., 2009)

The dysregulation of miRNAs is linked to a diverse range of phenotypes implicating their expression in nearly all biological processes. Their expression has been associated with cardiovascular disease, cancer, inflammation and viral infection. The wide range of miRNAs implicated in the immune response could potentially be used to diagnose and treat various diseases. The expression pattern of miRNAs is specific to various disease states (Alevizos and Illei, 2010; Schuster et al., 2010; Taylor and Gercel-Taylor, 2008; Wittmann and Jack, 2010). Because of their unique expression pattern, miRNAs are promising biomarkers in the diagnosis and prognosis of diseases like cancer and rheumatoid arthritis. Clusters of miRNAs are found in secreted exosomes of cells and depending on the disease state, a different cluster of miRNAs will be found in the exosome (De Smaele et al., 2010; Hunter et al., 2008; Kosaka et al., 2010b; Rabinowits et al., 2009). The use of small non-coding RNA like miRNA as small molecule inhibitors or mimics to enhance the expression of a miRNA are an emerging class of therapeutic

(Jackson and Linsley, 2010). Because miRNA are negative regulators and fine-tuners of gene expression the effects of therapeutically administering a single miRNA may have an impact on the expression of many target genes, not just one and this may manifest itself as a safety issue. However, these potential "off-target" effects have not deterred researchers from exploring miRNA therapies. Several companies are developing approaches to target miRNAs, most notably antagomirs and locked nucleic acid miRNA inhibitors (Stenvang et al., 2008). These approaches, if used to target TLR-regulated miRNAs could prove to have therapeutic benefits.

Some of the miRNAs used as positive controls of TLR activation in this study have tremendous therapeutic potential (See figure 1.5 for detailed diagram). miR-146a is upregulated in response to LPS and targets TRAF6 and IRAK1, which are important molecules in the TLR4 signaling pathway. The elimination of miR-146a expression could lead to a pro-inflammatory adjuvant effect in cancer or infection. miR-155 is upregulated in response to LPS and targets SHIP-1, which is a negative regulator of NF-κB signaling. The elimination of miR-155 could have an inhibitory effect on TLR signaling. miR-21 expression also increases in response to LPS and targets the IL-10 inhibitor PDCD4 leading to an increase in IL-10 production. The elimination of miR-21 would inhibit IL-10 production and have an immunostimulatory effect. Mimicking these miRNAs would potentially have an anti-inflammatory effect in response to stimuli like LPS. miR-155 overexpressing transgenic mice exhibit enhanced TNF-α production (Tili et al., 2007). I have demonstrated in the proliferation experiments in this study that the targeting of a single miRNA for knockdown or overexpression results in a less drastic functional result than the knockdown of a single gene or knocking out that gene. This result provides support for the notion that miRNAs could act as excellent small molecule inhibitors in many diseases.

miRNAs are a single type of negative regulator of TLR signaling. The phosphorylation and ubiquitination of proteins are processes that are also involved in the regulation of TLR signaling. These are key covalent modifications that lead to activation of NF-κB. Recent research has shown that modulating these modifications in cell signaling cascades can be beneficial in the treatment of

cancer, neurodegenerative disease, inflammation and viral infections (Nalepa et al., 2006; Petroski, 2008). Proteins targeted for degradation are tagged with a chain of ubiquitin molecules via ligation to lysine residues. K48-linked polyubiquitin is thought to be the primary form that is recognized by the proteasome for degradation and K63-linked seems to be regulatory (Nalepa et al., 2006). Ubiquitin-activating enzymes (E1), ubiquitin-conjugating enzymes (E2s), and ubiquitin ligases (E3s) all have a role in the process of ubiquitination in the cell. In the TLR signalling pathway TRAF6 (a target of miR-146a) has E3 ubiquitin-ligase activity and *in vitro* studies have demonstrated the capacity for inhibitors of TRAF6 to block autoubiquitination as well as cell proliferation (Guedat and Colland, 2007). Inhibitors of apoptosis proteins (IAPs) are another group of molecules that act as negative regulators of immune signalling (Cossu et al., 2009a). IAPs are upregulated in many cancers and exert their effect by inhibiting caspases. They are regulated via an endogenous inhibitor SMAC (Second mitochondria-derived activator of caspase) SMAC binds to IAPs and disrupts their ability to inhibit caspases, enzymes involved in apoptosis. cIAP1 and cIAP2 associate with TRAF1, TRAF2, and TRAF6 to participate in NF-κB activation by IL1R/TLR signalling molecules, TNF-α and CD40 which use TRAF6. Importantly the role of cIAP1 appears to be to mediate K48-linked ubiquitination of TRAF3 an inhibitor of TLR signalling (Vallabhapurapu et al., 2008). SMAC-mimetics can kill malignant cells by binding to cIAP1 and cIAP2, leading to TNF-receptor mediated apoptosis as well as possibly block cIAP1 and cIAP2 from degrading TRAF3 and inhibit subsequent NF-κB activation (Cossu et al., 2009b).

A study examining the effect of miR-146a on IRAK1 expression showed that overexpression of miR-146a directly affected IRAK1 as well as NF-κB resulting in an inhibition of invasion of pancreatic cancer cells (Li et al., 2010). The IRAKs (1, 2 & 4) are a class of proteins that are subject to negative regulation in TLR signaling and they have proven to be excellent targets for therapeutics to reduce the inflammatory response. The best understood of the family is IRAK4. Mice that express a catalytically inactive mutant of IRAK4 are completely resistant to septic shock and show impaired IL-1 activity (Cohen, 2009). Dendritic cells from these mice do not produce IFN-α in response to TLR7, 8 and 9 ligands or

following infection by influenza virus. Furthermore, these mice are resistant to joint inflammation and destruction, and also bone destruction in a model of arthritis, supporting the targeting of the kinase activity of IRAK-4 for chronic inflammation (Koziczak-Holbro et al., 2009). IRAK-M acts as a negative regulator of TLR signaling. IRAK-M activation prevented the formation of IRAK-TRAF6 complexes (Kobayashi et al., 2002a). IRAK-M deficient cells displayed increased cytokine production following TLR stimulation and the knockout mice showed increased inflammatory responses. I have described two levels of negative regulation, there is regulation of protein translation and there is regulation of mRNA and transcription. All aspects of negative regulation work in concert with each other resulting in an appropriate and hopefully effective immune response. The different levels of regulation demonstrate the tremendous importance of controlling signal transduction in the cell. Each of the negative regulators of immune signaling described here, including miRNAs exhibit tremendous therapeutic potential.

Similar to miRNAs, the abnormal expression of cyclins and the downregulation of CDK inhibitors (CDKi) have been linked to the progression of various cancers (Brotherton et al., 1998; Hirai et al., 2005; Lee et al., 2008; Sellers and Kaelin, 1997). The search for chemical inhibitors of CDKs is underway and some candidates are currently being evaluated in clinical trials as anti-cancer and anti-inflammatory therapies (Duffin et al., 2009; Leitch et al., 2009). CDKi drugs have shown significant effects on many cell types including lymphocytes and fibroblasts and have demonstrated pro-apoptotic potential (Rossi et al., 2006). Immune cells such as neutrophils undergo apoptosis during the resolution phase of inflammation, leading to the recognition and removal of the apoptotic bodies by macrophages. However, if macrophage phagocytosis or neutrophil apoptosis is impaired, chronic inflammation may occur. CDK inhibitors such as R-roscovitine have the therapeutic potential to treat inflammatory diseases by targeting neutrophils for apoptosis. It is suggested that key endogenous survival proteins like Mcl-1 are the targets of CDK inhibitors and may be of critical importance in the resolution of inflammation (Leitch et al., 2010). The CDKi $p21^{Cip1/Waf1}$ is specific towards CDK2, 4 and 6 and acts as a negative regulator of the activation of macrophages by reducing TNF-α and IL-1β production in response to LPS. p21

knockout mice demonstrated an increased susceptibility to LPS-induced shock brought about by increased levels of IL-1β (Lloberas and Celada, 2009; Scatizzi et al., 2009). The expression of p21 in lung epithelial cells resulted in a decrease in lung inflammation and reduced fibrosis. Patients who were given p21 via gene transfer exhibited down-regulation of IL-6, IL-8, monocytes chemoattractant protein-1 (MCP-1), and cathepsins (Nonomura et al., 2003). Based on the evidence obtained from my study, in disease situations where there is excessive inflammation precursor-miR-107 could act as a small-molecule inhibitor of CDK6 in a similar way as validated CDKi therapies but without the drawbacks and side effects of traditional CDKi therapies which include neutropenia and the possibility of redundancies amongst CDKs leading to lack of efficacy. A combination of RNA and CDKi therapies could prove to be beneficial.

Many additional experiments could be done in the future to further elucidate the importance of miR-107 in innate immune signaling as well as to reveal the currently unknown role of PanK1α in TLR signaling. As mentioned previously, there is no definitive role for CoA in immunity but based on the observation from this study that PanK1α decreases in response to LPS stimulation, there must be a role for CoA in TLR signaling. It is known that fatty acid oxidation and gluconeogenesis are decreased in response to LPS whereas inhibitors of NF-κB enhance fatty acid oxidation (Planavila et al., 2005). p65 is known to physically interact with PPARα. This is the first study to show that the decrease in PPARα is dependent on p65 suggesting that p65 is acting as some sort of repressor of PPARα activation. The link between metabolism and immunity is becoming more evident and the roles of miR-107, PanK1α and PPARα could be major players in these processes.

It will be of interest to extend the findings from this study to other targets of miR-107 to determine if there is a cooperative effect of miR-107 targets on functions like proliferation and motility. Table 5.3 lists other potential targets of miR-107 that increased in expression in response to LPS. The table describes if they are pro or anti-inflammatory as well as their role in cancer and disease. There may also be a cooperative effect between different miRNAs with defined roles in TLR signaling as shown in figure 1.5. There is the potential of a feedback loop between

miR-21 and miR-155. miR-21 expression increases in response to TLR stimuli to allow for the enhanced production of IL-10 which acts as a suppressor of miR-155 expression and this would turn off the Akt pathway leading to decreased NF-κB activity (McCoy et al., 2010; O'Connell et al., 2009; Sheedy et al., 2010). miR-107 also may potentially play a role in the regulation of these miRNAs. As shown in this study the overexpression of miR-107 led to a decrease in TNF-α secretion and the CDK6 deficient BMDM exhibited decreased TNF-α and IL-10 which would allow for the enhanced expression of miR-155. It will be interesting to further study Dicer1 as a potential target of miR-107. Because miR-107 downregulation in response to LPS occurs from 2 to 8 hours post-stimulation, this would increase Dicer1 expression leading to the processing of the miRNAs that are upregulated at later times post-stimulation like miR-155 and miR-21. It will be interesting to study other miRNA that are downregulated in response to LPS as well as to examine the precise mechanisms by which TLR signals leads to the downregulation of miR-107 and other miRNA. This study has demonstrated that manipulating a single 23 nucleotide miRNA can drastically affect a biological function like proliferation leaving no room for debate that miRNAs are anything but insignificant.

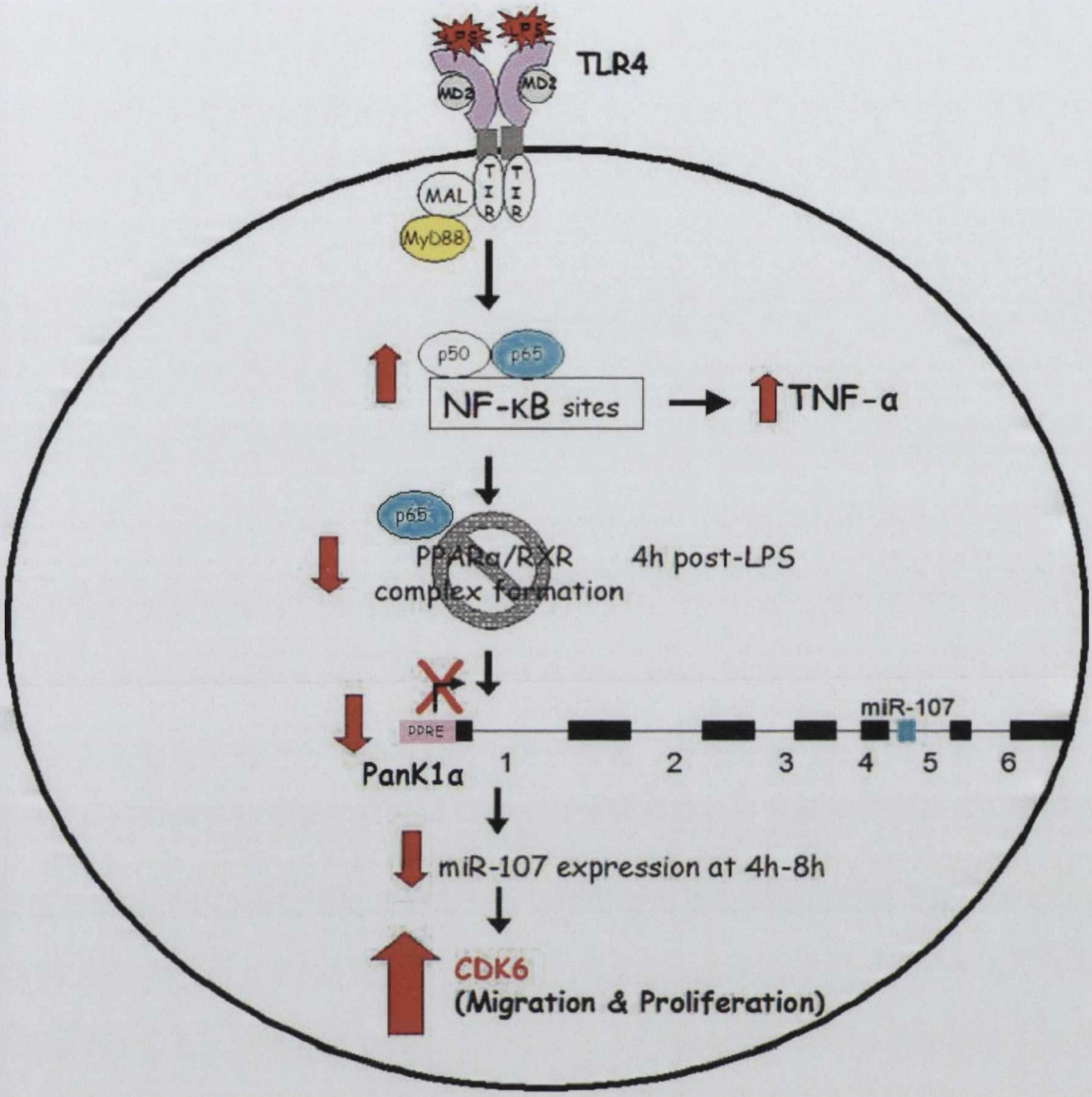


Figure 6.1. **Regulation of cellular proliferation and migration via the decrease in miR-107 expression in response to LPS which leads to an increase in CDK6 expression**. Model depicting the role of miR-107 in modulating TLR4 signaling.

CHAPTER 7

REFERENCES

Agnese, D., Calvano, J., Hahm, S., Coyle, S., Corbett, S., Calvano, S., and Lowry, S. (2002). Human toll-like receptor 4 mutations but not CD14 polymorphisms are associated with an increased risk of gram-negative infections. J Infect Dis *186*, 1522-1525.

Akira, S., and Takeda, K. (2004). Functions of toll-like receptors: lessons from KO mice. C R Biol *327*, 581-589.

Alevizos, I., and Illei, G.G. (2010). MicroRNAs as biomarkers in rheumatic diseases. Nat Rev Rheumatol *6*, 391-398.

Androulidaki, A., Iliopoulos, D., Arranz, A., Doxaki, C., Schworer, S., Zacharioudaki, V., Margioris, A.N., Tsichlis, P.N., and Tsatsanis, C. (2009). The kinase Akt1 controls macrophage response to lipopolysaccharide by regulating microRNAs. Immunity *31*, 220-231.

Arteel, G.E., Guo, L., Schlierf, T., Beier, J.I., Kaiser, J.P., Chen, T.S., Liu, M., Conklin, D.J., Miller, H.L., von Montfort, C., and States, J.C. (2008). Subhepatotoxic exposure to arsenic enhances lipopolysaccharide-induced liver injury in mice. Toxicol Appl Pharmacol *226*, 128-139.

Asirvatham, A., Gregorie, C., Hu, Z., Magner, W., and Tomasi, T. (2007). MicroRNA targets in immune genes and the Dicer/Argonaute and ARE machinery components. Mol Immunol.

Atamna, H., and Frey, W.H., 2nd (2007). Mechanisms of mitochondrial dysfunction and energy deficiency in Alzheimer's disease. Mitochondrion *7*, 297-310.

Barger, P.M., Browning, A.C., Garner, A.N., and Kelly, D.P. (2001). p38 mitogen-activated protein kinase activates peroxisome proliferator-activated receptor alpha: a potential role in the cardiac metabolic stress response. J Biol Chem *276*, 44495-44501.

Bazzoni, F., Rossato, M., Fabbri, M., Gaudiosi, D., Mirolo, M., Mori, L., Tamassia, N., Mantovani, A., Cassatella, M.A., and Locati, M. (2009). Induction and regulatory function of miR-9 in human monocytes and neutrophils exposed to proinflammatory signals. Proc Natl Acad Sci U S A *106*, 5282-5287.

Becker, J., Delayre-Orthez, C., Frossard, N., and Pons, F. (2008). Regulation of peroxisome proliferator-activated receptor-alpha expression during lung inflammation. Pulm Pharmacol Ther *21*, 324-330.

Beigneux, A.P., Moser, A.H., Shigenaga, J.K., Grunfeld, C., and Feingold, K.R. (2000). The acute phase response is associated with retinoid X receptor repression in rodent liver. J Biol Chem *275*, 16390-16399.

Belair, C., Darfeuille, F., and Staedel, C. (2009). Helicobacter pylori and gastric cancer: possible role of microRNAs in this intimate relationship. Clin Microbiol Infect *15*, 806-812.

Birney, E., Stamatoyannopoulos, J.A., Dutta, A., Guigo, R., Gingeras, T.R., Margulies, E.H., Weng, Z., Snyder, M., Dermitzakis, E.T., Thurman, R.E., *et al.* (2007). Identification and analysis of functional elements in 1% of the human genome by the ENCODE pilot project. Nature *447*, 799-816.

Blouin, C.C., Page, E.L., Soucy, G.M., and Richard, D.E. (2004). Hypoxic gene activation by lipopolysaccharide in macrophages: implication of hypoxia-inducible factor 1alpha. Blood *103*, 1124-1130.

Bohlig, L., Friedrich, M., and Engeland, K. (2010). p53 activates the PANK1/miRNA-107 gene leading to downregulation of CDK6 and p130 cell cycle proteins. Nucleic Acids Res.

Bowie, A., Kiss-Toth, E., Symons, J.A., Smith, G.L., Dower, S.K., and O'Neill, L.A. (2000). A46R and A52R from vaccinia virus are antagonists of host IL-1 and toll-like receptor signaling. Proc Natl Acad Sci U S A *97*, 10162-10167.

Brotherton, D.H., Dhanaraj, V., Wick, S., Brizuela, L., Domaille, P.J., Volyanik, E., Xu, X., Parisini, E., Smith, B.O., Archer, S.J., *et al.* (1998). Crystal structure of the complex of the cyclin D-dependent kinase Cdk6 bound to the cell-cycle inhibitor p19INK4d. Nature *395*, 244-250.

Brown, H. (1995). Ilya Mechnikov and his studies on comparative inflammation. Proc Soc Exp Biol Med *209*, 99-101.

Brown, J.W., Marshall, D.F., and Echeverria, M. (2008). Intronic noncoding RNAs and splicing. Trends Plant Sci *13*, 335-342.

Burns, K., Martinon, F., Esslinger, C., Pahl, H., Schneider, P., Bodmer, J.L., Di Marco, F., French, L., and Tschopp, J. (1998). MyD88, an adapter protein involved in interleukin-1 signaling. J Biol Chem *273*, 12203-12209.

Calin, G., Dumitru, C., Shimizu, M., Bichi, R., Zupo, S., Noch, E., Aldler, H., Rattan, S., Keating, M., Rai, K., *et al.* (2002). Frequent deletions and down-regulation of micro- RNA genes miR15 and miR16 at 13q14 in chronic lymphocytic leukemia. Proc Natl Acad Sci U S A *99*, 15524-15529.

Calin, G., Pekarsky, Y., and Croce, C. (2007). The role of microRNA and other non-coding RNA in the pathogenesis of chronic lymphocytic leukemia. Best Pract Res Clin Haematol *20*, 425-437.

Chen, C.Z., Li, L., Lodish, H.F., and Bartel, D.P. (2004). MicroRNAs modulate hematopoietic lineage differentiation. Science *303*, 83-86.

Chen, P.Y., and Meister, G. (2005). microRNA-guided posttranscriptional gene regulation. Biol Chem *386*, 1205-1218.

Chen, X., Splinter, P., O'Hara, S., and LaRusso, N. (2007). A cellular micro-RNA, let-7i, regulates Toll-like receptor 4 expression and contributes to cholangiocyte immune responses against Cryptosporidium parvum infection. J Biol Chem *282*, 28929-28938.

Chinetti, G., Fruchart, J.C., and Staels, B. (2000). Peroxisome proliferator-activated receptors (PPARs): nuclear receptors at the crossroads between lipid metabolism and inflammation. Inflamm Res *49*, 497-505.

Cho, W.C. (2007). OncomiRs: the discovery and progress of microRNAs in cancers. Mol Cancer *6*, 60.

Chow, T.F., Mankaruos, M., Scorilas, A., Youssef, Y., Girgis, A., Mossad, S., Metias, S., Rofael, Y., Honey, R.J., Stewart, R., *et al.* (2010). The miR-17-92 cluster is over expressed in and has an oncogenic effect on renal cell carcinoma. J Urol *183*, 743-751.

Cobb, B.S., Nesterova, T.B., Thompson, E., Hertweck, A., O'Connor, E., Godwin, J., Wilson, C.B., Brockdorff, N., Fisher, A.G., Smale, S.T., and Merkenschlager, M. (2005). T cell lineage choice and differentiation in the absence of the RNase III enzyme Dicer. J Exp Med *201*, 1367-1373.

Cohen, P. (2009). Targeting protein kinases for the development of anti-inflammatory drugs. Curr Opin Cell Biol *21*, 317-324.

Cohn, Z.A. (1963). The fate of bacteria within phagocytic cells. I. The degradation of isotopically labeled bacteria by polymorphonuclear leucocytes and macrophages. J Exp Med *117*, 27-42.

Cook, D., Hollingsworth, J.J., and Schwartz, D. (2003). Toll-like receptors and the genetics of innate immunity. Curr Opin Allergy Clin Immunol *3*, 523-529.

Cook, D., Pisetsky, D., and Schwartz, D. (2004). Toll-like receptors in the pathogenesis of human disease. Nat Immunol *5*, 975-979.

Cossu, F., Mastrangelo, E., Milani, M., Sorrentino, G., Lecis, D., Delia, D., Manzoni, L., Seneci, P., Scolastico, C., and Bolognesi, M. (2009a). Designing Smac-mimetics as antagonists of XIAP, cIAP1, and cIAP2. Biochem Biophys Res Commun *378*, 162-167.

Cossu, F., Milani, M., Mastrangelo, E., Vachette, P., Servida, F., Lecis, D., Canevari, G., Delia, D., Drago, C., Rizzo, V., *et al.* (2009b). Structural Basis for Bivalent Smac-Mimetics Recognition in the IAP Protein Family. J Mol Biol.

Criss, A.K., Ahlgren, D.M., Jou, T.S., McCormick, B.A., and Casanova, J.E. (2001). The GTPase Rac1 selectively regulates Salmonella invasion at the apical plasma membrane of polarized epithelial cells. J Cell Sci *114*, 1331-1341.

Cunard, R., DiCampli, D., Archer, D.C., Stevenson, J.L., Ricote, M., Glass, C.K., and Kelly, C.J. (2002). WY14,643, a PPAR alpha ligand, has profound effects on immune responses in vivo. J Immunol *169*, 6806-6812.

Curtale, G., Citarella, F., Carissimi, C., Goldoni, M., Carucci, N., Fulci, V., Franceschini, D., Meloni, F., Barnaba, V., and Macino, G. (2010). An emerging player in the adaptive immune response: microRNA-146a is a modulator of IL-2 expression and activation-induced cell death in T lymphocytes. Blood *115*, 265-273.

Czech, B., Zhou, R., Erlich, Y., Brennecke, J., Binari, R., Villalta, C., Gordon, A., Perrimon, N., and Hannon, G.J. (2009). Hierarchical rules for Argonaute loading in Drosophila. Mol Cell *36*, 445-456.

Daffis, S., Samuel, M.A., Suthar, M.S., Gale, M., Jr., and Diamond, M.S. (2008). Toll-like receptor 3 has a protective role against West Nile virus infection. J Virol *82*, 10349-10358.

De Smaele, E., Ferretti, E., and Gulino, A. (2010). MicroRNAs as biomarkers for CNS cancer and other disorders. Brain Res *1338*, 100-111.

Delerive, P., De Bosscher, K., Besnard, S., Vanden Berghe, W., Peters, J.M., Gonzalez, F.J., Fruchart, J.C., Tedgui, A., Haegeman, G., and Staels, B. (1999). Peroxisome proliferator-activated receptor alpha negatively regulates the vascular inflammatory gene response by negative cross-talk with transcription factors NF-kappaB and AP-1. J Biol Chem *274*, 32048-32054.

DiDonato, J.A., Hayakawa, M., Rothwarf, D.M., Zandi, E., and Karin, M. (1997). A cytokine-responsive IkappaB kinase that activates the transcription factor NF-kappaB. Nature *388*, 548-554.

Dolt, K.S., Mishra, M.K., Karar, J., Baig, M.A., Ahmed, Z., and Pasha, M.A. (2007). cDNA cloning, gene organization and variant specific expression of HIF-1 alpha in high altitude yak (Bos grunniens). Gene *386*, 73-80.

Duffin, R., Leitch, A.E., Sheldrake, T.A., Hallett, J.M., Meyer, C., Fox, S., Alessandri, A.L., Martin, M.C., Brady, H.J., Teixeira, M.M., *et al.* (2009). The CDK inhibitor, R-roscovitine, promotes eosinophil apoptosis by down-regulation of Mcl-1. FEBS Lett *583*, 2540-2546.

Ericson, K.K., Krull, D., Slomiany, P., and Grossel, M.J. (2003). Expression of cyclin-dependent kinase 6, but not cyclin-dependent kinase 4, alters morphology of cultured mouse astrocytes. Mol Cancer Res *1*, 654-664.

Fahraeus, R., and Lane, D.P. (1999). The p16(INK4a) tumour suppressor protein inhibits alphavbeta3 integrin-mediated cell spreading on vitronectin by blocking PKC-dependent localization of alphavbeta3 to focal contacts. EMBO J *18*, 2106-2118.

Fearon, D., and Locksley, R. (1996). The instructive role of innate immunity in the acquired immune response. Science *272*, 50-53.

Feingold, K.R., Moser, A., Patsek, S.M., Shigenaga, J.K., and Grunfeld, C. (2009). Infection decreases fatty acid oxidation and nuclear hormone receptors in the diaphragm. J Lipid Res.

Feingold, K.R., Wang, Y., Moser, A., Shigenaga, J.K., and Grunfeld, C. (2008). LPS decreases fatty acid oxidation and nuclear hormone receptors in the kidney. J Lipid Res *49*, 2179-2187.

Fiaschi-Taesch, N.M., Salim, F., Kleinberger, J., Troxell, R., Cozar-Castellano, I., Selk, K., Cherok, E., Takane, K.K., Scott, D.K., and Stewart, A.F. (2010). Induction of human beta-cell proliferation and engraftment using a single G1/S regulatory molecule, cdk6. Diabetes *59*, 1926-1936.

Fidalgo, B.V., and Najjar, V.A. (1967). The physiological role of the lymphoid system. VI. The stimulatory effect of leucophilic gamma globulin (leucokinin) on the phagocytic activity of human polymorphonuclear leucocyte. Biochemistry *6*, 3386-3392.

Fitzgerald, K., Palsson-McDermott, E., Bowie, A., Jefferies, C., Mansell, A., Brady, G., Brint, E., Dunne, A., Gray, P., Harte, M., *et al.* (2001). Mal (MyD88-adapter-like) is required for Toll-like receptor-4 signal transduction. Nature *413*, 78-83.

Fitzgerald, K., Rowe, D., Barnes, B., Caffrey, D., Visintin, A., Latz, E., Monks, B., Pitha, P., and Golenbock, D. (2003). LPS-TLR4 signaling to IRF-3/7 and NF-kappaB involves the toll adapters TRAM and TRIF. J Exp Med *198*, 1043-1055.

Fontana, L., Pelosi, E., Greco, P., Racanicchi, S., Testa, U., Liuzzi, F., Croce, C.M., Brunetti, E., Grignani, F., and Peschle, C. (2007). MicroRNAs 17-5p-20a-106a control monocytopoiesis through AML1 targeting and M-CSF receptor upregulation. Nat Cell Biol *9*, 775-787.

Frankel, L., Christoffersen, N., Jacobsen, A., Lindow, M., Krogh, A., and Lund, A. (2008). Programmed cell death 4 (PDCD4) is an important functional target of the microRNA miR-21 in breast cancer cells. J Biol Chem *283*, 1026-1033.

Friedman, R.C., Farh, K.K., Burge, C.B., and Bartel, D.P. (2009). Most mammalian mRNAs are conserved targets of microRNAs. Genome Res *19*, 92-105.

Furuta, M., Kozaki, K.I., Tanaka, S., Arii, S., Imoto, I., and Inazawa, J. (2010). miR-124 and miR-203 are epigenetically silenced tumor-suppressive microRNAs in hepatocellular carcinoma. Carcinogenesis *31*, 766-776.

García-Mauriño, S., Pozo, D., Carrillo-Vico, A., Calvo, J., and Guerrero, J. (1999). Melatonin activates Th1 lymphocytes by increasing IL-12 production. Life Sci *65*, 2143-2150.

Garzon, R., Pichiorri, F., Palumbo, T., Visentini, M., Aqeilan, R., Cimmino, A., Wang, H., Sun, H., Volinia, S., Alder, H., *et al.* (2007). MicroRNA gene expression during retinoic acid-induced differentiation of human acute promyelocytic leukemia. Oncogene *26*, 4148-4157.

Gordon, S. (2002). Pattern recognition receptors: doubling up for the innate immune response. Cell *111*, 927-930.

Goto, M., Yoshioka, T., Battelino, T., Ravindranath, T., and Zeller, W.P. (2001). TNFalpha decreases gluconeogenesis in hepatocytes isolated from 10-day-old rats. Pediatr Res *49*, 552-557.

Goto, M., Zeller, W.P., and Lichtenberg, R.C. (1994). Decreased gluconeogenesis and increased glucose disposal without hyperinsulinemia in 10-day-old rats with endotoxic shock. Metabolism *43*, 1248-1254.

Gottesman, S. (2005). Micros for microbes: non-coding regulatory RNAs in bacteria. Trends Genet *21*, 399-404.

Gottwein, E., Mukherjee, N., Sachse, C., Frenzel, C., Majoros, W., Chi, J., Braich, R., Manoharan, M., Soutschek, J., Ohler, U., and Cullen, B. (2007). A viral microRNA functions as an orthologue of cellular miR-155. Nature *450*, 1096-1099.

Greenberg, S., and Grinstein, S. (2002). Phagocytosis and innate immunity. Curr Opin Immunol *14*, 136-145.

Grimson, A., Farh, K., Johnston, W., Garrett-Engele, P., Lim, L., and Bartel, D. (2007a). MicroRNA targeting specificity in mammals: determinants beyond seed pairing. Mol Cell *27*, 91-105.

Grimson, A., Farh, K.K., Johnston, W.K., Garrett-Engele, P., Lim, L.P., and Bartel, D.P. (2007b). MicroRNA targeting specificity in mammals: determinants beyond seed pairing. Mol Cell *27*, 91-105.

Grossel, M.J., and Hinds, P.W. (2006a). Beyond the cell cycle: a new role for Cdk6 in differentiation. J Cell Biochem *97*, 485-493.

Grossel, M.J., and Hinds, P.W. (2006b). From cell cycle to differentiation: an expanding role for cdk6. Cell Cycle *5*, 266-270.

Guedat, P., and Colland, F. (2007). Patented small molecule inhibitors in the ubiquitin proteasome system. BMC Biochem *8 Suppl 1*, S14.

Han, L., Witmer, P.D., Casey, E., Valle, D., and Sukumar, S. (2007). DNA methylation regulates MicroRNA expression. Cancer Biol Ther *6*, 1284-1288.

Harte, M.T., Haga, I.R., Maloney, G., Gray, P., Reading, P.C., Bartlett, N.W., Smith, G.L., Bowie, A., and O'Neill, L.A. (2003). The poxvirus protein A52R targets Toll-like receptor signaling complexes to suppress host defense. J Exp Med *197*, 343-351.

Hayashita, Y., Osada, H., Tatematsu, Y., Yamada, H., Yanagisawa, K., Tomida, S., Yatabe, Y., Kawahara, K., Sekido, Y., and Takahashi, T. (2005). A polycistronic microRNA cluster, miR-17-92, is overexpressed in human lung cancers and enhances cell proliferation. Cancer Res *65*, 9628-9632.

Hirai, H., Kawanishi, N., and Iwasawa, Y. (2005). Recent advances in the development of selective small molecule inhibitors for cyclin-dependent kinases. Curr Top Med Chem *5*, 167-179.

Hunter, M.P., Ismail, N., Zhang, X., Aguda, B.D., Lee, E.J., Yu, L., Xiao, T., Schafer, J., Lee, M.L., Schmittgen, T.D., *et al.* (2008). Detection of microRNA expression in human peripheral blood microvesicles. PLoS One *3*, e3694.

Inohara, N., Ogura, Y., Chen, F.F., Muto, A., and Nunez, G. (2001). Human Nod1 confers responsiveness to bacterial lipopolysaccharides. J Biol Chem *276*, 2551-2554.

Iorio, M., Ferracin, M., Liu, C., Veronese, A., Spizzo, R., Sabbioni, S., Magri, E., Pedriali, M., Fabbri, M., Campiglio, M., *et al.* (2005). MicroRNA gene expression deregulation in human breast cancer. Cancer Res *65*, 7065-7070.

Jackson, A., and Linsley, P.S. (2010). The therapeutic potential of microRNA modulation. Discov Med *9*, 311-318.

Jaillon, O., Bouhouche, K., Gout, J.F., Aury, J.M., Noel, B., Saudemont, B., Nowacki, M., Serrano, V., Porcel, B.M., Segurens, B., *et al.* (2008). Translational control of intron splicing in eukaryotes. Nature *451*, 359-362.

Janeway, C.A., Jr. (2001). How the immune system protects the host from infection. Microbes Infect *3*, 1167-1171.

Janeway, C.J., and Medzhitov, R. (2002). Innate immune recognition. Annu Rev Immunol *20*, 197-216.

Jindra, P.T., Bagley, J., Godwin, J.G., and Iacomini, J. (2010). Costimulation-dependent expression of microRNA-214 increases the ability of T cells to proliferate by targeting Pten. J Immunol *185*, 990-997.

Johnson, C.D., Esquela-Kerscher, A., Stefani, G., Byrom, M., Kelnar, K., Ovcharenko, D., Wilson, M., Wang, X., Shelton, J., Shingara, J., *et al.* (2007). The let-7 microRNA represses cell proliferation pathways in human cells. Cancer Res *67*, 7713-7722.

Kaisho, T., and Akira, S. (2006). Toll-like receptor function and signaling. J Allergy Clin Immunol *117*, 979-987; quiz 988.

Kantor, P.F., Lucien, A., Kozak, R., and Lopaschuk, G.D. (2000). The antianginal drug trimetazidine shifts cardiac energy metabolism from fatty acid oxidation to glucose oxidation by inhibiting mitochondrial long-chain 3-ketoacyl coenzyme A thiolase. Circ Res *86*, 580-588.

Kawai, T., and Akira, S. (2005a). Pathogen recognition with Toll-like receptors. Curr Opin Immunol *17*, 338-344.

Kawai, T., and Akira, S. (2005b). Toll-like receptor downstream signaling. Arthritis Res Ther *7*, 12-19.

Kawai, T., and Akira, S. (2006). TLR signaling. Cell Death Differ *13*, 816-825.

Khabar, K. (2007). Rapid transit in the immune cells: the role of mRNA turnover regulation. J Leukoc Biol *81*, 1335-1344.

Khor, C.C., Chapman, S.J., Vannberg, F.O., Dunne, A., Murphy, C., Ling, E.Y., Frodsham, A.J., Walley, A.J., Kyrieleis, O., Khan, A., *et al.* (2007). A Mal functional variant is associated with protection against invasive pneumococcal disease, bacteremia, malaria and tuberculosis. Nat Genet *39*, 523-528.

Kiechl, S., Lorenz, E., Reindl, M., Wiedermann, C., Oberhollenzer, F., Bonora, E., Willeit, J., and Schwartz, D. (2002). Toll-like receptor 4 polymorphisms and atherogenesis. N Engl J Med *347*, 185-192.

Kim, V.N. (2005). MicroRNA biogenesis: coordinated cropping and dicing. Nat Rev Mol Cell Biol *6*, 376-385.

Kim, Y.K., and Kim, V.N. (2007). Processing of intronic microRNAs. EMBO J *26*, 775-783.

Kobayashi, K., Hernandez, L.D., Galan, J.E., Janeway, C.A., Jr., Medzhitov, R., and Flavell, R.A. (2002a). IRAK-M is a negative regulator of Toll-like receptor signaling. Cell *110*, 191-202.

Kobayashi, K., Inohara, N., Hernandez, L.D., Galan, J.E., Nunez, G., Janeway, C.A., Medzhitov, R., and Flavell, R.A. (2002b). RICK/Rip2/CARDIAK mediates signalling for receptors of the innate and adaptive immune systems. Nature *416*, 194-199.

Kontrogianni-Konstantopoulos, A., Jones, E.M., Van Rossum, D.B., and Bloch, R.J. (2003). Obscurin is a ligand for small ankyrin 1 in skeletal muscle. Mol Biol Cell *14*, 1138-1148.

Kosaka, N., Iguchi, H., and Ochiya, T. (2010a). Circulating microRNA in body fluid: a new potential biomarker for cancer diagnosis and prognosis. Cancer Sci.

Kosaka, N., Iguchi, H., and Ochiya, T. (2010b). Circulating microRNA in body fluid: a new potential biomarker for cancer diagnosis and prognosis. Cancer Sci *101*, 2087-2092.

Koziczak-Holbro, M., Littlewood-Evans, A., Pollinger, B., Kovarik, J., Dawson, J., Zenke, G., Burkhart, C., Muller, M., and Gram, H. (2009). The critical role of kinase activity of interleukin-1 receptor-associated kinase 4 in animal models of joint inflammation. Arthritis Rheum *60*, 1661-1671.

Kulshreshtha, R., Davuluri, R.V., Calin, G.A., and Ivan, M. (2008). A microRNA component of the hypoxic response. Cell Death Differ *15*, 667-671.

Kulshreshtha, R., Ferracin, M., Wojcik, S.E., Garzon, R., Alder, H., Agosto-Perez, F.J., Davuluri, R., Liu, C.G., Croce, C.M., Negrini, M., *et al.* (2007). A microRNA signature of hypoxia. Mol Cell Biol *27*, 1859-1867.

Lai, E.C. (2002). Micro RNAs are complementary to 3' UTR sequence motifs that mediate negative post-transcriptional regulation. Nat Genet *30*, 363-364.

Lamaze, C., Fujimoto, L.M., Yin, H.L., and Schmid, S.L. (1997). The actin cytoskeleton is required for receptor-mediated endocytosis in mammalian cells. J Biol Chem *272*, 20332-20335.

Lang, C.H., Spolarics, Z., Ottlakan, A., and Spitzer, J.J. (1993). Effect of high-dose endotoxin on glucose production and utilization. Metabolism *42*, 1351-1358.

Latz, E., Visintin, A., Lien, E., Fitzgerald, K., Monks, B., Kurt-Jones, E., Golenbock, D., and Espevik, T. (2002). Lipopolysaccharide rapidly traffics to and from the Golgi apparatus with the toll-like receptor 4-MD-2-CD14 complex in a process that is distinct from the initiation of signal transduction. J Biol Chem *277*, 47834-47843.

Lee, J., Choi, H., Kim, K.H., Jeong, S., Park, J.W., Baek, C.S., and Lee, S.H. (2008). Synthesis and biological evaluation of 3,5-diaminoindazoles as cyclin-dependent kinase inhibitors. Bioorg Med Chem Lett *18*, 2292-2295.

Lee, K.H., Lotterman, C., Karikari, C., Omura, N., Feldmann, G., Habbe, N., Goggins, M.G., Mendell, J.T., and Maitra, A. (2009). Epigenetic silencing of MicroRNA miR-107 regulates cyclin-dependent kinase 6 expression in pancreatic cancer. Pancreatology *9*, 293-301.

Lee, R.C., Feinbaum, R.L., and Ambros, V. (1993). The C. elegans heterochronic gene lin-4 encodes small RNAs with antisense complementarity to lin-14. Cell *75*, 843-854.

Leitch, A.E., Haslett, C., and Rossi, A.G. (2009). Cyclin-dependent kinase inhibitor drugs as potential novel anti-inflammatory and pro-resolution agents. Br J Pharmacol *158*, 1004-1016.

Leitch, A.E., Riley, N.A., Sheldrake, T.A., Festa, M., Fox, S., Duffin, R., Haslett, C., and Rossi, A.G. (2010). The cyclin-dependent kinase inhibitor R-roscovitine down-regulates Mcl-1 to override pro-inflammatory signalling and drive neutrophil apoptosis. Eur J Immunol *40*, 1127-1138.

Leonardi, R., Rehg, J.E., Rock, C.O., and Jackowski, S. (2010). Pantothenate kinase 1 is required to support the metabolic transition from the fed to the fasted state. PLoS One *5*, e11107.

Leonardi, R., Zhang, Y.M., Rock, C.O., and Jackowski, S. (2005). Coenzyme A: back in action. Prog Lipid Res *44*, 125-153.

Lewis, B., Shih, I., Jones-Rhoades, M., Bartel, D., and Burge, C. (2003). Prediction of mammalian microRNA targets. Cell *115*, 787-798.

Lewis, B.P., Burge, C.B., and Bartel, D.P. (2005). Conserved seed pairing, often flanked by adenosines, indicates that thousands of human genes are microRNA targets. Cell *120*, 15-20.

Li, C.B., Li, X.X., Chen, Y.G., Zhang, C., Zhang, M.X., Zhao, X.Q., Hao, M.X., Hou, X.Y., Gong, M.L., Zhao, Y.X., *et al.* (2009a). Effects and mechanisms of PPARalpha activator fenofibrate on myocardial remodelling in hypertension. J Cell Mol Med *13*, 4444-4452.

Li, Q.J., Chau, J., Ebert, P.J., Sylvester, G., Min, H., Liu, G., Braich, R., Manoharan, M., Soutschek, J., Skare, P., *et al.* (2007). miR-181a is an intrinsic modulator of T cell sensitivity and selection. Cell *129*, 147-161.

Li, Y., Chang, Y., Zhang, L., Feng, Q., Liu, Z., Zhang, Y., Zuo, J., Meng, Y., and Fang, F. (2005). High glucose upregulates pantothenate kinase 4 (PanK4) and thus affects M2-type pyruvate kinase (Pkm2). Mol Cell Biochem *277*, 117-125.

Li, Y., Guessous, F., Zhang, Y., Dipierro, C., Kefas, B., Johnson, E., Marcinkiewicz, L., Jiang, J., Yang, Y., Schmittgen, T.D., *et al.* (2009b).

MicroRNA-34a inhibits glioblastoma growth by targeting multiple oncogenes. Cancer Res *69*, 7569-7576.

Li, Y., Vandenboom, T.G., 2nd, Wang, Z., Kong, D., Ali, S., Philip, P.A., and Sarkar, F.H. (2010). miR-146a suppresses invasion of pancreatic cancer cells. Cancer Res *70*, 1486-1495.

Liang, Y., Ridzon, D., Wong, L., and Chen, C. (2007). Characterization of microRNA expression profiles in normal human tissues. BMC Genomics *8*, 166.

Liu, G., Friggeri, A., Yang, Y., Park, Y.J., Tsuruta, Y., and Abraham, E. (2009). miR-147, a microRNA that is induced upon Toll-like receptor stimulation, regulates murine macrophage inflammatory responses. Proc Natl Acad Sci U S A *106*, 15819-15824.

Liu, H., Brannon, A.R., Reddy, A.R., Alexe, G., Seiler, M.W., Arreola, A., Oza, J.H., Yao, M., Juan, D., Liou, L.S., *et al.* (2010a). Identifying mRNA targets of microRNA dysregulated in cancer: with application to clear cell Renal Cell Carcinoma. BMC Syst Biol *4*, 51.

Liu, Q., Fu, H., Sun, F., Zhang, H., Tie, Y., Zhu, J., Xing, R., Sun, Z., and Zheng, X. (2008). miR-16 family induces cell cycle arrest by regulating multiple cell cycle genes. Nucleic Acids Res *36*, 5391-5404.

Liu, X., Wang, T., Wakita, T., and Yang, W. (2010b). Systematic identification of microRNA and messenger RNA profiles in hepatitis C virus-infected human hepatoma cells. Virology *398*, 57-67.

Lloberas, J., and Celada, A. (2009). p21(waf1/CIP1), a CDK inhibitor and a negative feedback system that controls macrophage activation. Eur J Immunol *39*, 691-694.

Lokaj, J., and John, C. (2008). [Ilya Ilich Metchnikov and Paul Ehrlich: 1908 Nobel Prize winners for their research on immunity]. Epidemiol Mikrobiol Imunol *57*, 119-124.

Lorenz, E., Mira, J., Cornish, K., Arbour, N., and Schwartz, D. (2000). A novel polymorphism in the toll-like receptor 2 gene and its potential association with staphylococcal infection. Infect Immun *68*, 6398-6401.

Lu, J., Getz, G., Miska, E.A., Alvarez-Saavedra, E., Lamb, J., Peck, D., Sweet-Cordero, A., Ebert, B.L., Mak, R.H., Ferrando, A.A., *et al.* (2005). MicroRNA expression profiles classify human cancers. Nature *435*, 834-838.

Lu, L.F., and Liston, A. (2009). MicroRNA in the immune system, microRNA as an immune system. Immunology *127*, 291-298.

Lysakova-Devine, T., Keogh, B., Harrington, B., Nagpal, K., Halle, A., Golenbock, D.T., Monie, T., and Bowie, A.G. (2010). Viral Inhibitory Peptide of TLR4, a Peptide Derived from Vaccinia Protein A46, Specifically Inhibits TLR4 by Directly Targeting MyD88 Adaptor-Like and TRIF-Related Adaptor Molecule. J Immunol.

Maa, M.C., Chang, M.Y., Chen, Y.J., Lin, C.H., Yu, C.J., Yang, Y.L., Li, J., Chen, P.R., Tang, C.H., Lei, H.Y., and Leu, T.H. (2008). Requirement of inducible nitric-oxide synthase in lipopolysaccharide-mediated Src induction and macrophage migration. J Biol Chem *283*, 31408-31416.

Maitra, U., Chang, S., Singh, N., and Li, L. (2009). Molecular mechanism underlying the suppression of lipid oxidation during endotoxemia. Mol Immunol *47*, 420-425.

Martello, G., Rosato, A., Ferrari, F., Manfrin, A., Cordenonsi, M., Dupont, S., Enzo, E., Guzzardo, V., Rondina, M., Spruce, T., *et al.* A MicroRNA targeting dicer for metastasis control. Cell *141*, 1195-1207.

Martello, G., Rosato, A., Ferrari, F., Manfrin, A., Cordenonsi, M., Dupont, S., Enzo, E., Guzzardo, V., Rondina, M., Spruce, T., *et al.* (2010). A MicroRNA targeting dicer for metastasis control. Cell *141*, 1195-1207.

Martinon, F., Mayor, A., and Tschopp, J. (2009). The inflammasomes: guardians of the body. Annu Rev Immunol *27*, 229-265.

Marx, N., Mackman, N., Schonbeck, U., Yilmaz, N., Hombach, V., Libby, P., and Plutzky, J. (2001). PPARalpha activators inhibit tissue factor expression and activity in human monocytes. Circulation *103*, 213-219.

Marx, N., Sukhova, G.K., Collins, T., Libby, P., and Plutzky, J. (1999). PPARalpha activators inhibit cytokine-induced vascular cell adhesion molecule-1 expression in human endothelial cells. Circulation *99*, 3125-3131.

May, R.C., and Machesky, L.M. (2001). Phagocytosis and the actin cytoskeleton. J Cell Sci *114*, 1061-1077.

McCoy, C., and O'Neill, L. (2008). The role of toll-like receptors in macrophages. Front Biosci *13*, 62-70.

McCoy, C.E., Sheedy, F.J., Qualls, J.E., Doyle, S.L., Quinn, S.R., Murray, P.J., and O'Neill, L.A. (2010). IL-10 inhibits miR-155 induction by Toll-like receptors. J Biol Chem.

Medzhitov, R., and Janeway, C.J. (2000). The Toll receptor family and microbial recognition. Trends Microbiol *8*, 452-456.

Medzhitov, R., Preston-Hurlburt, P., and Janeway, C.J. (1997). A human homologue of the Drosophila Toll protein signals activation of adaptive immunity. Nature *388*, 394-397.

Memon, R.A., Bass, N.M., Moser, A.H., Fuller, J., Appel, R., Grunfeld, C., and Feingold, K.R. (1999). Down-regulation of liver and heart specific fatty acid binding proteins by endotoxin and cytokines in vivo. Biochim Biophys Acta *1440*, 118-126.

Memon, R.A., Fuller, J., Moser, A.H., Smith, P.J., Feingold, K.R., and Grunfeld, C. (1998). In vivo regulation of acyl-CoA synthetase mRNA and activity by endotoxin and cytokines. Am J Physiol *275*, E64-72.

Merkerova, M., Belickova, M., and Bruchova, H. (2008). Differential expression of microRNAs in hematopoietic cell lineages. Eur J Haematol *81*, 304-310.

Meyerson, M., and Harlow, E. (1994). Identification of G1 kinase activity for cdk6, a novel cyclin D partner. Mol Cell Biol *14*, 2077-2086.

Moore, R.N., Steeg, P.S., Mannel, D.N., and Mergenhagen, S.E. (1980). Role of lipopolysaccharide in regulating colony-stimulating factor-dependent macrophage proliferation in vitro. Infect Immun *30*, 797-804.

Moraes, L.A., Piqueras, L., and Bishop-Bailey, D. (2006). Peroxisome proliferator-activated receptors and inflammation. Pharmacol Ther *110*, 371-385.

Moschos, S., Williams, A., Perry, M., Birrell, M., Belvisi, M., and Lindsay, M. (2007). Expression profiling in vivo demonstrates rapid changes in lung microRNA levels following lipopolysaccharide-induced inflammation but not in the anti-inflammatory action of glucocorticoids. BMC Genomics *8*, 240.

Mu, P., Han, Y.C., Betel, D., Yao, E., Squatrito, M., Ogrodowski, P., de Stanchina, E., D'Andrea, A., Sander, C., and Ventura, A. (2009). Genetic dissection of the miR-17~92 cluster of microRNAs in Myc-induced B-cell lymphomas. Genes Dev *23*, 2806-2811.

Muljo, S.A., Ansel, K.M., Kanellopoulou, C., Livingston, D.M., Rao, A., and Rajewsky, K. (2005). Aberrant T cell differentiation in the absence of Dicer. J Exp Med *202*, 261-269.

Murakami, K., Bujo, H., Unoki, H., and Saito, Y. (2007). Effect of PPARalpha activation of macrophages on the secretion of inflammatory cytokines in cultured adipocytes. Eur J Pharmacol *561*, 206-213.

Murray, R.Z., Kay, J.G., Sangermani, D.G., and Stow, J.L. (2005). A role for the phagosome in cytokine secretion. Science *310*, 1492-1495.

Nalepa, G., Rolfe, M., and Harper, J.W. (2006). Drug discovery in the ubiquitin-proteasome system. Nat Rev Drug Discov *5*, 596-613.

Nelson, P.T., and Wang, W.X. (2010). MiR-107 is reduced in Alzheimer's disease brain neocortex: validation study. J Alzheimers Dis *21*, 75-79.

Nilsen, T.W. (2007). Mechanisms of microRNA-mediated gene regulation in animal cells. Trends Genet *23*, 243-249.

Ninomiya-Tsuji, J., Kishimoto, K., Hiyama, A., Inoue, J., Cao, Z., and Matsumoto, K. (1999). The kinase TAK1 can activate the NIK-I kappaB as well as the MAP kinase cascade in the IL-1 signalling pathway. Nature *398*, 252-256.

Nonomura, Y., Kohsaka, H., Nagasaka, K., and Miyasaka, N. (2003). Gene transfer of a cell cycle modulator exerts anti-inflammatory effects in the treatment of arthritis. J Immunol *171*, 4913-4919.

O'Carroll, D., Mecklenbrauker, I., Das, P.P., Santana, A., Koenig, U., Enright, A.J., Miska, E.A., and Tarakhovsky, A. (2007). A Slicer-independent role for Argonaute 2 in hematopoiesis and the microRNA pathway. Genes Dev *21*, 1999-2004.

O'Connell, R.M., Chaudhuri, A.A., Rao, D.S., and Baltimore, D. (2009). Inositol phosphatase SHIP1 is a primary target of miR-155. Proc Natl Acad Sci U S A *106*, 7113-7118.

O'Connell, R.M., Rao, D.S., Chaudhuri, A.A., Boldin, M.P., Taganov, K.D., Nicoll, J., Paquette, R.L., and Baltimore, D. (2008). Sustained expression of microRNA-155 in hematopoietic stem cells causes a myeloproliferative disorder. J Exp Med *205*, 585-594.

O'Connell, R.M., Taganov, K.D., Boldin, M.P., Cheng, G., and Baltimore, D. (2007). MicroRNA-155 is induced during the macrophage inflammatory response. Proc Natl Acad Sci U S A *104*, 1604-1609.

O'Neill, L., and Bowie, A. (2007). The family of five: TIR-domain-containing adaptors in Toll-like receptor signalling. Nat Rev Immunol *7*, 353-364.

O'Neill, L., Fitzgerald, K., and Bowie, A. (2003). The Toll-IL-1 receptor adaptor family grows to five members. Trends Immunol *24*, 286-290.

Okamura, K., Phillips, M.D., Tyler, D.M., Duan, H., Chou, Y.T., and Lai, E.C. (2008). The regulatory activity of microRNA* species has substantial influence on microRNA and 3' UTR evolution. Nat Struct Mol Biol *15*, 354-363.

Orom, U.A., and Lund, A.H. (2007). Isolation of microRNA targets using biotinylated synthetic microRNAs. Methods *43*, 162-165.

Orom, U.A., Nielsen, F.C., and Lund, A.H. (2008). MicroRNA-10a binds the 5'UTR of ribosomal protein mRNAs and enhances their translation. Mol Cell *30*, 460-471.

Ozsolak, F., Poling, L.L., Wang, Z., Liu, H., Liu, X.S., Roeder, R.G., Zhang, X., Song, J.S., and Fisher, D.E. (2008). Chromatin structure analyses identify miRNA promoters. Genes Dev *22*, 3172-3183.

Passilly, P., Schohn, H., Jannin, B., Cherkaoui Malki, M., Boscoboinik, D., Dauca, M., and Latruffe, N. (1999). Phosphorylation of peroxisome proliferator-activated receptor alpha in rat Fao cells and stimulation by ciprofibrate. Biochem Pharmacol *58*, 1001-1008.

Paukkeri, E.L., Leppanen, T., Sareila, O., Vuolteenaho, K., Kankaanranta, H., and Moilanen, E. (2007). PPARalpha agonists inhibit nitric oxide production by enhancing iNOS degradation in LPS-treated macrophages. Br J Pharmacol *152*, 1081-1091.

Peavy, D.L., Baughn, R.E., and Musher, D.M. (1978). Mitogenic activity of bacterial lipopolysaccharides in vivo: morphological and functinal characterization of responding cells. Infect Immun *19*, 71-78.

Pedersen, M.R., Jensen, S., Christensen, J.D., and Hansen, E.W. (1995). Lipopolysaccharide in concentrations above 40 ng/ml stimulates proliferation of the IL-6-dependent B9 cell line. J Immunol Methods *180*, 159-163.

Perry, M.M., Williams, A.E., Tsitsiou, E., Larner-Svensson, H.M., and Lindsay, M.A. (2009). Divergent intracellular pathways regulate interleukin-1beta-induced miR-146a and miR-146b expression and chemokine release in human alveolar epithelial cells. FEBS Lett *583*, 3349-3355.

Petroski, M.D. (2008). The ubiquitin system, disease, and drug discovery. BMC Biochem *9 Suppl 1*, S7.

Picard, C., Puel, A., Bonnet, M., Ku, C., Bustamante, J., Yang, K., Soudais, C., Dupuis, S., Feinberg, J., Fieschi, C., *et al.* (2003). Pyogenic bacterial infections in humans with IRAK-4 deficiency. Science *299*, 2076-2079.

Picard, C., von Bernuth, H., Ku, C., Yang, K., Puel, A., and Casanova, J. (2007). Inherited human IRAK-4 deficiency: an update. Immunol Res *38*, 347-352.

Pineda Torra, I., Jamshidi, Y., Flavell, D.M., Fruchart, J.C., and Staels, B. (2002). Characterization of the human PPARalpha promoter: identification of a functional nuclear receptor response element. Mol Endocrinol *16*, 1013-1028.

Planavila, A., Laguna, J.C., and Vazquez-Carrera, M. (2005). Nuclear factor-kappaB activation leads to down-regulation of fatty acid oxidation during cardiac hypertrophy. J Biol Chem *280*, 17464-17471.

Polster, B.J., Westaway, S.K., Nguyen, T.M., Yoon, M.Y., and Hayflick, S.J. (2010). Discordant expression of miR-103/7 and pantothenate kinase host genes in mouse. Mol Genet Metab.

Poltorak, A., He, X., Smirnova, I., Liu, M., Van Huffel, C., Du, X., Birdwell, D., Alejos, E., Silva, M., Galanos, C., *et al.* (1998). Defective LPS signaling in C3H/HeJ and C57BL/10ScCr mice: mutations in Tlr4 gene. Science *282*, 2085-2088.

Popovic, R., Riesbeck, L.E., Velu, C.S., Chaubey, A., Zhang, J., Achille, N.J., Erfurth, F.E., Eaton, K., Lu, J., Grimes, H.L., *et al.* (2009). Regulation of mir-196b by MLL and its overexpression by MLL fusions contributes to immortalization. Blood *113*, 3314-3322.

Pozzi, A., and Capdevila, J.H. (2008). PPARalpha Ligands as Antitumorigenic and Antiangiogenic Agents. PPAR Res *2008*, 906542.

Rabinowits, G., Gercel-Taylor, C., Day, J.M., Taylor, D.D., and Kloecker, G.H. (2009). Exosomal microRNA: a diagnostic marker for lung cancer. Clin Lung Cancer *10*, 42-46.

Rakoff-Nahoum, S., Paglino, J., Eslami-Varzaneh, F., Edberg, S., and Medzhitov, R. (2004). Recognition of commensal microflora by toll-like receptors is required for intestinal homeostasis. Cell *118*, 229-241.

Ramachandran, V., and Chen, X. (2008). Degradation of microRNAs by a family of exoribonucleases in Arabidopsis. Science *321*, 1490-1492.

Ramaswamy, G., Karim, M.A., Murti, K.G., and Jackowski, S. (2004). PPARalpha controls the intracellular coenzyme A concentration via regulation of PANK1alpha gene expression. J Lipid Res *45*, 17-31.

Redell, J.B., Liu, Y., and Dash, P.K. (2009). Traumatic brain injury alters expression of hippocampal microRNAs: potential regulators of multiple pathophysiological processes. J Neurosci Res *87*, 1435-1448.

Reindl, M., Lutterotti, A., Ingram, J., Schanda, K., Gassner, C., Deisenhammer, F., Berger, T., and Lorenz, E. (2003). Mutations in the gene for toll-like receptor 4 and multiple sclerosis. Tissue Antigens *61*, 85-88.

Reinhart, B.J., Weinstein, E.G., Rhoades, M.W., Bartel, B., and Bartel, D.P. (2002). MicroRNAs in plants. Genes Dev *16*, 1616-1626.

Rius, J., Guma, M., Schachtrup, C., Akassoglou, K., Zinkernagel, A.S., Nizet, V., Johnson, R.S., Haddad, G.G., and Karin, M. (2008). NF-kappaB links innate immunity to the hypoxic response through transcriptional regulation of HIF-1alpha. Nature *453*, 807-811.

Robishaw, J.D., Berkich, D., and Neely, J.R. (1982). Rate-limiting step and control of coenzyme A synthesis in cardiac muscle. J Biol Chem *257*, 10967-10972.

Rock, C.O., Calder, R.B., Karim, M.A., and Jackowski, S. (2000). Pantothenate kinase regulation of the intracellular concentration of coenzyme A. J Biol Chem *275*, 1377-1383.

Rodriguez, A., Griffiths-Jones, S., Ashurst, J.L., and Bradley, A. (2004). Identification of mammalian microRNA host genes and transcription units. Genome Res *14*, 1902-1910.

Rodriguez, A., Vigorito, E., Clare, S., Warren, M., Couttet, P., Soond, D., van Dongen, S., Grocock, R., Das, P., Miska, E., *et al.* (2007). Requirement of bic/microRNA-155 for normal immune function. Science *316*, 608-611.

Rossi, A.G., Sawatzky, D.A., Walker, A., Ward, C., Sheldrake, T.A., Riley, N.A., Caldicott, A., Martinez-Losa, M., Walker, T.R., Duffin, R., *et al.* (2006). Cyclin-dependent kinase inhibitors enhance the resolution of inflammation by promoting inflammatory cell apoptosis. Nat Med *12*, 1056-1064.

Rostand, K., and Esko, J. (1997). Microbial adherence to and invasion through proteoglycans. Infect Immun *65*, 1-8.

Rowley, D., and Turner, K.J. (1964). Increase in Macroglobulin Antibodies of Mouse and Pig Following Injection of Bacterial Lipopolysaccharide. Immunology *7*, 394-402.

Ryan, J.L., Gobran, L., and Morrison, D.C. (1986). Modulation of murine macrophage metabolism by glycolipids: inhibition of LPS-induced metabolism by specific gangliosides. J Leukoc Biol *40*, 367-379.

Sabroe, I., Read, R., Whyte, M., Dockrell, D., Vogel, S., and Dower, S. (2003). Toll-like receptors in health and disease: complex questions remain. J Immunol *171*, 1630-1635.

Sandberg, R., Neilson, J.R., Sarma, A., Sharp, P.A., and Burge, C.B. (2008). Proliferating cells express mRNAs with shortened 3' untranslated regions and fewer microRNA target sites. Science *320*, 1643-1647.

Sato, S., Sanjo, H., Takeda, K., Ninomiya-Tsuji, J., Yamamoto, M., Kawai, T., Matsumoto, K., Takeuchi, O., and Akira, S. (2005). Essential function for the

kinase TAK1 in innate and adaptive immune responses. Nat Immunol *6*, 1087-1095.

Scatizzi, J.C., Mavers, M., Hutcheson, J., Young, B., Shi, B., Pope, R.M., Ruderman, E.M., Samways, D.S., Corbett, J.A., Egan, T.M., and Perlman, H. (2009). The CDK domain of p21 is a suppressor of IL-1beta-mediated inflammation in activated macrophages. Eur J Immunol *39*, 820-825.

Schuster, C., Budczies, J., Faber, C., Kirchner, T., and Hlubek, F. (2010). MicroRNA expression profiling of specific cells in complex archival tissue stained by immunohistochemistry. Lab Invest.

Sellers, W.R., and Kaelin, W.G., Jr. (1997). Role of the retinoblastoma protein in the pathogenesis of human cancer. J Clin Oncol *15*, 3301-3312.

Sen, R., and Baltimore, D. (1986). Inducibility of kappa immunoglobulin enhancer-binding protein Nf-kappa B by a posttranslational mechanism. Cell *47*, 921-928.

Shah, Y.M., Morimura, K., Yang, Q., Tanabe, T., Takagi, M., and Gonzalez, F.J. (2007). Peroxisome proliferator-activated receptor alpha regulates a microRNA-mediated signaling cascade responsible for hepatocellular proliferation. Mol Cell Biol *27*, 4238-4247.

Shalev, A., Siegrist-Kaiser, C.A., Yen, P.M., Wahli, W., Burger, A.G., Chin, W.W., and Meier, C.A. (1996). The peroxisome proliferator-activated receptor alpha is a phosphoprotein: regulation by insulin. Endocrinology *137*, 4499-4502.

Sheedy, F.J., and O'Neill, L.A. (2008). Adding fuel to fire: microRNAs as a new class of mediators of inflammation. Ann Rheum Dis *67 Suppl 3*, iii50-55.

Sheedy, F.J., Palsson-McDermott, E., Hennessy, E.J., Martin, C., O'Leary, J.J., Ruan, Q., Johnson, D.S., Chen, Y., and O'Neill, L.A. (2010). Negative regulation of TLR4 via targeting of the proinflammatory tumor suppressor PDCD4 by the microRNA miR-21. Nat Immunol *11*, 141-147.

Shen, W.F., Hu, Y.L., Uttarwar, L., Passegue, E., and Largman, C. (2008). MicroRNA-126 regulates HOXA9 by binding to the homeobox. Mol Cell Biol *28*, 4609-4619.

Shi, L., Zhang, J., Pan, T., Zhou, J., Gong, W., Liu, N., Fu, Z., and You, Y. (2010). MiR-125b is critical for the suppression of human U251 glioma stem cell proliferation. Brain Res *1312*, 120-126.

Si, M., Zhu, S., Wu, H., Lu, Z., Wu, F., and Mo, Y. (2007). miR-21-mediated tumor growth. Oncogene *26*, 2799-2803.

Siomi, H., and Siomi, M.C. (2010). Posttranscriptional regulation of microRNA biogenesis in animals. Mol Cell *38*, 323-332.

Slomiany, P., Baker, T., Elliott, E.R., and Grossel, M.J. (2006). Changes in motility, gene expression and actin dynamics: Cdk6-induced cytoskeletal changes associated with differentiation in mouse astrocytes. J Cell Biochem *99*, 635-646.

Sperling, J., Azubel, M., and Sperling, R. (2008). Structure and function of the Pre-mRNA splicing machine. Structure *16*, 1605-1615.

Stack, J., Haga, I.R., Schroder, M., Bartlett, N.W., Maloney, G., Reading, P.C., Fitzgerald, K.A., Smith, G.L., and Bowie, A.G. (2005). Vaccinia virus protein A46R targets multiple Toll-like-interleukin-1 receptor adaptors and contributes to virulence. J Exp Med *201*, 1007-1018.

Stenvang, J., Silahtaroglu, A.N., Lindow, M., Elmen, J., and Kauppinen, S. (2008). The utility of LNA in microRNA-based cancer diagnostics and therapeutics. Semin Cancer Biol *18*, 89-102.

Stern-Ginossar, N., Elefant, N., Zimmermann, A., Wolf, D.G., Saleh, N., Biton, M., Horwitz, E., Prokocimer, Z., Prichard, M., Hahn, G., *et al.* (2007). Host immune system gene targeting by a viral miRNA. Science *317*, 376-381.

Stuart, L., and Ezekowitz, R. (2005). Phagocytosis: elegant complexity. Immunity *22*, 539-550.

Taganov, K., Boldin, M., Chang, K., and Baltimore, D. (2006). NF-kappaB-dependent induction of microRNA miR-146, an inhibitor targeted to signaling proteins of innate immune responses. Proc Natl Acad Sci U S A *103*, 12481-12486.

Takahashi, Y., Forrest, A.R., Maeno, E., Hashimoto, T., Daub, C.O., and Yasuda, J. (2009). MiR-107 and MiR-185 can induce cell cycle arrest in human non small cell lung cancer cell lines. PLoS One *4*, e6677.

Takeda, K., and Akira, S. (2004). TLR signaling pathways. Semin Immunol *16*, 3-9.

Takeda, K., and Akira, S. (2005). Toll-like receptors in innate immunity. Int Immunol *17*, 1-14.

Taylor, D.D., and Gercel-Taylor, C. (2008). MicroRNA signatures of tumor-derived exosomes as diagnostic biomarkers of ovarian cancer. Gynecol Oncol *110*, 13-21.

Thai, T., Calado, D., Casola, S., Ansel, K., Xiao, C., Xue, Y., Murphy, A., Frendewey, D., Valenzuela, D., Kutok, J., *et al.* (2007). Regulation of the germinal center response by microRNA-155. Science *316*, 604-608.

Thomson, J.M., Newman, M., Parker, J.S., Morin-Kensicki, E.M., Wright, T., and Hammond, S.M. (2006). Extensive post-transcriptional regulation of microRNAs and its implications for cancer. Genes Dev *20*, 2202-2207.

Tili, E., Michaille, J., Cimino, A., Costinean, S., Dumitru, C., Adair, B., Fabbri, M., Alder, H., Liu, C., Calin, G., and Croce, C. (2007). Modulation of miR-155 and miR-125b levels following lipopolysaccharide/TNF-alpha stimulation and their possible roles in regulating the response to endotoxin shock. J Immunol *179*, 5082-5089.

Uematsu, S., and Akira, S. (2005). [Role of toll-like receptor in immunological defence mechanism]. Nippon Naika Gakkai Zasshi *94*, 355-361.

Ulevitch, R. (2004). Therapeutics targeting the innate immune system. Nat Rev Immunol *4*, 512-520.

Underhill, D., and Ozinsky, A. (2002a). Phagocytosis of microbes: complexity in action. Annu Rev Immunol *20*, 825-852.

Underhill, D., and Ozinsky, A. (2002b). Toll-like receptors: key mediators of microbe detection. Curr Opin Immunol *14*, 103-110.

Underhill, D., Ozinsky, A., Hajjar, A., Stevens, A., Wilson, C., Bassetti, M., and Aderem, A. (1999). The Toll-like receptor 2 is recruited to macrophage phagosomes and discriminates between pathogens. Nature *401*, 811-815.

Vadiveloo, P.K. (1999). Macrophages--proliferation, activation, and cell cycle proteins. J Leukoc Biol *66*, 579-582.

Vallabhapurapu, S., Matsuzawa, A., Zhang, W., Tseng, P.H., Keats, J.J., Wang, H., Vignali, D.A., Bergsagel, P.L., and Karin, M. (2008). Nonredundant and complementary functions of TRAF2 and TRAF3 in a ubiquitination cascade that activates NIK-dependent alternative NF-kappaB signaling. Nat Immunol *9*, 1364-1370.

Velu, C.S., Baktula, A.M., and Grimes, H.L. (2009). Gfi1 regulates miR-21 and miR-196b to control myelopoiesis. Blood *113*, 4720-4728.

Verhoef, J., Peterson, P., and Verbrugh, H. (1979). Host-parasite relationship in staphylococcal infections: the role of the staphylococcal cell wall during the process of phagocytosis. Antonie Van Leeuwenhoek *45*, 49-53.

Vieira, O.V., Botelho, R.J., and Grinstein, S. (2002). Phagosome maturation: aging gracefully. Biochem J *366*, 689-704.

Vigorito, E., Perks, K., Abreu-Goodger, C., Bunting, S., Xiang, Z., Kohlhaas, S., Das, P., Miska, E., Rodriguez, A., Bradley, A., *et al.* (2007). microRNA-155 Regulates the Generation of Immunoglobulin Class-Switched Plasma Cells. Immunity *27*, 847-859.

Vogel, J., and Sharma, C.M. (2005). How to find small non-coding RNAs in bacteria. Biol Chem *386*, 1219-1238.

Vos, O. (1978). Effect of bacterial lipopolysaccharide on proliferation of CFU-S. Exp Hematol *6*, 688-693.

Wang, W.X., Rajeev, B.W., Stromberg, A.J., Ren, N., Tang, G., Huang, Q., Rigoutsos, I., and Nelson, P.T. (2008). The expression of microRNA miR-107 decreases early in Alzheimer's disease and may accelerate disease progression through regulation of beta-site amyloid precursor protein-cleaving enzyme 1. J Neurosci *28*, 1213-1223.

Wang, W.X., Wilfred, B.R., Madathil, S.K., Tang, G., Hu, Y., Dimayuga, J., Stromberg, A.J., Huang, Q., Saatman, K.E., and Nelson, P.T. (2010a). MiR-107 Regulates Granulin/Progranulin with Implications for Traumatic Brain Injury and Neurodegenerative Disease. Am J Pathol.

Wang, Y., Li, Z., He, C., Wang, D., Yuan, X., Chen, J., and Jin, J. (2010b). MicroRNAs expression signatures are associated with lineage and survival in acute leukemias. Blood Cells Mol Dis *44*, 191-197.

Weichert, H., Blechschmidt, I., Schroder, S., and Ambrosius, H. (1991). The MTT-assay as a rapid test for cell proliferation and cell killing: application to human peripheral blood lymphocytes (PBL). Allerg Immunol (Leipz) *37*, 139-144.

West, M.A., Prescott, A.R., Eskelinen, E.L., Ridley, A.J., and Watts, C. (2000). Rac is required for constitutive macropinocytosis by dendritic cells but does not control its downregulation. Curr Biol *10*, 839-848.

West, M.A., Wallin, R.P., Matthews, S.P., Svensson, H.G., Zaru, R., Ljunggren, H.G., Prescott, A.R., and Watts, C. (2004). Enhanced dendritic cell antigen capture via toll-like receptor-induced actin remodeling. Science *305*, 1153-1157.

Westra, J., Brouwer, E., van Roosmalen, I.A., Doornbos-van der Meer, B., van Leeuwen, M.A., Posthumus, M.D., and Kallenberg, C.G. (2010). Expression and regulation of HIF-1alpha in macrophages under inflammatory conditions; significant reduction of VEGF by CaMKII inhibitor. BMC Musculoskelet Disord *11*, 61.

Whitham, S., Dinesh-Kumar, S.P., Choi, D., Hehl, R., Corr, C., and Baker, B. (1994). The product of the tobacco mosaic virus resistance gene N: similarity to toll and the interleukin-1 receptor. Cell *78*, 1101-1115.

Wienholds, E., and Plasterk, R.H. (2005). MicroRNA function in animal development. FEBS Lett *579*, 5911-5922.

Wightman, B., Ha, I., and Ruvkun, G. (1993). Posttranscriptional regulation of the heterochronic gene lin-14 by lin-4 mediates temporal pattern formation in C. elegans. Cell *75*, 855-862.

Wilfred, B.R., Wang, W.X., and Nelson, P.T. (2007). Energizing miRNA research: a review of the role of miRNAs in lipid metabolism, with a prediction that miR-103/107 regulates human metabolic pathways. Mol Genet Metab *91*, 209-217.

Williams, L.M., and Ridley, A.J. (2000). Lipopolysaccharide induces actin reorganization and tyrosine phosphorylation of Pyk2 and paxillin in monocytes and macrophages. J Immunol *164*, 2028-2036.

Wittmann, J., and Jack, H.M. (2010). Serum microRNAs as powerful cancer biomarkers. Biochim Biophys Acta.

Wong, P., Iwasaki, M., Somervaille, T.C., Ficara, F., Carico, C., Arnold, C., Chen, C.Z., and Cleary, M.L. (2010). The miR-17-92 microRNA polycistron regulates MLL leukemia stem cell potential by modulating p21 expression. Cancer Res *70*, 3833-3842.

Wu, J., Qian, J., Li, C., Kwok, L., Cheng, F., Liu, P., Perdomo, C., Kotton, D., Vaziri, C., Anderlind, C., *et al.* (2010). miR-129 regulates cell proliferation by downregulating Cdk6 expression. Cell Cycle *9*, 1809-1818.

Xia, H., Qi, Y., Ng, S.S., Chen, X., Li, D., Chen, S., Ge, R., Jiang, S., Li, G., Chen, Y., *et al.* (2009). microRNA-146b inhibits glioma cell migration and invasion by targeting MMPs. Brain Res *1269*, 158-165.

Xiang, R.L., Yang, Y.L., Zuo, J., Xiao, X.H., Chang, Y.S., and De Fang, F. (2007). PanK4 inhibits pancreatic beta-cell apoptosis by decreasing the transcriptional level of pro-caspase-9. Cell Res *17*, 966-968.

Xiao, C., Calado, D.P., Galler, G., Thai, T.H., Patterson, H.C., Wang, J., Rajewsky, N., Bender, T.P., and Rajewsky, K. (2007). MiR-150 controls B cell differentiation by targeting the transcription factor c-Myb. Cell *131*, 146-159.

Xu, J., Storer, P.D., Chavis, J.A., Racke, M.K., and Drew, P.D. (2005). Agonists for the peroxisome proliferator-activated receptor-alpha and the retinoid X receptor inhibit inflammatory responses of microglia. J Neurosci Res *81*, 403-411.

Xu, T., Zhu, Y., Xiong, Y., Ge, Y.Y., Yun, J.P., and Zhuang, S.M. (2009). MicroRNA-195 suppresses tumorigenicity and regulates G1/S transition of human hepatocellular carcinoma cells. Hepatology *50*, 113-121.

Yamakuchi, M., Lotterman, C.D., Bao, C., Hruban, R.H., Karim, B., Mendell, J.T., Huso, D., and Lowenstein, C.J. P53-induced microRNA-107 inhibits HIF-1 and tumor angiogenesis. Proc Natl Acad Sci U S A *107*, 6334-6339.

Yamakuchi, M., Lotterman, C.D., Bao, C., Hruban, R.H., Karim, B., Mendell, J.T., Huso, D., and Lowenstein, C.J. (2010). P53-induced microRNA-107 inhibits HIF-1 and tumor angiogenesis. Proc Natl Acad Sci U S A *107*, 6334-6339.

Yang, H., Kong, W., He, L., Zhao, J.J., O'Donnell, J.D., Wang, J., Wenham, R.M., Coppola, D., Kruk, P.A., Nicosia, S.V., and Cheng, J.Q. (2008a). MicroRNA expression profiling in human ovarian cancer: miR-214 induces cell survival and cisplatin resistance by targeting PTEN. Cancer Res *68*, 425-433.

Yang, Q., Nagano, T., Shah, Y., Cheung, C., Ito, S., and Gonzalez, F.J. (2008b). The PPAR alpha-humanized mouse: a model to investigate species differences in liver toxicity mediated by PPAR alpha. Toxicol Sci *101*, 132-139.

Yang, X., Feng, M., Jiang, X., Wu, Z., Li, Z., Aau, M., and Yu, Q. (2009). miR-449a and miR-449b are direct transcriptional targets of E2F1 and negatively regulate pRb-E2F1 activity through a feedback loop by targeting CDK6 and CDC25A. Genes Dev *23*, 2388-2393.

Yin, Q., Wang, X., McBride, J., Fewell, C., and Flemington, E. (2008). B-cell receptor activation induces BIC/miR-155 expression through a conserved AP-1 element. J Biol Chem *283*, 2654-2662.

Yu, J.L., Rak, J.W., Coomber, B.L., Hicklin, D.J., and Kerbel, R.S. (2002). Effect of p53 status on tumor response to antiangiogenic therapy. Science *295*, 1526-1528.

Zahradka, P., Wright, B., Fuerst, M., Yurkova, N., Molnar, K., and Taylor, C.G. (2006). Peroxisome proliferator-activated receptor alpha and gamma ligands differentially affect smooth muscle cell proliferation and migration. J Pharmacol Exp Ther *317*, 651-659.

Zhang, Y.M., Chohnan, S., Virga, K.G., Stevens, R.D., Ilkayeva, O.R., Wenner, B.R., Bain, J.R., Newgard, C.B., Lee, R.E., Rock, C.O., and Jackowski, S. (2007). Chemical knockout of pantothenate kinase reveals the metabolic and genetic program responsible for hepatic coenzyme A homeostasis. Chem Biol *14*, 291-302.

Zhao, J.J., Lin, J., Lwin, T., Yang, H., Guo, J., Kong, W., Dessureault, S., Moscinski, L.C., Rezania, D., Dalton, W.S., *et al.* (2010). microRNA expression

profile and identification of miR-29 as a prognostic marker and pathogenetic factor by targeting CDK6 in mantle cell lymphoma. Blood *115*, 2630-2639.

Zhong, Z., Yeow, W.S., Zou, C., Wassell, R., Wang, C., Pestell, R.G., Quong, J.N., and Quong, A.A. (2010). Cyclin D1/cyclin-dependent kinase 4 interacts with filamin A and affects the migration and invasion potential of breast cancer cells. Cancer Res *70*, 2105-2114.

Zhou, B., Wang, S., Mayr, C., Bartel, D.P., and Lodish, H.F. (2007). miR-150, a microRNA expressed in mature B and T cells, blocks early B cell development when expressed prematurely. Proc Natl Acad Sci U S A *104*, 7080-7085.

Zhu, S., Si, M., Wu, H., and Mo, Y. (2007). MicroRNA-21 targets the tumor suppressor gene tropomyosin 1 (TPM1). J Biol Chem *282*, 14328-14336.

CHAPTER 8

APPENDICES

Publication Record

Poster Abstracts

Hennessy E.J., Sheedy F.J., and O'Neill, L.A. 2010 Keystone Symposia: Innate Immunity: Mechanism Linking with Adaptive Immunity. Dublin, Ireland 7th-12th June, 2010. "The role of miR-107 in the innate immune response and host-pathogen interactions."

Hennessy E.J., Sheedy F.J., and O'Neill, L.A. Viruses and Innate Immunity EMBO Workshop. Dublin, Ireland 5th-7th May, 2010. "The role of miR-107 in the innate immune response and host-pathogen interactions."

Published Articles

Hennessy, E.J., Parker, A.E., and O'Neill, L.A. (2010). Targeting Toll-like receptors: emerging therapeutics? Nat Rev Drug Discov *9*, 293-307

Hennessy, E.J. and O'Neill, L.A. Toll-like Receptors: very clever molecules. *Abcam Reviews*. 2010

Sheedy, F.J., Palsson-McDermott, E., Hennessy, E.J., Martin, C., O'Leary, J.J., Ruan, Q., Johnson, D.S., Chen, Y., and O'Neill, L.A. (2010). Negative regulation of TLR4 via targeting of the proinflammatory tumor suppressor PDCD4 by the microRNA miR-21. Nat Immunol *11*, 141-147

Articles in Review

Hennessy, E.J., Sheedy, F.J., Santamaria, D., Barbacid, M. and O'Neill, L.A. (2010). TLR4 Down-regulates miR-107 Leading to an Increase in Macrophage Proliferation and Migration Via CDK6.

THE ROLE OF MIR-107 IN THE INNATE IMMUNE RESPONSE AND HOST-PATHOGEN INTERACTIONS

Elizabeth J. Hennessy, Frederick J. Sheedy, Luke A.J. O'Neill. School of Biochemistry and Immunology, Trinity College Dublin, Dublin 2, Ireland

Toll-like receptors (TLRs) play a critical role in innate immunity and their activation leads to the stimulation of transcription factors such as NFκB and the induction of expression of a wide-range of immune and inflammatory proteins including cytokines like TNF-α. microRNAs (miRNA) are a novel class of small non-coding RNA regulatory molecules which post-transcriptionally regulate genes in a fine-tuning manner. "ImmunomiRs" are miRNA which have a specific role in regulating the expression of genes involved in the immune response. Our results have identified a miRNA, miR-107 that is downregulated specifically in many cell types including primary mouse and human cells in response to the TLR4 ligand lipopolysaccharide (LPS) in a MyD88-dependent manner. LPS stimulation also affects the gene that contains the sequence for miR-107, Pantothenate kinase-1α (Pank1α) by decreasing its mRNA and protein levels in a MyD88-dependent fashion. The transcription factor Peroxisome proliferator activating receptor-α (PPARα) which regulates Pank1α in the cell is also downregulated in response to LPS stimulation. Through the use of a chemical ligand specific to PPARα, and the manipulation of miR-107 levels in the cell, we found that miR-107 inhibits TNF-α secretion, and phagocytosis of live bacteria while also affecting cytoskeleton rearrangement. LPS stimulation therefore limits miR-107 thus releasing its "brake" on potential target genes such as Cyclin-dependent Kinase-6 (Cdk6) to allow these events to occur. It is possible that the known inhibitory effect of PPARα on LPS-induced TNF-α production involves upregulation of miR-107 which occurs at later stages of infection. Following the examination of the expression of miR-107 in response to bacterial stimuli and in biological processes such as phagocytosis, and actin cytoskeleton rearrangement, a possible mechanism for how the host responds to an invading pathogen has been uncovered. The results from this study may lead to a more complete understanding of how miRNA are regulated and to their role and function in the immune response.

This work was funded by the Health Research Board in Ireland under grant No. PhD / 20007/9.

Classification – Biological Sciences (Immunology)

TLR4 Down-regulates miR-107 Increasing Macrophage Proliferation and Migration Via Cyclin-dependent Kinase 6

Elizabeth J. Hennessy*, Frederick J. Sheedy*, David Santamaria†, Mariano Barbacid† and Luke A. J. O'Neill*‡

* School of Biochemistry and Immunology
Trinity College Dublin, Dublin 2, Ireland
† Centro Nacional de Investigaciones Oncológicas
Molecular Oncology Programme
E-28029 Madrid, Spain

‡ To whom correspondence should be addressed.
E-mail: laoneill@tcd.ie
Luke A.J. O'Neill
School of Biochemistry and Immunology
Trinity College Dublin
Dublin 2, Ireland
Tel: +353-1-8962439
FAX: +353-1-6772400

ABSTRACT

Toll-like receptors (TLRs) increase the expression of multiple microRNAs (miRNAs). Here we report the down-regulation of miR-107 by TLR4 in multiple cell types. The miR-107 sequence occurs in an intron within the sequence encoding the gene for Pantothenate kinase-1α (PanK1α) which is regulated by the transcription factor PPAR-α. PanK1α is also decreased in response to lipopolysaccharide (LPS). The effect on both miR-107 and PanK1α is via decreased PPAR-α. We have found that the putative miR-107 target cyclin-dependent-kinase 6 (CDK6) expression is increased by TLR4 as a result of the decrease in miR-107. This effect is required for increased proliferation and migration of macrophages in response to LPS, and CDK6-deficient mice are resistant to the lethal effect of LPS. We have therefore identified a mechanism for LPS signaling which involves a decrease in miR-107 leading to an increase in CDK6.

\body**INTRODUCTION**

TLRs are among the body's first line of defense where they recognize conserved structures from bacteria, viruses or fungi (1, 2). They play a critical role in innate immunity and their activation leads to the transcription of genes involved in the immune and inflammatory responses. miRNAs are an important family of small, non-coding RNAs which act as regulators of gene expression in a tissue and cell specific manner by base-pairing to a target messenger RNA (mRNA) sequence called a seed sequence. This leads to the partial or full degradation of the mRNA by RNases and the inhibition of its translation into a functional protein (3-5). miRNAs were originally found to have a role in cellular development, differentiation, proliferation and apoptosis and are now known to function in cancer and immunity (5-8). Stimulation of cells with the TLR4 specific ligand LPS from gram-negative bacteria results in an increase in the expression of several miRNAs including miR-21, miR-146a and miR-155. miR-21 has been linked to cell motility, invasion and adhesion, with target genes that include tropomyosin, PDCD4 and PTEN. It was recently shown to negatively regulate the immune response by promoting the anti-inflammatory response by eliminating PDCD4 and up-regulating IL-10 (9, 10). miR-146a acts as a negative regulator of TLR signaling and cytokine production. Two genes known to be involved in TLR4 signaling, TRAF6 and IRAK1 are targets of miR-146a and it was shown that LPS-induced activation of miR-146a is NF-κB-dependent (11). miR-155 has been shown to directly target SOCS1 and SHIP-1. Mice lacking miR-155 have defects in B cell differentiation, as well as having severe deficiencies in immune responses when exposed to pathogens (12-14). miRNAs have also been shown to be down-regulated in expression in response to LPS and TLR4 activation, including Let-7i and miR-125b, which have been shown to target TLR4 and TNF-α respectively. This aspect of miRNA biology has so far been less explored. (6, 15, 16).

Here we demonstrate that miR-107 is down-regulated in response to LPS. The mechanism involves a decrease in the transcription factor Peroxisome proliferator activating receptor-α (PPAR-α) (17). We also found decreases in the expression of PanK1α, an enzyme required for Coenzyme A (CoA) biosynthesis whose gene contains the miR-107 sequence in intron 5. We have found that CDK6 is an important target for miR-107. LPS causes an increase in CDK6 expression via the decrease in miR-107. This process is required for proliferation and migration of cells, and

indirectly affects phagocytosis. CDK6-deficient mice are also less susceptible to the lethal effect of LPS. We have therefore uncovered a loop activated by TLR4, which limits the expression of miR-107, leading to an increase in its target CDK6, thereby enhanced proliferation, motility and phagocytosis.

RESULTS

In a screen of miRNAs we found that as well as increasing a range of miRNAs (notably miR-146a, miR-155 and miR-21), LPS can down-regulate miRNAs, notably miR-149 and miR-107. We focused on miR-107 since we consistently observed a decrease in this miRNA in multiple cell types. Figure 1A shows that in primary BMDM (Upper) and human peripheral blood mononuclear cells (PBMC) (Lower), miR-107 expression is decreased by approximately four fold four hours post-LPS stimulation relative to the unstimulated sample. miR-146a is known to be up-regulated in response to LPS so it was used as a positive control for miRNA expression and it increased three fold over a 24 hour period in primary BMDM and five fold in PBMC over 24 hours of stimulation with LPS (Fig. 1B Upper and lower).

We next examined the primary (pri-miR) and precursor (pre-miR) transcripts of miR-107 to determine if the down-regulation of mature miR-107 in response to LPS is transcriptionally regulated. miR-107 is transcribed as a primary (pri-miR-107) transcript from the fifth intron of the pantothenate kinase 1α (PanK1α) gene found on chromosome 19 of the murine genome (18). Figure 1C shows that the pri-miR-107 transcript (Left) is down-regulated rapidly four to eight fold in response to LPS in primary BMDM. The pre-miR-107 transcript (Right) also decreased four fold following eight hours of LPS stimulation leading to the conclusion that the down-regulation of mature miR-107 is transcriptionally regulated. We next examined if the effect of LPS on miR-107 was dependent on MyD88 or Trif signaling pathways. We determined that the down-regulation of miR-107 is MyD88-dependent because there was no decrease in MyD88-deficient cells as shown in Figure 1D Left. Trif-deficient cells still showed the decrease. To determine if the effect is NF-κB-dependent we used p65-deficient MEF and we established that the decrease in miR-107 is dependent on p65 (Fig. 1D Right). miR-107 expression decreased approximately four fold in the wild-type MEF but did not decrease in the p65-deficient cells.

PanK1α expression was measured next to establish if miR-107 is co-transcribed with PanK1α since the miR-107 sequence occurs in intron 5 of the PanK1α gene. Figure 2A shows that PanK1α mRNA decreased in primary BMDM a four fold decrease being evident after eight hours of LPS stimulation and PanK1α protein level also decreased in primary cells over time. mRNA expression in the adaptor deficient and p65 deficient cells was also examined and similar to miR-107, PanK1α decreased in the wild-type and Trif deficient cells but failed to decrease in the MyD88 deficient cells (Fig 2B Left) and in p65 deficient cells (Fig 2B Right). Similar to miR-107 therefore, PanK1α expression is inhibited by LPS treatment in a MyD88 and p65-dependent fashion. We next examined the expression of the transcription factor PPAR-α which is known to regulate the expression of PanK1α. The PanK1α promoter region contains four putative peroxisome proliferator response elements (PPREs) for the transcription factor PPAR-α (17). PPAR-α has anti-inflammatory capabilities and prevents the binding of NF-κB and AP-1 to their target gene sequences possibly by preventing the phosphorylation of p65 and inhibiting the degradation of IκBα (19). We found that PPAR-α mRNA (Fig 2C Left) and protein expression (Fig 2C Right) decreased four fold following four to eight hours of LPS stimulation. Figure 2D (Left) shows PPAR-α mRNA in the adaptor deficient BMDM and similar to PanK1α and miR-107, PPAR-α decreased in the wild-type and Trif deficient cells but failed to decrease in the MyD88 deficient cells. Similarly in the MEF, PPAR-α decreased in the wild-type cells but failed to decrease in the p65 deficient cells (Fig 2D Right). These results suggest that all three transcripts are under the same mechanism leading to their down-regulation and that the decrease in PPAR-α might mediate the inhibition of both PanK1α and miR-107.

Having clearly demonstrated a decrease in miR-107 expression by LPS, we next investigated a functional outcome for this effect. CDK6 has emerged as a potentially important miR-107 target (20, 21). The seed sequence match between miR-107 and CDK6 is found at position 308-314 in the 3'UTR of CDK6. CDK6 expression was up-regulated by LPS at both the mRNA and protein levels with induction evident at four hours and declining at 24 hours (Fig. 3A). Figure 3B demonstrates that the upregulation of CDK6 in response to LPS is both MyD88 (Left) and p65-dependent (Right). We also examined other potential target genes of miR-107 to see if their mRNA expression also increased in response to LPS. Figure 3C shows the mRNA

expression of Dicer1 and HIF-1α. The expression of both of these genes increased more than two fold following four to eight hours of LPS stimulation. To verify that miR-107 was targeting CDK6 we transfected Immortalized BMDM (I-BMDM) with antisense-miR-107 (anti-miR-107) or precursor-miR-107 (pre-miR-107) molecules to knockdown or over-express miR-107 in the cells and then measured CDK6 mRNA and protein levels. We first examined the effect of using anti-sense to miR-107 on CDK6 mRNA and protein expression. We found that cells transfected with the anti-miR-107 exhibited at least a three fold increase in CDK6 mRNA and protein following eight hours of LPS stimulation compared to cells transfected with a non-targeting anti-miR-control molecule where CDK6 increased only two fold as shown in Figure 3D Left and Right. We also transfected I-BMDM with pre-miR-107 to observe the effect of over-expressing miR-107 on CDK6 mRNA and protein. We observed less CDK6 mRNA and protein following eight hours of LPS stimulation compared to pre-miR-control transfected cells where CDK6 mRNA expression increased two fold in response to LPS as shown in figure 3E Left and right. It is interesting to note the difference in response to LPS between cell-types. CDK6 mRNA expression increased more in the primary BMDM compared to the I-BMDM in response to LPS.

In order to confirm that miR-107 is directly targeting the 3`UTR of CDK6 a luciferase construct containing the 3`UTR of CDK6 with the wild-type miR-107 seed sequence located at position 308-314 or a mutated form at a single nucleotide. Because the luciferase construct contains an SV40 promoter and enhancer sequences there is constitutive expression of strong luciferase activity. Figure 3F shows that transfection of cells with anti-miR-107 does not have an affect on the luciferase activity because it is constitutive regardless of knocking-down miR-107. However, cells transfected with the wild-type CDK6 construct and pre-miR-107 exhibited a 75% decrease in luciferase indicating that miR-107 directly binds to the seed-sequence. Cells transfected with the mutant CDK6 luciferase and pre-miR-107 also exhibited a 30% decrease in response to transfection with pre-miR-107 but importantly this is less than in the wild-type construct. This 30% decrease is due to a second seed sequence in the CDK6 3`UTR at position 1815-1821 that the pre-miR-107 molecule is binding. These results indicate that miR-107 expression directly affects CDK6 mRNA and protein levels in the cell.

We next examined the functional relevance of miR-107 expression. For this we examined the cell cycle regulation of CDK6, a known target for miR-107. We therefore examined proliferation of macrophages. Figure 4A Left, shows cells transfected with the antisense-miR-107 exhibit increased proliferation over 24 hours of stimulation with LPS compared to cells transfected with a control oligonucleotide. As is common with miRNAs the functional effects are subtle but consistant with a two fold increase at eight hours. Figure 4A Right illustrates cells transfected with the precursor-miR-107 exhibited less proliferation following eight hours of LPS stimulation and continued to proliferate less through 24 hours of stimulation. Cell migration was also compared between cells stimulated with LPS and transfected with pre-miR-107. Migration is induced in response to LPS. Cells transfected with anti-miR-107 exhibited an enhanced migratory ability compared to the anti-miR-control transfected cells as shown in figure 4B Left. Cells transfected with pre-miR-107 showed a significant reduced ability to migrate compared to the pre-miR-control transfected cells as illustrated in Figure 4B Right. The ability to phagocytose live bacteria by macrophages that lacked miR-107 or were over-expressing miR-107 was also measured. Figure 4C shows that cells overexpressing miR-107 have a decreased ability to phagocytose live *E. coli*. This difference may be due to reduced cell number due to reduced proliferation in response to LPS. Apoptosis was measured in cells transfected with the miR-oligonucleotides to ensure that the decrease in proliferation was not due to more cell death of cells transfected with pre-miR-107 or CDK6 siRNA. We found that there were no differences in percent of apoptotic cells.

CDK6 has a known role in cellular proliferation and LPS induces cellular proliferation (22-28). A previous study demonstrated that over-expression of CDK6 leads to an increased ability to migrate (29, 30). Cells were transfected with siRNA for CDK6 to observe its effect on proliferation of cells stimulated with LPS over a 24 hour period to observe if the effect observed in cells over-expressing miR-107 was due to targeting of CDK6. As shown in Figure 5A Left, cells in which CDK6 was knocked down with siRNA proliferate significantly less compared to control siRNA transfected cells. We also obtained bone marrow from CDK6-deficient mice. BMDM isolated from the bone marrow also exhibited significantly less proliferation in response to LPS as shown in figure 5A Right, compared to the wild-type counterpart BMDM.

To examine the role of CDK6 in TLR signaling and inflammation further, we injected CDK6-deficient and wild-type control mice with LPS and monitored their survival. CDK6-deficient mice were less susceptible to LPS, with lower mortality than wild-type mice (Fig. 5C). Analysis of circulating cytokine concentrations 1 h after LPS injection showed that TNF-α concentrations were lower in CDK6-deficient mice treated with LPS (Fig. 5D Left), consistent with lower susceptibility. Analysis of IL-10 concentrations at 4 h after LPS injection showed that serum concentrations in CDK6-deficient mice were greater than those in wild-type mice (Fig 5D Right). These data indicate that CDK6 has a pro-inflammatory role in LPS signaling. Overall, therefore, our results indicate that a decrease in miR-107 induced by LPS leads to an increase in CDK6 expression, which is turn leads to macrophage proliferation and migration with CDK6 also having a role in LPS lethality *in vivo*.

DISCUSSION

miR-107 and PanK1α are down-regulated in a MyD88/NF-κB/PPAR-α-dependent fashion in response to LPS. Following the modulation of miR-107 levels we found that the decrease in miR-107 leads to an increase in CDK6 thereby promoting proliferation and migration and indirectly affecting phagocytosis. We have therefore found a regulatory loop requiring a decrease in miR-107 and PanK1α via PPAR-α leading to increased CDK6 expression and subsequent proliferation and migration of macrophages. Both PanK1α and PPAR-α have known roles in lipid metabolism in the cell but little is known about their possible roles in TLR and immune signaling. PanK1α is involved in the first and most highly regulated step in the synthesis of CoA an essential cofactor in fatty acid oxidation or the metabolism of carboxylic acids which includes short and long chain fatty acids. Intracellular CoA levels decrease in response to glucose and insulin. LPS stimulation induces hypoglycemia and decreases liver gluconeogenesis in rats and decreases fatty acid oxidation during sepsis (31-36). Hepatocytes from rats were isolated and incubated with recombinant TNF-α to evaluate its effects on gluconeogenesis and glucose uptake (37). There was a decrease in gluconeogenesis and an increase in glucose uptake indicating a mutual inhibition between TNF-α stimulation and gluconeogenesis. LPS and TNF-α may decrease gluconeogenesis and fatty acid oxidation as a way to conserve glucose during infection but this decrease can be detrimental in some tissues and beneficial in other

tissues like the heart (38). We have shown that PanK1α is decreased in response to LPS and this could be a mechanism for the decrease observed in gluconeogenesis and fatty acid oxidation seen in the previous studies.

We have found that LPS stimulation leads to a decrease in PPAR-α mRNA and protein expression. Previous studies have shown that recombinant TNF-α or LPS stimulation decreases PPAR-α mRNA expression in rat liver hepatocytes. In mice exposed to TNF-α or LPS, PPAR-α mRNA in the lungs was decreased by 50-60% (39). In our study, the down-regulation of PPAR-α was maximal at 4 hours post LPS challenge. The precise mechanism of PPAR-α down-regulation by LPS is not known. LPS stimulates the expression of c-Jun, a component of the AP-1 signaling pathway and also activates NF-κB. A glutathione S-transferase pull-down experiment demonstrated that PPAR-α physically interacts with c-Jun and the NF-κB subunit p65 and that there is a bidirectional antagonism between PPAR-α, c-Jun and p65 (40). It is known that PPAR-α can positively auto-regulate its own expression because the PPAR-α/RXR complex can directly bind to the PPAR-α promoter (41). We have shown that following activation of TLR4 by LPS, NF-κB is activated which is required for the decrease in PPAR-α expression. Through the use of p65-deficient cells we have shown that the decrease in PPAR-α mRNA in response to LPS is p65 dependent. This suggests that p65 plays a role in the inhibition of the formation of the PPAR-α/RXR complex directly or it is interacting directly at the PPAR-α promoter preventing its transcription. There may also be an unknown factor involved and p65 is affecting this cofactor resulting in the inhibition of either the formation of the complex or the transcription of PPAR-α leading to a decrease in PPAR-α, PanK1α and miR-107 expression.

This study is the first to directly link any of the cyclin-dependent kinases as LPS responsive genes. CDK6 has a prominent role in the cell cycle. It is required to progress cells from G1 to S phases of the cell cycle. To regulate the onset of DNA replication, CDKs like CDK6 and its partner CDK4 associate with cyclins to phosphorylate the Rb protein and subsequently activate genes necessary for DNA replication (42, 43). Two families of CDK inhibitor proteins function to bind to CDKs so that they can no longer bind to cyclins and phosphorylate Rb thus controlling the progression of cells into S phase. The CDK inhibitor $p21^{Cip1/Waf1}$ is specific towards

CDK2, 4 and 6 and acts as a negative regulator of the activation of macrophages by reducing TNF-α and IL-1β production in response to LPS. p21 knockout mice demonstrated an increased susceptibility to LPS-induced shock brought about by increased levels of IL-1β (44, 45). The expression of p21 in lung epithelial cells resulted in decreased lung inflammation and reduced fibrosis. Based on the evidence obtained from our study, in disease situations where there is excessive inflammation precursor-miR-107 could act as a small-molecule inhibitor of CDK6 in a similar way to $p21^{Cip1/Waf1}$.

TLR stimulation has been shown to induce cell proliferation (23-28, 46). LPS stimulation has been shown to enhance the proliferation of the B9 cell line in a dose-dependent manner. A study examining the effect of arsenic on proliferation of mouse liver hepatocytes showed that arsenic exposure inhibited LPS induced proliferation through changes in mediators of cell cycle progression like CDK6 (47). We have found that LPS induces the proliferation of macrophages and the overexpression of miR-107 or silencing of CDK6 interferes with this process. CDK expression has also been linked to migration and motility of cells (48). A recent study showed that decreasing the activity of cyclin D1 decreased the kinase activity of CDK4/6 resulting in decreased motility of a breast cancer cell line. Overexpression of CDK6 suppressed the CDK inhibitor $p16^{INK4a}$ resulting in a decrease in cell spreading (49). CDK6 was shown to localize to the ruffling edge of spreading cells, indicating a function for CDK6 in controlling matrix-dependent cell spreading.

Several studies have shown that stimulation of cells with LPS results in an increase in cellular motility and in some cases an increase in wound repair (27, 50). Migration of cells is essential for proper wound healing so we next observed the effect of overexpressing miR-107 or inhibiting miR-107 expression on migration of I-BMDM stimulated with LPS. We have shown that cells overexpressing miR-107 exhibited a decreased ability to migrate into a wounded area whereas cells lacking miR-107 displayed an enhanced capacity. All cells exhibited an enhanced ability to migrate following LPS stimulation for 18 hours. The consequence of having decreased cellular proliferation and motility are a decrease in the overall immune response including a decrease in phagocytosis. Microbes, apoptotic cells, necrotic cells and cellular debris are all recognized by receptors like TLRs and they are internalized

through a cytoskeleton-dependent process of engulfment called phagocytosis (51). We have found that macrophages exhibited a decreased ability to phagocytose live *E. coli* when miR-107 was overexpressed compared to control transfected cells. Whereas cells lacking miR-107 displayed an enhanced ability to phagocytose live *E. coli* compared to anti-control transfected cells. (27, 52). We also found that CDK6 is important for LPS lethality since CDK6-deficiant mice were resistant to LPS. This is likely due to a macrophage defect as was indicated from decreased TNF-α and increased IL-10 production in CDK6-deficient mice.

Apart from CDK6, we also found two other potential miR-107 targets to be upregulated by LPS, HIF-1α and Dicer1. LPS is a known inducer of hypoxia signaling in a time and dose-dependent manner and this could be promoted by decreased miR-107 leading to increased HIF-1α (53). miR-107 has been shown to mediate p53 regulated hypoxic signaling by targeting HIF-1β (18). We also found that Dicer1 mRNA expression increased 2 fold following 1 to 2 hours of LPS stimulation. Elevated levels of miR-107 expression have been found in human breast cancer and these cells were shown to target Dicer1 mRNA resulting in overall miRNA down-regulation (54). The effect of LPS on Dicer1 here may therefore regulate other miRNAs.

Overall therefore, our data indicate a role for miR-107 in the regulation of TLR signaling. The decrease in miR-107 impacts on CDK6 levels, which in turn promotes proliferation and migration and in vivo is involved in the lethal effect of LPS. As more miR-107 targets are validated more functional consequences related to the expression of miR-107 will be established. The more that is understood regarding the role of miR-107 in TLR signaling, the greater the prospect of targeting it therapeutically for infections and inflammatory diseases.

EXPERIMENTAL PROCEDURES

Reagents

LPS from *Escherichia coli*, Serotype 0111:B4, was from Alexis. Anti-sense (anti-107), Precursor-miR-107 (pre-107), anti-miR-control (anti-control) and precursor-miR-control (pre-control) oligonucleotides, TaqMan mmu-miR-107 primer/probe

expression assay, primary-miR-107 probe and mCDK6 gene expression assay were obtained from Applied Biosystems.

Cell Culture

Immortalized wild-type bone marrow-derived macrophages (I-BMDM), MyD88-deficient and TRIF-deficient I-BMDM were a kind gift from Douglas Golenbock (University of Massachusetts), Wild-type and CDK6-deficient bone marrow was obtained from Dr. David Santamaria (Centro Nacional de Investigaciones Oncológicas, Madrid Spain). Marrow was isolated from the tibias and femurs of C57/Bl6 mice, and primary BMDM were generated as described previously (9). Human peripheral blood mononuclear cells (PBMC) were isolated from whole blood using a Ficoll gradient (55). HEK293T cells were obtained from the European collection of Animal cell cultures. In all cases, Dulbecco's modified Eagle's medium was supplemented with 10% fetal calf serum, 2 mm l-glutamine, 1% penicillin/streptomycin solution (v/v).

Mice

CDK6 -/- mice were generated as previously described (56). Mice were maintained according to the animal care standards established by the European Union.

RT-PCR

Immortalized BMDM (I-BMDM) and differentiated primary BMDM or PBMC were set up at 3×10^5/ml or 1×10^6/ml, respectively, in 24-well plates 1 day prior to stimulation. Cells were stimulated with LPS as indicated in the figure legend. Total RNA was extracted using the RNeasy kit (Qiagen), modified to obtain small RNA species. For miRNA analysis, miRNA TaqMan assays for miR-107 or miR-146a and RNU6B (Applied Biosystems) were used according to the manufacturer's instructions where 5 ng/ml total RNA was used as starting material. For mRNA expression analysis, cDNA was prepared from 20 to 100 ng/ml total RNA using the High-Capacity cDNA archive kit (Applied Biosystems) according to the manufacturer's instructions. mRNA expression was then monitored using either TaqMan gene expression assays with Fast Universal PCR Master Mix or SYBR Green-based chemistry (Invitrogen) using the following primers:

mmu-pre-107, 5′- GTGCTTTCAGCTTCTTTACAGTG -3′, forward,
5′- TCTCTGTGCTTTGATAGCCCTGT -3′, reverse;
glyceraldehyde-3-phosphate dehydrogenase (GAPDH),
5′- GAACGGGAAGCTTGTCATCAA -3′, forward,
5′- CTAAGCAGTTGGTGGTGCAG -3′, reverse;
mPanK1α, 5'- CTGCGGAGGAGGATGGACT -3', forward,
5'- CCACCGATATCCATACCAAACC -3', reverse;
mPPAR-α 5'- GCAGCTCGTACAGGTCATCA -3', forward,
5'- CTCTTCATCCCCAAGCGTAG -3', reverse.

miRNA and mRNA expression were measured on the 7900 RT-PCR system (Applied Biosystems), and fold changes in expression were calculated by the Delta Delta CT method using RNU6b as an endogenous control for miRNA analysis and GAPDH as an endogenous control for mRNA expression. All fold changes are expressed normalized to an unstimulated control for each cell type.

Enzyme-linked Immunosorbent Assay

Murine TNF-α and IL-10 expression were measured from the supernatants of stimulated cells using an enzyme-linked immunosorbent assay DuoSet kit (R&D Biosystems) according to the manufacturer's instructions.

Luciferase Assays

CDK6 3'UTR luciferase plasmid was obtained from Labomics. HEK293T cells seeded at 3×10^5/ml in 24-well plates were transfected using 2% Lipofectamine2000 (Invitrogen) with wild-type or mutant plasmid and TK-Renilla and 50 nm murine anti-control-miR, pre-control-miR, or 50 nM anti-miR-107 or pre-miR-107 (Applied Biosystems). In all cases, cells were lysed in passive lysis buffer before being analyzed for both luciferase and TK-Renilla activity as described previously (57). Data were normalized to TK-Renilla activity. In all cases results are expressed as mean ± S.E.M. of triplicate determinations from three separate experiments where fold changes are expressed normalized to control transfected cells.

Protein Expression

Primary BMDM seeded at 1×10^6/ml in 6-well plates were stimulated with LPS as indicated in the figure legends. Cells were lysed in low stringency lysis buffer

complete with protease inhibitors, and protein concentration was determined using the Coomassie Bradford reagent (Pierce). Lysates were resolved on 12% SDS-PAGE gels and transferred onto polyvinylidene difluoride membrane before being immunoblotted with a mouse monoclonal anti-CDK6 antibody (Cell Signaling Technology Inc.), a rabbit polyclonal anti-PanK1α antibody (a kind gift from Dr. Suzanne Jackowski from St. Jude Children's Research Hospital, Memphis, TN), a rabbit polyclonal anti-PPAR-α antibody (BioVision) or a mouse anti-β-actin (AC-15, Sigma). Blots were developed by enhanced chemiluminescence (ECL) (Cell Signaling Technology Inc.).

MTT Proliferation Assay

I-BMDM seeded at 3×10^5/ml in 96-well plates were transfected with 50 nm anti-sense or precursor miRNA oligonucleotides or 50 nM siRNA-CDK6 or siRNA-Control. Cells were stimulated with LPS as indicated in the figure legend. Four hours before the end of stimulation, 20 µl of 5 mg/ml MTT (3-(4,5-Dimethylthiazol-2-yl)-2,5-diphenyltetrazolium bromide) reagent was added to the cells (58). Following the four hour incubation media was removed and 100% isopropanol containing 4 mM HCl and 0.1% Nondet P-40 (NP40) was added and the plate was agitated for 15 minutes covered in foil at room temperature after which the optical density of the wells was read at 590 nm with a reference filter of 620 nm.

Wound Assay

I-BMDM seeded at 3×10^5/ml in 12-well plates were transfected with 50 nM anti-sense or precursor miRNA oligonucleotides for 24 hours. A sterile 10µl pipette tip was used to scratch wounds through the cell monolayer. After scraping, cells were washed twice in PBS to remove loose cells and new media was added. Cells were stimulated with LPS as indicated and incubated at 37°C as indicated in the figure legend. Digital images were taken at 0 and 24 hours after scraping. Images were superimposed with a 0.3mm x 0.3mm grid to quantify wound closure. Percent wound closure was calculated by comparing the number of grids in the defined wound area not occupied by cells after 24 hours of LPS stimulation (29).

Gentamicin Protection Assay

I-BMDM seeded at 3×10^5/ml in 12-well plates were transfected with 50 nM anti-sense or precursor miRNA oligonucleotides for 24 hours. Cells were stimulated with

live *E. coli* at a multiplicity of infection of 1:10. The plate was incubated in a 37°C 5% CO_2 incubator for one hour. After this time, the plates were washed 3 times with ice cold 1X PBS. One ml of 100 μg/ml gentamicin in DMEM was added to each well, and the plates were incubated in a 37°C 5% CO_2 incubator for one hour. After incubation, cells were washed 3 times in 1X PBS and then lysed with 100 μl ice cold dH_2O for 5 minutes at room temperature. Serial dilutions of 1:10, 1:100 and 1:1000 were then made, and samples were spot plated (10 μl) on LB plates and incubated overnight at 37°C. Colony forming units (CFUs) were counted approximately 12 hours later and an internalization index was calculated comparing the initial number of bacteria to the bacteria internalized (59).

Statistical analysis

All statistical tests were carried out on the mean results of at least three independent experiments unless otherwise indicated. A paired two-tailed and two-sample student t-test was performed to determine if samples were significantly different with Microsoft Excel. Levels of significance are indicated using asterisks: * $P \leq 0.05$, ** $P \leq 0.01$, *** ≤ 0.001.

ACKNOWLEDGEMENTS

We thank D. Golenbock (University of Massachusetts) for wild-type, MyD88-deficient and TRIF-deficient BMDMs immortalized by retrovirus; R. Hay (University of St. Andrews) for p65-deficient and matched wild-type control mouse embryonic fibroblasts; S. Jackowski (St. Jude Children's Research Hospital, Memphis, TN) for mouse polyclonal PanK1α antibody; and C.E. McCoy for critical reading of this manuscript. Supported by Science Foundation Ireland and the Health Research Board Ireland (No. PhD / 20007/9).

REFERENCES

1. Kawai T & Akira S (2006) TLR signaling. *Cell Death Differ* **13,** 816-825.
2. Takeda K & Akira S (2004) TLR signaling pathways. *Semin Immunol* **16,** 3-9.
3. Chen PY & Meister G (2005) microRNA-guided posttranscriptional gene regulation *Biol Chem* **386,** 1205-1218.
4. Gantier M, Sadler A, & Williams B (2007) Fine-tuning of the innate immune response by microRNAs. *Immunol Cell Biol* **85,** 458-462.
5. Sheedy FJ & O'Neill LA (2008) Adding fuel to fire: microRNAs as a new class of mediators of inflammation *Ann Rheum Dis* **67 Suppl 3,** iii50-55.

6. Lu LF & Liston A (2009) MicroRNA in the immune system, microRNA as an immune system *Immunology* **127,** 291-298.
7. Pauley KM & Chan EK (2008) MicroRNAs and their emerging roles in immunology *Ann N Y Acad Sci* **1143,** 226-239.
8. Xiao C & Rajewsky K (2009) MicroRNA control in the immune system: basic principles *Cell* **136,** 26-36.
9. Sheedy FJ, Palsson-McDermott E, Hennessy EJ, Martin C, O'Leary JJ, *et al.* (2010) Negative regulation of TLR4 via targeting of the proinflammatory tumor suppressor PDCD4 by the microRNA miR-21 *Nat Immunol* **11,** 141-147.
10. Frankel L, Christoffersen N, Jacobsen A, Lindow M, Krogh A, *et al.* (2008) Programmed cell death 4 (PDCD4) is an important functional target of the microRNA miR-21 in breast cancer cells. *J Biol Chem* **283,** 1026-1033.
11. Taganov K, Boldin M, Chang K, & Baltimore D (2006) NF-kappaB-dependent induction of microRNA miR-146, an inhibitor targeted to signaling proteins of innate immune responses. *Proc Natl Acad Sci U S A* **103,** 12481-12486.
12. McCoy CE, Sheedy FJ, Qualls JE, Doyle SL, Quinn SR, *et al.* (2010) IL-10 inhibits miR-155 induction by Toll-like receptors *J Biol Chem.*
13. O'Connell RM, Chaudhuri AA, Rao DS, & Baltimore D (2009) Inositol phosphatase SHIP1 is a primary target of miR-155 *Proc Natl Acad Sci U S A* **106,** 7113-7118.
14. Yin Q, Wang X, McBride J, Fewell C, & Flemington E (2008) B-cell receptor activation induces BIC/miR-155 expression through a conserved AP-1 element *J Biol Chem* **283,** 2654-2662.
15. Chen X, Splinter P, O'Hara S, & LaRusso N (2007) A cellular micro-RNA, let-7i, regulates Toll-like receptor 4 expression and contributes to cholangiocyte immune responses against Cryptosporidium parvum infection. *J Biol Chem* **282,** 28929-28938.
16. Tili E, Michaille J, Cimino A, Costinean S, Dumitru C, *et al.* (2007) Modulation of miR-155 and miR-125b levels following lipopolysaccharide/TNF-alpha stimulation and their possible roles in regulating the response to endotoxin shock. *J Immunol* **179,** 5082-5089.
17. Ramaswamy G, Karim MA, Murti KG, & Jackowski S (2004) PPARalpha controls the intracellular coenzyme A concentration via regulation of PANK1alpha gene expression *J Lipid Res* **45,** 17-31.
18. Yamakuchi M, Lotterman CD, Bao C, Hruban RH, Karim B, *et al.* (2010) P53-induced microRNA-107 inhibits HIF-1 and tumor angiogenesis *Proc Natl Acad Sci U S A* **107,** 6334-6339.
19. Murakami K, Bujo H, Unoki H, & Saito Y (2007) Effect of PPARalpha activation of macrophages on the secretion of inflammatory cytokines in cultured adipocytes *Eur J Pharmacol* **561,** 206-213.
20. Lee KH, Lotterman C, Karikari C, Omura N, Feldmann G, *et al.* (2009) Epigenetic silencing of MicroRNA miR-107 regulates cyclin-dependent kinase 6 expression in pancreatic cancer *Pancreatology* **9,** 293-301.
21. Takahashi Y, Forrest AR, Maeno E, Hashimoto T, Daub CO, *et al.* (2009) MiR-107 and MiR-185 can induce cell cycle arrest in human non small cell lung cancer cell lines *PLoS One* **4,** e6677.
22. Wu J, Qian J, Li C, Kwok L, Cheng F, *et al.* (2010) miR-129 regulates cell proliferation by downregulating Cdk6 expression *Cell Cycle* **9,** 1809-1818.

23. Fiaschi-Taesch NM, Salim F, Kleinberger J, Troxell R, Cozar-Castellano I, *et al.* (2010) Induction of human beta-cell proliferation and engraftment using a single G1/S regulatory molecule, cdk6 *Diabetes* **59,** 1926-1936.
24. Peavy DL, Baughn RE, & Musher DM (1978) Mitogenic activity of bacterial lipopolysaccharides in vivo: morphological and functinal characterization of responding cells *Infect Immun* **19,** 71-78.
25. Vos O (1978) Effect of bacterial lipopolysaccharide on proliferation of CFU-S *Exp Hematol* **6,** 688-693.
26. Moore RN, Steeg PS, Mannel DN, & Mergenhagen SE (1980) Role of lipopolysaccharide in regulating colony-stimulating factor-dependent macrophage proliferation in vitro *Infect Immun* **30,** 797-804.
27. Williams LM & Ridley AJ (2000) Lipopolysaccharide induces actin reorganization and tyrosine phosphorylation of Pyk2 and paxillin in monocytes and macrophages *J Immunol* **164,** 2028-2036.
28. Pedersen MR, Jensen S, Christensen JD, & Hansen EW (1995) Lipopolysaccharide in concentrations above 40 ng/ml stimulates proliferation of the IL-6-dependent B9 cell line *J Immunol Methods* **180,** 159-163.
29. Slomiany P, Baker T, Elliott ER, & Grossel MJ (2006) Changes in motility, gene expression and actin dynamics: Cdk6-induced cytoskeletal changes associated with differentiation in mouse astrocytes *J Cell Biochem* **99,** 635-646.
30. Lucas JJ, Domenico J, & Gelfand EW (2004) Cyclin-dependent kinase 6 inhibits proliferation of human mammary epithelial cells *Mol Cancer Res* **2,** 105-114.
31. Goto M, Zeller WP, & Lichtenberg RC (1994) Decreased gluconeogenesis and increased glucose disposal without hyperinsulinemia in 10-day-old rats with endotoxic shock *Metabolism* **43,** 1248-1254.
32. Lang CH, Spolarics Z, Ottlakan A, & Spitzer JJ (1993) Effect of high-dose endotoxin on glucose production and utilization *Metabolism* **42,** 1351-1358.
33. Memon RA, Fuller J, Moser AH, Smith PJ, Feingold KR, *et al.* (1998) In vivo regulation of acyl-CoA synthetase mRNA and activity by endotoxin and cytokines *Am J Physiol* **275,** E64-72.
34. Memon RA, Bass NM, Moser AH, Fuller J, Appel R, *et al.* (1999) Down-regulation of liver and heart specific fatty acid binding proteins by endotoxin and cytokines in vivo *Biochim Biophys Acta* **1440,** 118-126.
35. Feingold KR, Wang Y, Moser A, Shigenaga JK, & Grunfeld C (2008) LPS decreases fatty acid oxidation and nuclear hormone receptors in the kidney *J Lipid Res* **49,** 2179-2187.
36. Feingold KR, Moser A, Patsek SM, Shigenaga JK, & Grunfeld C (2009) Infection decreases fatty acid oxidation and nuclear hormone receptors in the diaphragm *J Lipid Res*.
37. Goto M, Yoshioka T, Battelino T, Ravindranath T, & Zeller WP (2001) TNFalpha decreases gluconeogenesis in hepatocytes isolated from 10-day-old rats *Pediatr Res* **49,** 552-557.
38. Kantor PF, Lucien A, Kozak R, & Lopaschuk GD (2000) The antianginal drug trimetazidine shifts cardiac energy metabolism from fatty acid oxidation to glucose oxidation by inhibiting mitochondrial long-chain 3-ketoacyl coenzyme A thiolase *Circ Res* **86,** 580-588.

39. Becker J, Delayre-Orthez C, Frossard N, & Pons F (2008) Regulation of peroxisome proliferator-activated receptor-alpha expression during lung inflammation *Pulm Pharmacol Ther* **21,** 324-330.
40. Delerive P, De Bosscher K, Besnard S, Vanden Berghe W, Peters JM, *et al.* (1999) Peroxisome proliferator-activated receptor alpha negatively regulates the vascular inflammatory gene response by negative cross-talk with transcription factors NF-kappaB and AP-1 *J Biol Chem* **274,** 32048-32054.
41. Pineda Torra I, Jamshidi Y, Flavell DM, Fruchart JC, & Staels B (2002) Characterization of the human PPARalpha promoter: identification of a functional nuclear receptor response element *Mol Endocrinol* **16,** 1013-1028.
42. Grossel MJ & Hinds PW (2006) From cell cycle to differentiation: an expanding role for cdk6 *Cell Cycle* **5,** 266-270.
43. Grossel MJ & Hinds PW (2006) Beyond the cell cycle: a new role for Cdk6 in differentiation *J Cell Biochem* **97,** 485-493.
44. Lloberas J & Celada A (2009) p21(waf1/CIP1), a CDK inhibitor and a negative feedback system that controls macrophage activation *Eur J Immunol* **39,** 691-694.
45. Scatizzi JC, Mavers M, Hutcheson J, Young B, Shi B, *et al.* (2009) The CDK domain of p21 is a suppressor of IL-1beta-mediated inflammation in activated macrophages *Eur J Immunol* **39,** 820-825.
46. Hasan UA, Trinchieri G, & Vlach J (2005) Toll-like receptor signaling stimulates cell cycle entry and progression in fibroblasts *J Biol Chem* **280,** 20620-20627.
47. Arteel GE, Guo L, Schlierf T, Beier JI, Kaiser JP, *et al.* (2008) Subhepatotoxic exposure to arsenic enhances lipopolysaccharide-induced liver injury in mice *Toxicol Appl Pharmacol* **226,** 128-139.
48. Zhong Z, Yeow WS, Zou C, Wassell R, Wang C, *et al.* (2010) Cyclin D1/cyclin-dependent kinase 4 interacts with filamin A and affects the migration and invasion potential of breast cancer cells *Cancer Res* **70,** 2105-2114.
49. Fahraeus R & Lane DP (1999) The p16(INK4a) tumour suppressor protein inhibits alphavbeta3 integrin-mediated cell spreading on vitronectin by blocking PKC-dependent localization of alphavbeta3 to focal contacts *EMBO J* **18,** 2106-2118.
50. Maa MC, Chang MY, Chen YJ, Lin CH, Yu CJ, *et al.* (2008) Requirement of inducible nitric-oxide synthase in lipopolysaccharide-mediated Src induction and macrophage migration *J Biol Chem* **283,** 31408-31416.
51. Janeway CJ & Medzhitov R (2002) Innate immune recognition. *Annu Rev Immunol* **20,** 197-216.
52. West MA, Prescott AR, Eskelinen EL, Ridley AJ, & Watts C (2000) Rac is required for constitutive macropinocytosis by dendritic cells but does not control its downregulation *Curr Biol* **10,** 839-848.
53. Blouin CC, Page EL, Soucy GM, & Richard DE (2004) Hypoxic gene activation by lipopolysaccharide in macrophages: implication of hypoxia-inducible factor 1alpha *Blood* **103,** 1124-1130.
54. Martello G, Rosato A, Ferrari F, Manfrin A, Cordenonsi M, *et al.* (2010) A MicroRNA targeting dicer for metastasis control *Cell* **141,** 1195-1207.
55. Palsson-McDermott EM, Doyle SL, McGettrick AF, Hardy M, Husebye H, *et al.* (2009) TAG, a splice variant of the adaptor TRAM, negatively regulates the adaptor MyD88-independent TLR4 pathway *Nat Immunol* **10,** 579-586.

56. Malumbres M, Sotillo R, Santamaria D, Galan J, Cerezo A, *et al.* (2004) Mammalian cells cycle without the D-type cyclin-dependent kinases Cdk4 and Cdk6 *Cell* **118,** 493-504.
57. McCoy CE, Carpenter S, Palsson-McDermott EM, Gearing LJ, & O'Neill LA (2008) Glucocorticoids inhibit IRF3 phosphorylation in response to Toll-like receptor-3 and -4 by targeting TBK1 activation *J Biol Chem* **283,** 14277-14285.
58. Weichert H, Blechschmidt I, Schroder S, & Ambrosius H (1991) The MTT-assay as a rapid test for cell proliferation and cell killing: application to human peripheral blood lymphocytes (PBL) *Allerg Immunol (Leipz)* **37,** 139-144.
59. Criss AK, Ahlgren DM, Jou TS, McCormick BA, & Casanova JE (2001) The GTPase Rac1 selectively regulates Salmonella invasion at the apical plasma membrane of polarized epithelial cells *J Cell Sci* **114,** 1331-1341.

FIGURE LEGENDS

Fig 1. miR-107 is down-regulated in response to LPS over time in a MyD88 and p65 dependent manner. (A) (Upper) Primary BMDM and (Lower) PBMC were stimulated with LPS (100 ng/ml), for the times indicated. Expression of miR-107 was measured by RT-PCR. Results were normalized to the endogenous control RNU6b, a ribosomal RNA and represented as fold stimulation over the unstimulated control. Results in all cases are shown as relative expression (R.E.). (B) (Upper) Primary BMDM and (Lower) PBMC were stimulated with LPS (100 ng/ml), for the times indicated. Expression of miR-146a was measured by RT-PCR. Results were normalized to the endogenous control RNU6b, a ribosomal RNA and represented as fold stimulation over the unstimulated control. (C) Primary BMDM were stimulated with LPS (100 ng/ml), for the times indicated and (Left) pri-miR-107 and (Right) pre-miR-107 were measured by RT-PCR. (D) (Left) WT I-BMDM, MyD88 deficient I-BMDM and Trif deficient I-BMDM were stimulated with LPS (100 ng/ml) for 8 or 24 h. (Right) WT MEF or p65 deficient MEF were stimulated with LPS (100 ng/ml) for the times indicated. The horizontal axis in all graphs represents time in hours of stimulation. In all cases, results are expressed as mean ± S.E.M. of triplicate determinations from three separate experiments.

Fig. 2. PanK1α and PPAR-α are down-regulated in response to LPS over time, similar to miR-107. (A) (Left) Primary BMDM were stimulated with LPS (100 ng/ml), for the times indicated. Expression of PanK1α was measured by RT-PCR. Results were normalized to the endogenous control GAPDH and represented as fold stimulation over the non-stimulated control. (Right) Primary BMDM were stimulated with LPS

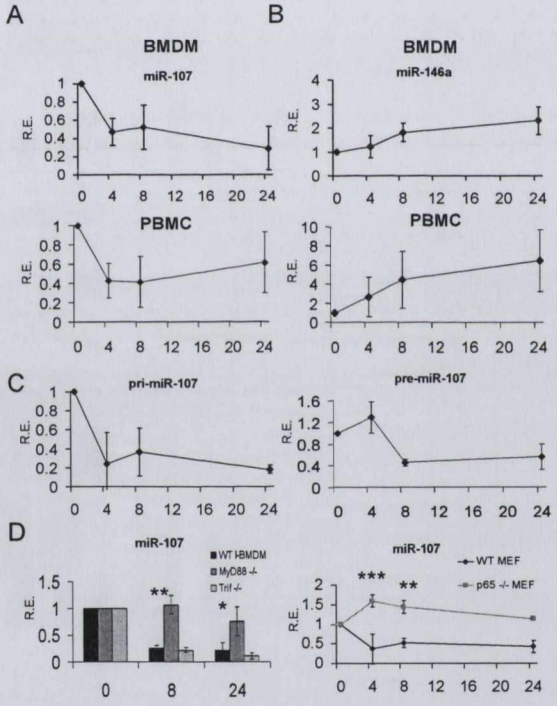
(100 ng/ml), for the times indicated and assessed for PanK1α and β-actin. Relative intensity (R.I) is shown to compare intensity of the western blot bands. (B) (Left) WT I-BMDM, MyD88 deficient I-BMDM and Trif deficient I-BMDM were stimulated with LPS (100 ng/ml) for 8 or 24 h. (Right) WT MEF or p65 deficient MEF were stimulated with LPS (100 ng/ml) for the times indicated. (C) (Left) Primary BMDM were stimulated with LPS (100 ng/ml), for the times indicated. Expression of PPAR-α was measured by RT-PCR. Results were normalized to the endogenous control GAPDH and represented as fold stimulation over the non-stimulated control. (Right) Primary BMDM were stimulated with LPS (100 ng/ml), for the times indicated and assessed for PPAR-α and β-actin, R.I. is shown below. (D) (Left) WT I-BMDM, MyD88 deficient I-BMDM and Trif deficient I-BMDM were stimulated with LPS (100 ng/ml) for 8 or 24 h. (Right) WT MEF or p65 deficient MEF were stimulated with LPS (100 ng/ml) for the times indicated. In all cases, results are expressed as mean ± S.E.M. of triplicate determinations from three separate experiments.

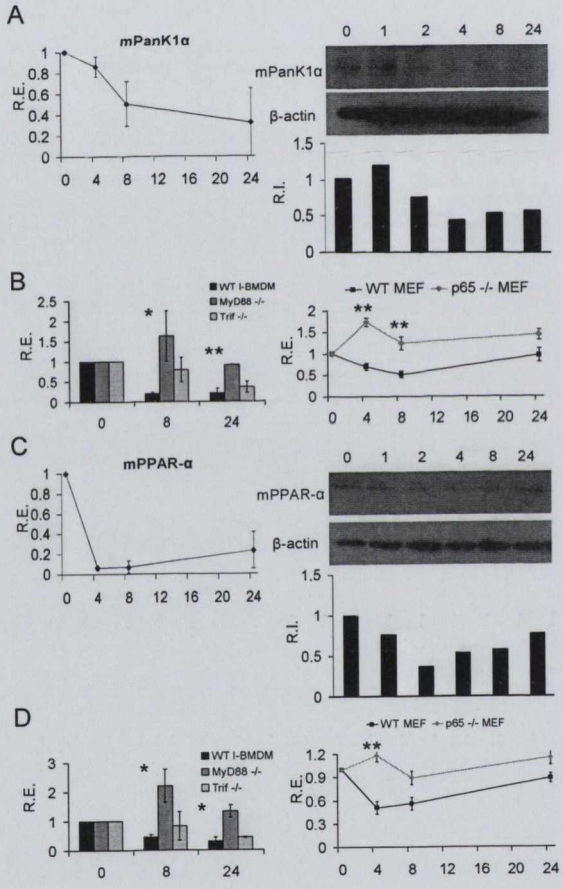
Fig. 3. CDK6, Dicer1 and HIF-1α are up-regulated in response to LPS over time and CDK6 is affected by miR-107 expression. (A) (Left) Primary BMDM were stimulated with LPS (100 ng/ml), for the times indicated. Expression of CDK6 was measured by RT-PCR. Results were normalized to the endogenous control GAPDH and represented as fold stimulation over the non-stimulated control. (Right) Cells were also assessed for CDK6 and β-actin protein expression. R.I. is shown below. (B) (Left) WT I-BMDM, MyD88 deficient I-BMDM and Trif deficient I-BMDM were stimulated with LPS (100 ng/ml) for 8 or 24 h and analyzed for CDK6 expression by RT-PCR. (Right) WT MEF or p65 deficient MEF were stimulated with LPS (100 ng/ml) for the times indicated and analyzed for CDK6 expression by RT-PCR. (C) I-BMDM were stimulated with LPS (100 ng/ml), for the times indicated. Expression of (Left) Dicer1 and (Right) HIF-1α were measured by RT-PCR in the same manner as CDK6. Results were normalized to the endogenous control GAPDH and represented as fold stimulation over the non-stimulated control. (D) (Left) I-BMDM were transfected with 50 nM anti-sense miRNA oligonucleotides and stimulated with LPS (100 ng/ml), for the times indicated. Expression of CDK6 was measured as before. (Right) Cells were also assessed for CDK6 and β-actin protein expression in response to LPS for the times indicated. R.I. is shown below. (E) (Left) I-BMDM were transfected with 50 nM precursor miRNA oligonucleotides and stimulated with LPS

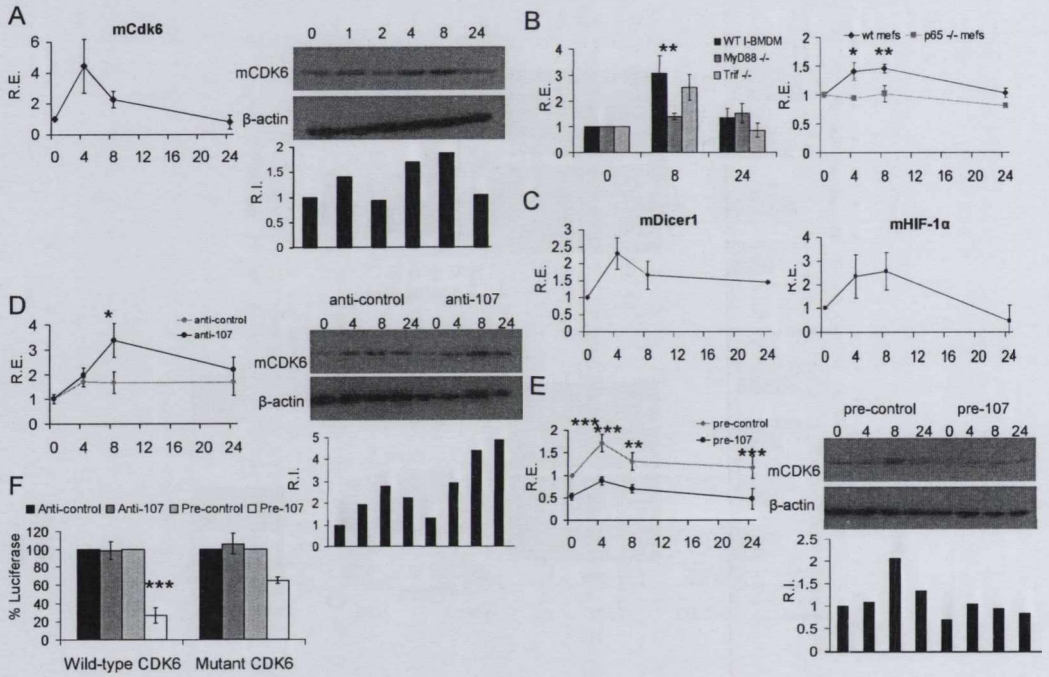
(100 ng/ml), for the times indicated. Expression of CDK6 was measured as before. (Right) Cells were also assessed for CDK6 and β-actin protein expression in response to LPS for the times indicated. R.I. is shown below. (F) CDK6 3'UTR luciferase plasmid and CDK6 mutant 3'UTR luciferase plasmid were co-transfected with 50 nM anti-miR-107, anti-miR-control, pre-miR-107 or pre-miR-control in HEK293T cells. Luciferase activity was measured and results were normalized for TK-Renilla activity, data is shown as percent luciferase relative to control. In all cases, results are expressed as mean ± S.E.M. of triplicate determinations from three separate experiments.

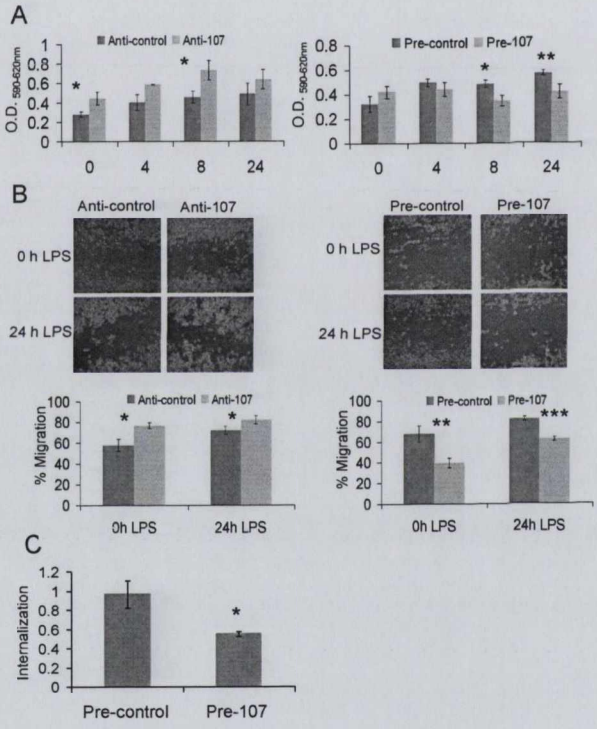
Fig. 4. Inhibition of proliferation, migration, phagocytosis and activation of the actin cytoskeleton by cells over-expressing miR-107. (A) (Left) I-BMDM were transfected with 50 nM anti-miR-107 or anti-miR-control and stimulated with LPS (100 ng/ml), for the times indicated and proliferation was assessed using 5mg/ml of MTT reagent. (Right) I-BMDM were transfected with 50 nM pre-miR-107 or pre-miR-control and stimulated with LPS (100 ng/ml), for the times indicated and assessed for proliferation as above. (B) (Upper Left) I-BMDM were transfected with 50 nM anti-miR-107 or anti-miR-control and a wound was introduced into the monolayer with a 10μl pipette tip at 0 h. Cells were than stimulated with LPS (100 ng/ml), for 24 h. The migration of the cells was monitored at 24 h post-stimulation. Triplicate photographs of the wound were taken and photos were displayed over a grid and empty wells were counted. (Lower Left) Results are represented as percent of wound closure. (Upper Right) I-BMDM were transfected with 50 nM pre-miR-107 or pre-miR-control and a wound was introduced into the monolayer with a 10μl pipette tip at 0 h. Cells were than stimulated with LPS (100 ng/ml), for 24 h. The migration of the cells was monitored at 24 h post-stimulation and analyzed and plotted as above. (C) Internalization of live *E. coli* was assessed using the gentamicin protection assay. Briefly, I-BMDM were transfected as above. *E. coli* was introduced to the cells at an MOI of 10:1 for 1 hour, cells were treated with 100μg/ml gentamicin for 1 h. Cells were lysed and CFU were counted. Data shown is a ratio of initial bacteria versus recovered bacteria or the internalization index. In all cases, results are expressed as mean ± S.E.M. of triplicate determinations from three separate experiments.

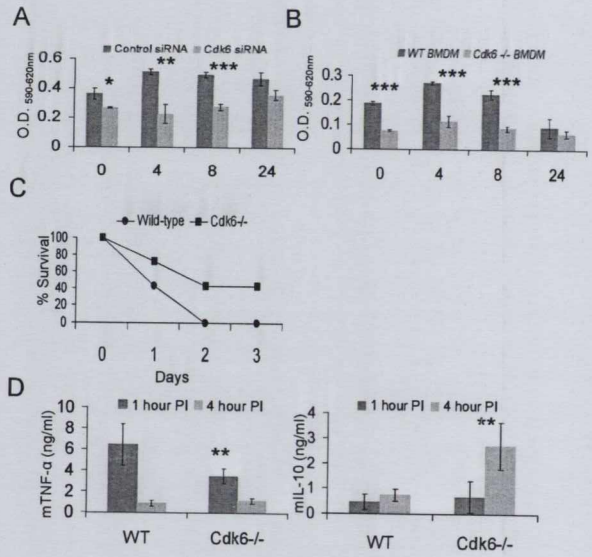
Fig. 5. Inhibition of proliferation, and cytokine production by cells lacking CDK6 and CDK6 deficient mice are protected from the lethality of LPS. (A) I-BMDM were transfected with 50 nM CDK6 siRNA or 50 nM control siRNA and stimulated with LPS (100 ng/ml), for the times indicated and proliferation was assessed using 5mg/ml of MTT reagent. (B) CDK6 knockout BMDM or wild-type BMDM were stimulated with LPS (100 ng/ml), for the times indicated and proliferation was assessed using 5mg/ml of MTT reagent. (C) Survival of wild-type (WT) control mice and CDK6-deficient (Cdk6-/-) mice 8 weeks of age were injected intraperitoneally with LPS (30 mg/ml), and monitored over a period of 3 d; results are plotted as a percentage of total numbers (n = 7 mice per group). (D) Enzyme-linked immunosorbent assay (ELISA) of mouse (Left) TNF-α and mouse (Right) IL-10 in blood samples from wild-type and CDK6-deficient mice (n = 7 mice per group), 1 h and 4 h after LPS injection. Data are representative of one independent experiment. In all cases, results are expressed as mean ± S.E.M. of triplicate determinations from three separate experiments


A
B
BMDM
miR-107
R.E.
BMDM
miR-146a
R.E.
PBMC
R.E.
PBMC
R.E.
C
pri-miR-107
R.E.
pre-miR-107
R.E.
D
miR-107
WT HBMDM
MyD88 -/-
Trif -/-
R.E.
**
*
miR-107
WT MEF
p65 -/- MEF
R.E.
***
**


A
mPanK1α
R.E.
0 4 8 12 16 20 24
0 1 2 4 8 24
mPanK1α
β-actin
R.I.
B
WT I-BMDM
MyD88 -/-
Trif -/-
R.E.
0 8 24
WT MEF
p65 -/- MEF
R.E.
0 4 8 12 16 20 24
C
mPPAR-α
R.E.
0 4 8 12 16 20 24
0 1 2 4 8 24
mPPAR-α
β-actin
R.I.
D
WT I-BMDM
MyD88 -/-
Trif -/-
R.E.
0 8 24
WT MEF
p65 -/- MEF
R.E.
0 4 8 12 16 20 24


A
mCdk6
R.E.
0 1 2 4 8 24
mCDK6
β-actin
R.I.
B
WT I-BMDM
MyD88 -/-
Trif -/-
R.E.
wt mefs
p65 -/- mefs
C
mDicer1
mHIF-1α
D
anti-control
anti-107
E
pre-control
pre-107
F
Anti-control Anti-107 Pre-control Pre-107
% Luciferase
Wild-type CDK6
Mutant CDK6


A
Anti-control
Anti-107
O.D. 590-620nm
1
0.8
0.6
0.4
0.2
0
*
*
0
4
8
24
Pre-control
Pre-107
O.D. 590-620nm
0.8
0.6
0.4
0.2
0
*
**
0
4
8
24
B
Anti-control
Anti-107
0 h LPS
24 h LPS
Pre-control
Pre-107
0 h LPS
24 h LPS
Anti-control
Anti-107
% Migration
100
80
60
40
20
0
*
*
0h LPS
24h LPS
Pre-control
Pre-107
% Migration
100
80
60
40
20
0
**
***
0h LPS
24h LPS
C
Internalization
1.2
1
0.8
0.6
0.4
0.2
0
*
Pre-control
Pre-107


A
Control siRNA
Cdk6 siRNA
O.D. 590-620nm
0.6
0.4
0.2
0
*
**
***
0
4
8
24
B
WT BMDM
Cdk6 -/- BMDM
O.D. 590-620nm
0.3
0.2
0.1
0
***
***
***
0
4
8
24
C
Wild-type
Cdk6-/-
% Survival
100
80
60
40
20
0
0
1
2
3
Days
D
1 hour PI
4 hour PI
mTNF-α (ng/ml)
10
8
6
4
2
0
**
WT
Cdk6-/-
1 hour PI
4 hour PI
mIL-10 (ng/ml)
4
3
2
1
0
**
WT
Cdk6-/-